

Winter 2014

OBJECT ORIENTED SCOUR ANALYSIS FOR MANMADE OBJECTS WITHIN AN ARTIFICIAL REEF

Clinton Bowman Lawson
University of New Hampshire, Durham

Follow this and additional works at: <https://scholars.unh.edu/thesis>

Recommended Citation

Lawson, Clinton Bowman, "OBJECT ORIENTED SCOUR ANALYSIS FOR MANMADE OBJECTS WITHIN AN ARTIFICIAL REEF" (2014). *Master's Theses and Capstones*. 1007.
<https://scholars.unh.edu/thesis/1007>

This Thesis is brought to you for free and open access by the Student Scholarship at University of New Hampshire Scholars' Repository. It has been accepted for inclusion in Master's Theses and Capstones by an authorized administrator of University of New Hampshire Scholars' Repository. For more information, please contact nicole.hentz@unh.edu.

OBJECT ORIENTED SCOUR ANALYSIS FOR MANMADE OBJECTS
WITHIN AN ARTIFICIAL REEF

BY

CLINTON LAWSON

B.S. Ocean Engineering, United States Naval Academy, 2008

THESIS

Submitted to the University of New Hampshire

in Partial Fulfillment of

the Requirements for the Degree of

Master of Science

in

Ocean Engineering

December, 2014

This thesis/dissertation has been examined and approved in partial fulfillment of the requirements for the degree of

Masters of Science in Ocean Engineering by:

Thesis Director, Diane Foster, Associate Professor of
Mechanical and Ocean Engineering

Kenneth C. Baldwin, Director ,Center for Ocean Engineering

Arthur Trembanis, Director Coastal Sediments
Hydrodynamics & Engineering Lab

On December 11th, 2014

Original approval signatures are on file with the University of New Hampshire Graduate School.

ACKNOWLEDGEMENTS

With the completion of this thesis, there are numerous people to whom I owe a debt of gratitude. First and foremost, the support and motivation provided by my wife, Molly, and our son, Daniel, have been pivotal to the completion of this work. The guidance and assistance provided by my advisor, Dr. Diane Foster was always welcomed and extremely helpful. To that end, I would also like to thank my committee members, Dr. Ken Baldwin and Dr. Art Trembanis. Further, I would like to thank Dr. Larry Mayer, Dr. Jim Gardner, and Val Schmidt for their contributions by way of discussion and review of my work. The community of support provided by the UNH School of Marine Science and Ocean Engineering was always extremely helpful and encouraging and for that I am very grateful.

TABLE OF CONTENTS

ACKNOWLEDGEMENTS	iii
LIST OF TABLES	vii
LIST OF FIGURES	viii
ABSTRACT	xii
I. INTRODUCTION.....	1
1.1 Motivation for Research.....	1
1.2 Scope of Research	2
1.2.1 Bathymetric Survey	3
1.2.2 Scour	4
1.3 Data Background	6
1.3.1 Location	7
1.3.2 Data Acquisition.....	9
1.3.3 Hydrodynamic Background	10
II. OBSERVATIONS	12
2.1 Dataset Visualization	12
2.1.1 Datum Determination.....	12
2.1.2 Overview	14
3.1 Data Organization	18
3.2 Major Axis Digitization.....	22
3.3 Masking Procedure.....	27
3.4 Setup.....	28
3.5 Car Orientation	28
3.6 Car Depth and Height above the Seabed Determination	29
3.7 Orientation Evaluation	30
IV. ANALYSIS AND RESULTS	32
4.1 Vertical Settlement of Cars General Scour, Moat and Pit Formation, Evolution, and Sediment Transport	32
4.2 MBES Analysis.....	34
4.3 Hydrodynamic Conditions.....	35
4.4 Localized Bathymetric Change Analysis	37

4.4.1 Case 1: “ Bathymetric Change from October 26, 2012 to November 11 th , 2012”	38
4.4.2 Case 2: “Bathymetric Change from November to December.....	39
4.4.3 Case 3: “Bathymetric Change from December, 6 th to 2012, March 28 th , 2013”	40
4.4.4 Subcase Alpha: Case 2- Case 1 Difference in Bathymetric Change	41
4.5 Object Based Localized Scour Analysis.....	44
4.5.1 MBES Artificial Reef Survey Area Object Field Characteristics	46
4.5.2 Case 1a: Object Based Scour Analysis of November – October Bathymetric Change Surface.....	48
4.5.3 Case 3- Object Based Analysis of March–December Bathymetric Difference Surfaces	51
4.6 Orientation Based Object Analysis.....	52
4.6.1 Case 1 Orientation Based Analysis	52
4.6.2 Case 3 Orientation Based Analysis	54
4.7 Refinements	58
V. CONCLUSIONS.....	59
5.1 MBES Applicability in Scour Research	59
5.2 Object Based Data products from Assimilated MBES surveys.....	59
5.3 General Impacts of Car Orientation on the Scour/Accretion Records.....	59
VI. CONSIDERATIONS AND REMARKS	60
LIST OF REFERENCES	62
APPENDIX I- Scour/Accretion Plots.....	64
APPENDIX II- Orientation Plots	141
APPENDIX III- Difference Surface Statistics	142
APPENDIX IV- MATLAB Script: Numeric Profiler.....	143
APPENDIX V- MATLAB Scripts:10X Script.....	147
APPENDIX VI- MATLAB Script: Wave Data	149
APPENDIX VII- MATLAB Script: COMPWAVES	153
APPENDIX VIII- MATLAB Script: Final Wave Plots	155
APPENDIX IX- MATLAB Script: Find Minor Scour.....	157
APPENDIX X- MATLAB Script: Find Major Scour	163

APPENDIX XI- MATLAB Script: Scour Orientation Minor	169
APPENDIX XII- MATLAB Script Find Scour Orientation Major.....	173

LIST OF TABLES

TABLE 1- SURVEY OFFSET STATISTICS	14
TABLE 2- THE GRAPHICAL REPRESENTATION IN FIGURE 21 SHOWS THE MEANING OF COLUMNS 1 AND 2 IN THE TABLE. COLUMNS 2/3 AND 4/5 DEFINE THE LOCAL AND GLOBAL COORDINATE SYSTEM RESPECTIVELY.	26
TABLE 3-10X HAND DIGITIZATION TABLE. ACCURATE VISIBLE INTERPRETATION OF ORIENTATION IS ASSUMED. PRECISION OF THIS METHOD IS SHOWN THROUGH THE STANDARD DEVIATION OF EACH REQUIRED PARAMETER.	32
TABLE 4- SUMMARY OF HOW DIFFERENT SCENARIOS IMPACT THE OUTCOME OF A BATHYMETRIC CHANGE DIFFERENCE SURFACE	41
TABLE 5- CHARACTERIZING ATTRIBUTERS OF ALL CARS	45

LIST OF FIGURES

FIGURE 1- GEOGRAPHIC OVERVIEW OF RED BIRD REEF, LOCATED SOUTH OF CAPE MAY, NJ AND WEST OF NORTHERN DELAWARE. THIS FIGURE WAS EXTRACTED FROM RAINEAULT ET AL. 2013.	7
FIGURE 2-DIGITAL ELEVATION MODEL OF THE MID-ATLANTIC SHELF SHOWS THE BATHYMETRIC AND MORPHOLOGICAL ATTRIBUTES OF THE RED BIRD REEF SITE ON A LARGE SCALE (NOAA COASTAL RELIEF MODEL 90-M GRIDDED BATHYMETRY VE=200). THIS FIGURE WAS TAKEN FROM RAINEAULT ET AL., 2013.	8
FIGURE 3- SURVEY INSTRUMENTATION: (A) AUTONOMOUS UNDERWATER VEHICLE DATA WAS NOT USED FOR THIS STUDY (B) THE MBES SURVEYS COLLECTED FROM THE R/V HUGH R. SHARP IS THE FOCUS OF THIS ANALYSIS. (C) THE TELEDYNE RDI 60KHZ ADCP IS THE ONE OF THE SOURCES OF HYDRODYNAMIC DATA USED IN THIS ANALYSIS. THIS FIGURE WAS TAKEN FROM TREMBANIS ET AL. (2013).	9
FIGURE 4- HURRICANE SANDY'S PATH AS PROJECTED HERE SHOWS THE CENTER OF THE STORM PASSING DIRECTLY OVER RED BIRD REEF. THE ADCP RECORDS INDICATE A STRONG STORM INDUCED HYDRODYNAMIC ENVIRONMENT FROM HURRICANE SANDY. IMAGE TAKEN FROM PORTLAND WEATHER- WWW.BRUCESUSMAN.COM.	11
FIGURE 5- BATHYMETRIC SURVEY OF RED BIRD REEF FIELD SITE. THE SEVEN LOCATIONS FOR DATUM OFFSET CALCULATIONS ARE IDENTIFIED WITH YELLOW BOXES WHICH INCLUDE THE PERIMETER BOX WHICH ENCOMPASSES ENTIRE SURVEY AREA.	13
FIGURE 6- FIGURE FROM RAINEAULT ET AL. (2013) SHOWS AN AUTO SEGMENTATION OF A BACKSCATTER DATA COLLECTED FROM THE SEAFLOOR AT RED BIRD REEF IN 2011. THE TAN AREAS REPRESENT COARSE SANDY GRAVEL. THE BLUE AREAS OF THE MOSAIC REPRESENT SAND WITH SILT AND CLAY. THE GREEN REPRESENT ARTIFICIAL REEF OBJECTS.	15
FIGURE 7-DIGITAL TERRAIN MODEL REPRESENTING THE SURVEY DATA COLLECTED OCTOBER 26TH 2012. THE COLOR BAR RANGES FROM 26.5M WATER DEPTH REPRESENTED IN RED TO 28.5M WATER DEPTH REPRESENTED IN PURPLE	16
FIGURE 8 – DIGITAL TERRAIN MODEL REPRESENTING THE SURVEY DATA COLLECTED NOVEMBER 11TH 2012	17
FIGURE 9 – DIGITAL TERRAIN MODEL REPRESENTING THE SURVEY DATA COLLECTED DECEMBER 6TH 2012	17
FIGURE 10 – DIGITAL TERRAIN MODEL REPRESENTING THE SURVEY DATA COLLECTED MARCH 28TH 2013	18
FIGURE 11- THE ENTIRE DATA SET IS SEGMENTED INTO 4 SECTIONS THAT CLUSTER CARS OF SIMILAR LOCATION TOGETHER.	19
FIGURE 12- SECTION 1 CONTAINS FOUR OF THE SUBWAY CARS OF THIS ANALYSIS. SECTION 1 IS LOCATED ON THE EXTREME SOUTHWEST CORNER OF THE DATA SET.	19
FIGURE 13- SECTION 2 CONTAINS SEVEN CARS AND IS LOCATED DIRECTLY EAST OF SECTION 1.	20
FIGURE 14- SECTION 3 CONTAINS 13 CARS AND IS LOCATED TO THE EAST OF BOTH SECTIONS 1 AND 2.	21
FIGURE 15- SECTION 4 CONTAINS 14 CARS AND IS LOCATED IN THE SOUTHEAST CORNER OF THE DATSET..	21
FIGURE 16- A SAMPLE OF THE MAJOR AXIS IDENTIFICATION AND ORIENTATION ANALYSIS PREFORMED. THE DTM OF A CAR PICTURED HERE IS CAR NUMBER 18 IN THE DATA SET. THE	

LINE PICTURED IS REFERRED TO AS THE PARENT PROFILE OR MAJOR AXIS. THE COLOR SHADE REPRESENTS THE DEPTH IN ACCORDANCE WITH THE COLOR BAR TO THE RIGHT OF THE CAR. 23

FIGURE 17- MAJOR AXIS PROFILE SHOWING SCOUR SURROUNDING CAR NUMBER 18. THE Y-AXIS IS DEPTH AND THE X-AXIS IS LENGTH ALONG PARENT (MAJOR AXIS). VERTICAL COLOR SHADING IS CONSISTENT WITH FIGURE 7 AND IDENTIFIES ELEVATION OF SUBSURFACE PROFILE. CAR EXTENDS FROM ROUGHLY 8 M TO 24 M. THE FAR FIELD BED ELEVATION IS AT APPROXIMATELY -27.75 M. 23

FIGURE 18- CROSS PROFILE OF CAR #18 SHOWING THE EXTENTS OF THE EACH SUB DATA SET COLLECTED AND USED FOR CAR SPECIFIC ANALYSIS. CROSS PROFILES WERE COLLECTED EVERY 25 CM ON AXIS AND EVERY 25 CM ALONG THE PARENTS PROFILE TO MAINTAIN THE 25 CM RESOLUTION OF THE SCENE. 24

FIGURE 19- MINOR AXIS PROFILE SHOWING THE PLOTTED OUTPUT OF THE COLLECTED DATA. THE BOLD VERTICAL LINE AT X=0 M REPRESENTS THE CENTERLINE OF THE CAR AND THE PROFILE DATA PRESENTED IS THE DATA COLLECTED ORTHOGONALLY TO THE MAJOR AXIS AT TOP (LOCAL CAR REFERENCE) OF THE SUB-DATASET. 25

FIGURE 20-THE CROSS PROFILE INTERVAL ALONG THE PARENT AND THE SAMPLING INTERVAL ALONG THE CROSS PROFILE FORM A 25CM GRID OF SAMPLES OVER THE AREA SHOWN ABOVE WHICH REPRESENTS THE TYPICAL SAMPLING AREA. 25

FIGURE 21- THE PRODUCT OF THE SAMPLING GRID IS AN ASCII FILE IN WHICH DEFINE THE SAMPLING POINT'S LOCATION IN TERMS OF THE GLOBAL AND LOCAL COORDINATE SYSTEM. 26

FIGURE 22- THE TRANSITION FROM SEABED TO OBJECT LAYING ON THE SEABED IS SHOWN IN GREEN AND YELLOW 27

FIGURE 23-CAR ORIENTATION IS DEFINE AS COUNTER CLOCKWISE ROTATION FROM EAST. THE DETERMINATION OF ORIENTATION USES THE FIRST AND LAST DATA POINTS ALONG THE PARENT PROFILE. 29

FIGURE 24-EACH CAR WAS SAMPLED SUCH THAT THE FAR FIELD BOTTOM DEPTH WAS DETERMINED USING THE SECTIONS OF SEAFLOOR SHOWN ABOVE TO THE LEFT AND RIGHT OF THE CAR. LIKEWISE, THE TOP OF THE CAR WAS DETERMINED USING THE SAMPLING REGION SHOWN ON TOP OF THE CAR. 30

FIGURE 25- CAR #14 WAS USED TO EVALUATE THE ACCURACY OF HAND DIGITIZATION OF ORIENTATION. TABLE 3-10X HAND DIGITIZATION TABLE SHOWS THE ORIENTATION AND THE ASSOCIATED STANDARD DEVIATION OF THE METHOD. 31

FIGURE 26- VISIBLE MOATS CAN BE SEEN ON THE INITIAL SURVEY RECORD. VISUAL ANALYSIS WOULD INDICATE A FAR FIELD BOTTOM DEPTH AT APPROXIMATELY -27.7 ON THE WEST SIDE OF CAR 18 AND -27.3 ON THE EAST SIDE WITH MOATS AS DEEP AS 0.75M AROUND THE CAR. 32

FIGURE 27- (A) CAR ORIENTATION VS. HEIGHT OF CAR (B) DEPTH OF CAR VS HEIGHT OF CAR (C) ORIENTATION (DEG) VS DEPTH OF CAR (M) 33

FIGURE 28 – WAVE AND CURRENT DATA BETWEEN OCTOBER 26TH AND NOVEMBER 10TH WAS COLLECTED FROM THE DEPLOYED ADCP AT RED BIRD REEF. 36

FIGURE 29 – CASE 1: OCTOBER TO NOVEMBER DIFFERENCE SURFACE. THE STANDARD COLOR IS SHOWN IN THE TOP RIGHT OF THE FIGURE. SIGNIFICANT SCOUR IS SHOWN IN PURPLE WHILE A SIGNIFICANT ACCRETION IS SHOWN IN YELLOW AND RED. 39

FIGURE 30- NOVEMBER TO DECEMBER BATHYMETRIC CHANGE SHOWING A PERIOD OF BENIGN WAVE CONDITIONS THAT PRODUCED LITTLE DETECTABLE CHANGE AND SHOWS THE IMPACT

OF A VERTICAL OFFSET INTRODUCED BY TIDALLY REFERENCING DEPTH MEASUREMENTS DURING PERIODS OF LOST GPS SIGNAL.	40
FIGURE 31 – CASE 3: THE DECEMBER TO MARCH DIFFERENCE SURFACE VISUALLY SHOWS SIGNIFICANT BORROW PIT BEHAVIOR AND A MORE GENERAL SMOOTHING OF THE SEDIMENT FEATURES SEEN IN FIGURE 29.	41
FIGURE 32- SUBCASE ALPHA SHOWS THE AREAS WHERE THE MAGNITUDE OF THE CHANGE SURFACE WAS LARGE IN BOTH CASE 1 AND 3 BUT THE DIRECTIONS WERE OPPOSED. THE RED AREAS ON THE FIGURE REPRESENT AREAS WHERE SANDY SIGNIFICANTLY CHANGED THE SEAFLOOR DEPTH AND THE WEATHER EVENTS IN CASE 3 HAD A LARGE AFFECT IN THE SAME LOCATION BUT CHANGED THE SEAFLOOR DEPTH IN THE OPPOSITE DIRECTION. THE BLACK IN THE FIGURE REPRESENTS THE MASK APPLIED TO THE ARTIFICIAL REEF OBJECTS.	42
FIGURE 33- SUBCASE ALPHA OVERLAID ON CASE 1 SHOWS THE RELATIONSHIP BETWEEN THE CASE 1 DIFFERENCE SURFACE AND THE SUBCASE ALPHA SURFACE. THE COLOR SCALE IS THE SAME AS THE CASE 1 AND 2 SURFACES BUT THE RED IN THE FIGURE IS SUBCASE ALPHA.	42
FIGURE 34- SUBCASE ALPHA OVERLAID ON CASE 3 IS A SIMILAR PRODUCT TO FIGURE 35 BUT IS NOW SHOWN OVER CASE 3.	43
FIGURE 35-SUBCASE ALPHA OVERLAID ON AUTO SEGMENTATION MAP FROM RAINEAULT ET AL (2013). THE RED AREAS REPRESENT THE LARGE OPPOSED CHANGES BETWEEN BATHYMETRIC CHANGE SURFACES.	44
FIGURE 36- THE SUMMARY PLOT OF THE DEFINING CAR PARAMETERS SHOWING EACH CAR'S ASSOCIATED ORIENTATION (DEGREES CCW FROM EAST) (TOP), HEIGHT ABOVE THE SEABED (M) (MIDDLE), AND FAR FIELD DEPTH (M) (BOTTOM).	46
FIGURE 37- THE DISTRIBUTIONS OF ORIENTATION, HEIGHT OF CAR, AND FAR FIELD DEPTH SHOW HOW THE CARS ARE ORGANIZED BY THEIR ASSOCIATED PARAMETERS.	47
FIGURE 38- DIAGRAM SHOWING CONCEPTUAL LAYOUT AND EXTENTS OF ANALYSIS.	48
FIGURE 39 – THE OBJECT BASED MAJOR AXIS SCOUR ANALYSIS IS SHOWS ALL THE CARS IN THE DATASET FOR CASE I BATHYMETRIC CHANGE SURFACE. THE SHOWS THE VOLUMETRIC GAIN/LOSS IN $M^3/.25$ M STRIP ALONG MINOR AXIS CAR WIDTH. THE PLOT OF THE RIGHT SHOWS THE SUM OF THOSE GAINS/LOSSES FROM THE MIDPOINT OF THE MAJOR AXIS TO EITHER END OF THE CAR.	49
FIGURE 40- SUBPROFILE SCOUR ANALYSIS OF CASE 1 SHOWS THE SCOUR/DEPOSITION BEHAVIOR AS A FUNCTION OF 25 CM WIDTH ALONG THE MINOR AXIS.	50
FIGURE 41- CASE 3 SHOWING ALL CARS SHOWS THE VOLUMETRIC CHANGE(M^3) PER .25 M WIDTH FROM THE TOP AND BOTTOM OF THE CARS RUNNING ALONG THE MAJOR AXIS. THE PLOT SHOWS THE CHANGE GIVEN AND POSITION ALONG THE CAR'S MAJOR AXIS.	51
FIGURE 42-SUBPROFILE SCOUR ANALYSIS OF CASE 3 SHOWS THE SCOUR/ ACCRETION BEHAVIOR AS A FUNCTION OF 25CM WIDTH ALONG THE MAJOR AXIS (LEFT) AND THE CUMULATIVE EFFECTS (RIGHT)	52
FIGURE 43- CASE 1 SCOUR ACCRETION PLOTS FOR CARS FACING -25.5 TO 8.5 DEGREES CLOCKWISE FROM NORTH.	53
FIGURE 44: CASE 1 SCOUR ACCRETION PLOTS FOR CARS FACING 73 TO 107 DEGREES CLOCKWISE FROM NORTH	54
FIGURE 45- CASE 3 NORTH ORIENTED CARS: VOLUMETRIC SCOUR (MAJOR-RIGHT, MINOR-LEFT)	54
FIGURE 46-CASE 1 SCOUR ACCRETION PLOTS FOR CARS FACING -25.5 TO 8.5 DEGREES CLOCKWISE FROM NORTH	55

FIGURE 47-CASE 3 SCOUR ACCRETION PLOTS FOR CARS FACING 73 TO 107 DEGREES CLOCKWISE FROM NORTH.	56
FIGURE 48- CASE 1 AND 3 (NORTH ORIENTED CARS) SCOUR ACCRETION PLOTS TOGETHER.	57
FIGURE 49-CASE 1 AND 3 (EAST ORIENTED CARS) SCOUR ACCRETION PLOTS TOGETHER.	57

ABSTRACT

OBJECT ORIENTED SCOUR ANALYSIS FOR MANMADE OBJECTS

WITHIN AN ARTIFICIAL REEF

by

Clinton B. Lawson

University of New Hampshire, December, 2014

Scour in and around structures placed on the seafloor occurs on varying spatio-temporal scales in response to changing hydrodynamic conditions. This effort examines the scour surrounding submerged railway cars in an artificial reef environment, Red Bird Reef, located off the shores of Delaware. Repeated high resolution multibeam sonar data from a Reson 7125 Multibeam Echo Sounder is used to evaluate the sensitivity of localized scour to car orientation, water depth, sediment heterogeneity, and hydrodynamic forcing. Red Bird Reef shows unambiguous differences in scour/accretion response to varying wave climates and varying response to object based parameters such as object proximity, orientation, depth and height. This study examines the overall local scour and accretion surrounding 38 decommissioned R-26 "Redbird" subway cars placed on the seafloor functioning as an artificial reef system. Scour was shown to have axial asymmetries and is sensitive to the car orientation relative to wave direction. The observations show that the local influence area is greater than 8 times the objects width wide and 2 times the length long.

The use of bathymetric difference surfaces suggests areas where previous estimates of sediment composition transition from coarse to fine sediment are concomitant with regions of high scour variability. This result suggests that sediment grain size heterogeneity could be a significant influence on variability of submarine scour.

I. INTRODUCTION

1.1 Motivation for Research

The purpose of this study is to analyze the characteristics of marine scour around man made or artificial objects laying on or embedded in the seabed to further understand specifically how orientation, size, and local proximity affect the signature. Understanding the evolution of scour and the major associated parameters therein is critical to improving construction methods of ocean infrastructure. Minimizing scour can decrease the lifecycle costs of deployed and constructed infrastructure. By improving our understanding of the hydrodynamic conditions leading to scour, best practices can be refined and improved.

Another potential application of improving the ability to predict scour and accretion is improving the capability to detect objects lying on or partially buried in the seabed. The ocean is both a physically and economically challenging environment to operate in for extended periods of times. The ability to quickly identify objects that might pose a risk to marine traffic is hugely important both in permissive and non-permissive areas.

Understanding the onset and minimization of scour during conception is important but also presents the opportunity to look retroactively at a single or time-lapse bathymetric survey and gain valuable data about the site specific hydrodynamic regimes that exist there. This extrapolated information can be used to better plan movements of goods, materials, and people through less trafficked waters.

This will also serve to further reinforce a multi-beam echo sounder's (MBES) applicability in analyzing the seabed on finer length scales as higher resolution systems

develop. As uncertainties of position and depth decrease with refinement within the multi-beam processing pipeline and hardware, more refined conclusions can be ascertained.

1.2 Scope of Research

The automated use of underwater survey data is expanding rapidly. Underwater survey is becoming more economically viable, more widely used, and in turn becoming more refined, reliable, and accurate. The expansions in application for this data are growing as the horizontal and vertical uncertainties are minimized. The data collected today can be used on much finer length scales than ever before.

The use of these systems is currently constrained to uncertainties incurred through the integration process from positioning, data collection, and processing. However, as this uncertainty becomes smaller and the resolution becomes finer, this technology allows for expansion of use in the defense, commercial, and consumer sectors.

While the impacts of manmade objects on the seafloor are well documented in regards to hydrodynamics and erosion, there is still headway to be made in terms of characteristic properties that affect erosion. This study will focus on 38 subway cars placed on the seabed as artificial reef objects. The seafloor around these cars will be analyzed using an object based approach where each car and associated area on the seabed will be specifically analyzed to determine the effective parameters of the car that impact the response to local hydrodynamic forces measured by instruments deployed at the field site, wave buoy data in the vicinity, and forecasted models.

The goal of this study is to achieve a greater understanding of the various characteristic parameters of scour and sediment transport in a high energy inner-

continental shelf region specifically targeting local scour around objects placed in an artificial reef environment. The primary research objectives of this study are to :

1. process MBES data into data products that identify hydrodynamic/scour influences
2. illustrate scour as a function of distance from major and minor axis of square cylindrical artificial reef objects
3. investigate the cumulative scour as a function of distance
4. qualitatively analyze local scour for each survey relative to the associated hydrodynamics
5. evaluate the impacts of orientation, car height, and car depth on cumulative local scour

1.2.1 Bathymetric Survey

Bathymetric survey techniques have been employed by marine scientists since the early 19th century. Initially, depth measurement was performed via lead line methods with associated sextant positioning. While providing some insight into the bottom depths at relatively approximate locations, the spatiotemporal resolution was not sufficient for any use other than general situational awareness during navigational passage.

As the military and civilian need for more accurate and rapid surveys increased and technology improved, the single beam echo sounder became the method of choice early in 20th century. The first large deployment of this technology was completed in the 1920's by a German Atlantic Expedition, the Research Vessel Meteor (Wüst et al., 1936). With advances in sonar technology and computing, the multi-beam

echo sounder process was developed. With computer size decreasing and capability increasing, the applicability of multi beam sonar bathymetric survey surged tremendously. Single beam and multibeam echo-sounders (SBES and MBES) are now commonplace in maritime archaeology and survey (Momber et al., 2000; Lawrence et al., 2002; McNinch et al, 2006; Quinn et al., 2006).

The application of high resolution swath sonar (MBES) to study bed forms in the vicinity of manmade seabed objects and their associated spatio-temporal length scales is critical to further understanding the energetic littoral zone (Trembanis et al., 2013). The spatial coverage of swath sonar and its ability to measure depth and the dimensions of manmade objects enable a unique and accurate means of directly determining scour magnitudes from remotely sensed data (Mayer et al., 2007). Time-lapse MBES bathymetric surveys can accurately and rapidly capture morphological change at the seafloor and sites of interest such as shipwrecks, minefields and artificial reefs. Accretion-erosion models derived from these surveys can help quantify the magnitude and rate of change in fully submerged sites and objects at depth (Quinn et al., 2010).

1.2.2 Scour

As suggested in previous works, wave-induced scour can be predicted using simple models that utilize grain-size, wave orbital velocity and the physical dimensions of the subject object (Whitehouse et al., 1998). These steady flow parameters work adequately in fine grain sand. In areas of coarse sand, corrections to the prediction can be made by assuming scour and burial decreases as the disruption created by the object approaches that of the ripple field (Trembanis et al., 2007). This suggests that in

coarse sediment fields or in the presence of ripple fields, the objects scour is directly related to the sedimentary properties in the vicinity. However, further investigation is warranted, as the majority of research has been concentrated on major benchmark cases and flow environments. Scour processes around objects in combined wave and current environments should be analyzed further (Sumer et al., 2010).

In addition, morphologic models describing scour/deposition processes often do not include the effects of externally generated disruptions. The Meyer-Peter and Muller, (1948) model and Engelund and Fredsoe (1976) models were developed for internally generated boundary layer conditions. This is not applicable around manmade objects where processes such as horseshoe vortices and shedding need to be accounted for (Sumer et al., 2010). McNinch et al., (2006), also emphasize the importance of several hydrodynamic effects that are vital to understanding scour around objects. The effects are horseshoe vortices around the front and sides; spatially accelerated flow which is deflected around the object; and wake-vortices in the lee of the object are critical to understanding scour (McNinch et al., 2006). Furthermore the Tairua dataset used in Green et al. (2004), suggests that sediment suspension changes through time with changes in bedforms, mixing, entrainment, and cross-shelf variability (Green et al., 2004).

Seabed scour also occurs on varying spatial scales. At a shipwreck site, it is believed that scour effects are created on spatial scales varying from the complete wreck site itself down to the individual debris located within the field. The spatial extent of the scour depends on the orientation, shape, and size of the object itself as well as the seafloor geology, water depth and associated hydrodynamics. Scour also varies

under different regimes of hydrodynamic conditions including waves, tides, currents, and other estuarine flows (Quinn et al., 2006).

Under similar flow conditions, orientation will affect the direction, extent, and number of scour signatures created by an object on the seabed. The orientation will affect the evolution of the overall signature as well. Under oscillatory flow, the object might generate a triple scour signature or three distinct marks parallel to the peak flow. Yet at higher energy levels the triple scour signature will become unstable and transform into an expanded semi-elliptical single scour (Quinn et al., 2006).

Large scale marine scour at the Redbird Reef Site shows the removal of fine sediments and the formation of moats 1-30 m in diameter and 0.5 m-1 m deep around the reef objects and settling of the reef objects >1 m into the seabed. Local wave and current conditions could impact decisions on object clustering and orientation to decrease scour impacts in the future (Raineault et al., 2013). Conversely, scour/accretion patterns around objects on the seabed can offer valuable information on the hydrodynamic conditions of the environment (Plets et al., 2010).

1.3 Data Background

The data collection effort for this experiment was conducted as part of an Office of Naval Research (ONR) sponsored program to understand and characterize the ripple dynamics and scour processes in an energetic heterogeneous inner-shelf setting. A series of high-resolution acoustic surveys were conducted over a wide array of weather and associated hydrodynamic conditions. While the preponderance of analysis thus far in the project has been the application of methods to interpret the

ripple field behavior, this work will investigate the behavior of marine scour and sediment transport around individual objects placed within an artificial reef site.

1.3.1 Location

The artificial reef is located 29km east of the Indian River Inlet off the coast of Slaughter Beach, Delaware. The vicinity of Redbird Reef experiences both significant buoyant/tidal current forcing via the Delaware Estuary and from periodic significant storm events. The reef is primarily made up of the 997 retired NYC subway cars but also contains decommissioned military vehicles, tugboats, ballasted tires and barges

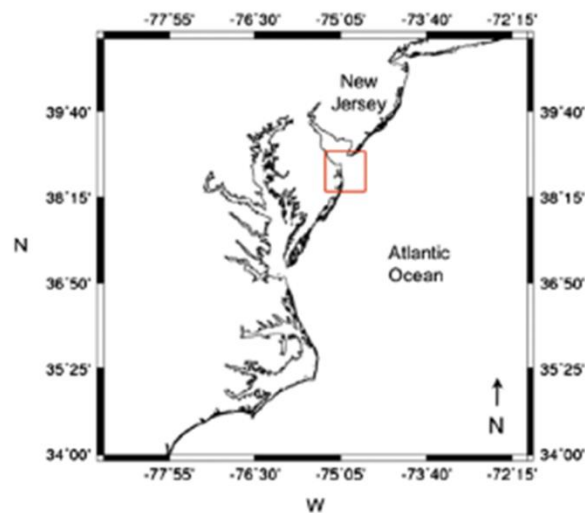


Figure 1- Geographic Overview of Red Bird Reef, located south of Cape May, NJ and West of northern Delaware. This figure was extracted from Raineault et al. 2013.

covering 4.5 km². The contents of the reef were added starting in 1996 and concluded in 2009 (Raineault et al., 2013). The reef itself was created by the Delaware Department of Natural Resources and Environmental Control (DNREC).

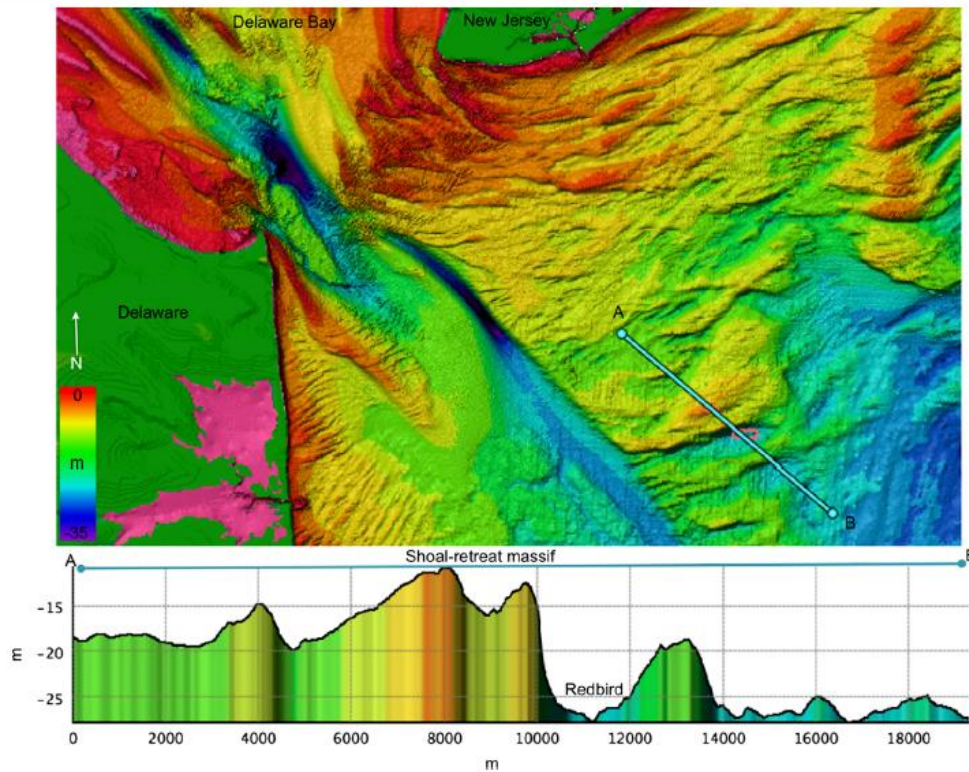


Figure 2-Digital elevation model of the mid-Atlantic shelf shows the bathymetric and morphological attributes of the Red Bird Reef site on a large scale (NOAA Coastal Relief Model 90-m gridded bathymetry VE=200). This figure was taken from Raineault et al., 2013.

A total of 997 subway cars were placed in curricular clusters with diameters of 150 m-250 m. The cars themselves have all had the windows and doors removed as well as any other potentially hazardous material. Large objects of note that were placed on the reef include six tug boats varying in length from 16 m to 28 m, a 48 m barge, and a 22 m push boat (Raineault et al. 2013)

The MBES surveys were conducted on October 26th, 2012, November 10th 2012, December, 6th, 2012, March 28th, 2013, and July 29th, 2013. This thesis will focus on the analysis of the high resolution MBES data to capture the evolution of scour and accretion at a higher resolution than previously studied during significant weather events. The data available presents a unique opportunity to look at the evolution of

scour around many cars during two distinct weather events and their respective response to time varying wave and current induced orbital velocities in a shallow water environment.

1.3.2 Data Acquisition

The data used in this study was acquired from the Research Vessel Hugh R. Sharp using a Reson 7125 multibeam echo sounder operated at both 200 and 400 kHz. The R/V Hugh R. Sharp is 44.5m in length. The surveys analyzed were conducted over a 1.0x0.5 km area using 400 kHz. 1.0 x 0.5 degree beam widths were utilized on transmit and receive enabling lateral resolution of 0.5 m x 0.25 m in the water depth at Redbird reef which is around 27 m.

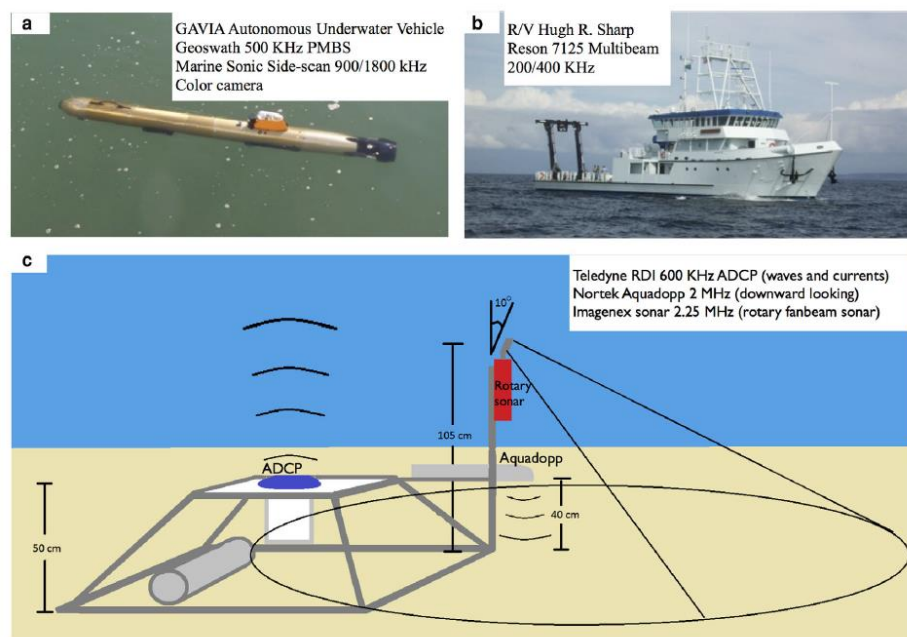


Figure 3- Survey Instrumentation: (a) Autonomous Underwater Vehicle data was not used for this study (b) The MBES surveys collected from the R/V Hugh R. Sharp is the focus of this analysis. (c) The Teledyne RDI 60kHz ADCP is the one of the sources of hydrodynamic data used in this analysis. This figure was taken from Trembanis et al. (2013).

An Applanix POSMV 330(V5) was used to refine raw global positioning system measurements and then post processed using Applanix POSPac MMS to reduce positioning uncertainties in the vertical and horizontal directions. Post processing is used to further correct GPS measurements from knowledge of specific satellite constellation orbits, outstanding clock corrections, calculated atmospheric delays etc. The advantage of post processing the data is improved accuracies that enable an ellipsoidally referenced position and depth across the swath and eliminate uncertainties associated with tidal forecasting/hind casting, heave measurements, and settlement and squat concerns. Vertical repeatability between surveys is on the order of 10-15cm (Trembanis et al., 2013).

In conjunction with the multibeam sonar, bottom mounted instrumentation was deployed to capture measurements at the field site critical to understanding the localized hydrodynamics. An RDI Workhorse Sentinel ADCP configured to measure profiles of currents every 30 minutes and a 5 minute wave burst every hour was deployed.

1.3.3 Hydrodynamic Background

The tidal influences are dominated by the semi-diurnal (M2) tide that controls the surface currents regionally (Muscarella et al. 2011), outside of significant weather events (Raineault et al. 2013). As mentioned above, hydrographic surveys were completed October 26th, 2012, November 10th 2012, December, 6th, 2012, March 28th, 2013, and July 29th, 2013. A unique aspect of these data sets is they offer multiple representations of

the seafloor over a time period in which there was significant storm induced scour and sediment transport under various orientations and of varying local proximity.

The first survey was completed on October 26, 2012. Four days prior, what is known today as Super Storm Sandy started as a tropical wave in the Caribbean Sea. Sandy quickly escalated to a Tropical Storm six hours later, and then moved northward as it intensified. Sandy hit Kingston, Jamaica as a hurricane and continued to increase in intensity as it again moved over the Caribbean Sea. Three days after the storm's formation, Hurricane Sandy hit Cuba as a Category 3 hurricane and quickly weakened to a Category 1.

Sandy made landfall north of Atlantic City, NJ on October 29th 2012. The proximity of Red Bird Reef to Atlantic City, NJ is shown in Figure 4.



Figure 4- Hurricane Sandy's path as projected here shows the center of the storm passing directly over Red Bird Reef. The ADCP records indicate a strong storm induced hydrodynamic environment from Hurricane Sandy. Image taken from Portland Weather-www.bruceusman.com.

The 26-October survey acts as a baseline both for the impacts of Hurricane Sandy and the large Nor'easter that followed during the first week of November. This survey enables the ability to look at the impacts globally (entire reef structure) and locally (individual cars) with respect to scour and sediment transport.

The survey that follows the October 29th, 2012 survey is the November 10th, 2012 survey. From these two overlapping surveys, products can be created to be qualitatively and quantitatively analyzed. The remaining surveys can be used to gain a more general idea of what the normal conditions create in terms of seasonal scour and transport.

II. OBSERVATIONS

2.1 Dataset Visualization

As mentioned in Mayer et al. (2007), 3-D and 4-D visualization of remotely sensed data is becoming increasingly important in expanding the rapid understanding of site specific hydrodynamic conditions in the littoral zone. In this analysis, QPS's Fledermaus software was utilized to visualize the point data in 0.25m gridded pixels. This resolution ensured adequate point density for this analysis. The Fledermaus scenes were created by Jonathan Beaudoin, UNH Center for Coastal and Ocean Mapping.

2.1.1 Datum Determination

In order to provide meaningful comparative analysis of each data set against each other, the data sets themselves had to be transformed to reflect a common datum upon which the depth was measured. This step is necessary, because the shipboard GPS of at least one survey was not functional. The data sets were cropped so

each data set contained the same number of pixels. To determine the offset of any particular data set from the averaged surface, seven common polygons were used to define areas of comparison. The location of these polygons can be seen in Figure 5. To ensure that the analysis could identify finer resolution changes in the bathymetry and associated ripple fields, each survey was compared to the initial bathymetric survey completed in October of 2012 and had an appropriate offset applied so as all the surveys were of similar vertical position as the October 2012 survey. Data manipulation and analysis was performed using the Fledermaus software package from QPS.

The seven polygon locations were chosen in such a way as to minimize the possibility of spatial variability while using the barge as a common, assumed to fixed location. The results of this differencing process can be found in

Table 1.

7

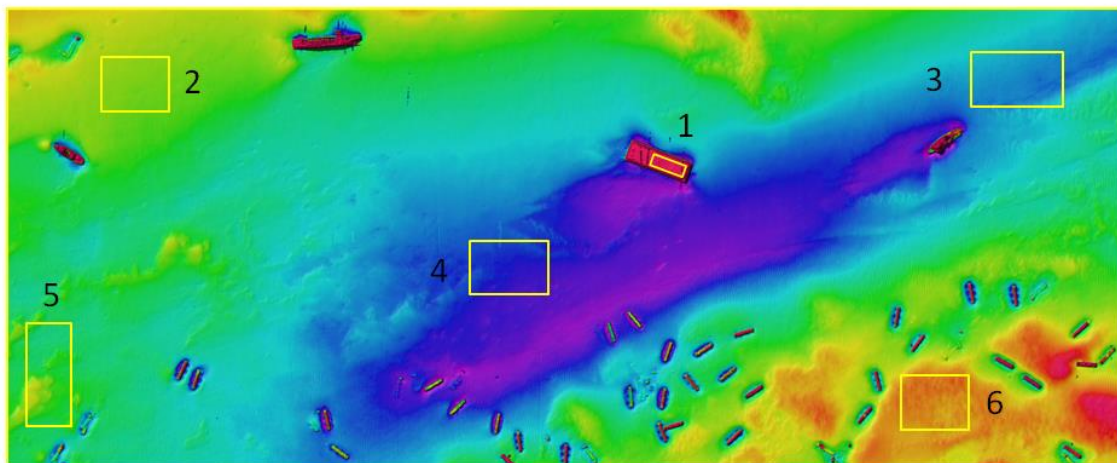


Figure 5- Bathymetric survey of Red Bird Reef field site. The seven locations for datum offset calculations are identified with yellow boxes which include the perimeter box which encompasses entire survey area.

Table 1- Survey Offset Statistics

	10-Nov-12		26-Dec-12		28-Mar-13		29-Jul-13	
	Mean Diff	STD	Mean Diff	STD	Mean Diff	STD	Mean Diff	STD
Barge	0.1	0.08	0.12	0.88	0.27	0.06	0.36	0.08
NW Patch	0.11	0.02	0.36	0.02	0.32	0.03	0.42	0.02
NE Patch	0.16	0.04	0.39	0.04	0.33	0.03	0.41	0.05
Center Patch	0.1	0.02	0.42	0.02	0.31	0.03	0.37	0.03
SW Patch	0.06	0.12	0.35	0.12	0.2	0.09	0.3	0.09
SE Patch	0.12	0.08	0.41	0.05	0.34	0.05	0.42	0.05
Entire Survey	0.09	0.12	0.36	0.13	0.25	0.14	0.35	0.14
	0.11	0.08	0.34	0.34	0.29	0.07	0.38	0.08
	AVG Mean	AVG STDEV	AVG Mean	AVG STDEV	AVG Mean	AVG STDEV	AVG Mean	AVG STDEV
	0.1		0.36		0.31		0.37	
	MEDIAN		MEDIAN		MEDIAN		MEDIAN	

The median offsets found in

Table 1 were applied to the respective surfaces. The median was used to avoid the incorporation of any particular anomalies used in the processing calculations. The barge was used as the lynch pin where positive values mean all pixels in section were higher than that of the October survey.

2.1.2 Overview

From the figure below, taken from Raineault et al. (2013), the sediment type within the reef structure varies primarily from north to south. This product is called an auto-segmentation map and was produced using QTC SWATHVIEW. The program uses

cluster analysis to determine the optimal number of distinct classes based on backscatter (Preston et al., 2004). Figure 6 serves to illustrate potential variability within the data set and potentially where the greatest variation from expectations might occur as well as help to explain any similar effects identified within similar sediment types.

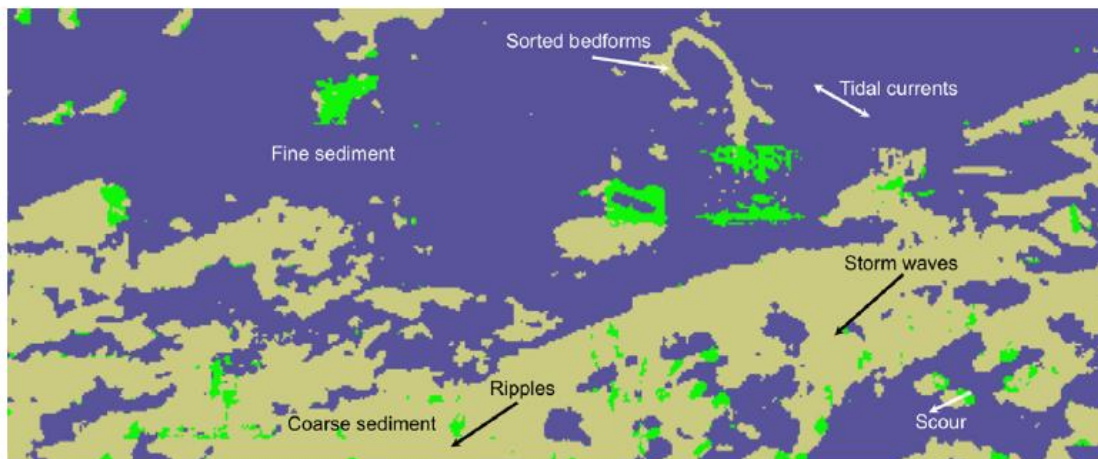


Figure 6- Figure from Raineault et al. (2013) shows an auto segmentation of a backscatter data collected from the seafloor at Red Bird Reef in 2011. The tan areas represent coarse sandy gravel. The blue areas of the mosaic represent sand with silt and clay. The green represent artificial reef objects.

Settling of artificial reef objects is discussed in Quinn et al. (2006). Quinn explains that the objects act as a stationary nucleus in rotary tidal currents, which creates scour and in turn causes the object to settle or be buried. Raineault et al. (2013) later concluded that at the Redbird site, the hard gravel substrate prevents further settling of objects. Similarly, McNinch et al. (2006) notes that a sandy gravel layer acts as a hindrance to further settling at the site of the studied shipwreck site, Queen Anne's Revenge. To that end, it is concluded in Raineault et al. (2013) that the cars have stopped settling by the 2008 survey.

As noted in Caston et al. (1979), and confirmed in Raineault et al. (2013), the cars develop asymmetrical scour moats that have relatively shallow depth in relation to their associated width and length. Other noticed attributes of the bathymetry are that the scour moat geometries and scour marks are dependent on the car's orientation with respect to the dominant flow. As such, the cars that are orientated broadside to the flow produce the largest marks while the other orientations produced narrower scours.

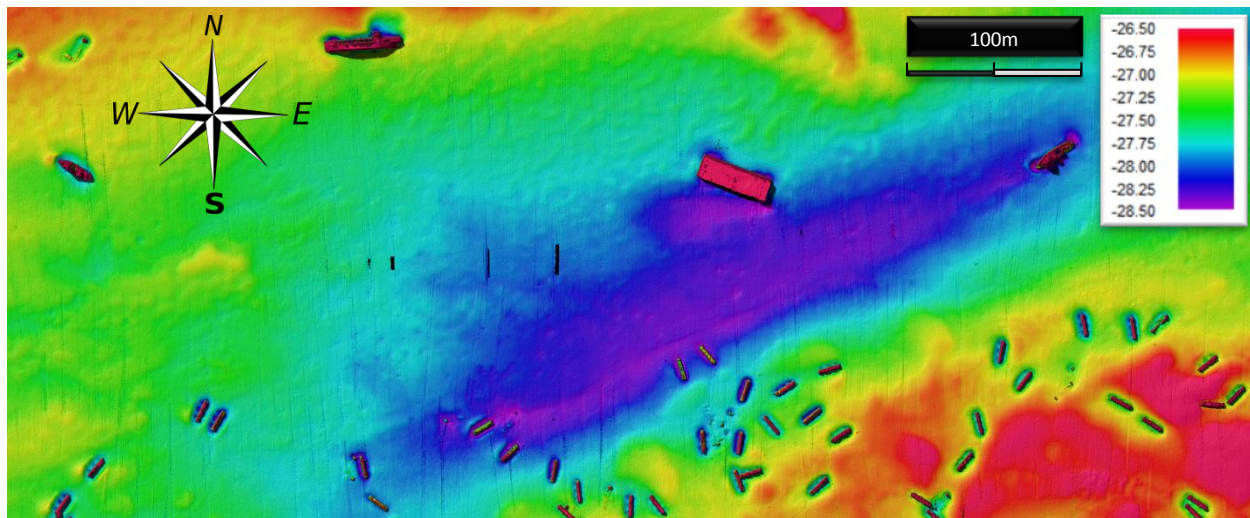


Figure 7-Digital Terrain Model representing the survey data collected October 26th 2012. The color bar ranges from 26.5m water depth represented in red to 28.5m water depth represented in purple

Figure 7 is a digital terrain model (DTM) of the survey conducted on October 26th 2012. This survey was performed days before Hurricane Sandy and the large Nor'easter that followed. Scour around a collection of cars shows a potential interaction of groups of cars on the seabed. The scour moats around the individual cars remains a property of the car itself, but the scour marks around cars in proximity to each other amalgamate on time scales of years. This effect is a product of the distance between the cars in the direction of sediment transport (Raineault et al. 2013).

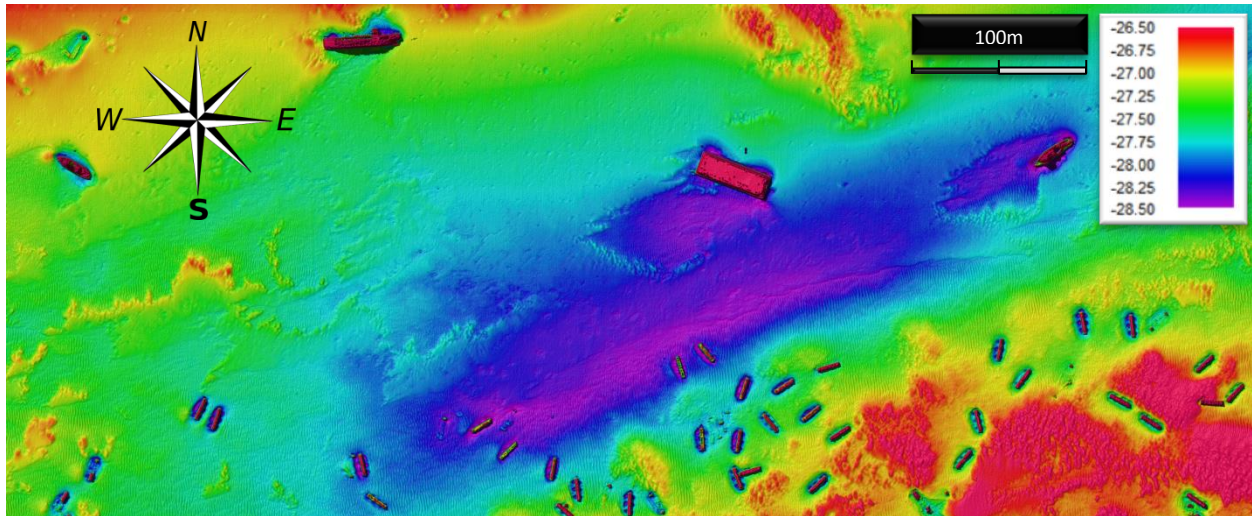


Figure 8 – Digital Terrain Model representing the survey data collected November 11th 2012

The digital terrain model representing the November 11th survey, Figure 8, shows an increase in seabed variability when compared to the other data sets contained within this analysis. The relatively steep gradients are washed away in the subsequent surveys. This survey data allows for the examination of the impacts of Hurricane Sandy and the Nor'easter as they surveys are closely preceding and following the storms.

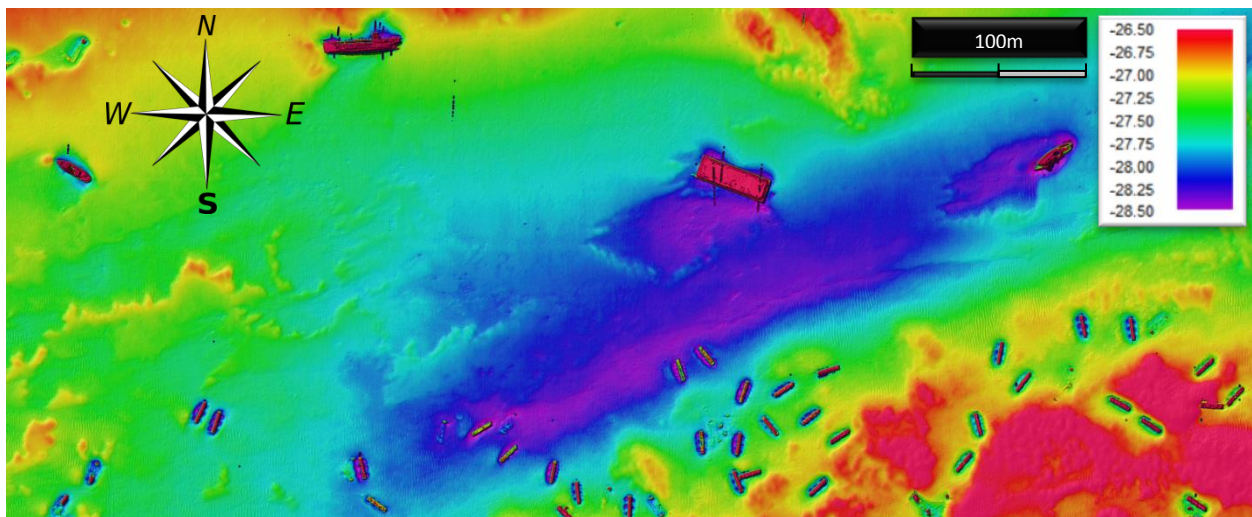


Figure 9 – Digital Terrain Model representing the survey data collected December 6th 2012

The November and December MBES data occurs during a calm period representing benign winter conditions. The December and March MBES surveys will allow for the comparison of bottom depths and associated changes during relatively typical winter conditions.

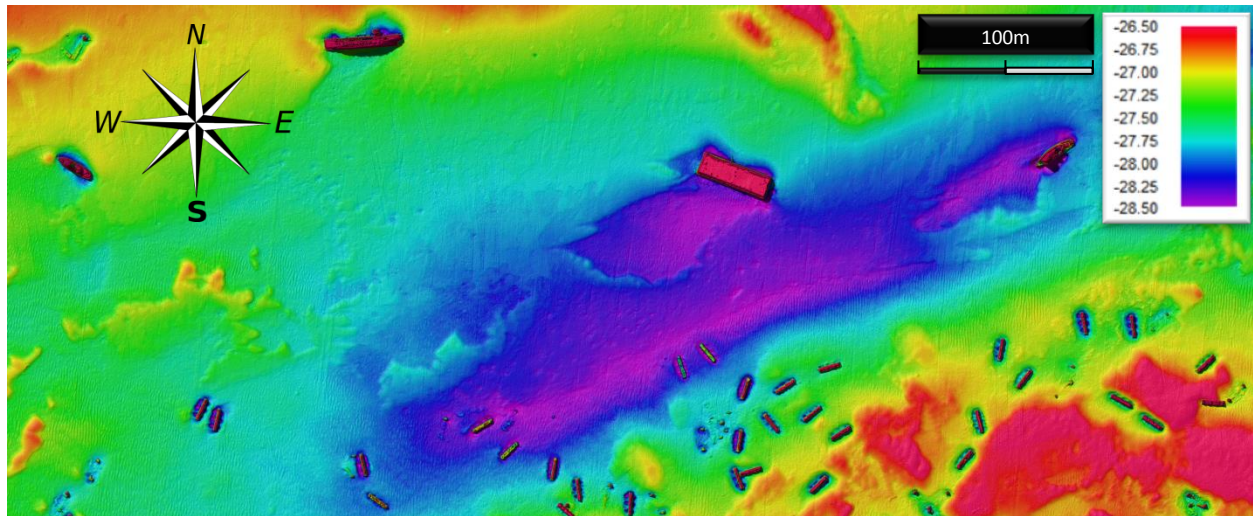


Figure 10 – Digital Terrain Model representing the survey data collected March 28th 2013

III. METHODS

3.1 Data Organization

This analysis will use the data collected around each car individually and as such the differentiation of the cars is required. Figure 11 shows the overall data set with identified sections defined that will be more closely examined.

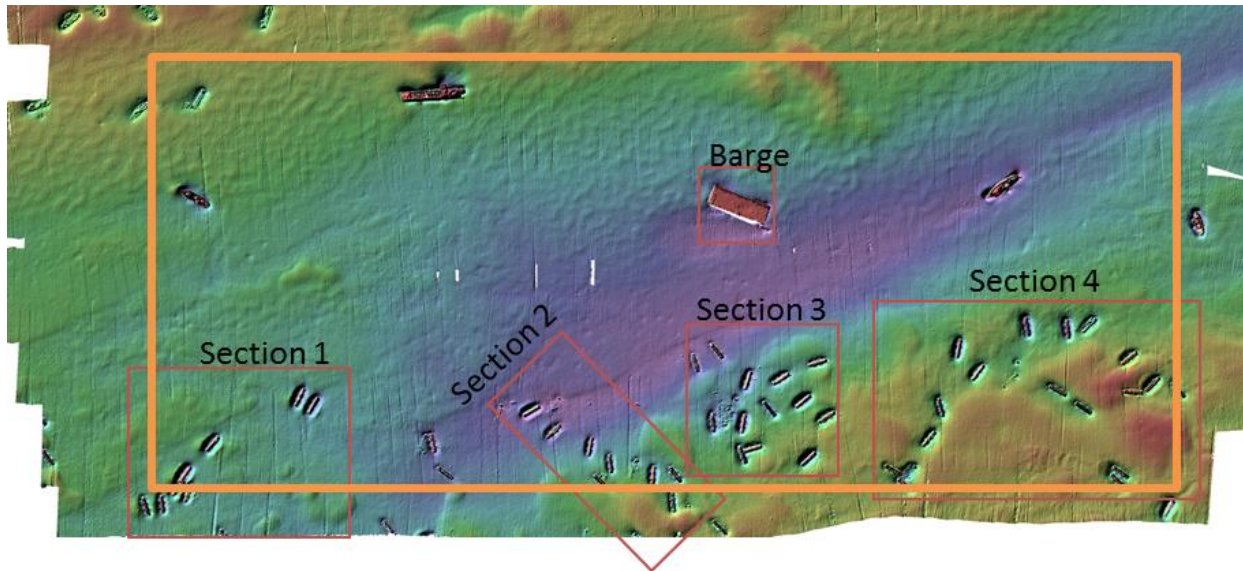


Figure 11- The entire data set is segmented into 4 sections that cluster cars of similar location together.

Represented in Figure 11, the dataset is divided into sections that determine more specific locations within the dataset. Sections 1-4 are listed from left to right, respectively. Section 1 contains four subway cars and is located in the southwest corner of the field site. The cars in section 1 are all oriented in similar directions and located at similar water depths.

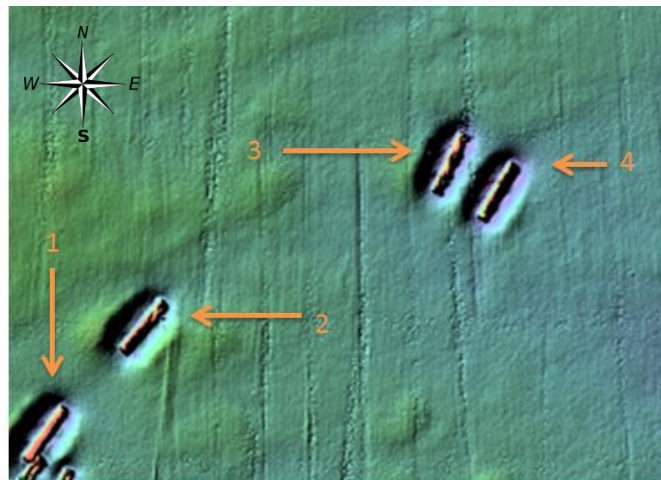


Figure 12- Section 1 contains four of the subway cars of this analysis. Section 1 is located on the extreme southwest corner of the data set.

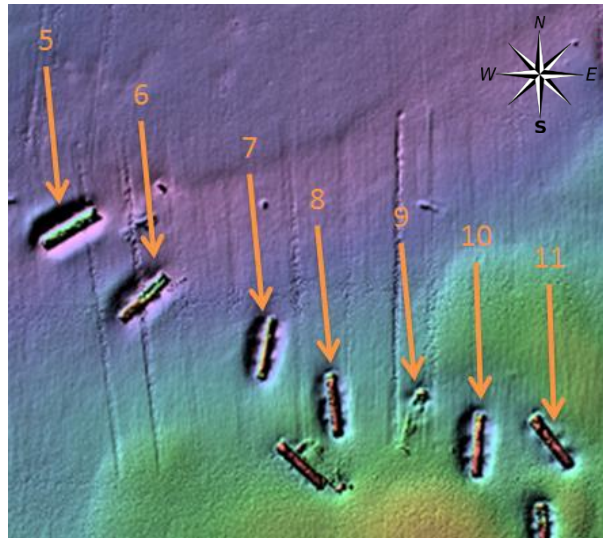


Figure 13- Section 2 contains seven cars and is located directly east of Section 1.

Section 2 contains seven cars and is located due east of section 1. The northern half of section 2 contains deeper water depths than the southern half of the section. The car orientations have a greater range of values than in section 1. Section 3 is located again due east of section 2. This section, represented in Figure 14, contains a greater number of cars than both sections 1 and 2. The cars in this section have a large variation of car orientations. In addition, the water depth in this section is deepest in the northwest corner and becomes shallower moving toward the southeast corner.

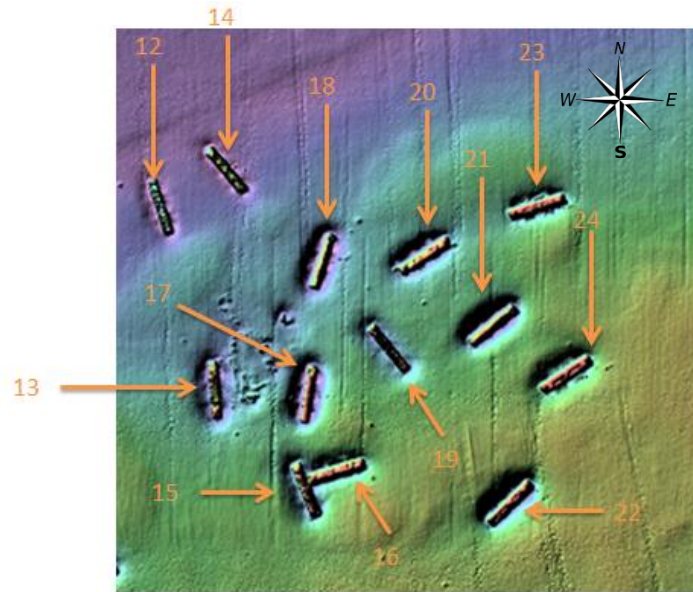


Figure 14- Section 3 contains 13 cars and is located to the east of both sections 1 and 2.

Section 4, represented in Figure 15, contains the greatest number of cars. This section is located in the southeast corner of the field site. The orientation and depth variability in this section is high. Of note, the clustering in this section is also tighter than the other sections within the data set.

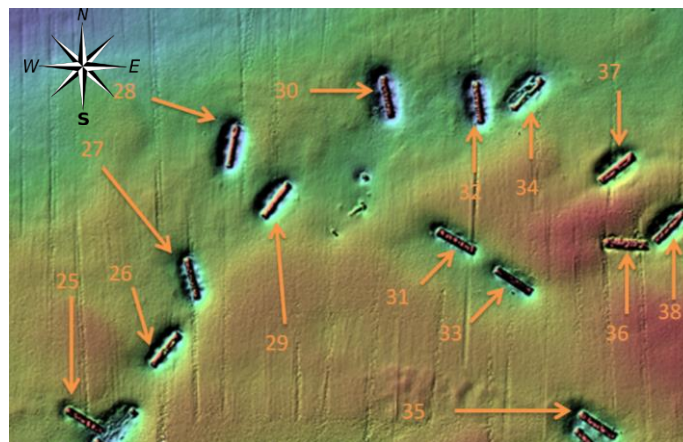


Figure 15- Section 4 contains 14 cars and is located in the southeast corner of the dataset..

3.2 Major Axis Digitization

This investigation will use orientation as a major parameter in the analysis. The method of determining the orientation of the car will be a hand digitization of the major axis created via a profile object in the QPS Fledermaus software package. To ensure that this method is robust, a means to determine the uncertainty of the process itself and how it compares to the required uncertainty is necessary to provide meaningful results. In this analysis, required uncertainty is assumed to be acceptable within ± 1 degree of orientation. The ability to repeatedly produce an accurate orientation will be proven through measuring the orientation of a particular car ten times separately. The results are then compared to the uncertainty requirements of the analysis.

The major axis digitation profile is used in conjunction with the process to determine the height of the car, discussed later, and the far field depth. The physical parameters of the line are described by factors of the R26 Redbird subway cars physical length (15.56 m) and width (2.67 m). For the purposes of the orientation line, the length of the line is two times the overall length of the car. This yields a length of approximately thirty two meters. The line itself starts approximately eight meters ahead of the start of the car and terminates eight meters beyond the tail of the car. The concept can be seen below in Figure 16.

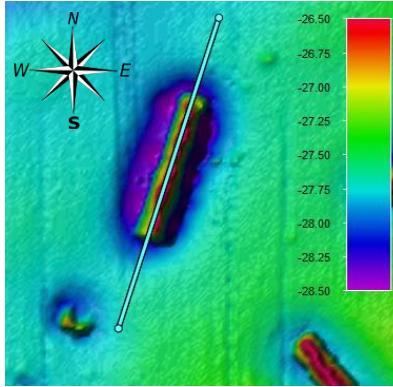


Figure 16- A sample of the major axis identification and orientation analysis preformed. The DTM of a car pictured here is car number 18 in the data set. The line pictured is referred to as the parent profile or major axis. The color shade represents the depth in accordance with the color bar to the right of the car.

This process creates an additional coordinate system. The global coordinate system is World Geodetic System 84 (WGS84)- Universal Transverse Mercator (UTM) Zone 19 North. The WGS 84 ellipsoid uses the Earth Gravitation Model of 1996 (EGM96) geoid which utilizes spherical harmonics to determine nominal sea-level. UTM Zone 19N is one of sixty, six-degree longitudinal zones that define the Universal Transverse Mercator conformal projection that utilizes the common coordinate system used in this analysis.

The local coordinate system that is generated as a result of this analysis process is specific to each car and has coordinates of location along parent profile (Major Axis), distance away from parent profile (negative /left, positive/right), and depth. This allows for the object based analysis that is a major part of this research.

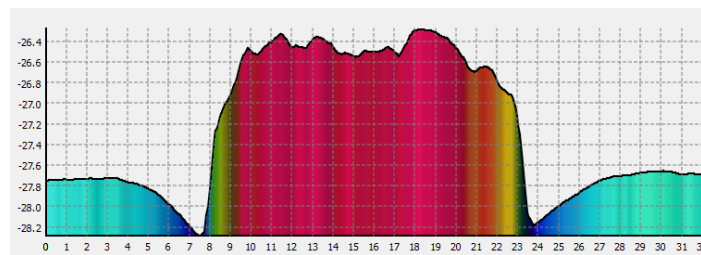


Figure 17- Major Axis Profile showing scour surrounding Car number 18. The Y-axis is depth and the X-axis is length along parent (major axis). Vertical color shading is

consistent with Figure 7 and identifies elevation of subsurface profile. Car extends from roughly 8 m to 24 m. The far field bed elevation is at approximately -27.75 m.

From this digitization, a profile object is created in Fledermaus that enables the creation of a cross-profile object. A cross profile object creates sampling profiles orthogonal to the major axis at any specified interval along the axis as seen in Figure 17. Again, the parameters of the cross profile object are defined by the physical attributes of the subway car. The R26 subway car is physically 2.67 m wide and 15.56 m long. The width of the cross profile lines are six times the width of the car. This can be seen below in Figure 18.

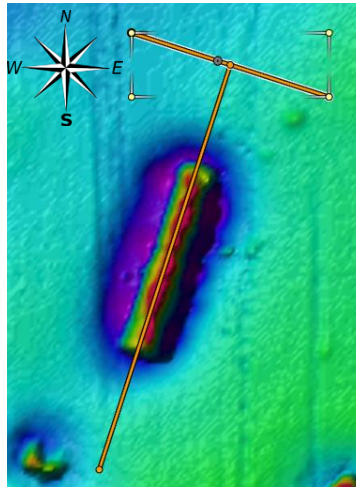


Figure 18- Cross profile of Car #18 showing the extents of the each sub data set collected and used for car specific analysis. Cross profiles were collected every 25 cm on axis and every 25 cm along the parents profile to maintain the 25 cm resolution of the scene.

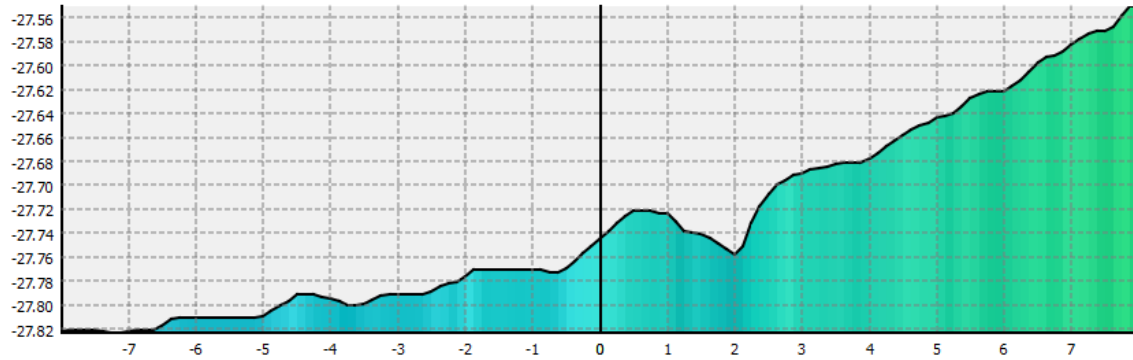


Figure 19- Minor Axis Profile showing the plotted output of the collected data. The bold vertical line at X=0 m represents the centerline of the car and the profile data presented is the data collected orthogonally to the major axis at top (local car reference) of the sub-dataset.

Cross profiles are created so the sample resolution of the ASCII file matches the native resolution of the scene. Cross profiles are cast every 25cm. A sample cross profile is shown in Figure 19. Figure 20 shows the visualization of cross profiles cast every 25cm resulting in a grid.

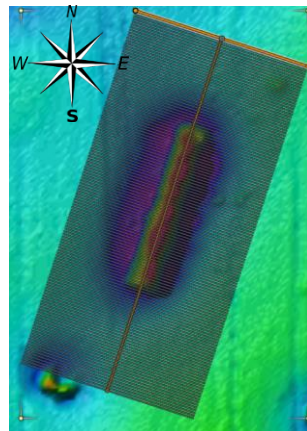


Figure 20-The cross profile interval along the parent and the sampling interval along the cross profile form a 25cm grid of samples over the area shown above which represents the typical sampling area.

This data grid is now oriented relative to the digitization orientation line discussed above. This grid was then exported as an ASCII file in a 25 cm resolution scale to be analyzed further in MATLAB. The ASCII format that is exported contains the columns of

the profile number, distance along the parent profile, the distances from the center, and the associated X,Y, Z values. This is shown in Figure 21.

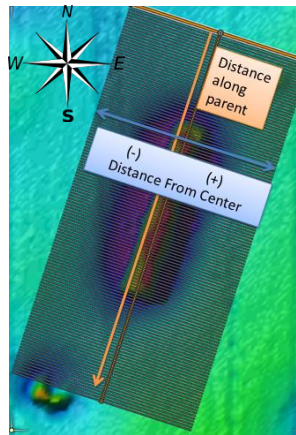


Figure 21- The product of the sampling grid is an ASCII file in which define the sampling point's location in terms of the global and local coordinate system.

Profile Number	Distance Along Parent Profile	Distance From Center	X	Y	Z
0	0	-5.425	523430.4257	4280372.307	-27.7822
0	0	-5.25	523430.2919	4280372.194	-27.7777
0	0	-5	523430.1006	4280372.033	-27.7485
0	0	-4.75	523429.9094	4280371.872	-27.7216

Table 2- The graphical representation in Figure 21 shows the meaning of columns 1 and 2 in the table. Columns 2/3 and 4/5 define the local and global coordinate system respectively.

In summary, the hand digitalization was performed for each car in the data set. This process produced 38 ASCII files for each survey gridded at 25cm resolution in the format above in Table 2.

3.3 Masking Procedure

To eliminate the potential influence of the railway cars shifting over time and any MBES binning or bottom picking errors on the cars themselves, a conservative mask was defined and applied to each data set. FM-Command was again utilized to merge the surfaces together. The merging constraints used were 0.25 m resolution and shoalest depth. This would encompass the top of each car at each survey and ensure the footprint of all the cars, stationary or moving, would be masked from each surface.

The masking surface was created and imported into Fledermaus using the shoalest points of each survey. The slope of the surface was then established and imported as a separate surface. These two products were then multiplied together to further show the transition from bed form to railway car. This surface was then masked based on pixel value. The pixel value was determined from a conservative visual estimate of bed form/railcar transition and then masked over the entire surface.

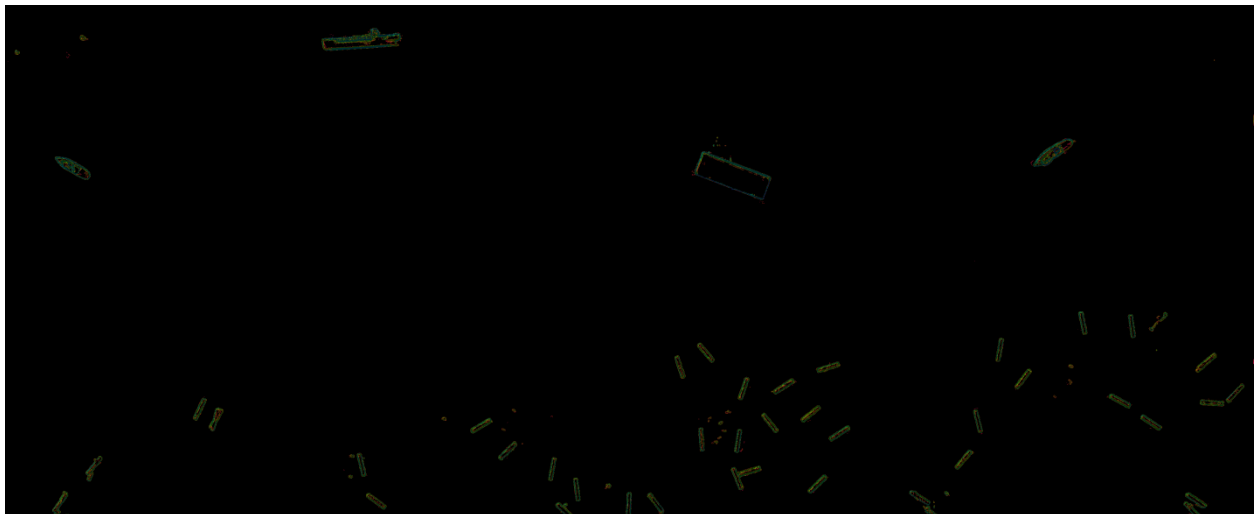


Figure 22- The transition from seabed to object laying on the seabed is shown in green and yellow

3.4 Setup

With each respective dataset on the same vertical plane, the datasets can be compared for scour and deposition between subsequent surveys. The concentration of this analysis will focus on the impact of orientation on the scour and accretion patterns surrounding each specific car or group of cars. Each car will have associated parameters that describe its physical location within the data set.

The quantitative parameters that describe each car are the section number which indicates the general horizontal location within the dataset, the car number that describes the left to right position within the section, the orientation of the car with respect to east, the height of the top of the car, and the bottom depth. From these parameters, the orientation relative to the dominant current and wave forces is determined as well as the height of the car protruding from the seabed.

3.5 Car Orientation

Car orientation is a key component to this analysis. The evaluation of the hand digitization process is vital to show that this method is a sufficient means to determine the orientation of the car. The digitization profile line was drawn 10 separate times and exported into MATLAB for analysis to show the acceptability of this method.

The 10 data sets were analyzed using a MATLAB script which can be found in APPENDIX V- MATLAB Scripts:10X Script. The program determines orientation of the car (Figure 23), far field depth of the seabed around the car (Figure 24), and the height of the car above the seabed. The input parameters used for car orientation were only the values along the centerline itself. The data were queried to determine the slope of the

line between the first data point along the parent and the last data point along the parent (displayed in degrees increasing counterclockwise above the horizontal). This is shown in Figure 25.

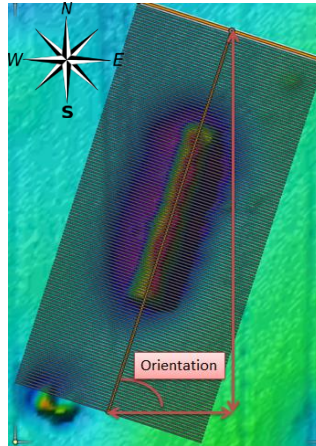


Figure 23-Car Orientation is define as counter clockwise rotation from east. The determination of orientation uses the first and last data points along the parent profile.

3.6 Car Depth and Height above the Seabed Determination

While determining a reliable means to determine car orientation was the primary goal of the repeated analysis, the impact of the method's variability should be looked at as well. The other key metrics of the car that are needed for this analysis are the height of the car above the seabed and the depth of the surrounding far field seabed, meaning the seabed depth outside of the scour influence zone. To determine the bottom depth, the depth was averaged over a strip of seabed on the outer limits of the cross profile object both on the left and right sides of the car. This concept can be seen below in Figure 24.

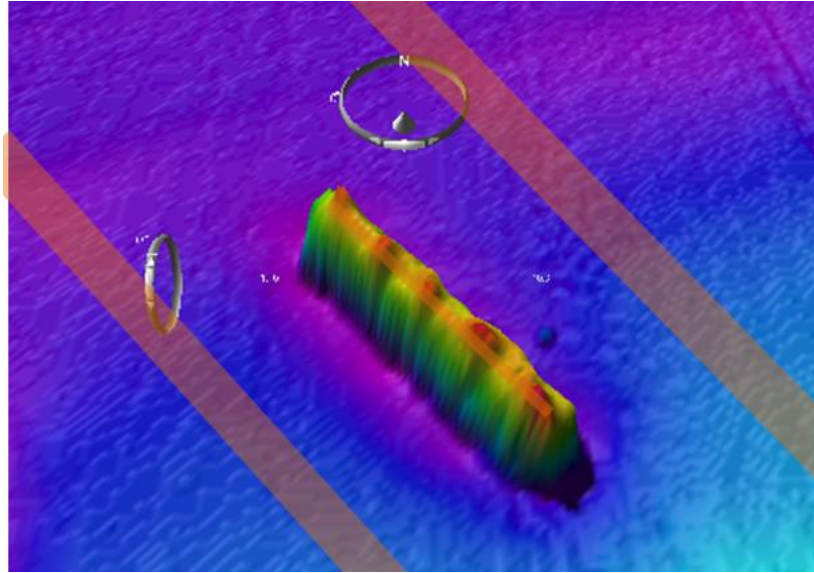


Figure 24-Each car was sampled such that the far field bottom depth was determined using the sections of seafloor shown above to the left and right of the car. Likewise, the top of the car was determined using the sampling region shown on top of the car.

3.7 Orientation Evaluation

After running the MATLAB script on the 10X repeated hand digitization of the car's orientation, the output values for orientation, bottom depth and car height were compared to determine if the hand digitization was a valid approach for determining the car orientation and the uncertainty impact on the associated depth measurements. The results can be seen below in Table 3-10X Hand Digitization Table.

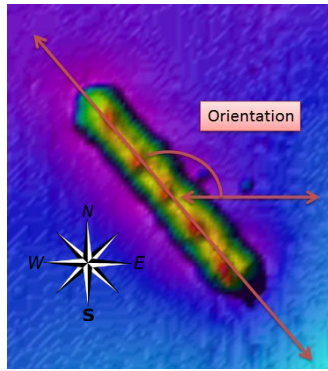


Figure 25- Car #14 was used to evaluate the accuracy of hand digitization of orientation. Table 3-10X Hand Digitization Table shows the orientation and the associated standard deviation of the method.

Trail #	Orientation (Degrees from East)	Bottom CC Depth (meters)	Top of Car (Meters)	Height of Car (Meters)
1	130.9	-28.01	-26.64	-1.36
2	130.5	-28.02	-26.65	-1.37
3	130.4	-28.02	-26.65	-1.37
4	131.0	-28.01	-26.65	-1.37
5	130.7	-28.02	-26.66	-1.36
6	130.9	-28.01	-26.65	-1.36
7	130.2	-28.02	-26.67	-1.35
8	130.7	-28.02	-26.65	-1.37
9	131.0	-28.01	-26.65	-1.37
10	130.4	-28.02	-26.65	-1.37
Mean	130.7	-28.01	-26.65	-1.36
Standard Deviation	0.3	0.004	0.006	0.005

Table 3-10X Hand Digitization Table. Accurate visible interpretation of orientation is assumed. Precision of this method is shown through the standard deviation of each required parameter.

As shown above, the variability in the hand digitalization of the car's orientation and subsequent impact on depth measurements is very small. Repeatability of 0.27 degrees is more than acceptable as it provides acceptable resolution to distinguish more general trends based on orientation.

IV. ANALYSIS AND RESULTS

4.1 Vertical Settlement of Cars General Scour, Moat and Pit Formation, Evolution, and Sediment Transport

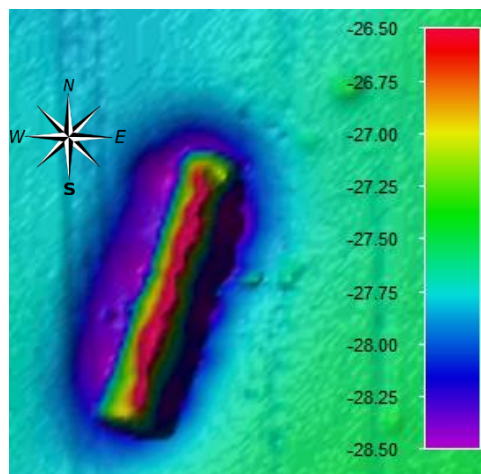


Figure 26- Visible moats can be seen on the initial survey record. Visual analysis would indicate a far field bottom depth at approximately -27.7 on the west side of Car 18 and -27.3 on the east side with moats as deep as 0.75m around the car.

As mentioned in Raineault et al. (2013), the cars are considered to be vertically stationary over the sampling window in relation to substrate below. What is evident and changing, however, is the formation or destruction of scour moats around the individual

cars themselves. These moats are clearly present and developed in the first survey (OCT 2012) and change throughout the time period in which this data was collected.

The car settlement relative to local water depth or initial orientation of car is determined in Figure 27 and shows an evaluation of the height of many cars relative to local far field seafloor depth relative to the water depth and orientation. As shown in Figure 27, there is no evidence of a correlation between the amount of settlement in relation to orientation. Given that the water depth is relatively uniform, it is not surprising that there is no trend for Car Depth relative to Car Height. This is to say that this analysis shows no dependence between settlement and orientation or depth.

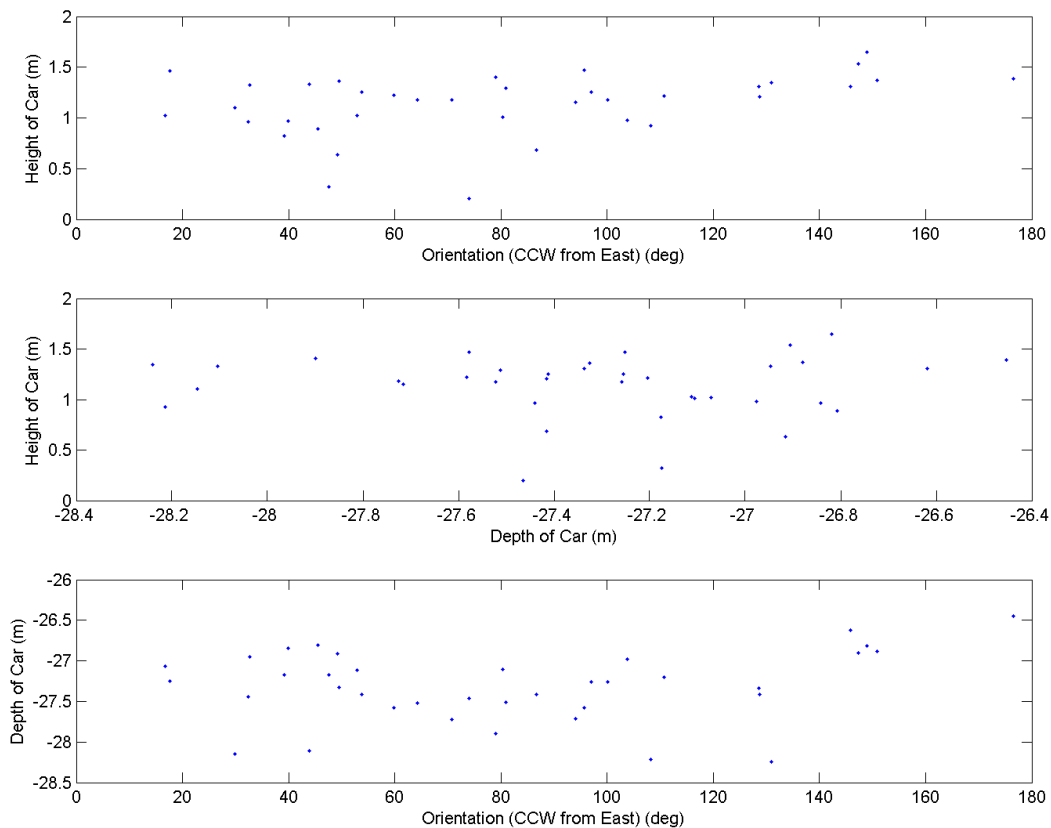


Figure 27- (a) Car Orientation vs. Height of Car (b) Depth of Car vs Height of Car (c) Orientation (deg) vs Depth of Car (m)

4.2 MBES Analysis

Scour pits that are present in the data tend to form in two different regimes. The cars that were placed with the windows facing the seafloor and the sea surface tend to have relatively uniform scour pits as the flow field obstruction created represents a basic rectangular box. The cars that were placed with the windows facing the flow or as it would sit on subway rails showed signs of scour pits in which deposition and scour differed because of the altered flow field. The along car frequency variation or the scour plots was qualitatively most correlated with the orientation of the car relative to dominant wave direction. This is, the windows influenced the flow fields most noticeably when the car was orthogonally aligned with the incoming dominant wave direction during the survey period.

Additionally, scour moat characteristics were noted in Raineault et al. (2013). The conclusion from Raineault et al. (2013) determines that car orientation affected the scour moat size. It was found that the east-west oriented cars have the shallowest moats and are generally asymmetrical. The northeast/southwest oriented cars have greater scour along the northwest face. The cars that were oriented northwest to southeast were noted to have the deepest mean moat depth of -0.67m. Raineault et al. (2013) concludes that the car orientations oblique to the current demonstrate the steepest moat sides.

4.3 Hydrodynamic Conditions

The five recurrent surveys provide an opportunity for examining the response of the seafloor to varying wave conditions. Three cases were defined for analysis. The first case includes Hurricane Sandy and a large Nor'easter that followed close behind. The second case represents benign hydrodynamic conditions typical of the season. The third condition represents more typical winter storm behavior with significant wave induced velocities at the bed.

The velocities at the bed are primarily current driven forces running 160/340 degrees (Munchow et al. 1992). In CASE I and similarly in CASE III, the current driven hydrodynamic forces at the bottom are impacted by large wave events approaching from offshore. The impact of these events can be seen from the *in-situ* wave and current data recorded by the ADCP at the Redbird Reef site. The two storms shown in the data are Hurricane Sandy and a large nor'easter the follow closely after.

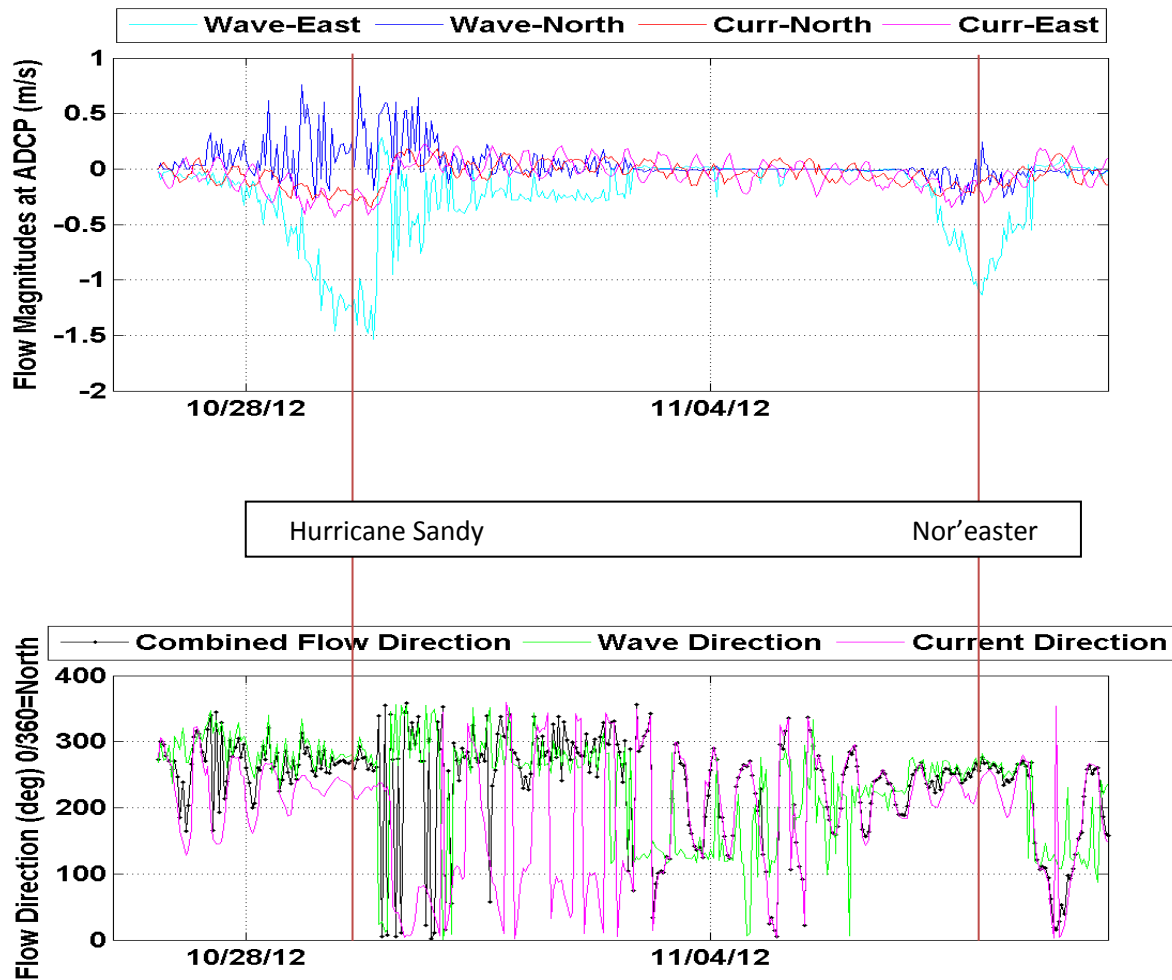


Figure 28 – Wave and current data between October 26th and November 10th was collected from the deployed ADCP at Red Bird Reef.

From October 26, 2012 to November 10, 2012 the survey area experienced two very significant storms that produced unique hydrodynamic conditions creating a very dynamic bed state leading to a large amount of marine scour and transport. The large contributions by the storms are evident in the difference surfaces produced by subtracting the depth measurements represented by each pixel value of the November 11, 2012 survey (Figure 8) from the initial October 26, 2012 survey (Figure 7).

The wave data above recorded by the *in-situ* ADCP indicates two significant wave events. The wave heights created during Hurricane Sandy had higher than average wave heights. The prominent forcing mechanism from Hurricane Sandy was above average wave heights approaching from offshore. The next significant weather event in the survey time period is the Nor'easter that followed Sandy. Case 3 represents a typical winter storm conditions. The combined current and wave induced forces on the bed are similar to Case 1.

Case 2 represents the benign winter conditions. During this period there are no significant wave events which eliminate a majority of wave induced forces on the bottom. The currents running 160/340 degrees are the greatest contribution to the hydrodynamic influence (Munchow et al., 1992) as there are no large wave events during this period.

4.4 Localized Bathymetric Change Analysis

The localized bathymetric change is evaluated by calculating difference surfaces between subsequent surveys surrounding significant weather events. Weather events were identified as large hydrodynamic events leading to detectable change in localized scour in some fraction of the field site. Case 1 considers the bathymetric change between the pre-survey on October 26th 2012 and post survey on November 11th 2012 that surrounded Hurricane Sandy on October 29th, 2012 and a Nor-easter that occurred on November 7th, 2012. Case 2 represents benign winter conditions for comparison. Case 3 considers the winter storm events from December 26th, 2012 to

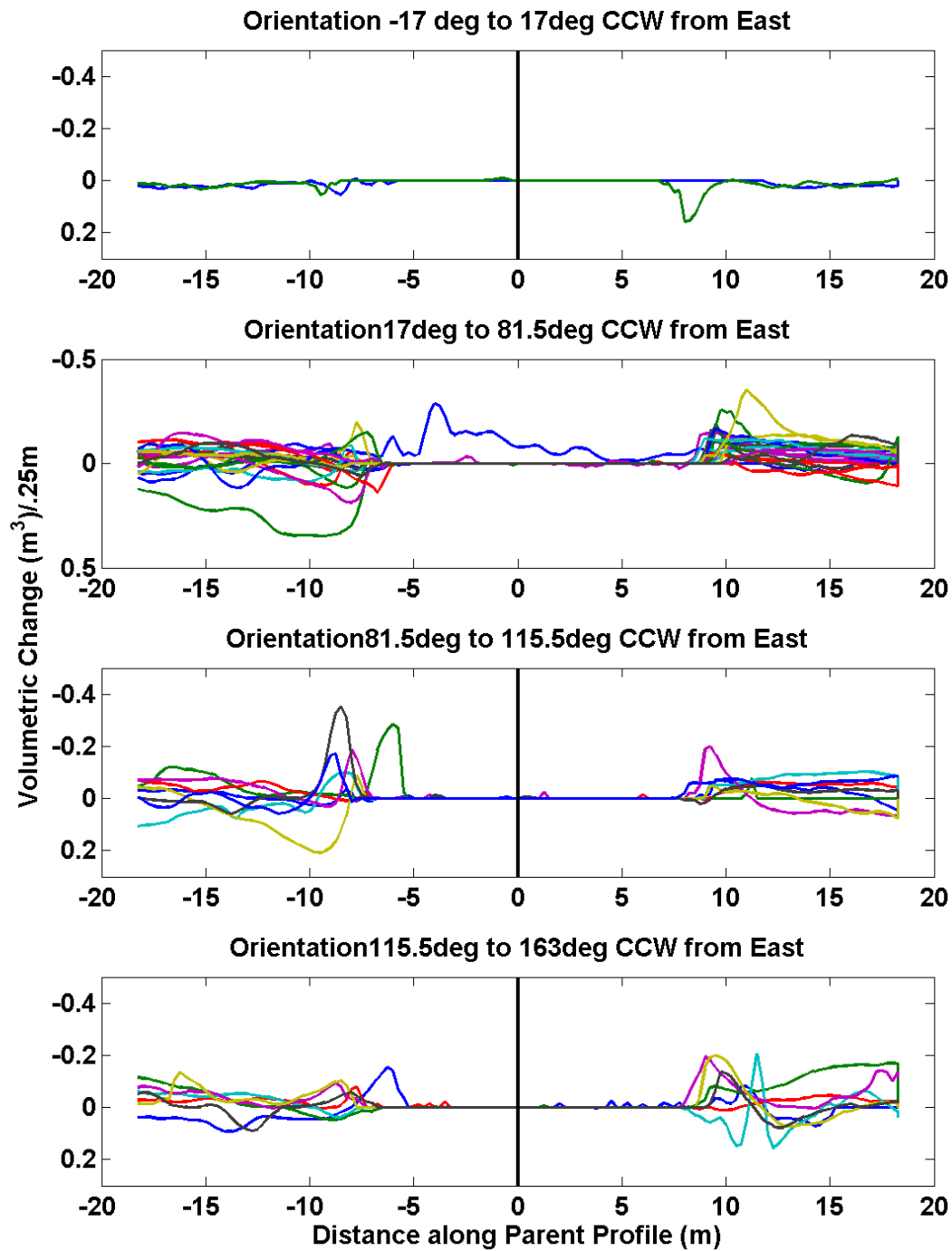
March 28th, 2013. Both Case 1 and Case 3 produced changes in the bathymetry that are larger than the uncertainties associated with the individual surveys.

The bathymetric change is represented by a surface difference product that displays the change in pixel values from one survey to another. The difference surface calculation subtracts the older survey's pixel value from the latest survey pixel value. A positive pixel difference value indicates that accretion and a negative value indicates scour.

4.4.1 Case 1: " Bathymetric Change from October 26, 2012 to November 11th, 2012"

The Case 1 difference surface statistics show a total volumetric loss over the entire survey surface of -3,135.44 cubic meters as shown in APPENDIX II- Orientation Plots

CASE III Major Axis by Orientation



APPENDIX III- Difference Surface Statistics. From Raineault et al. (2013), the typical wave conditions do not produce adequate orbital velocities at the bed to exceed the

threshold for motion U_{cr} . However, with the hydrodynamic conditions experienced during Hurricane Sandy and the large storm that followed shortly thereafter the effects can be clearly seen in Figure 29. As noted in Raineault et al. (2013), the presence of scour marks that align with the Northeast winds indicate that the larger scour and sediment transport cases are caused by waves associated with episodic storm events.

Specific to this difference surface, a visual analysis would indicate that scour pits evolve during this period and the sediment is transported due south until the velocities are conducive to deposition which is seen below as yellow to dark red. The storms' effect on the bottom is evident through the steep changes located throughout the survey area and increased sediment movement around the cars.

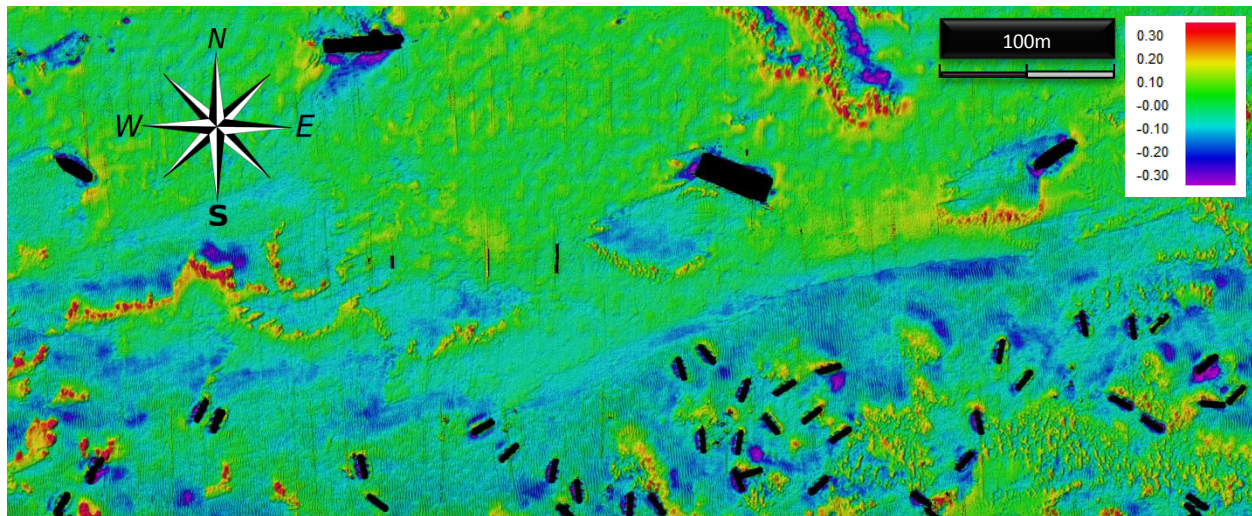


Figure 29 – Case 1: October to November Difference Surface. The standard color is shown in the top right of the figure. Significant scour is shown in purple while a significant accretion is shown in yellow and red.

4.4.2 Case 2: "Bathymetric Change from November to December"

An example of a bathymetric change that is on the same order of magnitude as the noise and error is shown in Figure 30. Of note is the offset introduced during a

period that required tidal referenced MBES data located just below the vertical midpoint of the survey that runs the complete length of the survey area west to east. This reference was required due to loss of GPS during this period.

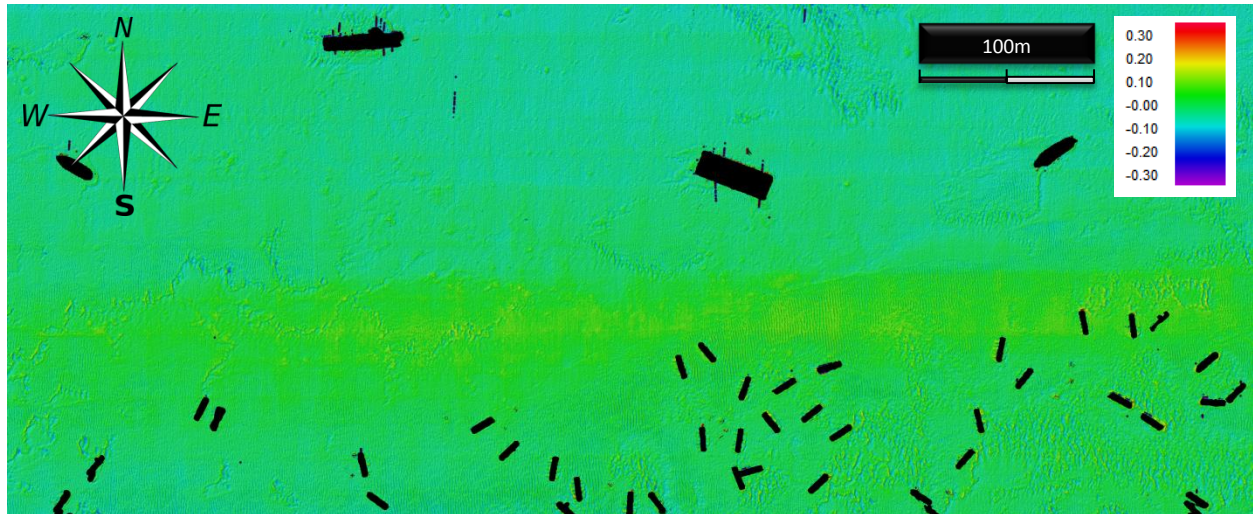


Figure 30- November to December Bathymetric change showing a period of benign wave conditions that produced little detectable change and shows the impact of a vertical offset introduced by tidally referencing depth measurements during periods of lost GPS signal.

4.4.3 Case 3: "Bathymetric Change from December, 6th to 2012, March 28th, 2013"

Figure 31, shown below, continues to show the major scour marks that remain from the major episodic storm referenced in Raineault et al. (2013). The sediment's behavior during this period is similar to the previous difference surface in the areas of minor change. However, in the areas of major scour or deposition in the October-November surface, the magnitudes of change remain large but where there was accretion in October-November there is significant scour in December-March. This difference surface represented a net volumetric loss of -15,213 cubic meters of material from the dataset area. This is consistent with winter erosional behavior typical of the

northeast region. Also of note for this case are the significant scour pits developing throughout the survey area identified by purple.

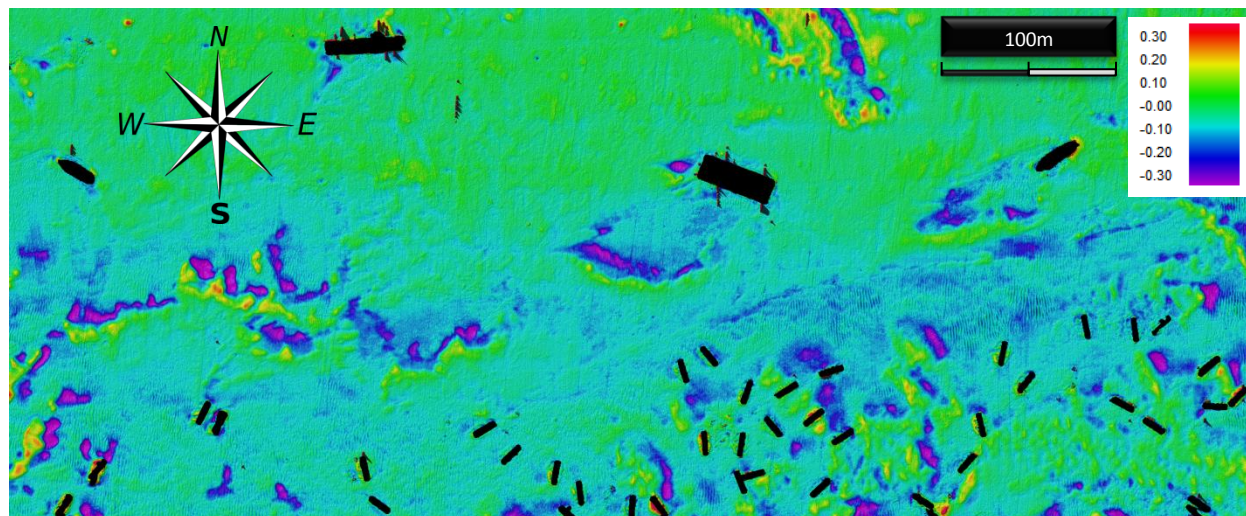


Figure 31 – Case 3: The December to March Difference Surface visually shows significant borrow pit behavior and a more general smoothing of the sediment features seen in Figure 29.

4.4.4 Subcase Alpha: Case 2- Case 1 Difference in Bathymetric Change

Figure 32 shows the areas of the artificial reef that experienced relatively large and opposed scour/accretion patterns. Red in the figure represents areas Case 1 and Case 2 had common areas of bathymetric change that was large in magnitude but opposite in direction. The figure below shows the particular areas in the reef where the transport was large and opposed from Case 1 to Case 2.

$$ABS(Pixel Value) = CASE 3 - CASE 1$$

CASE 3 Scour (-) – CASE 1 Accretion (+)	(-) - (+) = Large Negative
CASE 3 Scour (-) – CASE 1 Scour (-)	(-) - (-) = Small Negative or Offsetting
CASE 3 Accretion (+) – CASE 1 Accretion(+)	(+) - (+) = Small Positive or Offsetting

CASE 3 Accretion(+) - CASE 1 Scour (-)	(+) – (-) = Large Positive
--	----------------------------

Table 4- Summary of how different scenarios impact the outcome of a Bathymetric Change Difference Surface

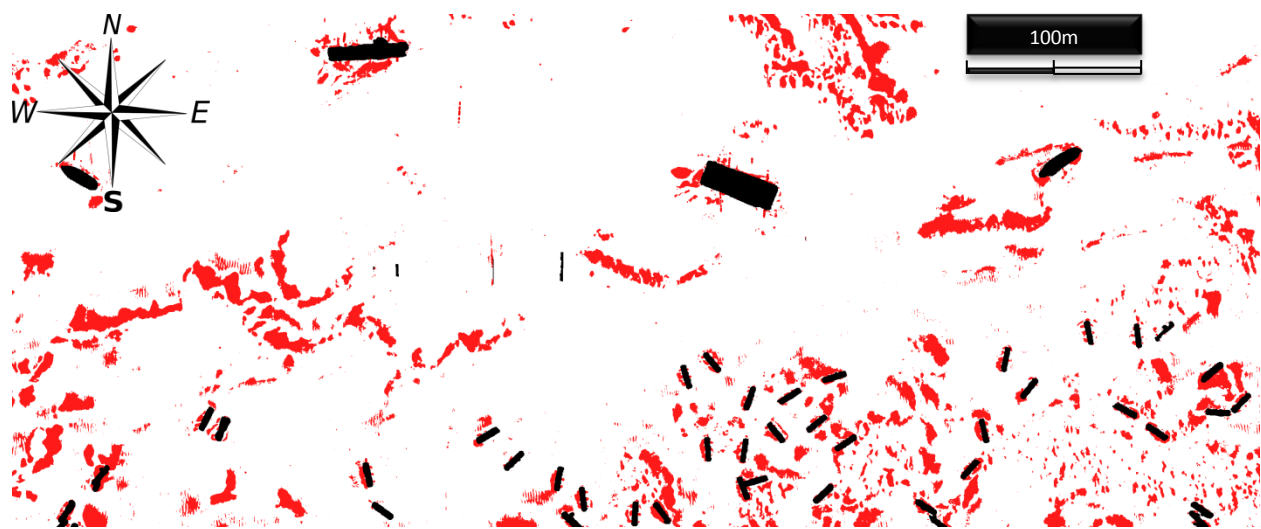


Figure 32- Subcase Alpha shows the areas where the magnitude of the change surface was large in both Case 1 and 3 but the directions were opposed. The red areas on the figure represent areas where Sandy significantly changed the seafloor depth and the weather events in Case 3 had a large affect in the same location but changed the seafloor depth in the opposite direction. The black in the figure represents the mask applied to the artificial reef objects.

Figure 33 shows where Subcase Alpha exists compared to the Case 1 bathymetric change. Subcase Alpha exists in some cases at the intuitive location when overlaid on Case 1, Figure 33, but then not necessarily in the intuitive location when overlaid on the Case 2 bathymetric change surface, Figure 34.

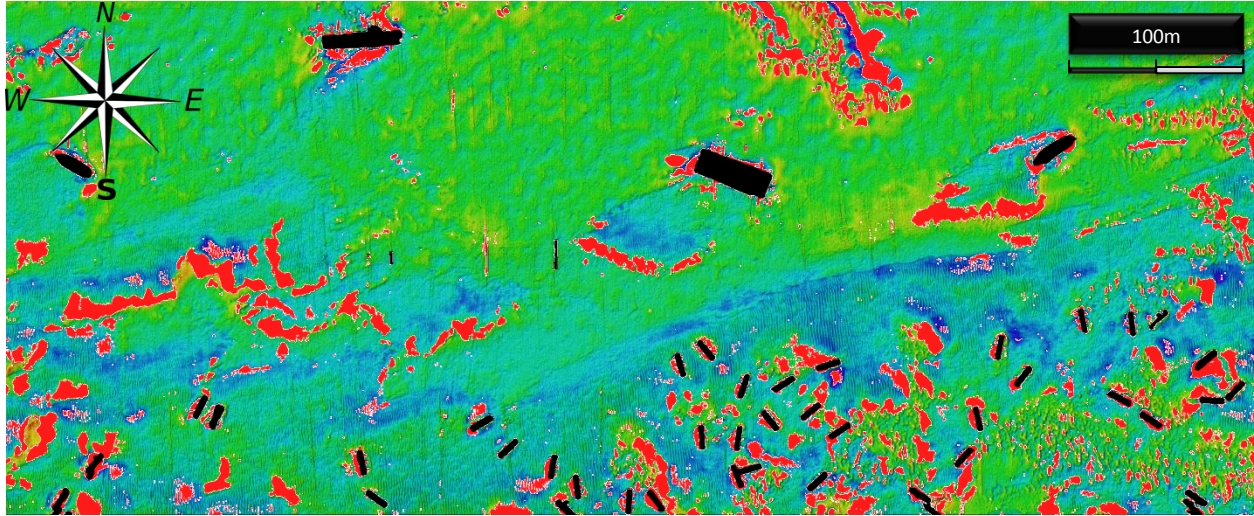


Figure 33- Subcase Alpha Overlaid on Case 1 shows the relationship between the Case 1 difference surface and the Subcase Alpha surface. The color scale is the same as the Case 1 and 2 surfaces but the red in the figure is Subcase Alpha.

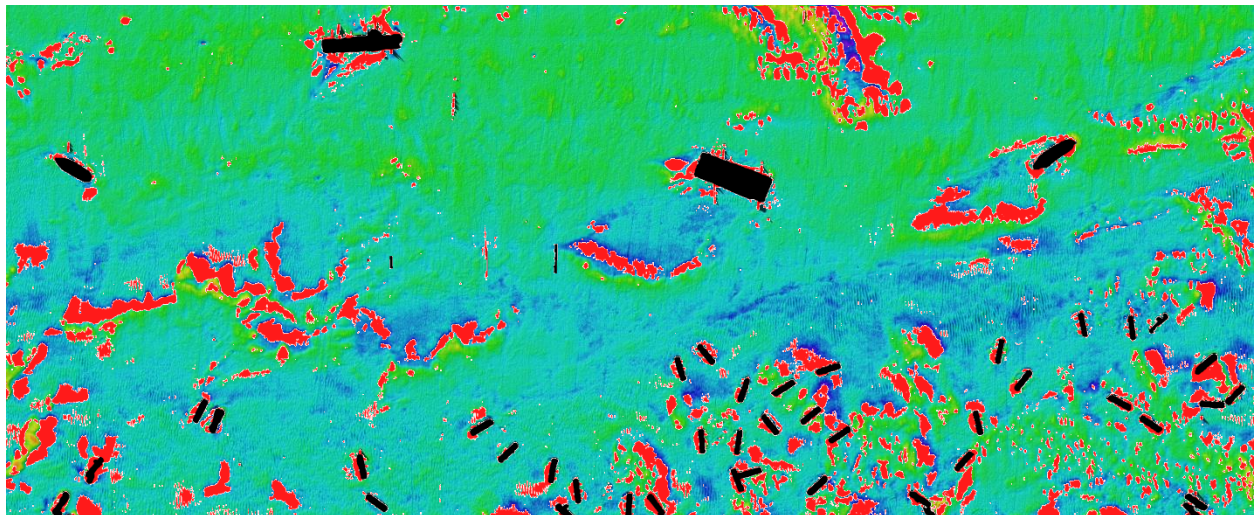


Figure 34- Subcase Alpha Overlaid on Case 3 is a similar product to Figure 33 but is now shown over Case 3.

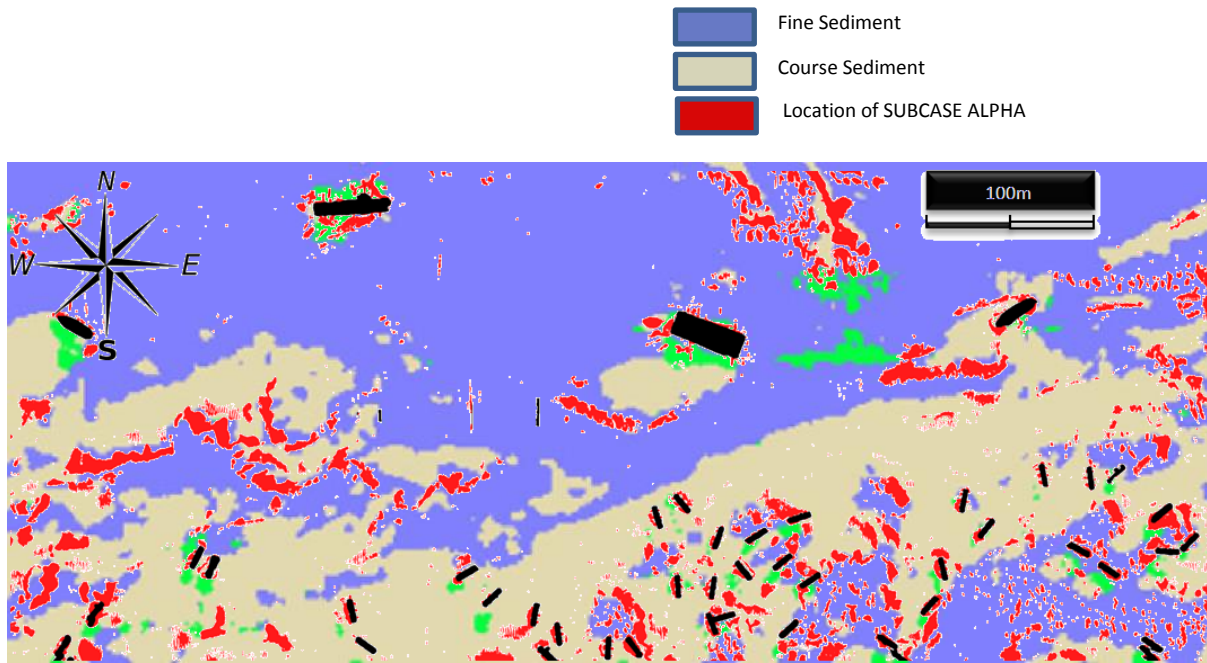


Figure 35-Subcase Alpha Overlaid on auto segmentation map from Raineault et al (2013). The red areas represent the large opposed changes between bathymetric change surfaces.

However, when Subcase Alpha is overlaid on the auto segmented figure from Raineault et al. (2013), Figure 35, the areas where Subcase Alpha is high in magnitude appear to align with transition areas from coarse to fine sediment. The auto segmentation uses a statistically based approach to segment the backscatter data into separate areas based on the acoustic properties of the medium. This auto segmentation product was produced from QTC SWATHVIEW.

4.5 Object Based Localized Scour Analysis

Another method of looking at this data set is in an object based approach that will examine the change in the seafloor as a spatial function of object lengths and widths and will present the data oriented by the objects direction. This will allow the data to be grouped based on the objects attributes within the dataset such as height, depth, and orientation. The characterizing attributes are shown in Table 5.

Car Number	Orientation	Car Height	Depth of Car
1	53.78	1.25	-27.41
2	49.44	1.36	-27.32
3	64.21	1.18	-27.52
4	59.82	1.22	-27.58
5	29.84	1.10	-28.15
6	43.95	1.33	-28.10
7	78.95	1.41	-27.90
8	95.64	1.47	-27.58
9	73.98	0.20	-27.46
10	86.66	0.69	-27.42
11	128.53	1.31	-27.34
12	108.20	0.92	-28.21
13	94.00	1.15	-27.72
14	130.93	1.35	-28.24
15	110.76	1.21	-27.20
16	16.79	1.02	-27.07
17	80.86	1.29	-27.51
18	70.75	1.18	-27.73
19	128.75	1.20	-27.42
20	32.41	0.96	-27.44
21	39.12	0.82	-27.18
22	49.19	0.63	-26.92
23	17.58	1.47	-27.25
24	32.71	1.33	-26.95
25	148.88	1.65	-26.82
26	49.19	0.63	-26.92
27	103.77	0.98	-26.98
28	80.41	1.01	-27.11
29	52.96	1.03	-27.11
30	100.13	1.18	-27.26
31	150.91	1.37	-26.88
32	96.97	1.25	-27.26
33	147.37	1.54	-26.91
34	47.58	0.32	-27.17
35	145.88	1.31	-26.62
36	176.47	1.39	-26.45
37	39.87	0.97	-26.84
38	45.50	0.89	-26.81

Table 5- Characterizing Attributers of all Cars

4.5.1 MBES Artificial Reef Survey Area Object Field Characteristics

The purpose of hand digitizing the major axis of the subway cars over the October survey and the subsequent Case 1 and Case 2 bathymetric change surfaces

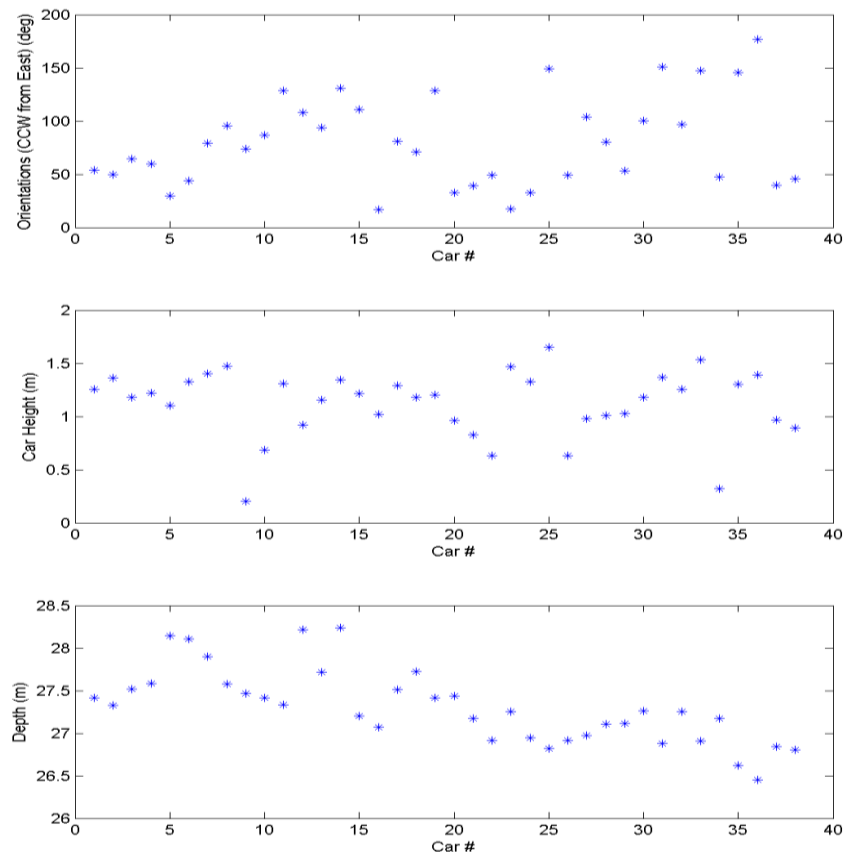


Figure 36- The summary plot of the defining car parameters showing each car's associated orientation (degrees CCW from East) (top), Height above the seabed (m) (middle), and far field depth (m) (bottom).

was to gather data on parameters that are specific to the cars and use those parameters to group the cars together and analyze the behavior around each group of cars. Figure 37 shows the distribution of the 38 cars organized by orientation, height, and depth.

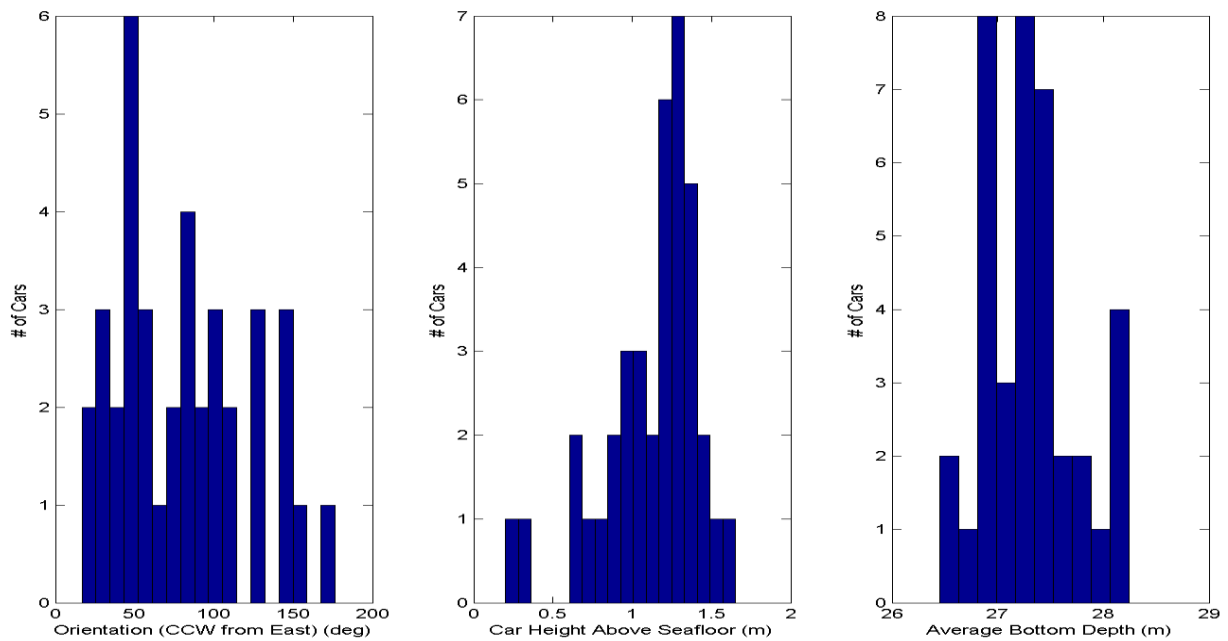


Figure 37- The distributions of Orientation, Height of Car, and Far Field Depth show how the cars are organized by their associated parameters.

Figure 38, shows the object based approach that defines depth and bathymetric change relative to a local coordinate system. Each blue rectangle represents the area over which the changes in bathymetry were averaged to determine the average change per unit width (.25 m) from a section that was L (length of the car = 15.56 m) tall or W (width of the car = 2.67 m) wide. The average of the blue rectangles are shown as volumetric change per unit width in the plots that follow.

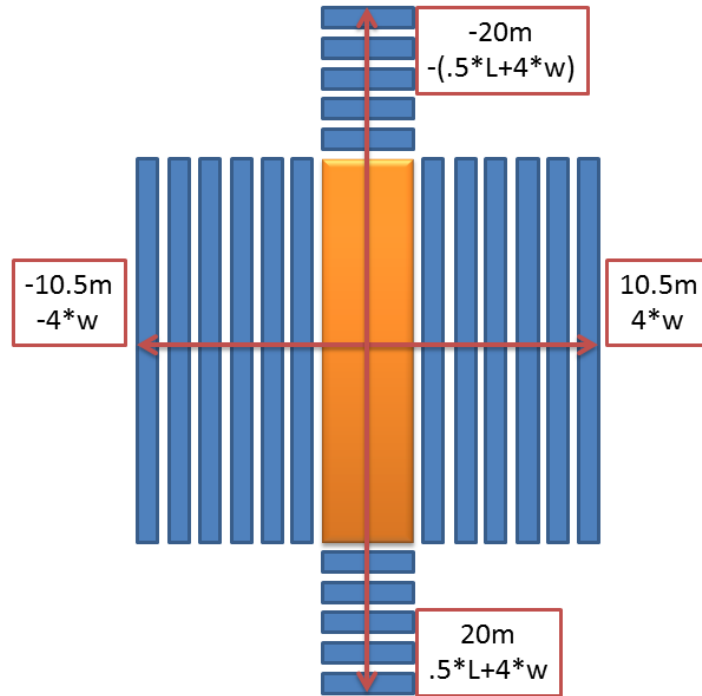


Figure 38- Diagram showing conceptual layout and extents of analysis.

4.5.2 Case 1a: Object Based Scour Analysis of November – October Bathymetric Change Surface

The volumetric change per 25 cm strip with length equal to 4 car widths plus the length of the car is shown as a function of car widths away from the car's major axis. Figure 39 shows, for all cars, the volumetric change per 25 cm strip of seafloor for any particular position along the car's major axis (left). The plot represents the spatial behavior of the sediment accretion/erosion patterns as a function of distance from the ends of the cars oriented along the cars' major axis.

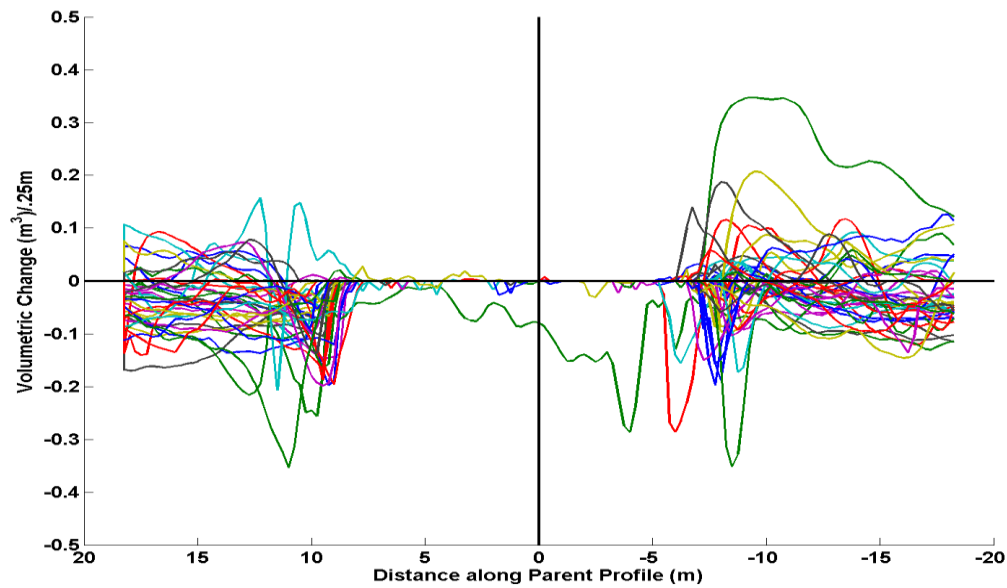


Figure 39 – The object based major axis scour analysis is shows all the cars in the dataset for Case I Bathymetric change surface. The shows the volumetric gain/loss in $m^3/.25m$ strip along minor axis car width. The plot of the right shows the sum of those gains/losses from the midpoint of the major axis to either end of the car.

Similarly, Figure 40 shows, for all cars, the volumetric loss per 25 cm width for the length of the car along the minor axis. The plots show variability in sediment behavior around each car.

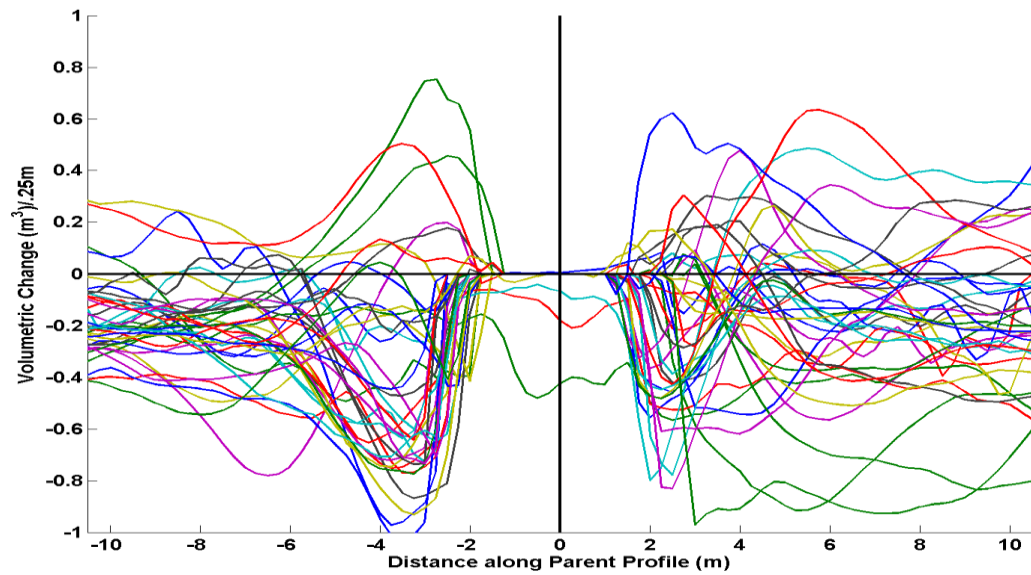


Figure 40- Subprofile Scour Analysis of Case 1 shows the scour/deposition behavior as a function of 25 cm width along the minor axis.

A majority of both the major and minor scour plots show scour and erosion locally around the cars. The magnitude of the scour varies as one might expect. However, there is a distinct change in erosional/accretion pattern that occurs at $x=-4$ m ($\sim 1.5 \cdot w$) and at $x=2.5$ ($\sim 1 \cdot w$) in Figure 40.

4.5.3 Case 3- Object Based Analysis of March–December Bathymetric Difference Surfaces

Case 3 results are more closely related and have a smaller range of over scour/accretion values than Case 1. Figure 41 and Figure 42, major and minor scour/accretion plots respectively, show a majority of cars experienced accretion during the Case 3 duration. Also, the sediment behavior was more similar between cars within the dataset.

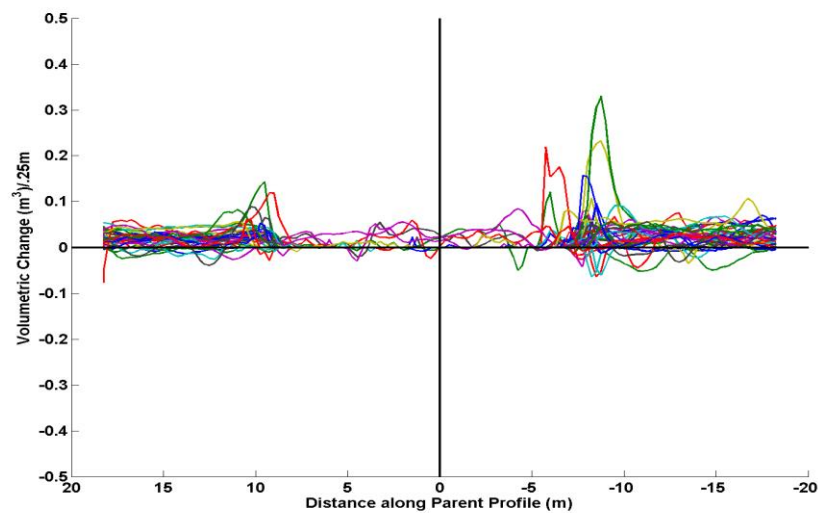


Figure 41- Case 3 showing all cars shows the volumetric change(m^3) per .25 m width from the top and bottom of the cars running along the major axis. The plot shows the change given and position along the car's major axis.

Case 3 plots show a much less variability and change not only between different cars but also within the same data series of one car. The inflection points in the plots are much less distinct and noticable in Case 3 when compared with Case 1. The major axis volumetric loss (Figure 41 left plot) shows a faint transition point at -10.5 m ($4 \cdot w$) or $1 \cdot w$ length from the end of the car.

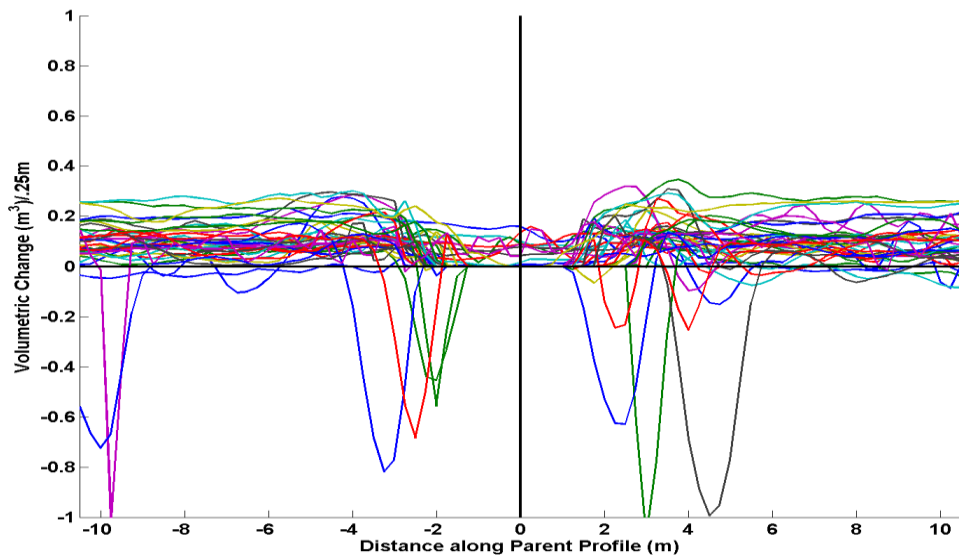


Figure 42-Subprofile Scour Analysis of Case 3 shows the scour/ Accretion behavior as a function of 25cm width along the major axis (left) and the cumulative effects (right)

4.6 Orientation Based Object Analysis

4.6.1 Case 1 Orientation Based Analysis

There are two scour/accretion signatures that are easily distinguishable in Case 1. Figure 43 shows symmetrical behavior and captures all the cars oriented from 81.5 to 115.5 deg CCW from east or -25.58 to 8.5° CW from north.

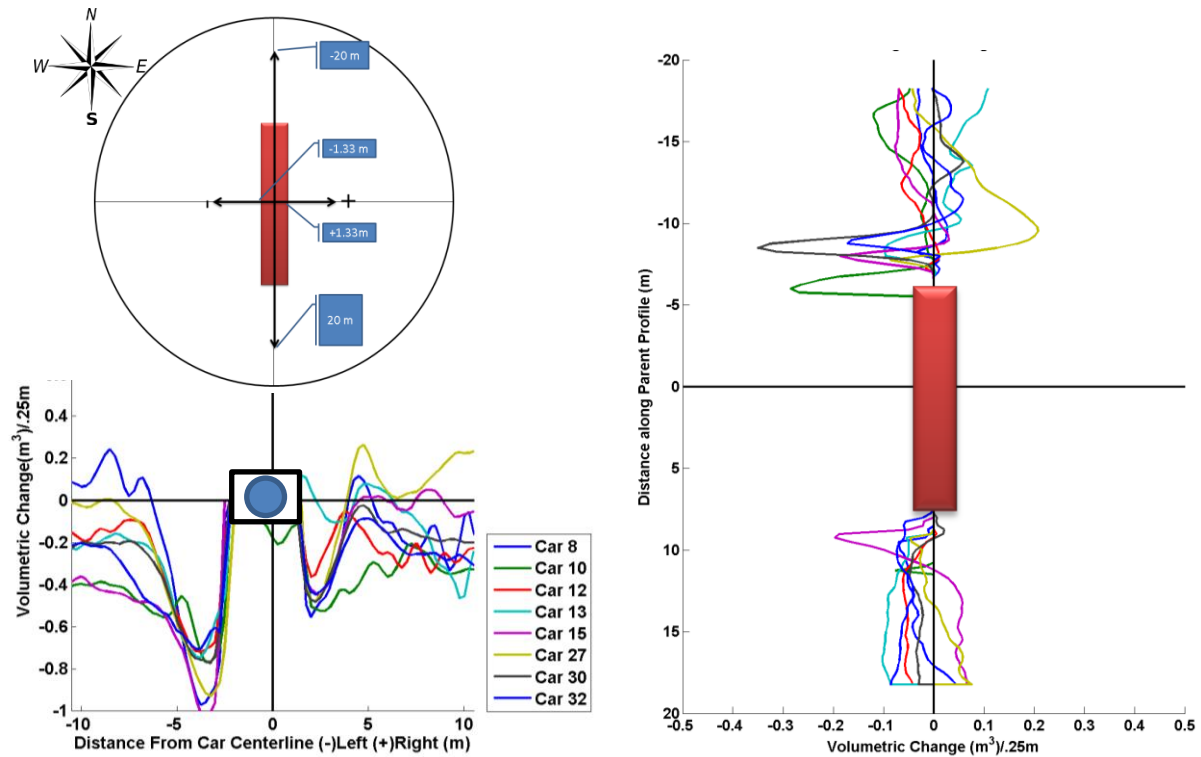


Figure 43- Case 1 scour accretion plots for cars facing -25.5 to 8.5 degrees clockwise from north.

For cars oriented -17 to 17 deg CCW from East or 73 to 106 deg CW from north have an asymmetrical scour/accretion signature (Figure 44). The northward facing side of the cars major axis shows accretion while the southern facing side of the car shows scour over the entire side. Of note, cars 16 and 36 both abut other cars in the field site. This primarily affects the major axis scour profiles.

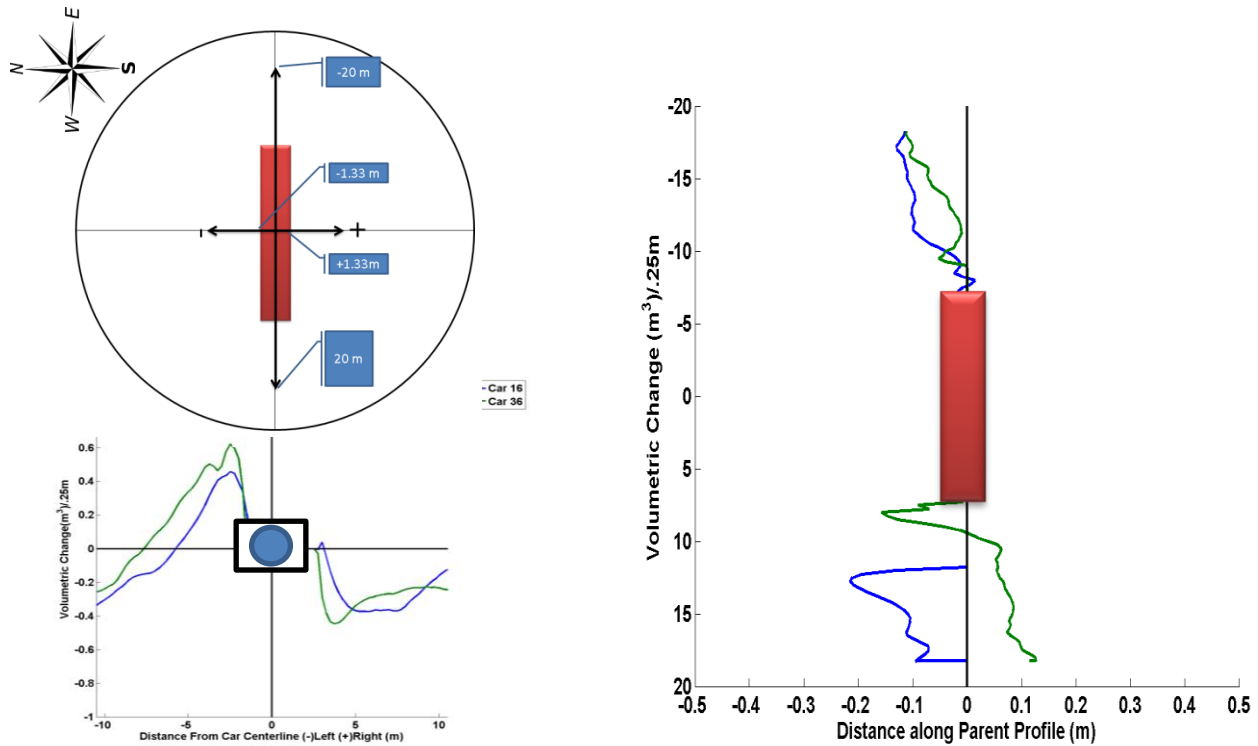


Figure 44: Case 1 scour accretion plots for cars facing 73 to 107 degrees clockwise from north

4.6.2 Case 3 Orientation Based Analysis

Similarly to Case 1. The Case 3 orientation analysis shows two distinct cases with similar orientation ranges by which the cars were discriminated. The discriminated ranges for Case 2 were -17 to 17 deg CCW from East or 73 to 106 deg CW from north and 81.5 to 115.5 deg CCW from east or -25 to 8.5 deg CW from north.

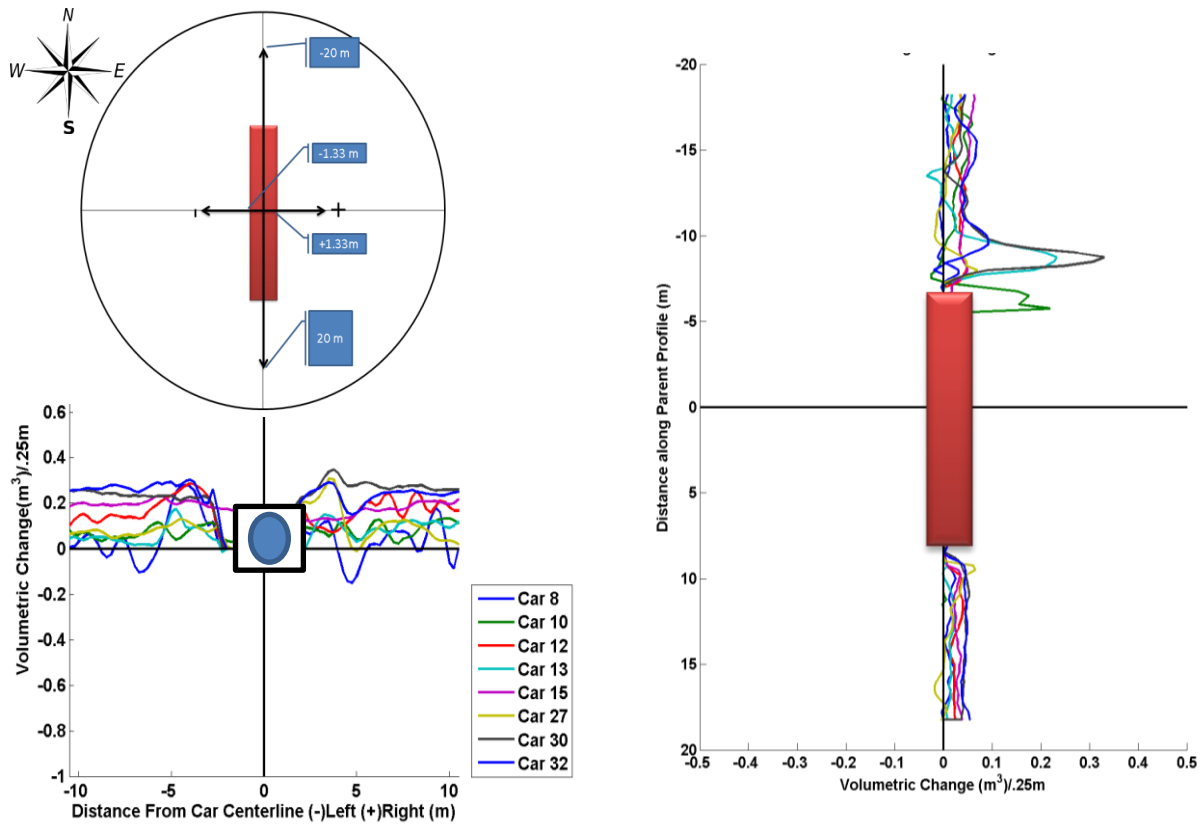


Figure 46-Case 1 scour accretion plots for cars facing -25.5 to 8.5 degrees clockwise from north

While Case 3 had more variability in the results, the two cases were distinctly different. The cars that were oriented east/west showed asymmetrical scour/accretion. Scour was demonstrated on the northward facing side and accretion was seen on the southward side. This is perhaps better seen in Figure 47, where there is clearly asymmetrical behavior for the east/west oriented cars and rather symmetrical accretion for the cars oriented north/south.

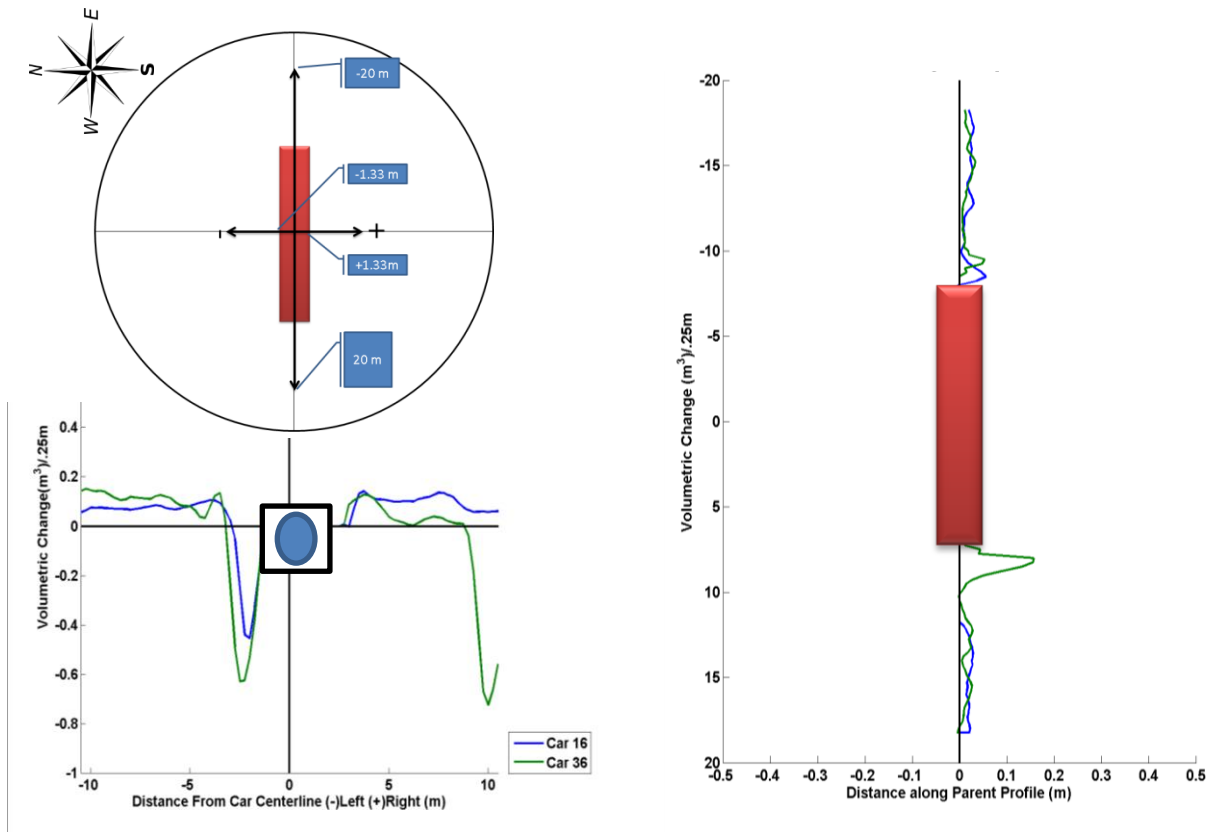


Figure 47-Case 3 scour accretion plots for cars facing 73 to 107 degrees clockwise from north.

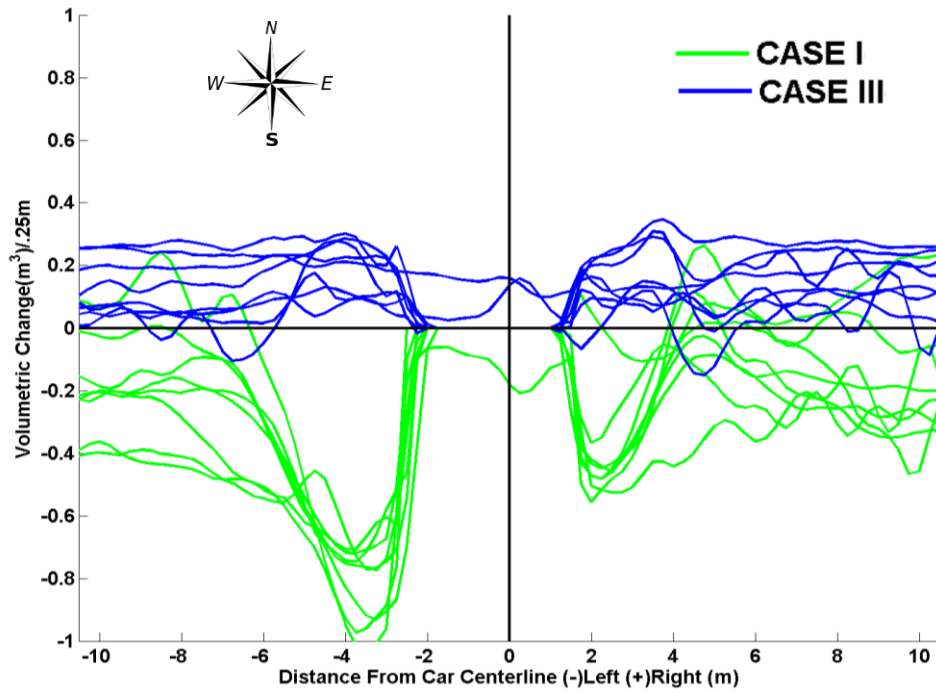


Figure 48- Case 1 and 3 (north oriented cars) scour accretion plots together.

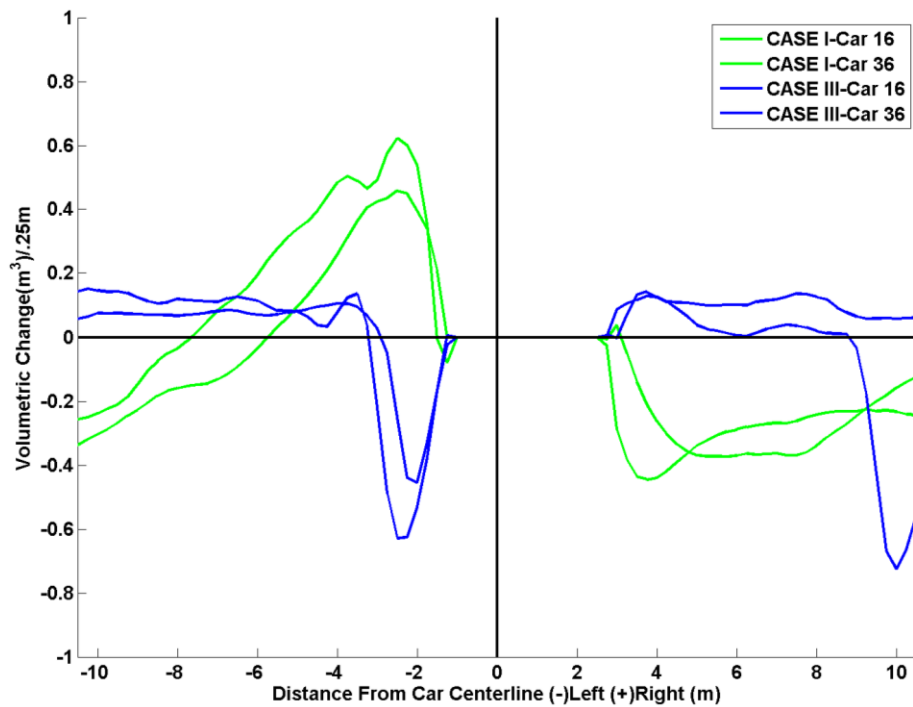


Figure 49-Case 1 and 3 (east oriented cars) scour accretion plots together.

Figure 48, and Figure 49 show both cases plotted together. The sediments response to these two time periods and associated hydrodynamic conditions shows opposed behavior. Where sediment was deposited during Sandy, it was removed during the winter storm in Case 3. These plots illustrate the dynamic behavior of the same area of seafloor in the inner continental shelf region.

4.7 Refinements

Over the course of this analysis, many factors surfaced that could impact the results while excluding them from consideration would not leave this work incomplete. One of the areas that should be investigated further is the evidence of shielding, or one car blocking another, within this dataset and how it affects the individual signatures. Also, along similar lines, what proximity eliminates the ability to discriminate two cars from each other and the cars act as one big artificial reef object.

Another area needing further consideration is the sediment analysis performed in Raineault et al. (2013) and its impact on the data seen here. It is evident that the transition zones between coarse and fine sediment have an empirical impact on the on the locations within the field site that exhibit highly variable scour behavior.

One immediate improvement to this analysis is to normalize the erosion/accretion data by multiplying the values by $(\text{car depth}/\text{car height})$. This dimensionless ratio factors in reduced bed velocities due to depth increase with increased flow obstruction with car height. At first glance, this appears to bring the plots together more tightly.

V. CONCLUSIONS

5.1 MBES Applicability in Scour Research

From the research performed in this analysis and the results provided, it is evident that the use of MBES systems are relevant to scour research. MBES enable the collection of large amounts of both bathymetric and backscatter data that help to identify bottom depth at fine length scales, determine depth and backscatter variability within the survey area, and perhaps the most important aspect is the accurate repeatability of the surveys from today's integrated MBES systems. The behavior of almost 40 distinct artificial reef objects in response to two time periods both of which contain significant weather is shown through the surveys. Leveraging MBES technology for scour research allows for the rapid and expansive analysis of scour behavior varying on temporal and spatial scales.

5.2 Object Based Data products from Assimilated MBES surveys

Using object based methods to organize MBES data is shown to be a powerful way to determine characteristic behavior within a particular area. Looking generally at the surveys themselves, one can ascertain qualitative information about the characteristics of the seafloor, dominant weather, and alike. However, when the data is queried and organized to display similar data for particular objects based on their characteristics, the depth of analysis expanded.

5.3 General Impacts of Car Orientation on the Scour/Accretion Records

The general impact of object orientation on scour/accretion is that within the field site studied during this analysis and the associated hydrodynamic conditions

associated with the CASE 1 and CASE 3 time periods, orientation dictated the scour/accretion pattern around each object. The response was spatially consistent and dependent on the cars orientation.

The scour/accretion response showed scour/accretion asymmetries in the cross object profiles and symmetries in the along object profiles for objects oriented orthogonally to the flow field while showing scour/accretion symmetries in the across object profiles and asymmetries in the along object profiles for cars oriented in line with the flow field. The asymmetrical response was opposed in magnitude between Case 1 and Case 3 suggesting that the inner continental shelf region is dynamic and changing on varying spatio-temporal scales.

VI. CONSIDERATIONS AND REMARKS

The ocean is very large and difficult environment to operate on, in, or around. The ability to gather, process, and analyze data from the ocean more efficiently is vital to a more accurate picture of this environment. The overall goal of this research was to infer hydrodynamic information data from scour accretion records and conversely infer scour/accretion data from hydrodynamic information.

The opportunity to study an artificial reef containing numerous and similar shaped objects over varying temporal scales is unique and presents an opportunity to produce a quantitative analysis of an intuitive process. While one could easily qualitatively analyze the bathymetric difference surfaces or the survey, the ability to query all the objects in the data set by defining characteristics and study the

scour/accretion profiles on both major and minor axis is unique and has proved to be a method to discriminate scour/accretion behavior.

The ability to refine predictive models of scour/accretion based on local hydrodynamics is extremely important. Ultimately the need for scour/accretion predictions in real time primarily applies to object detection in turbid and live environments such as in the inner continental shelf region. Object detection algorithms already exist and are relatively well established. Alternatively, seafloor bottom picking and sediment prediction algorithms exist and are also well established. This allows for a great understanding of bottom and *in-situ* object characteristics. Future investigations could look to incorporate the real time analysis of scour around in-situ objects on the seafloor that would allow for real time updating of predictive object detection algorithms and bottom composition models.

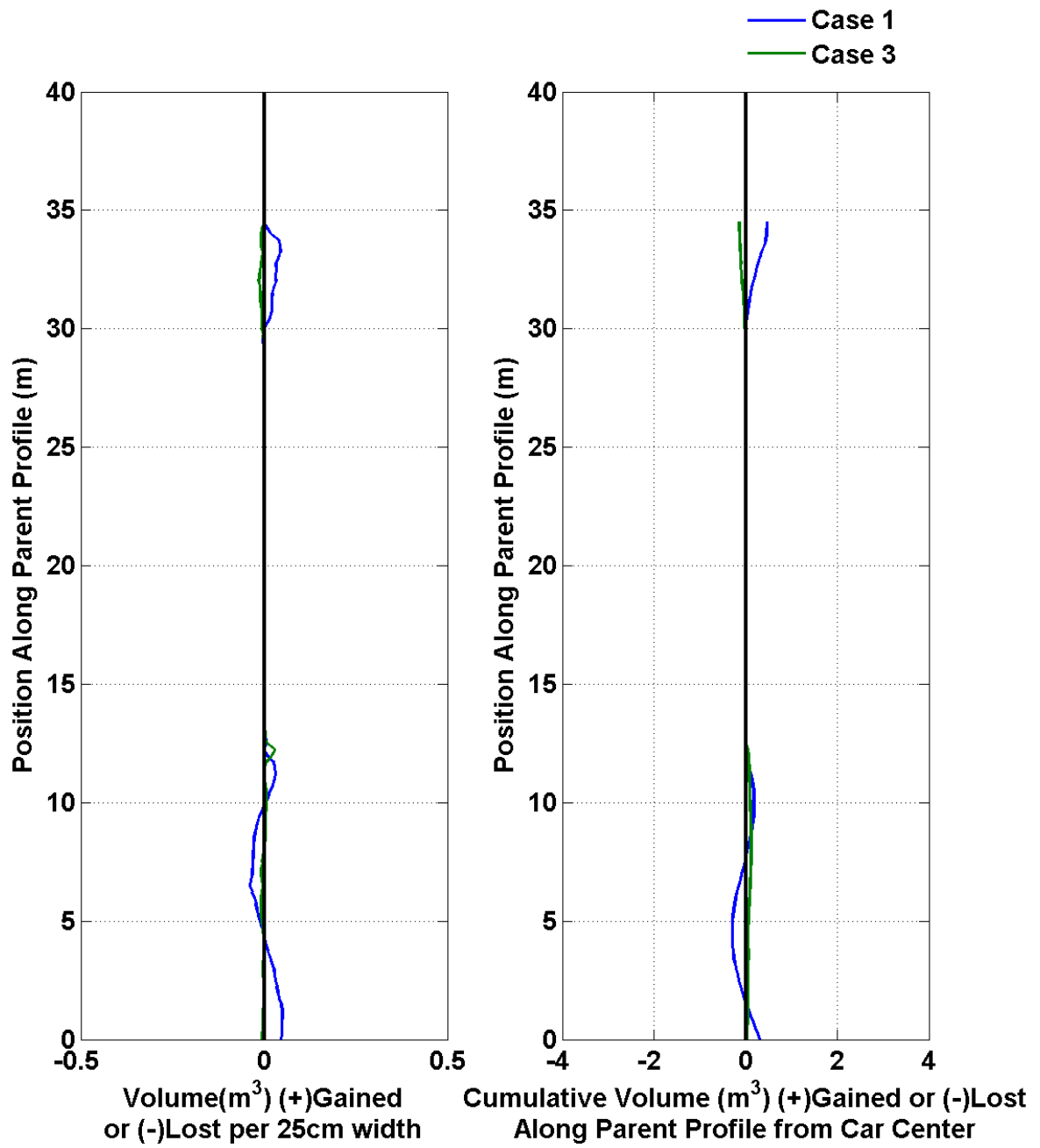
LIST OF REFERENCES

- Andreas Munchow, A. K. (1992). Astronomical and nonlinear tidal currents in a coupled estuary shelf system. *Continental Shelf Research*, 471-498.
- Arthur C. Trembanis, C. T. (2007). Predicting Seabed Burial of Cylinders by Wave-Induced Scour: Application to the Sandy Inner Shelf Off Florida and Massachusetts. *IEEE JOURNAL OF OCEANIC ENGINEERING*, 167-184.
- Arthur C. Trembanis, L. M. (n.d.). Bedform Parameterization and Object Detection from Sonar.
- DDNREC. (2009). 44 More Subway Cars Sunk at Redbird Reef. *News of the Delaware Department of Natural Resources and Environmental Control*, 182.
- DNREC. (2009-2010). *Delaware Reef Guide*. State of Delaware Department of Natural Resources and Environmental Control.
- FitzGerald, D. (1993). *Formation and Evolution of Multiple Tidal Inlets*. Washington, DC: American Geophysical Union.
- G. Momber, M. G. (2000). The application of the Submetrix ISIS 100 swath bathymetry system to the management of underwater sites. *International Journal of Nautical Archaeology*, 154-162.
- Hanson, H. (2014, 04 24). TVRL. Retrieved 04 24, 2014, from Lund University: http://www.tvrl.lth.se/fileadmin/tvrl/files/vvr040/6_Design_3pp.pdf
- J. McNinch, J. W. (2006). Predicting the Fate of Artefacts in Energetic, Shallow Marine. *The International Journal of Nautical Archaeology*, 290-309.
- M. Green, C. V. (2004). Suspension of coarse and fine sand on a wave-dominated. *Continental Shelf Research*, 317-335.
- M.I. Lawrence, C. B. (2002). Acoustic ground discrimination techniques for submerged archaeological site investigations. *Marine Technology Society Journal*, 65-73.
- Mayer, L. R., Glang, G., Richardson, M., Traykovski, P., & Trembanis, A. (2007). High-Resolution Mapping of Mines and Ripples at the Martha's Vineyard Coastal Observatory. *IEEE*, 133-149.
- N. Raineault, A. T. (2013). Interannual changes in seafloor surficial geology at an artificial reef site on the inner continental shelf. *Continental Shelf Research*, 67-78.

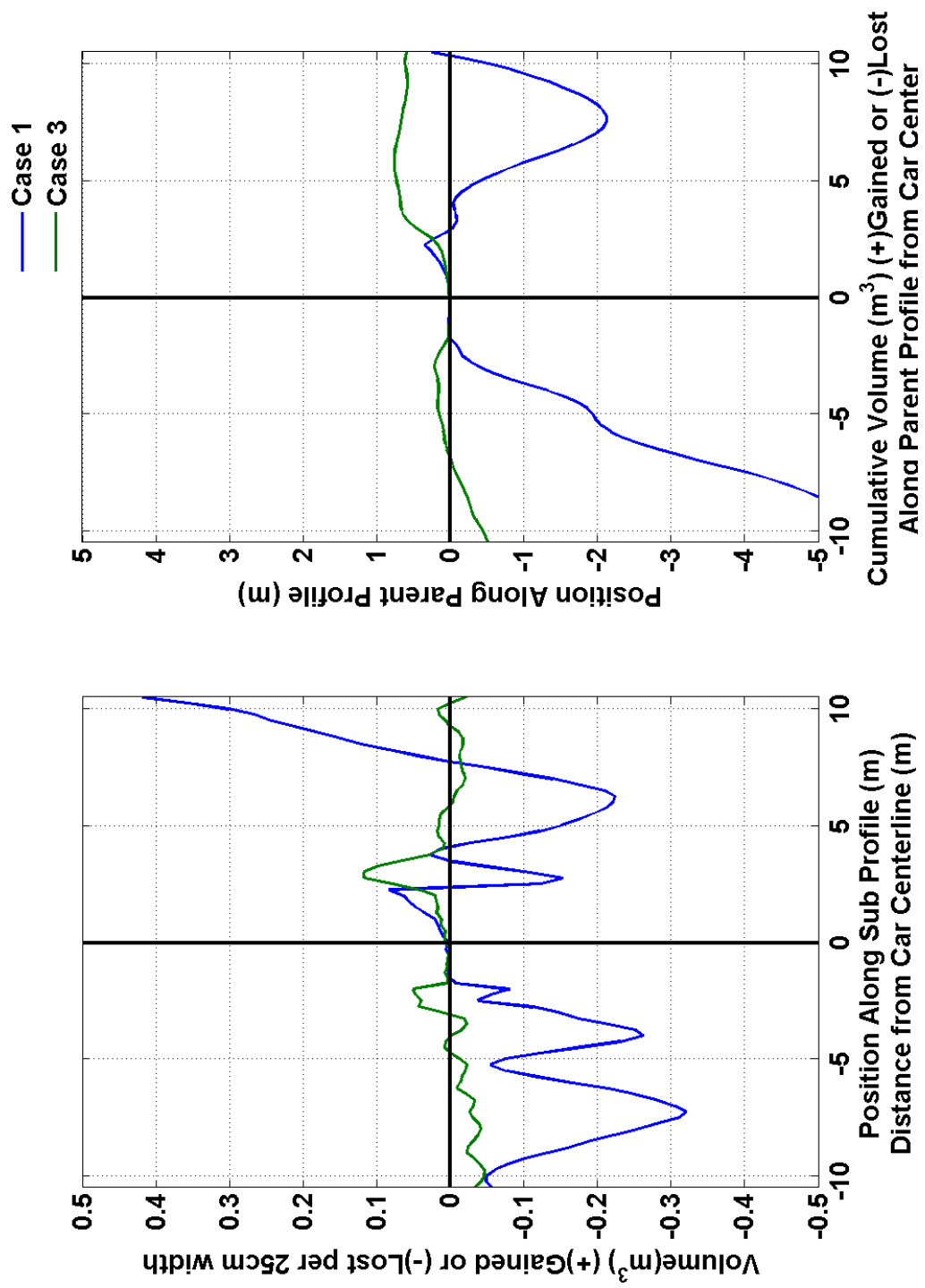
- NOAA. (2014, 04 24). *What percentage of the American Population Lives Near the Coast?* Retrieved 04 24, 2014, from NOAA:
<http://oceanservice.noaa.gov/facts/population.html>
- P.A. Muscarella, N. B. (2011). Surface currents and wind sat the Delaware Bay mouth. *Continental Shelf Research*, 1282-1293.
- Pope, J. (1997). Responding to Coastal Erosion and Flooding Damages. *Coastal Education & Research Foundation, Inc*, 704-710.
- Quinn, R. (2006). The role of scour in shipwreck site formation processes and the preservation of wreck-associated scour signatures in the sedimentary record e evidence from seabed and sub-surface data. *Journal of Archaeological Science*, 1419-1432.
- Randall, R. E. (1940). *Elements of Ocean Engineering*. Jersey City, NJ: SNAME.
- Richard P. Stumpf, K. H. (2003). Determination of water depth with high-resolution satellite imagery over variable bottom types. *American Society of Limnology and Oceanography*.
- Rory Quinn, D. B. (2010). The role of time-lapse bathymetric surveys in assessing morphological change at shipwreck sites. *Journal of Archaeological Science*, 2938-2946.
- Ruth Plets, R. Q. (2010). Using Multibeam Echo-Sounder Data to Identify Shipwreck Sites: archaeological assessment of the Joint Irish Bathymetric Survey data. *International Journal of Nautical Archaeology*, 87-98.
- Sumer, B. M. (2010). Mathematical modelling of scour: A review. *Journal of Hydraulic Research*, 729-731.
- Trembanis, A. C. (2013). A detailed seabed signature from Hurricane Sandy revealed in bed forms and scour. *Geochem. Geophys. Geosyst.*
- Whitcomb. (199). Combined Doppler/LBL Based Navigation of Underwater Vehicles. *UUST99*.
- Whitehouse. (1998). *Scour at Marine Structures*. London.
- Wüst, G. D. (1936). Atlas of the stratification and circulation of the Atlantic Ocean. *Walther de Gruyter & Co.*

APPENDIX I- Scour/Accretion Plots

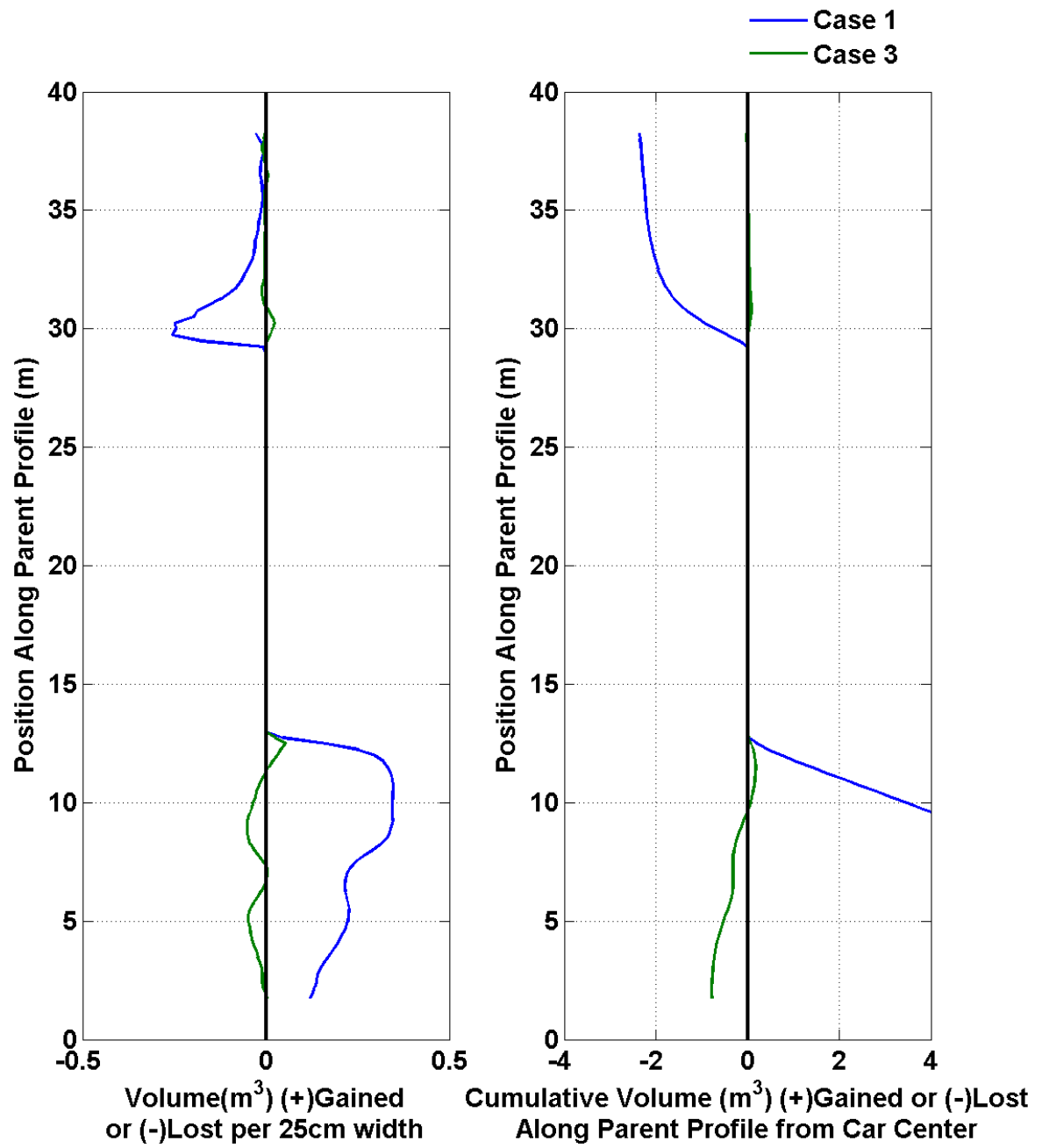
Car #1



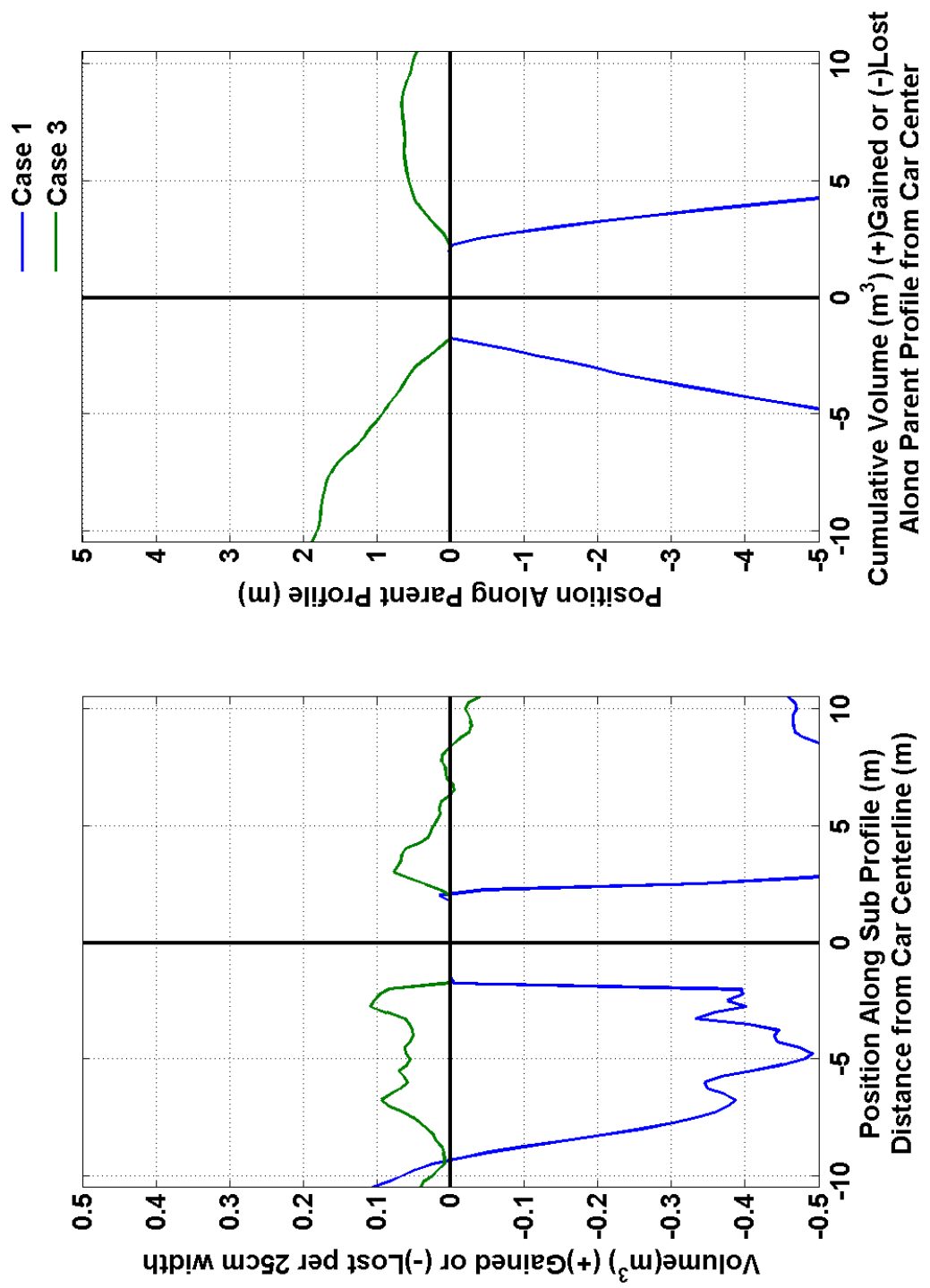
Car #1



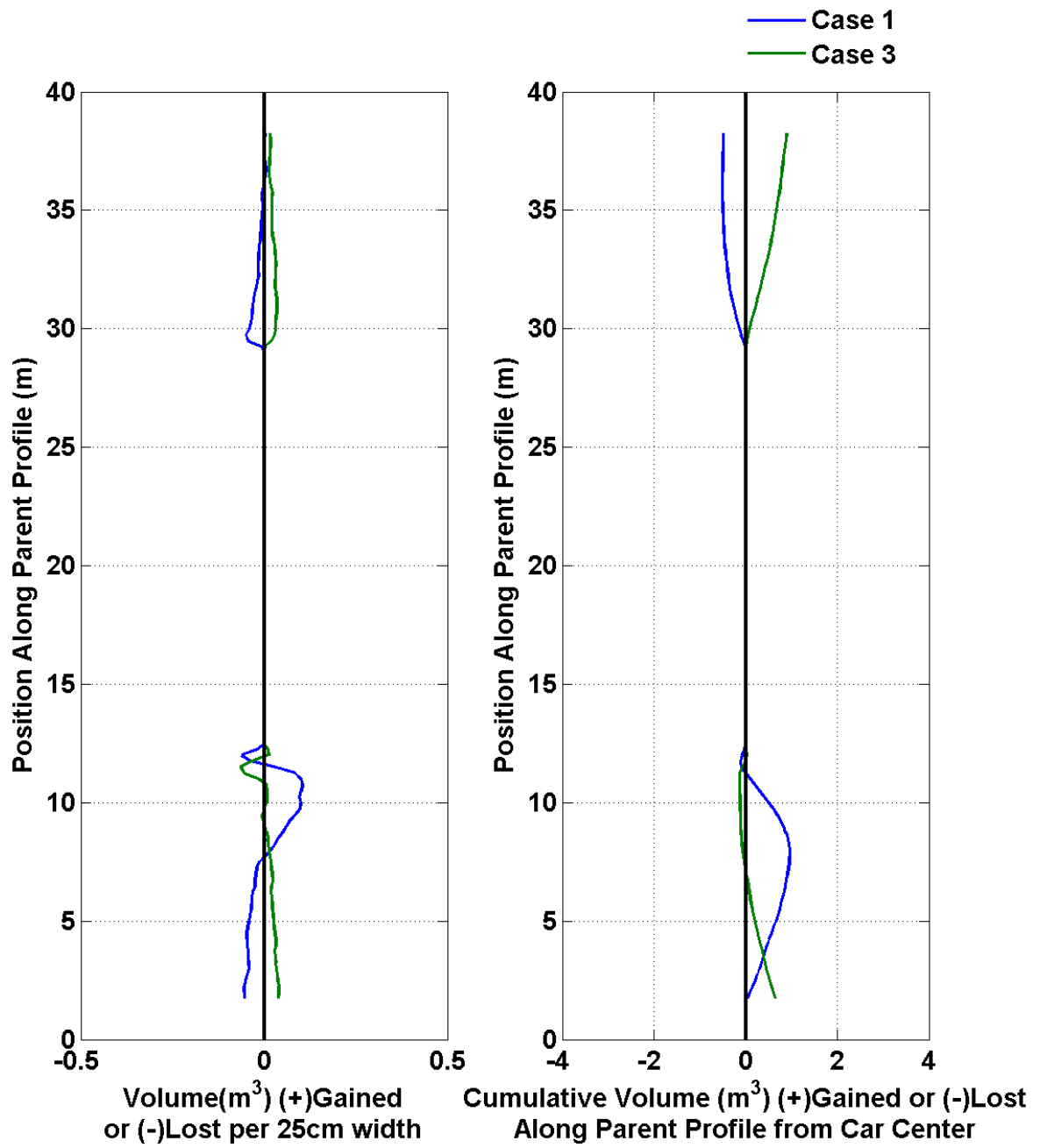
Car #2



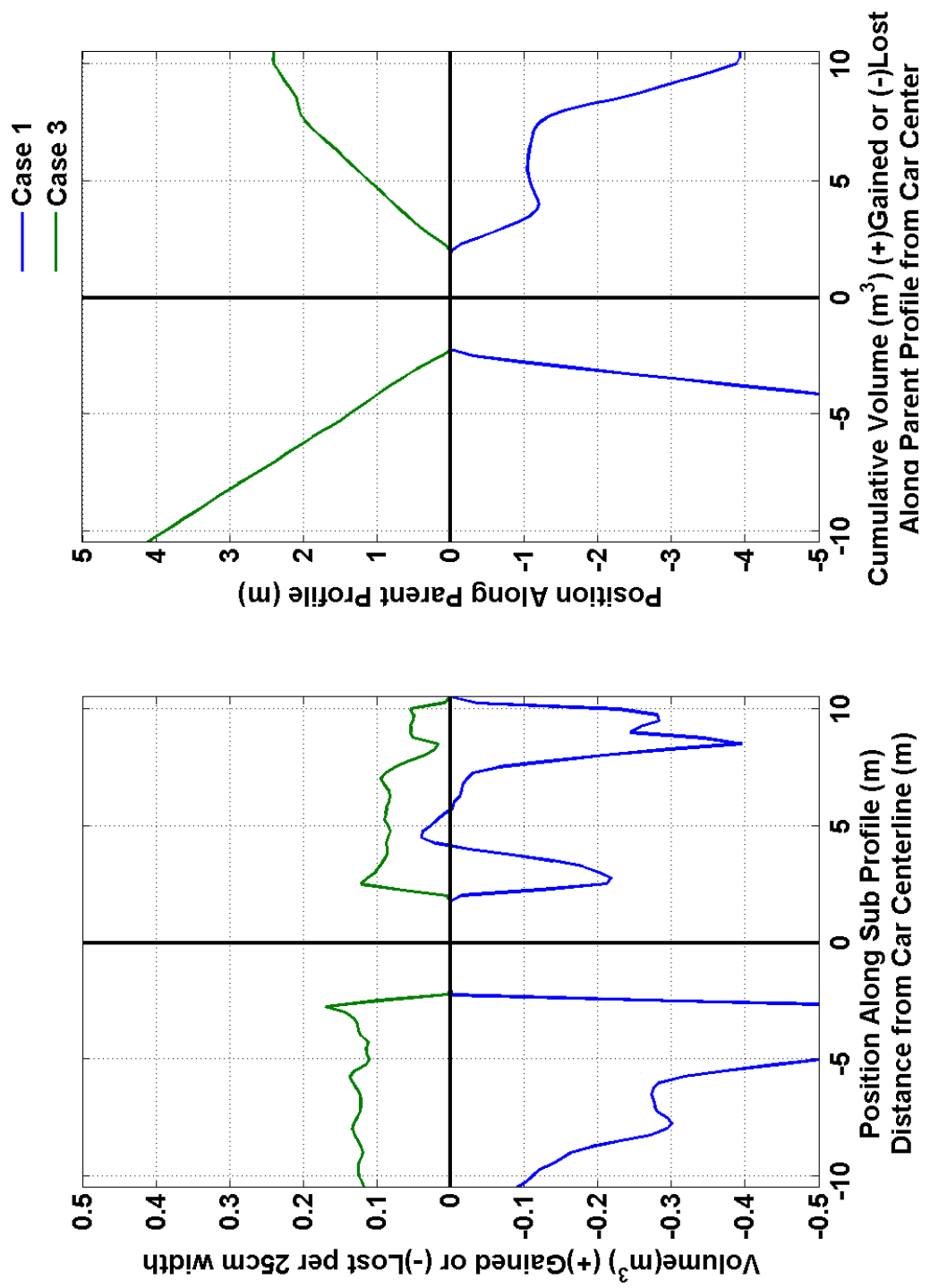
Car #2



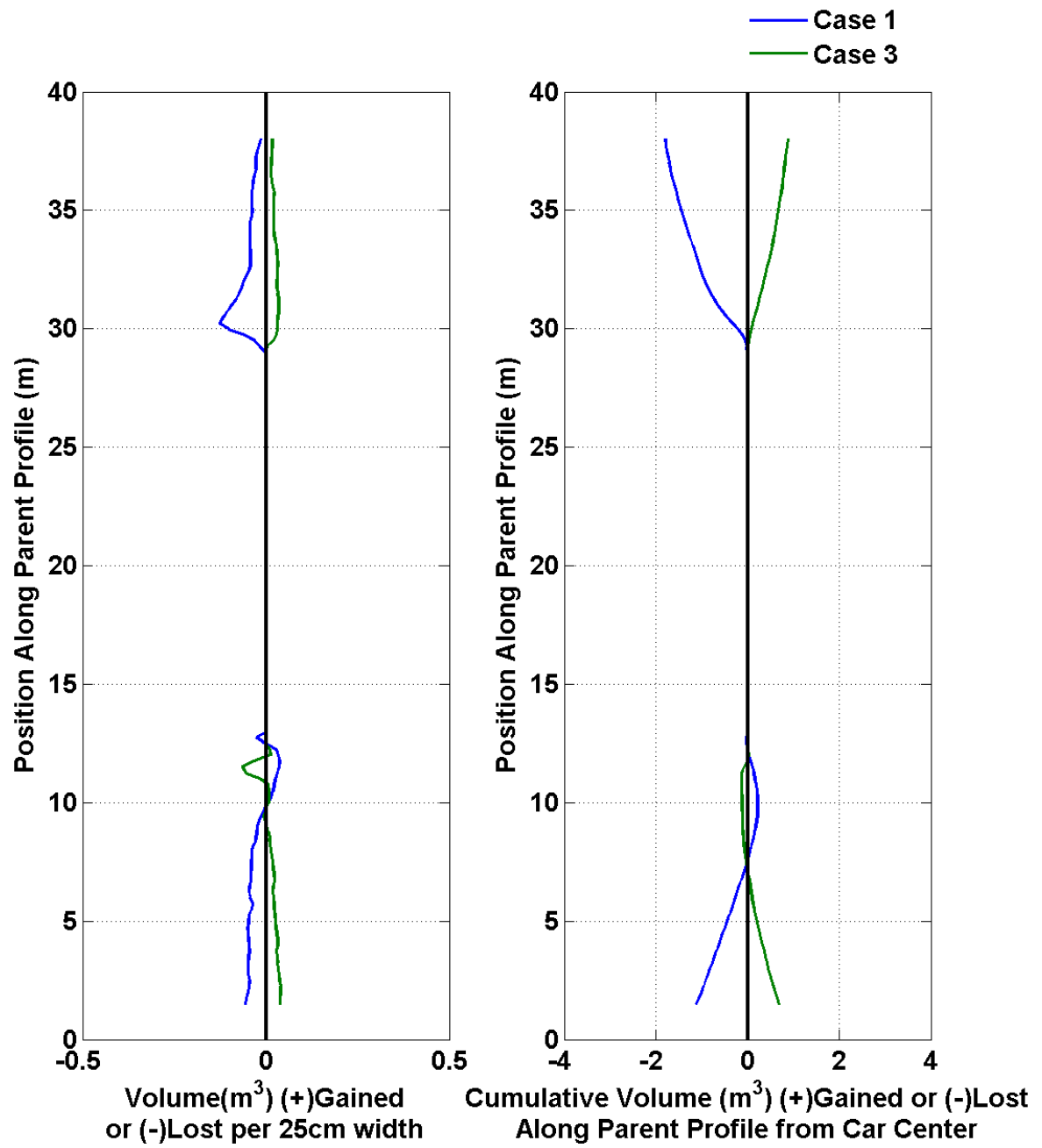
Car #3



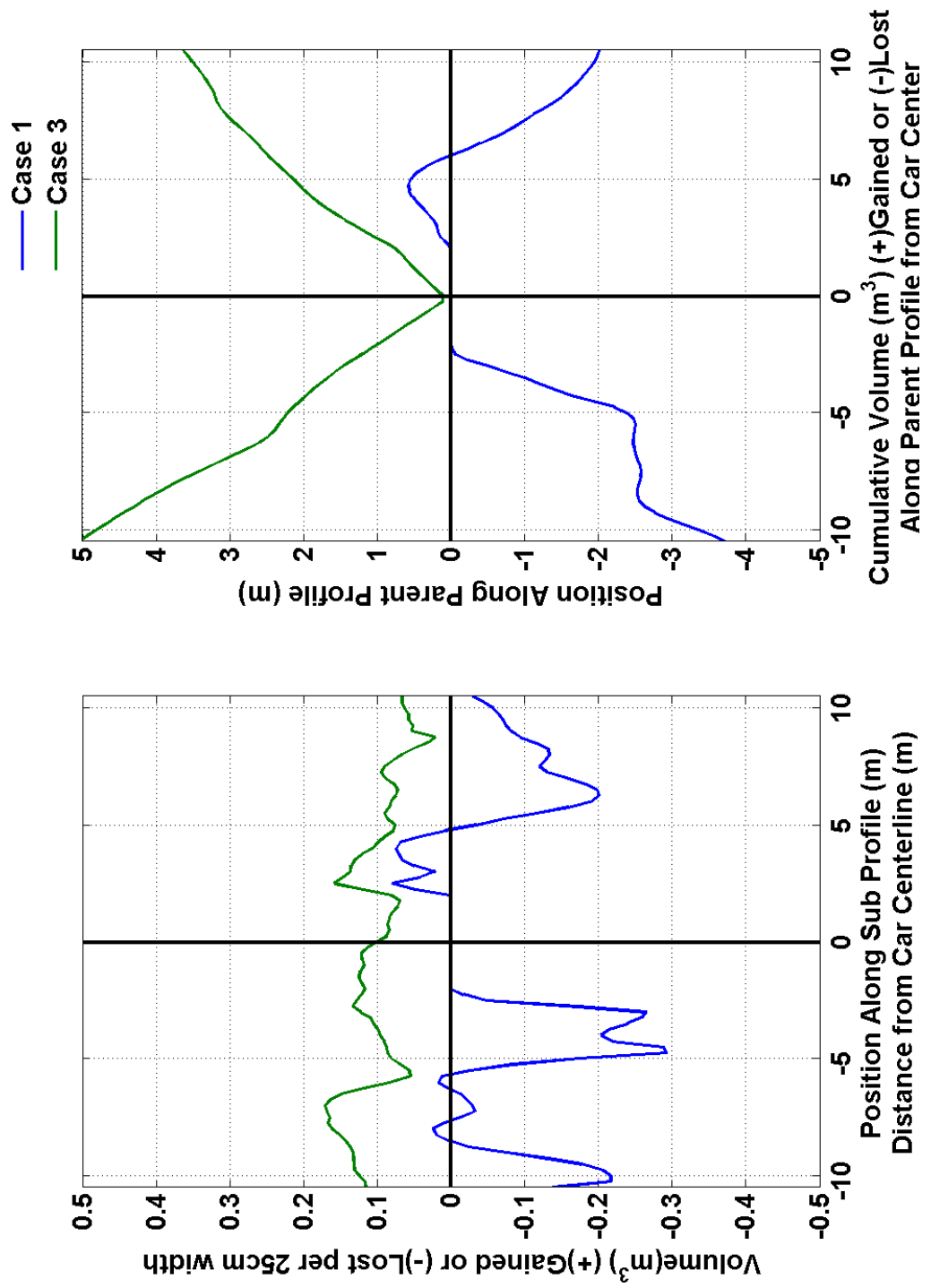
Car #3



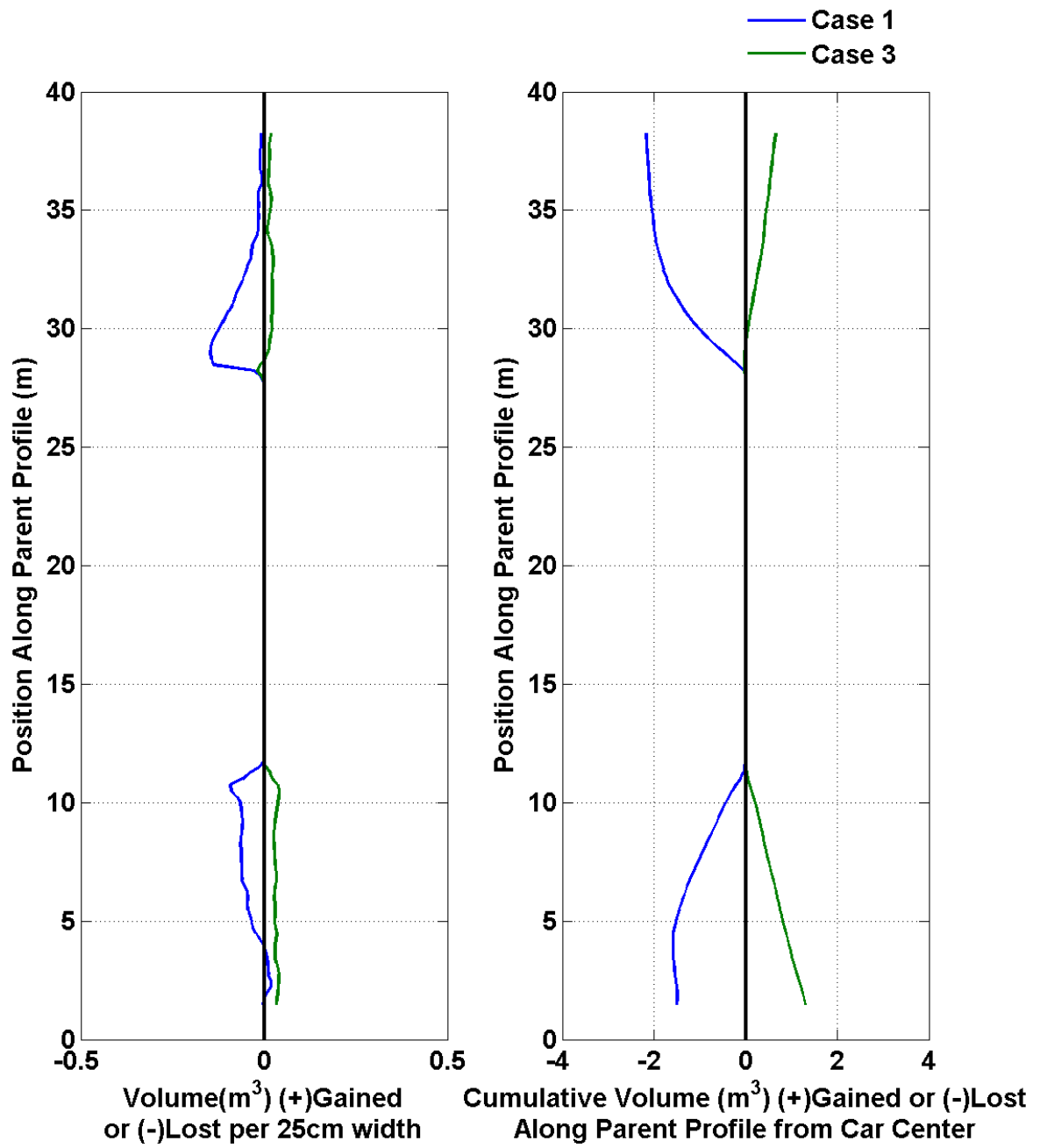
Car #4



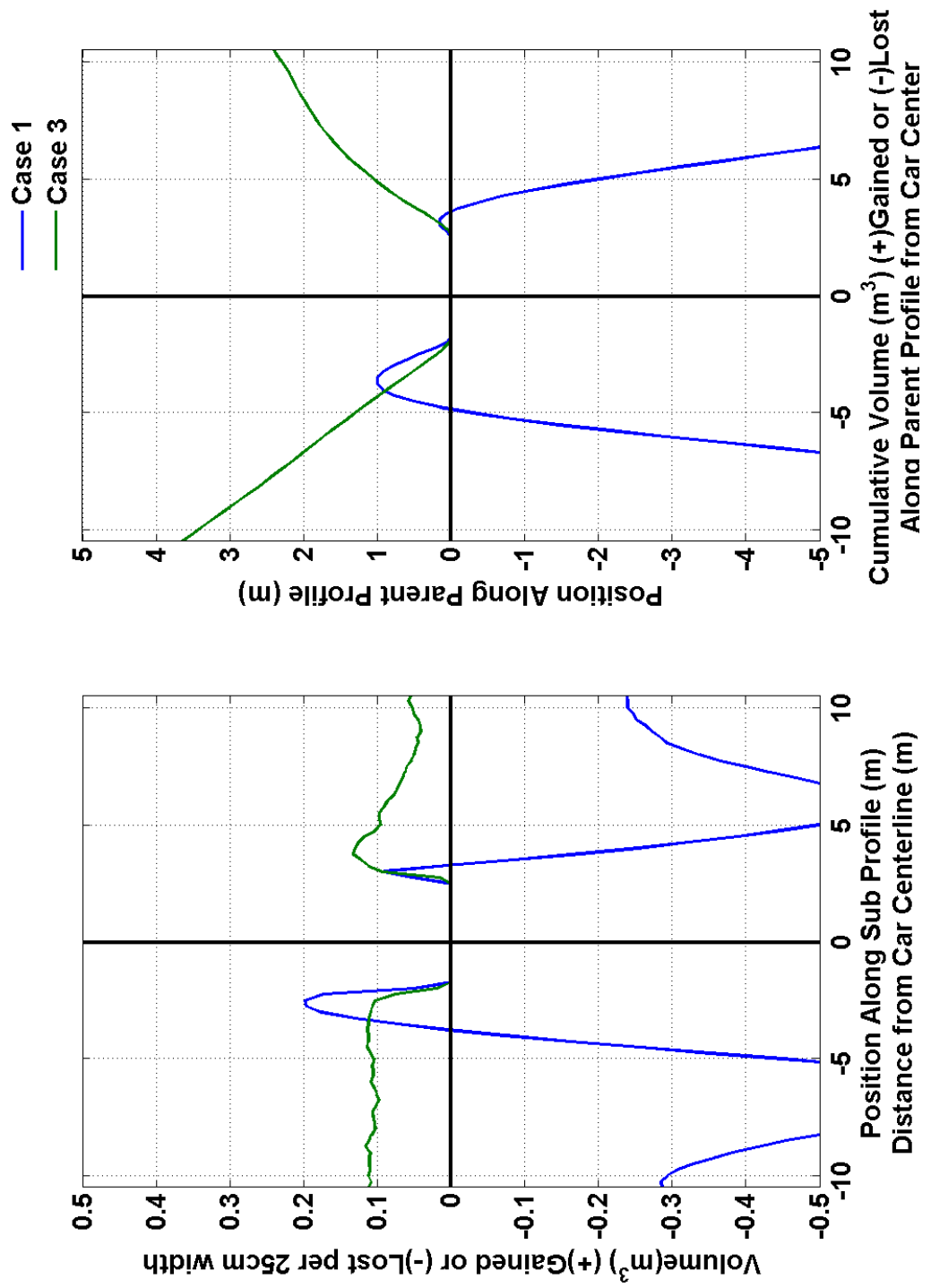
Car #4



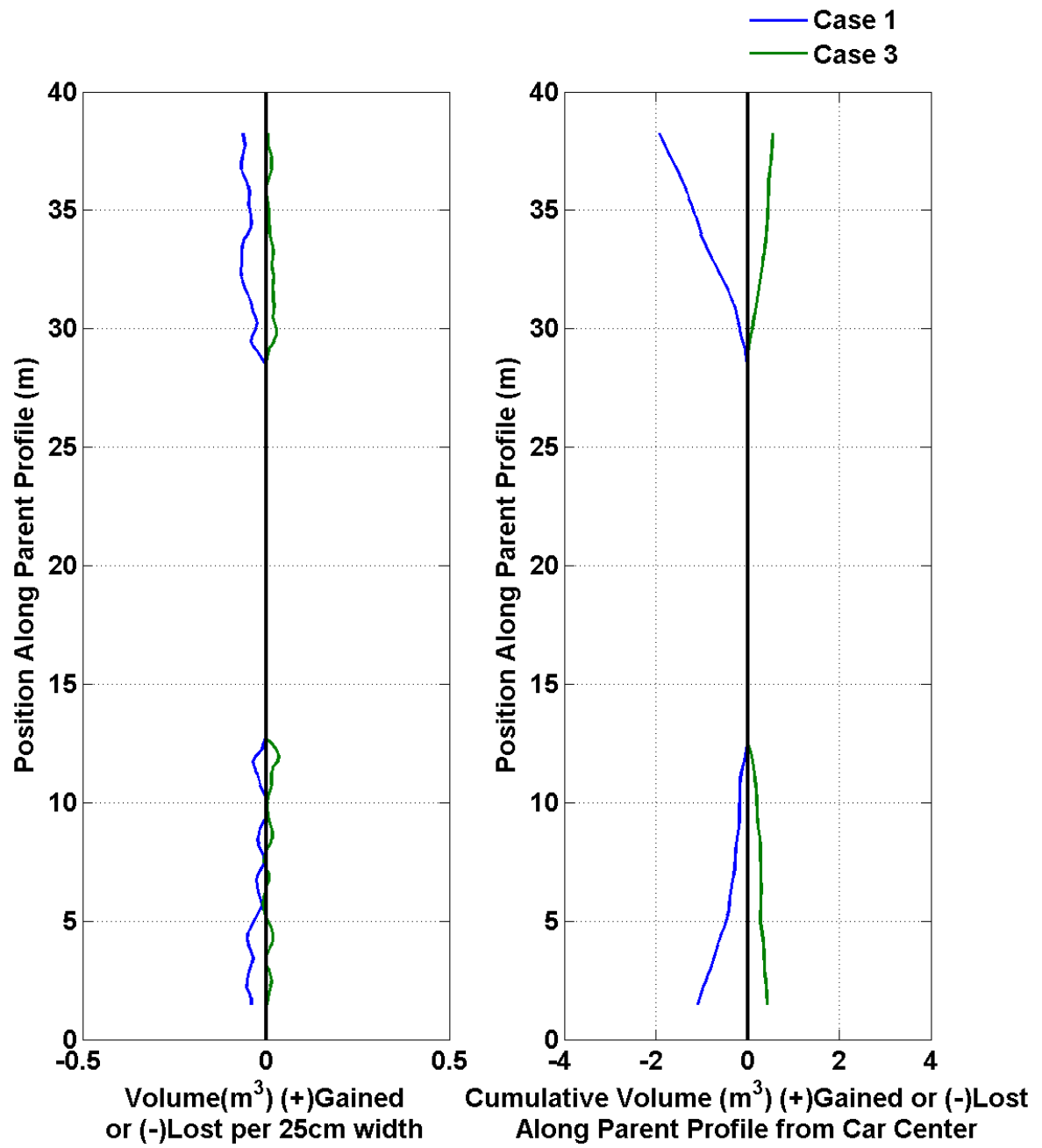
Car #5



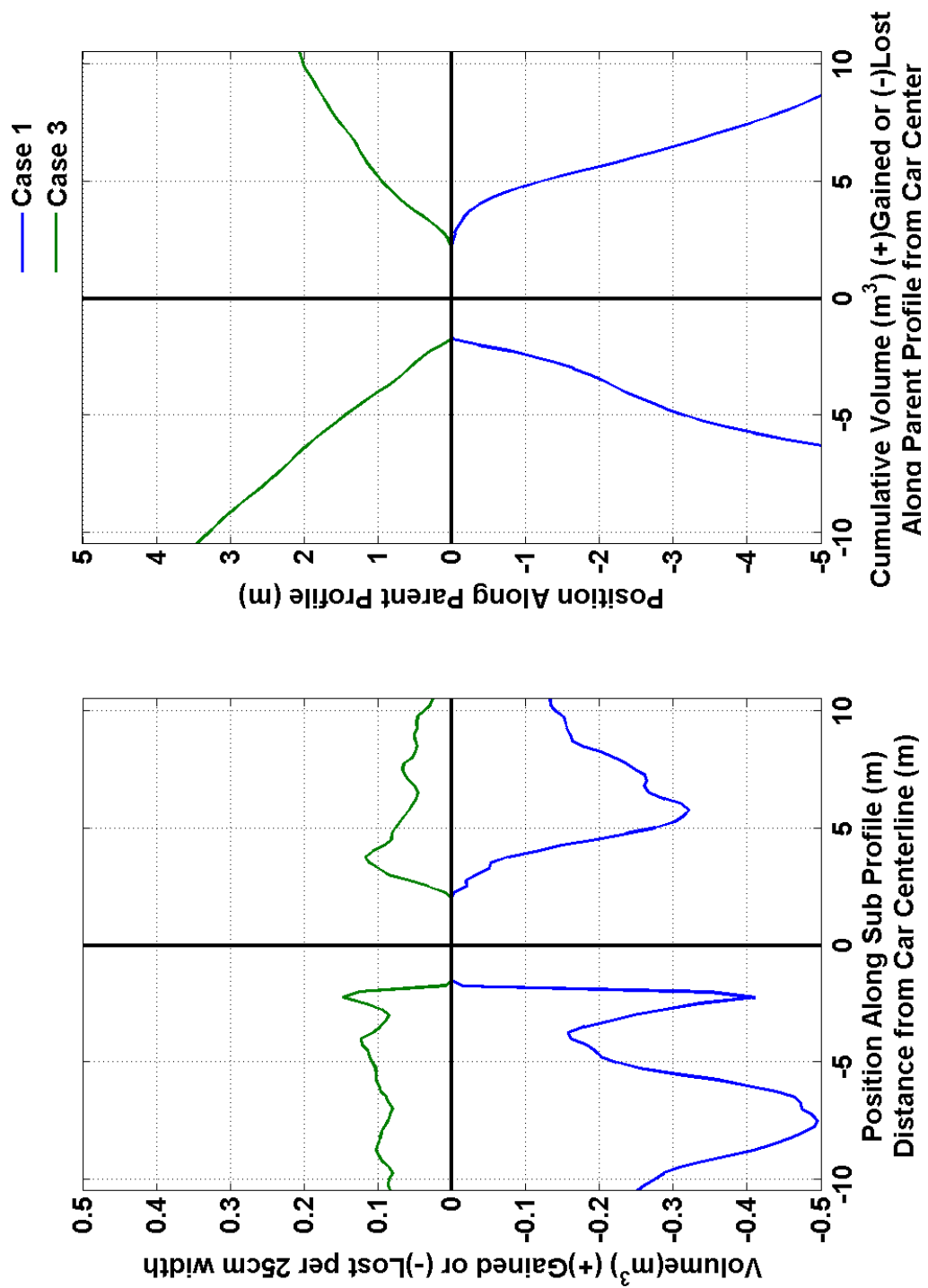
Car #5



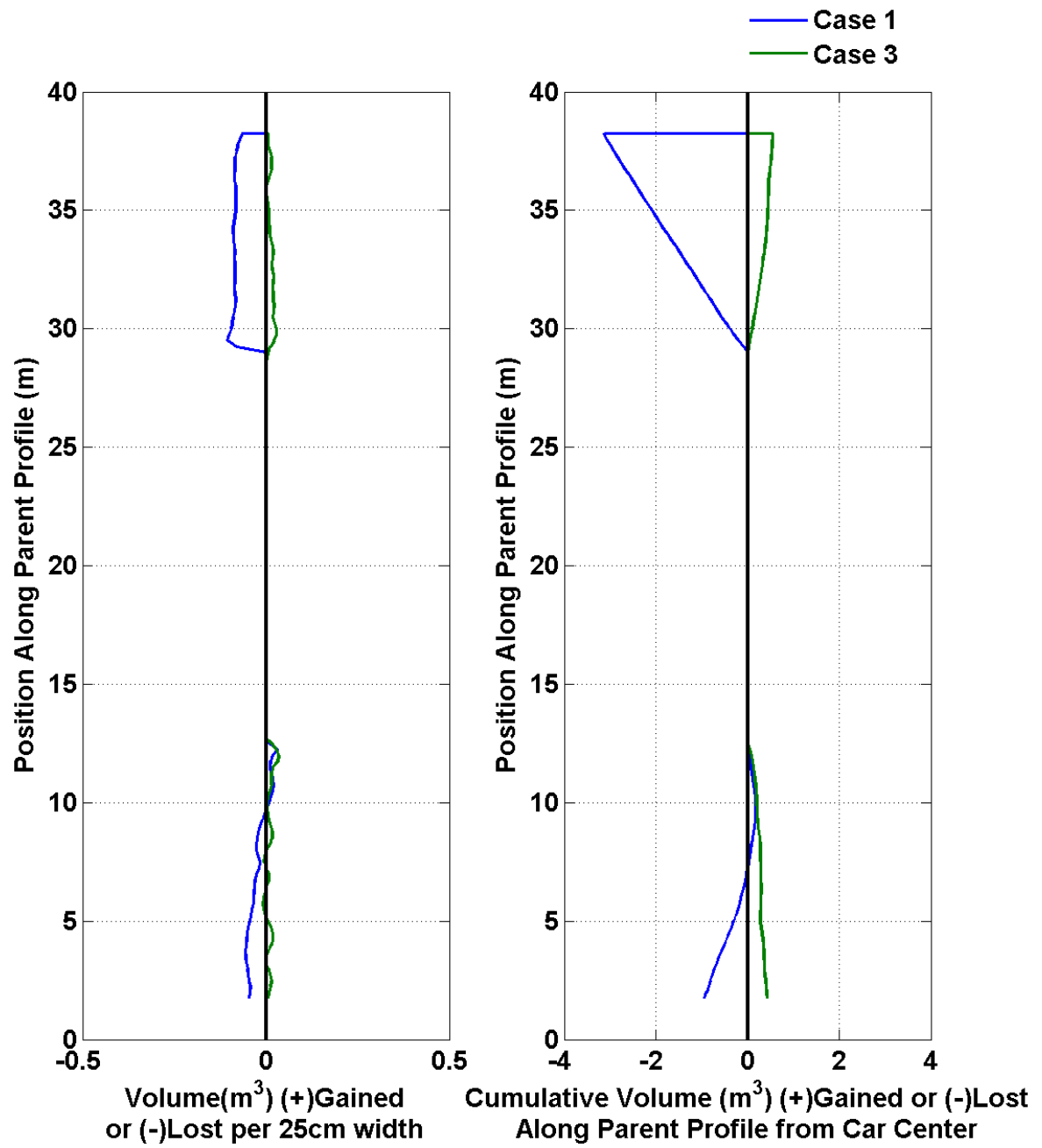
Car #6



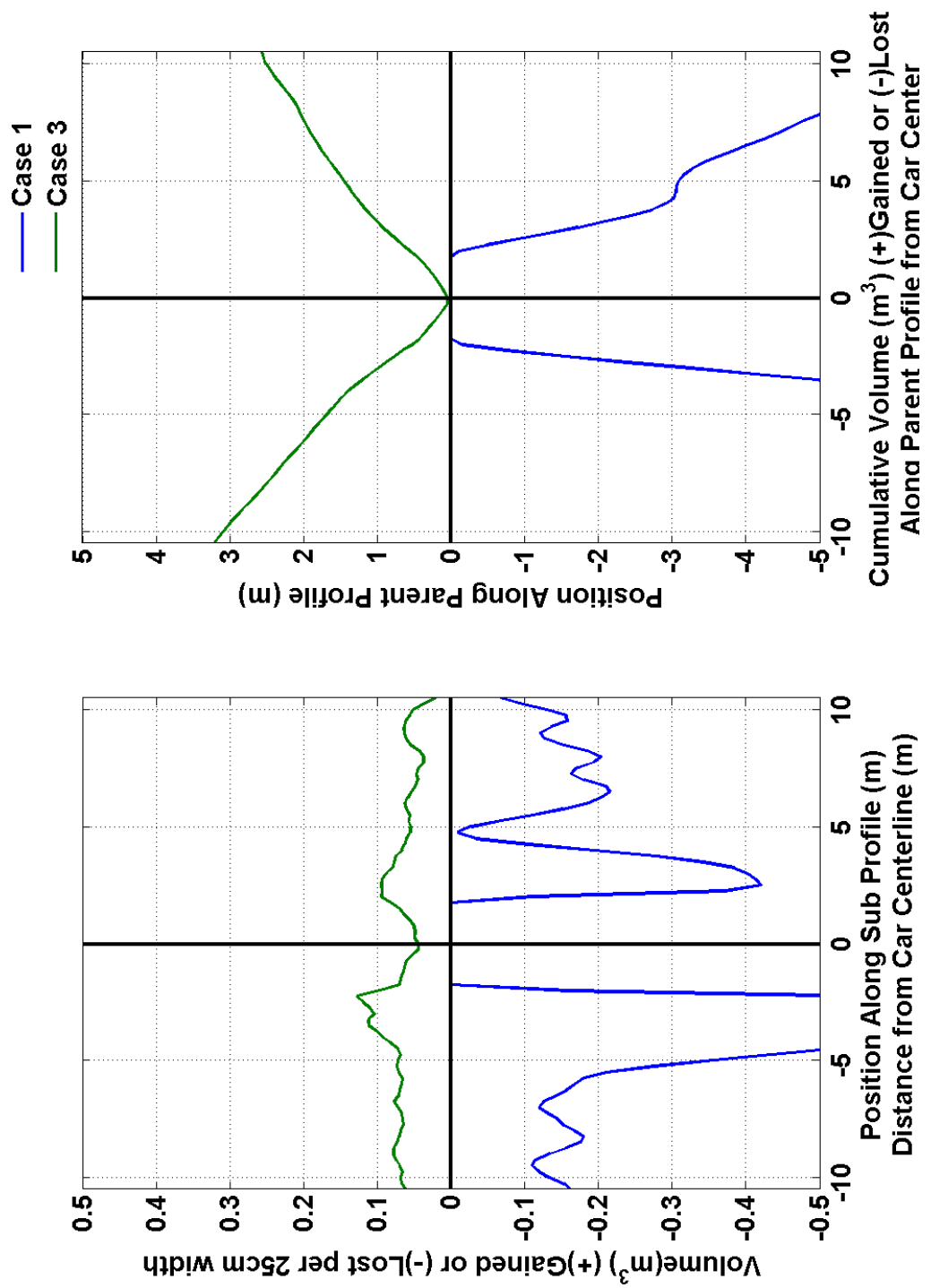
Car #6



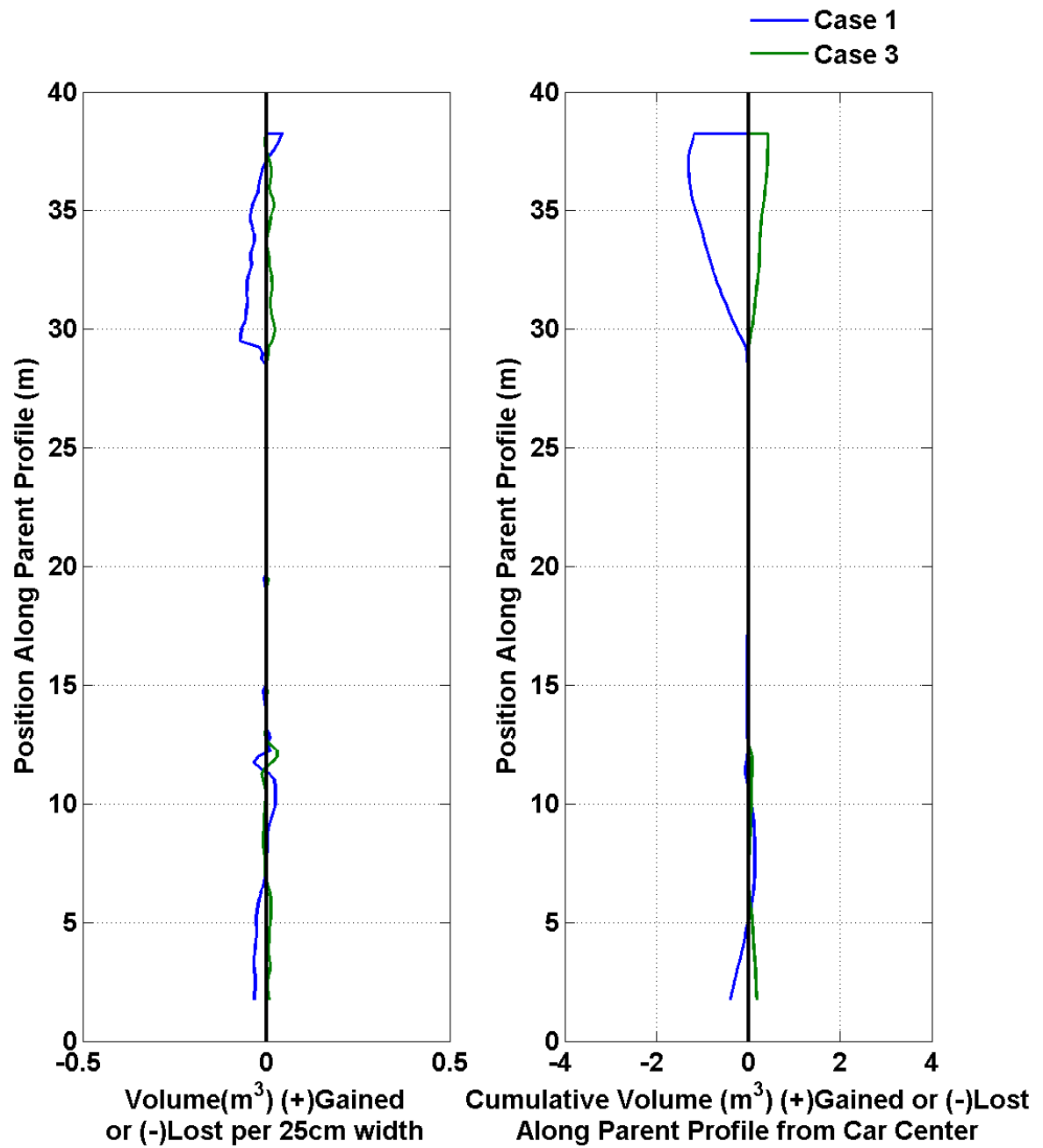
Car #7



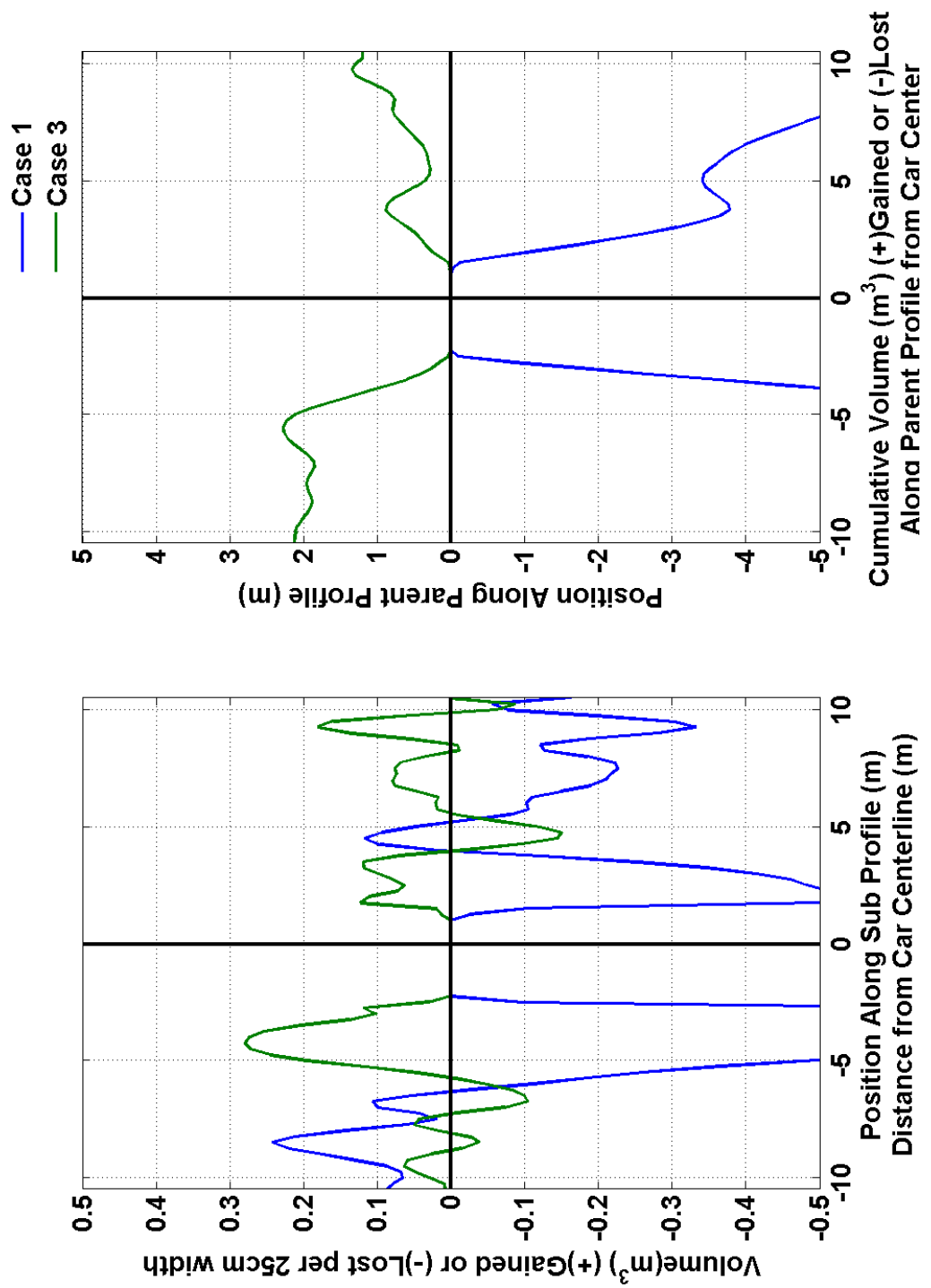
Car #7



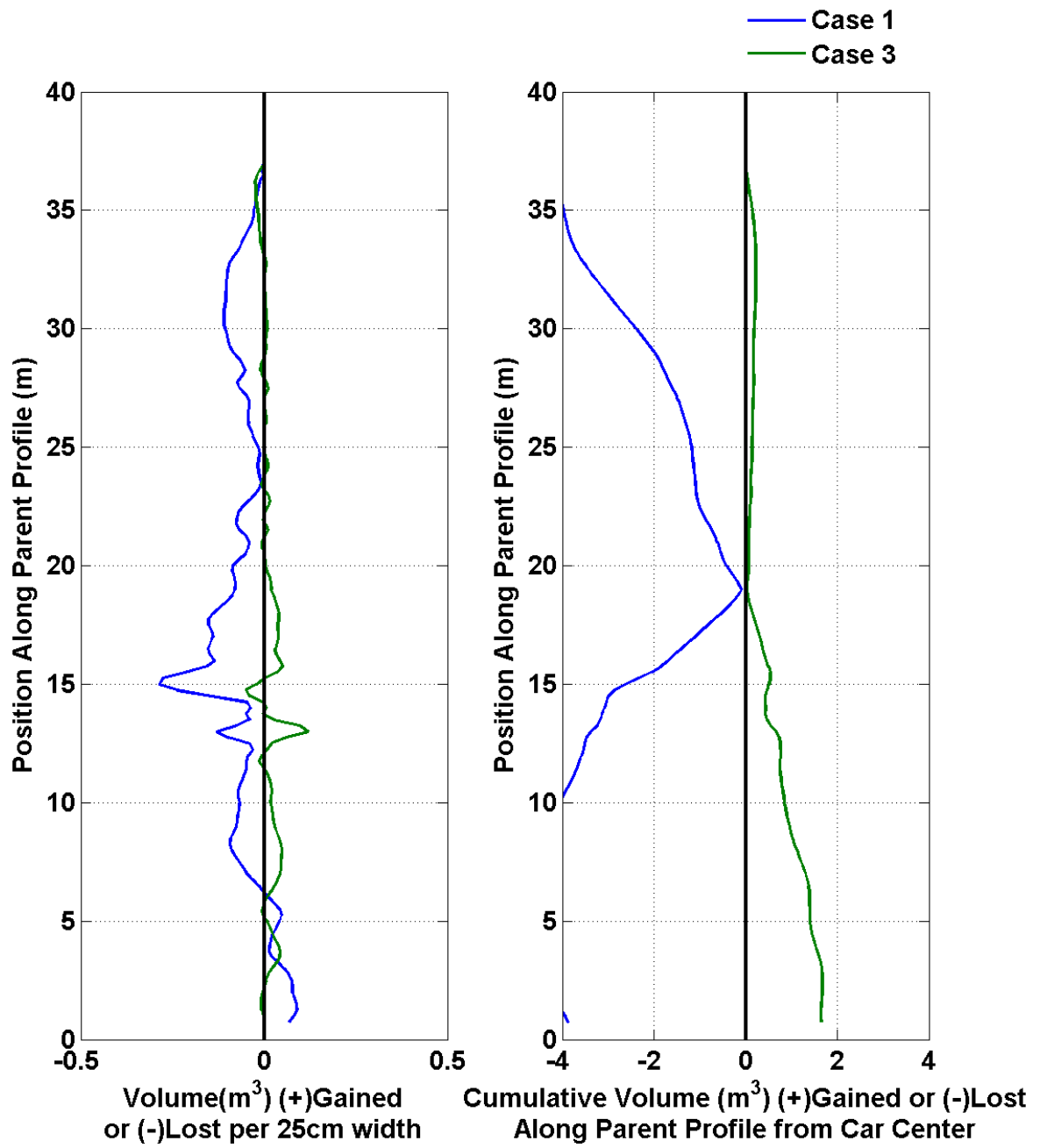
Car #8



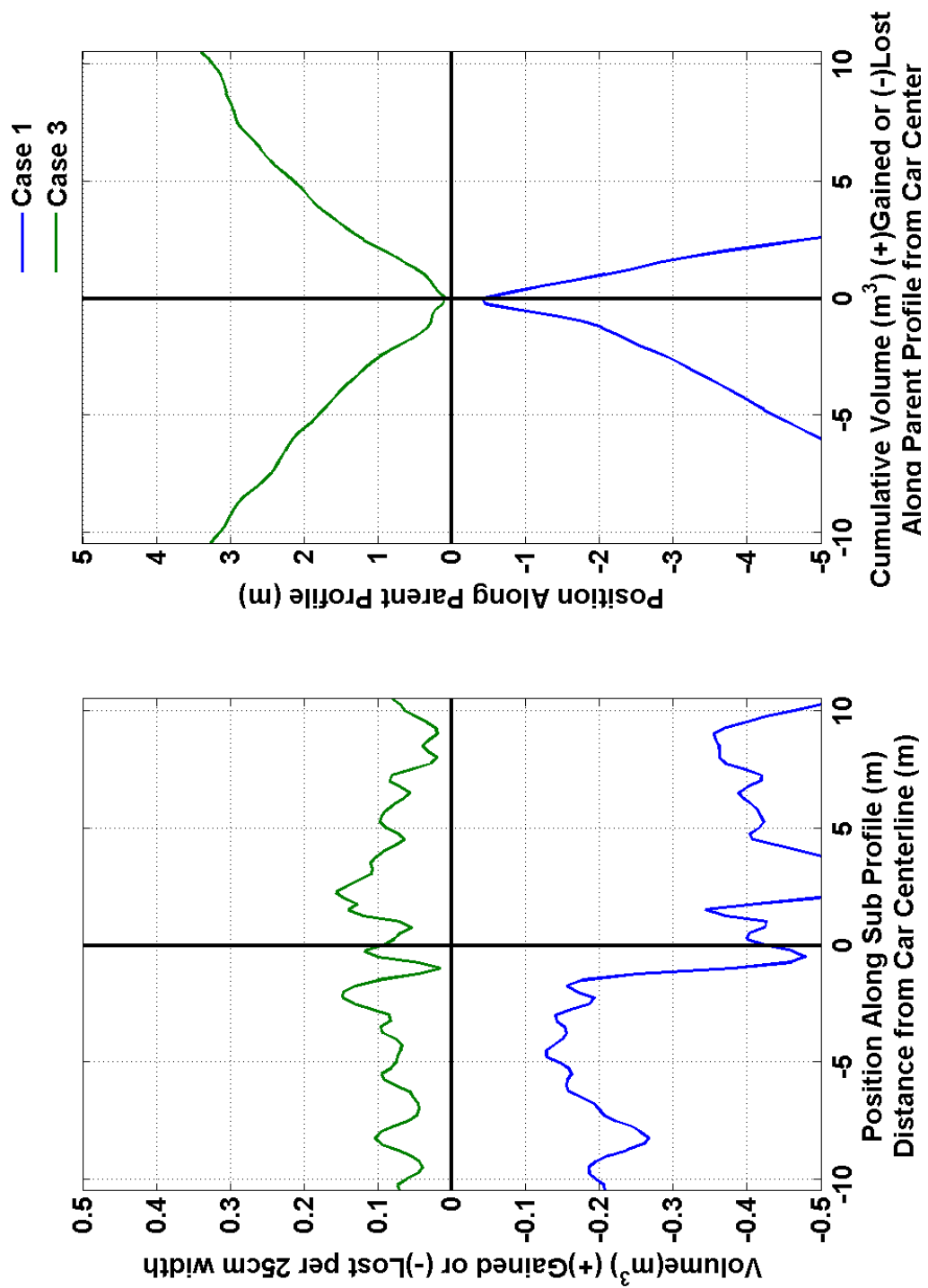
Car #8



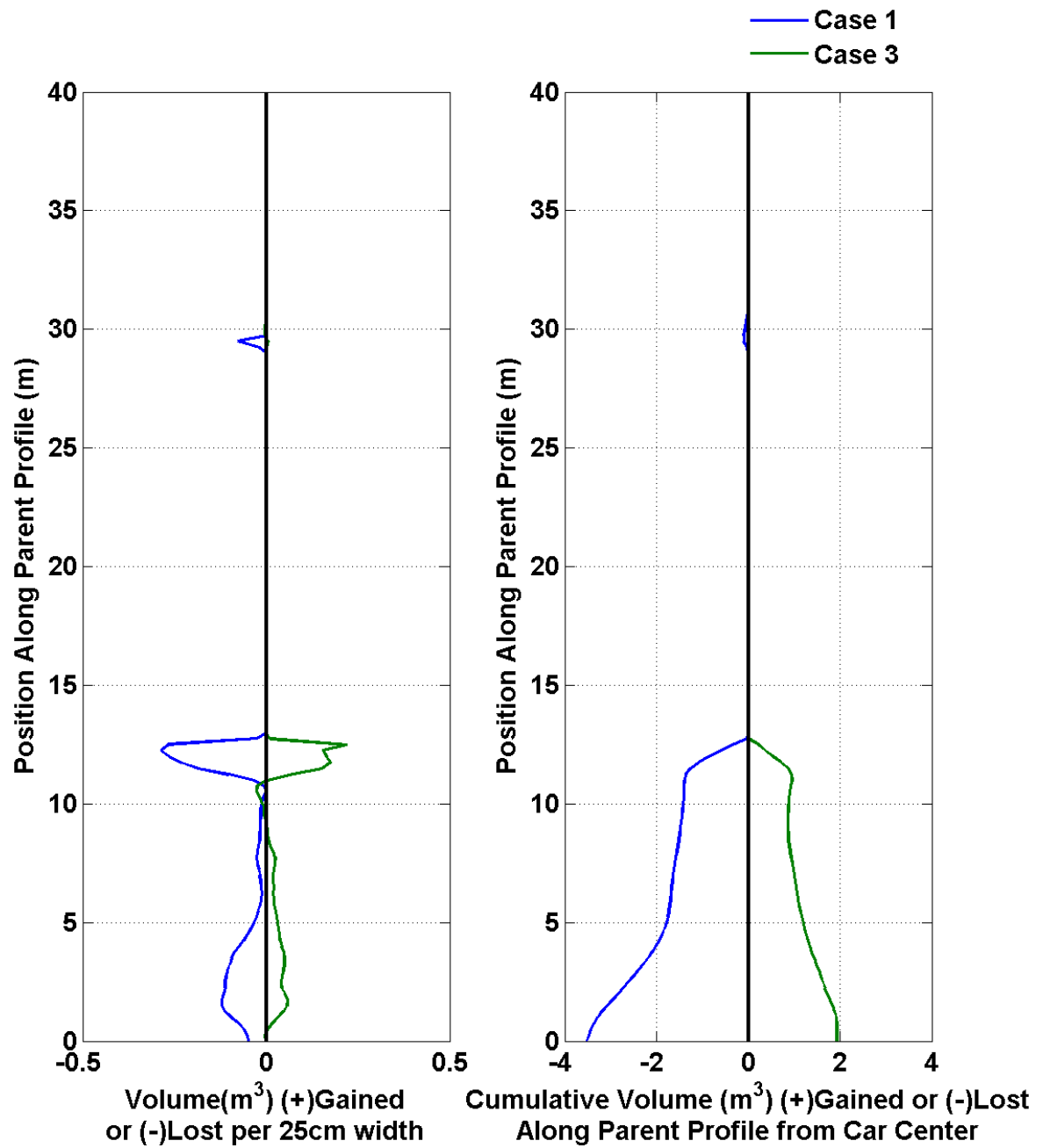
Car #9



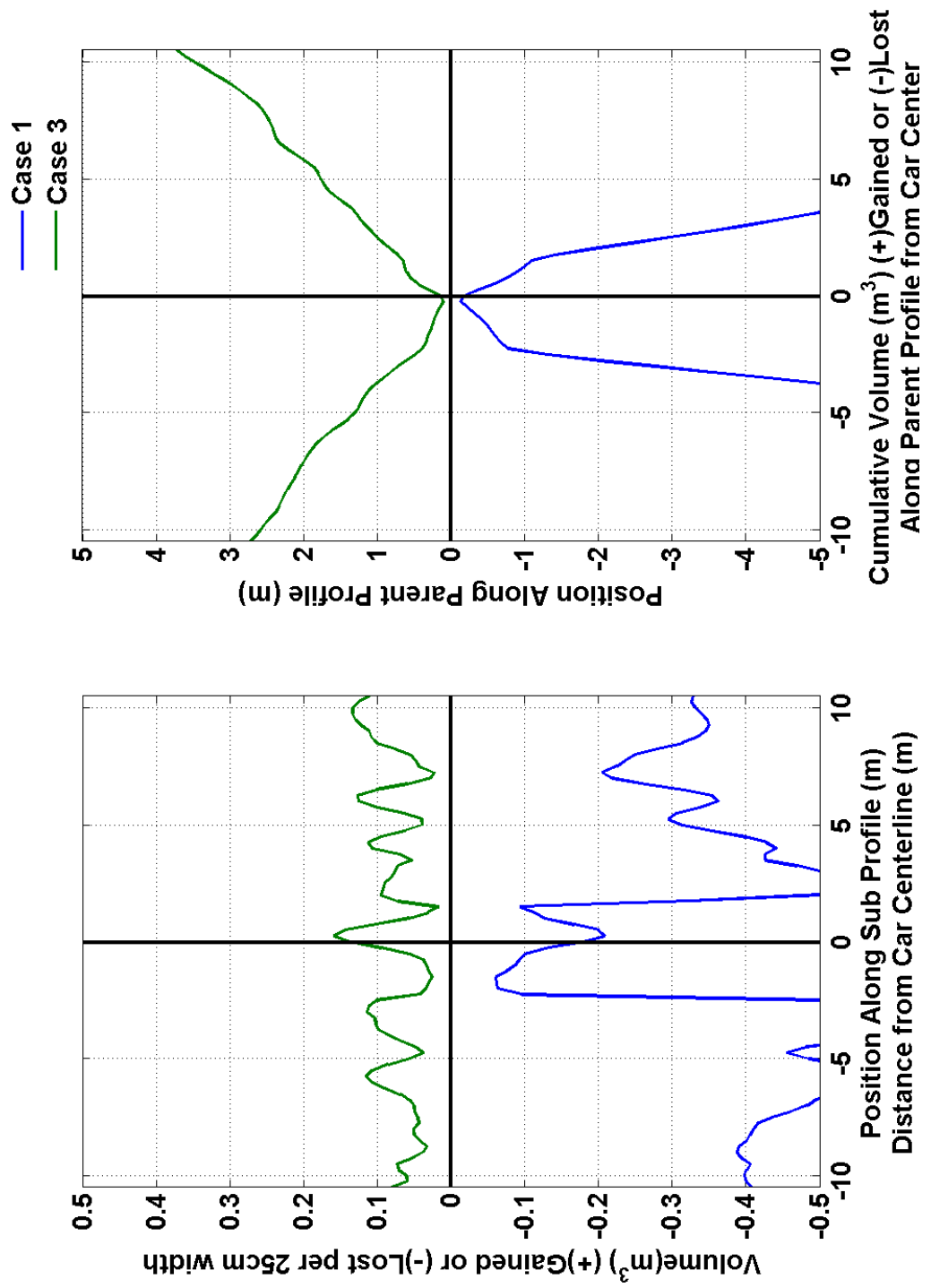
Car #9



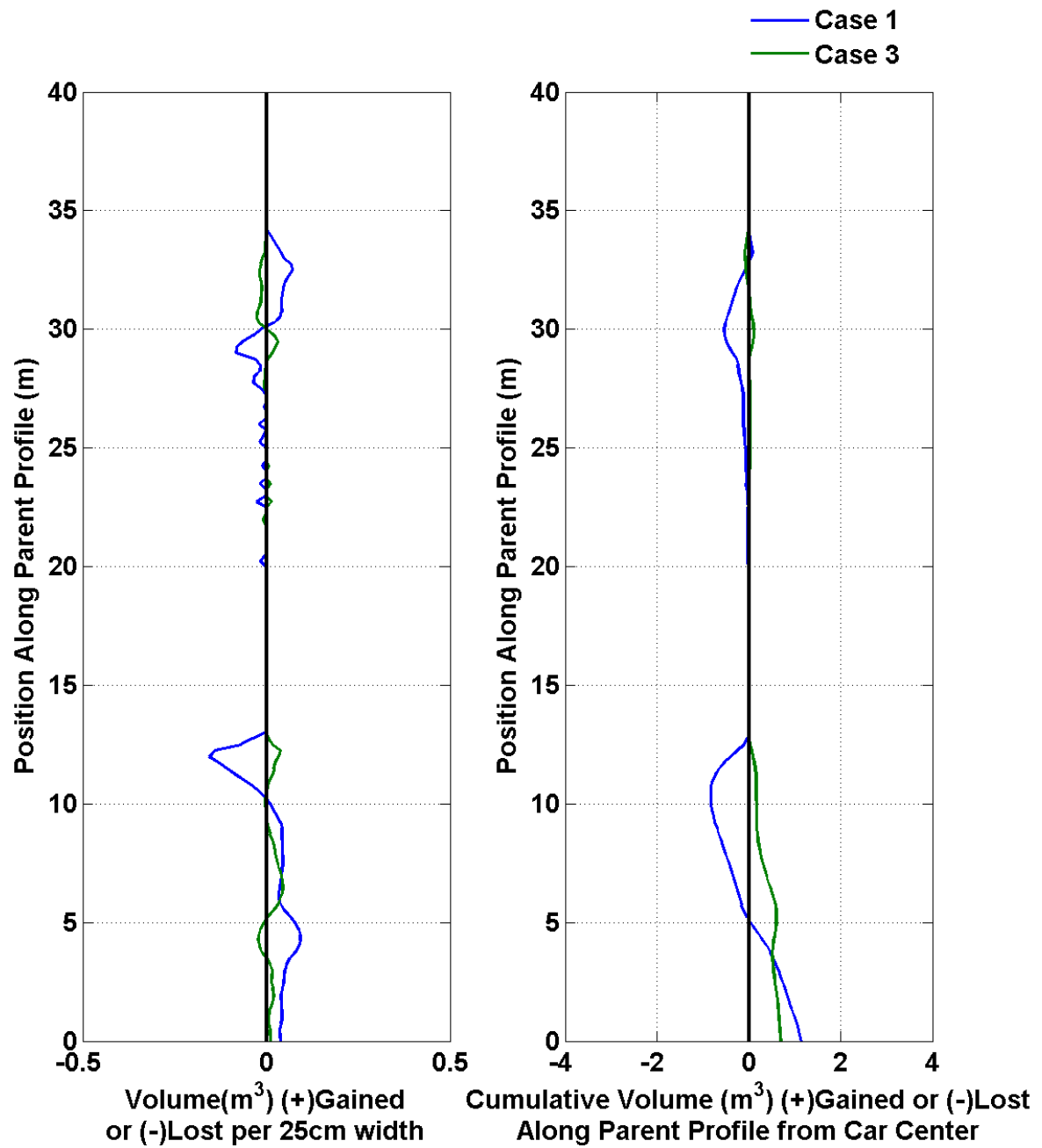
Car #10



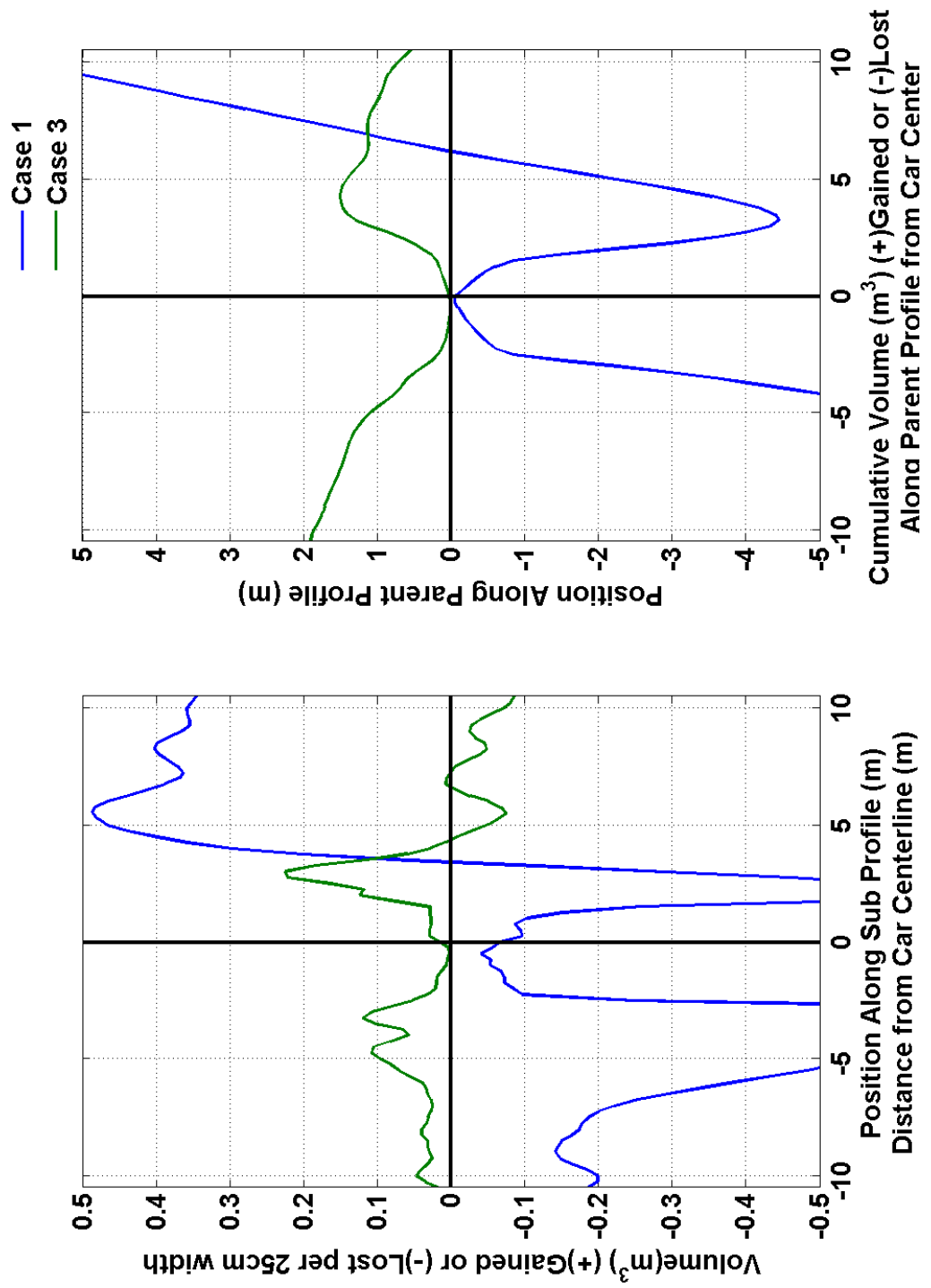
Car #10



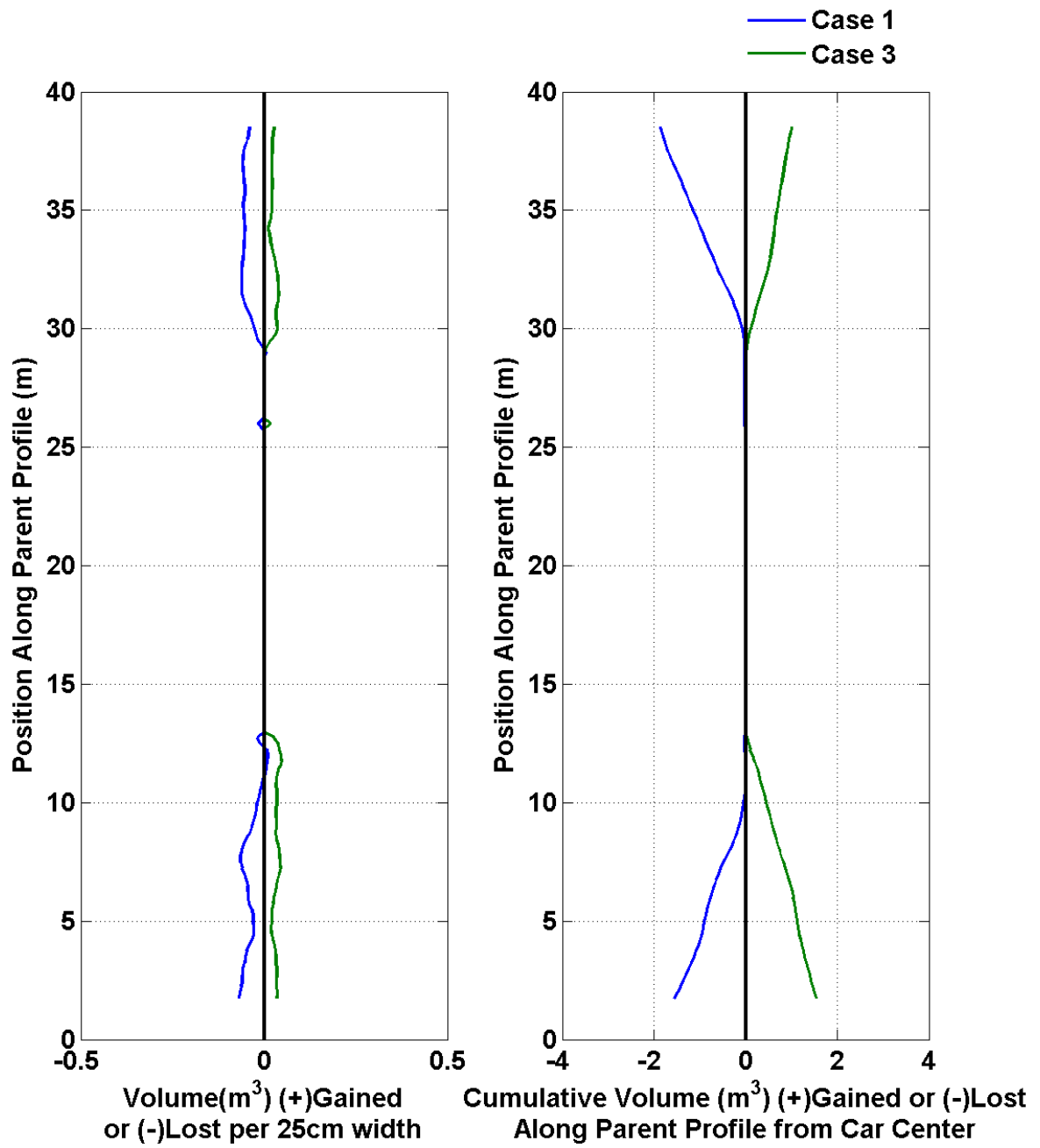
Car #11



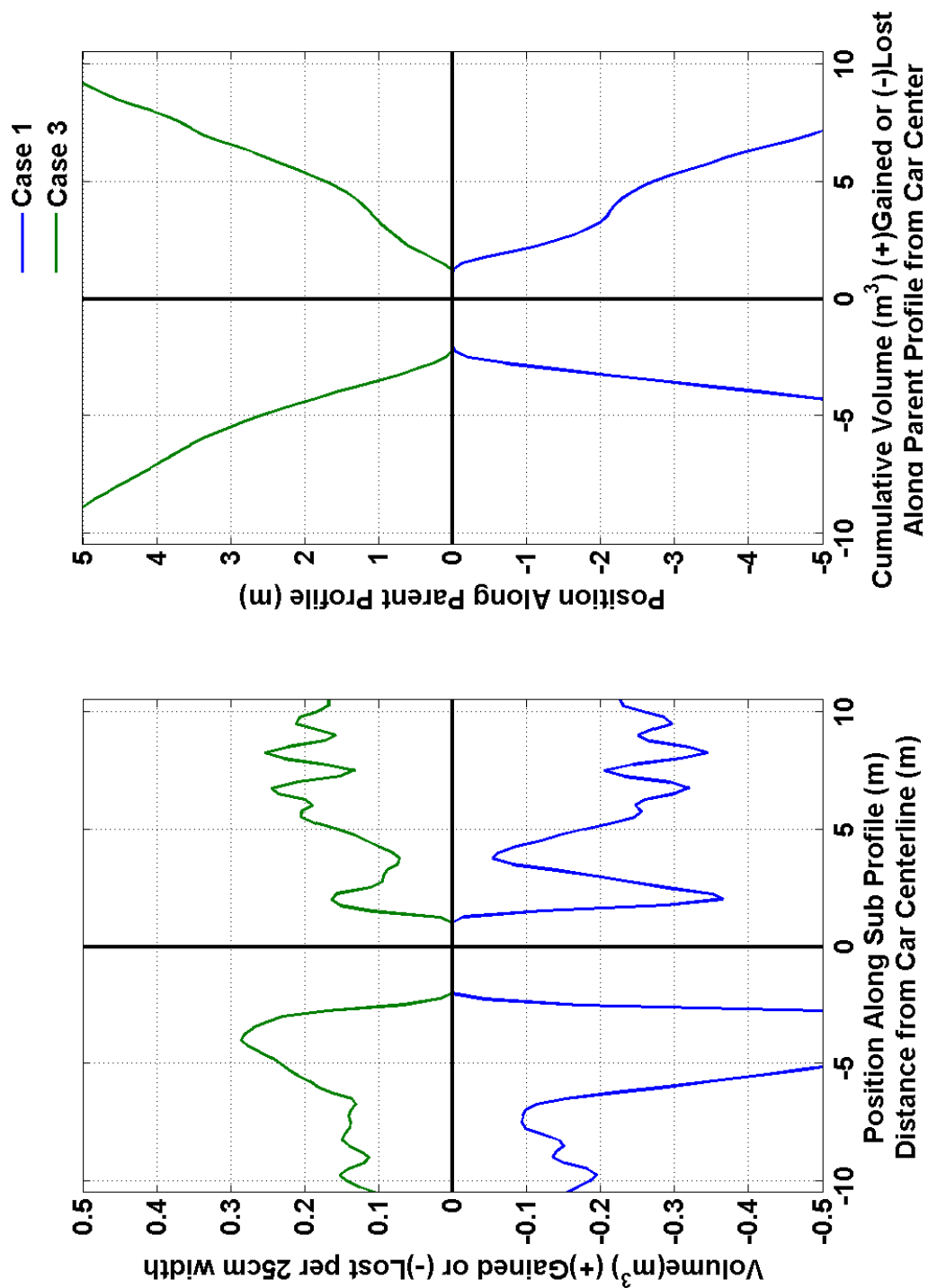
Car #11



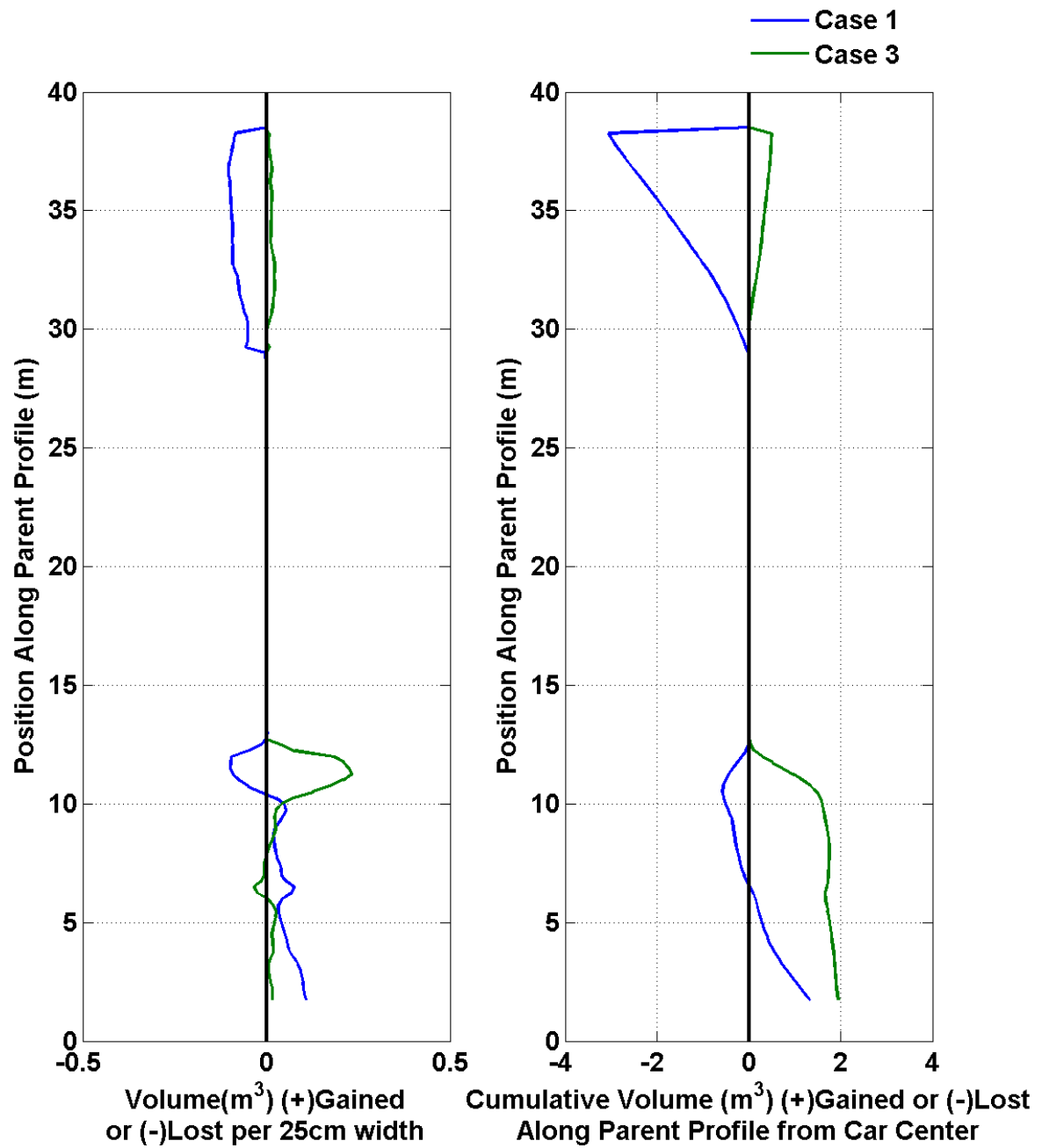
Car #12



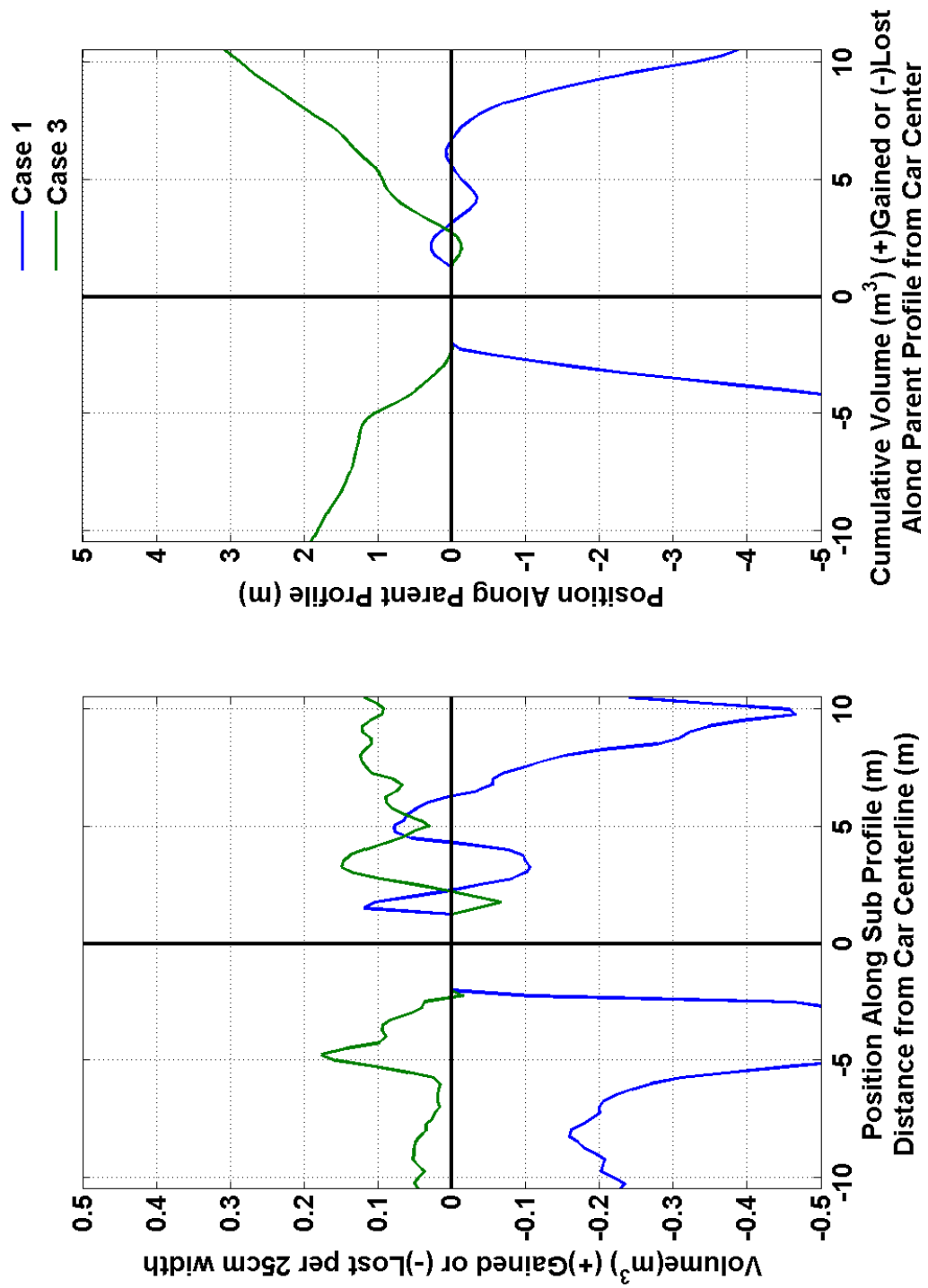
Car #12



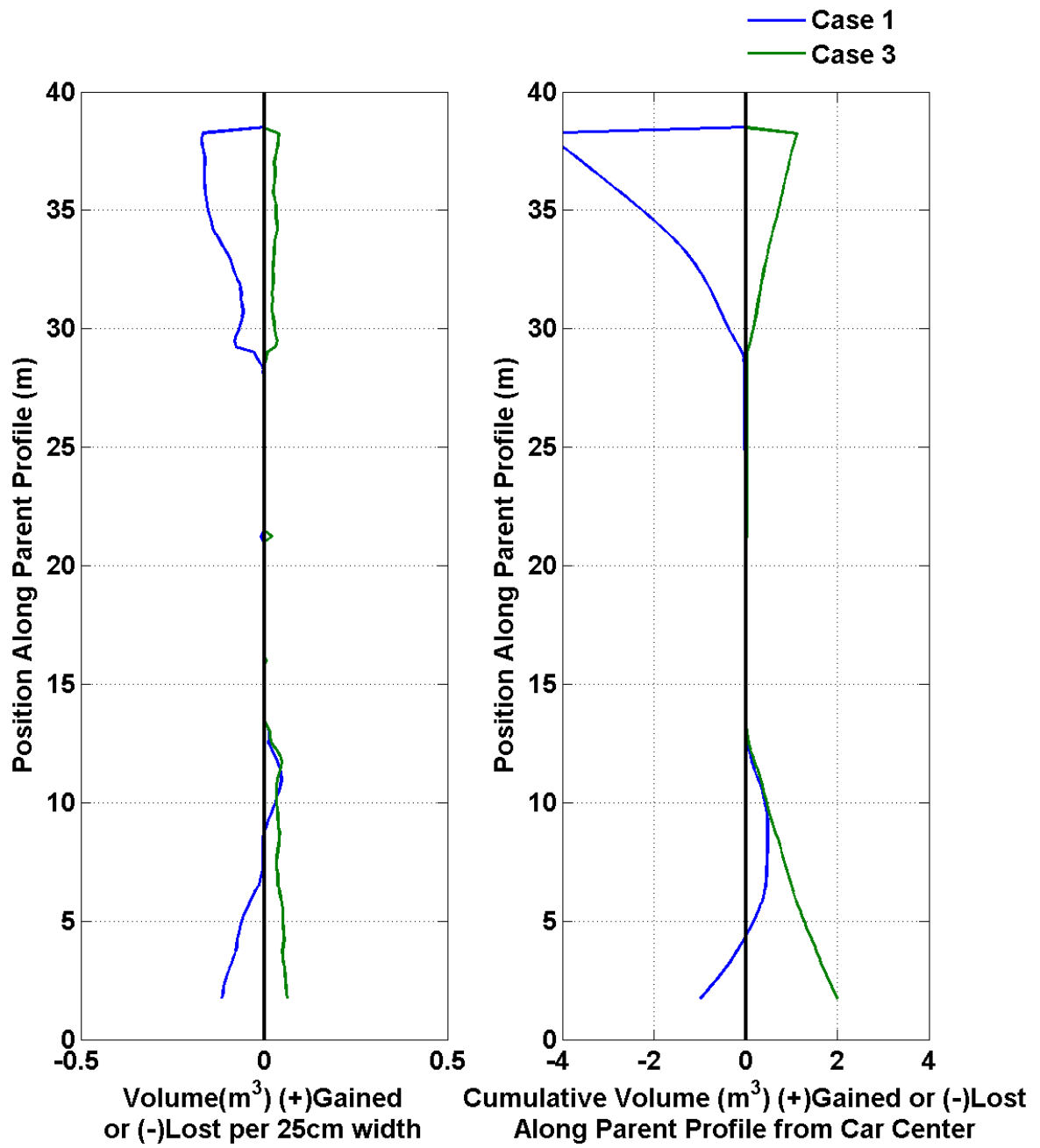
Car #13



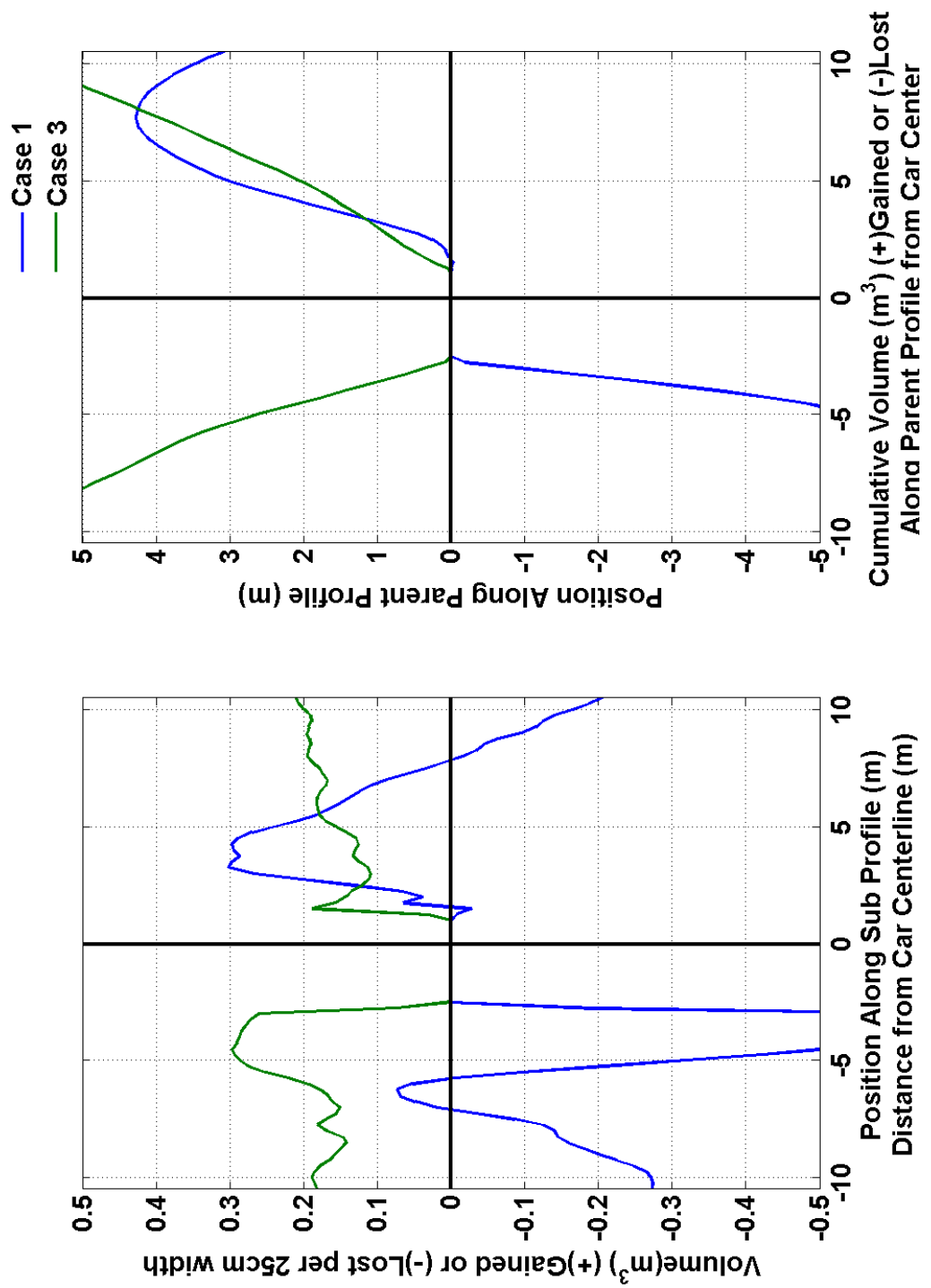
Car #13



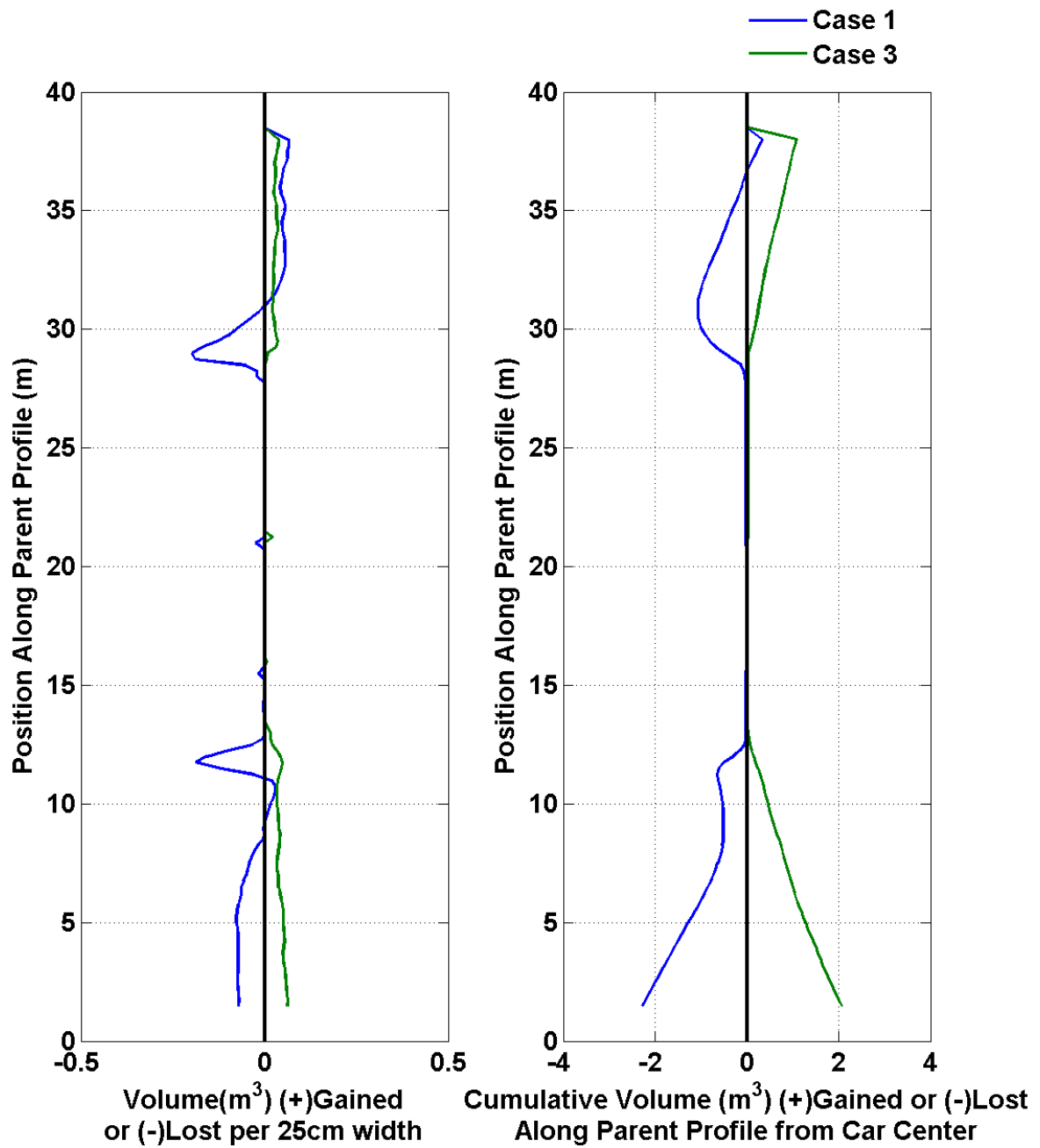
Car #14



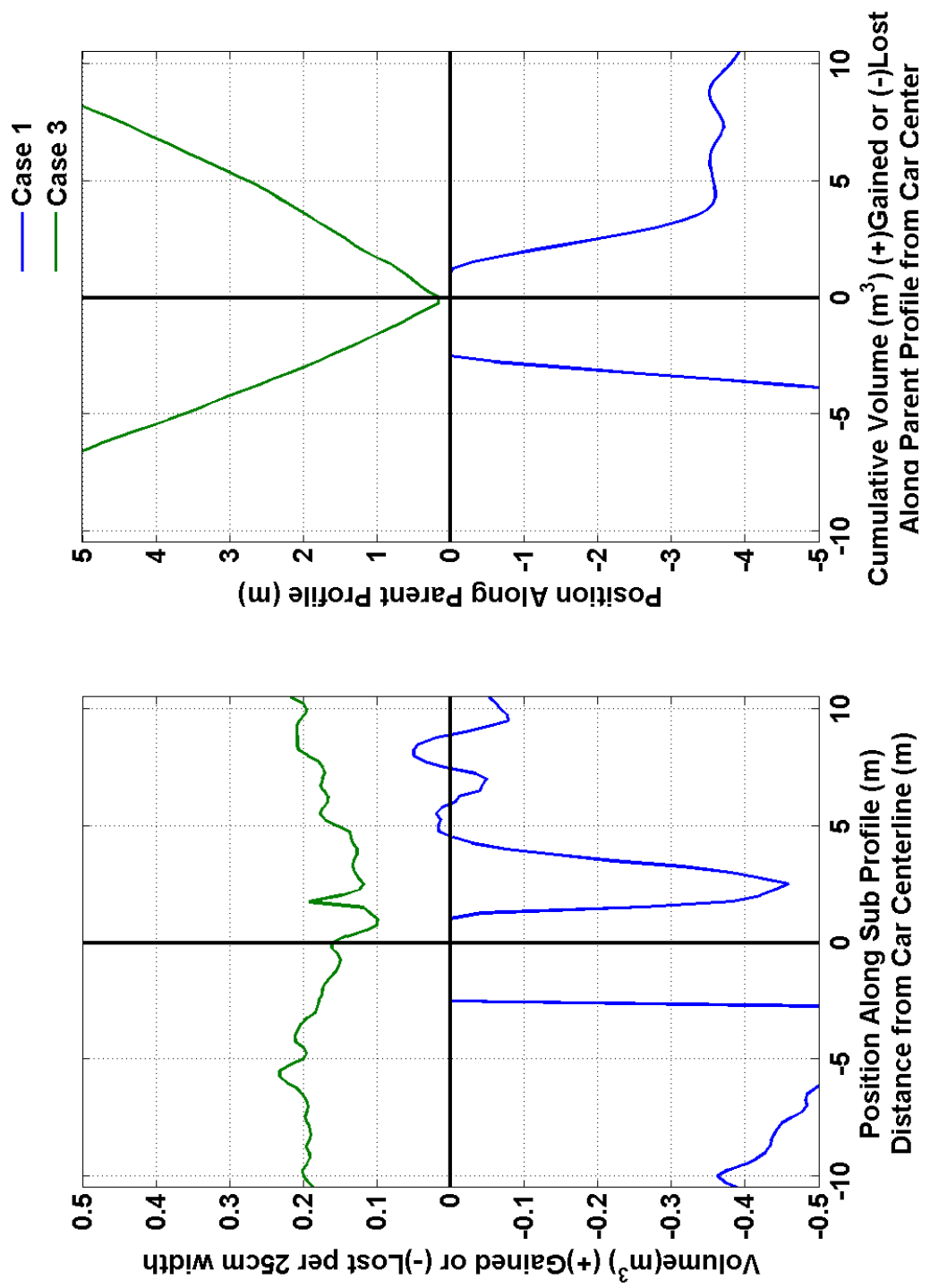
Car #14



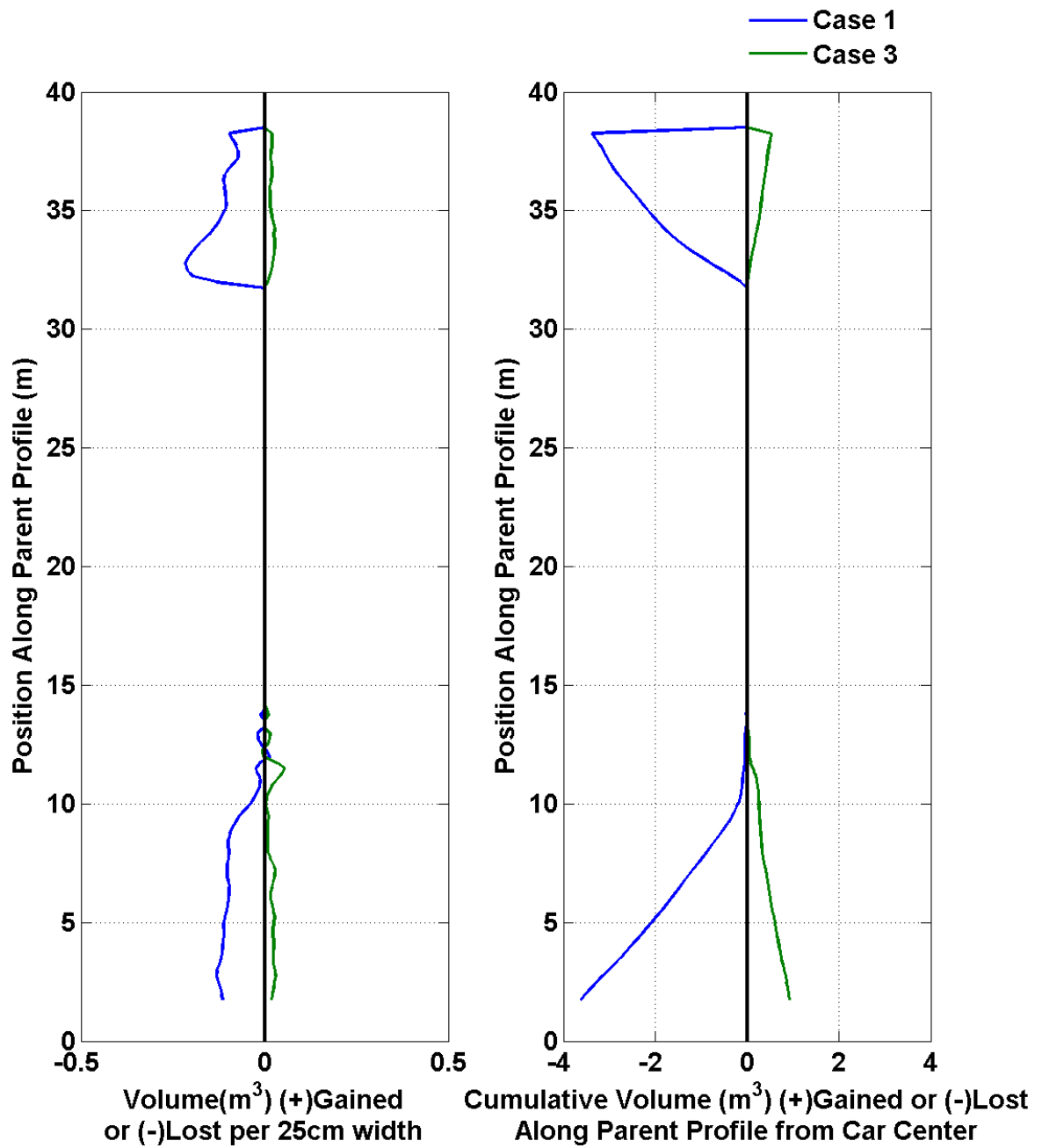
Car #15



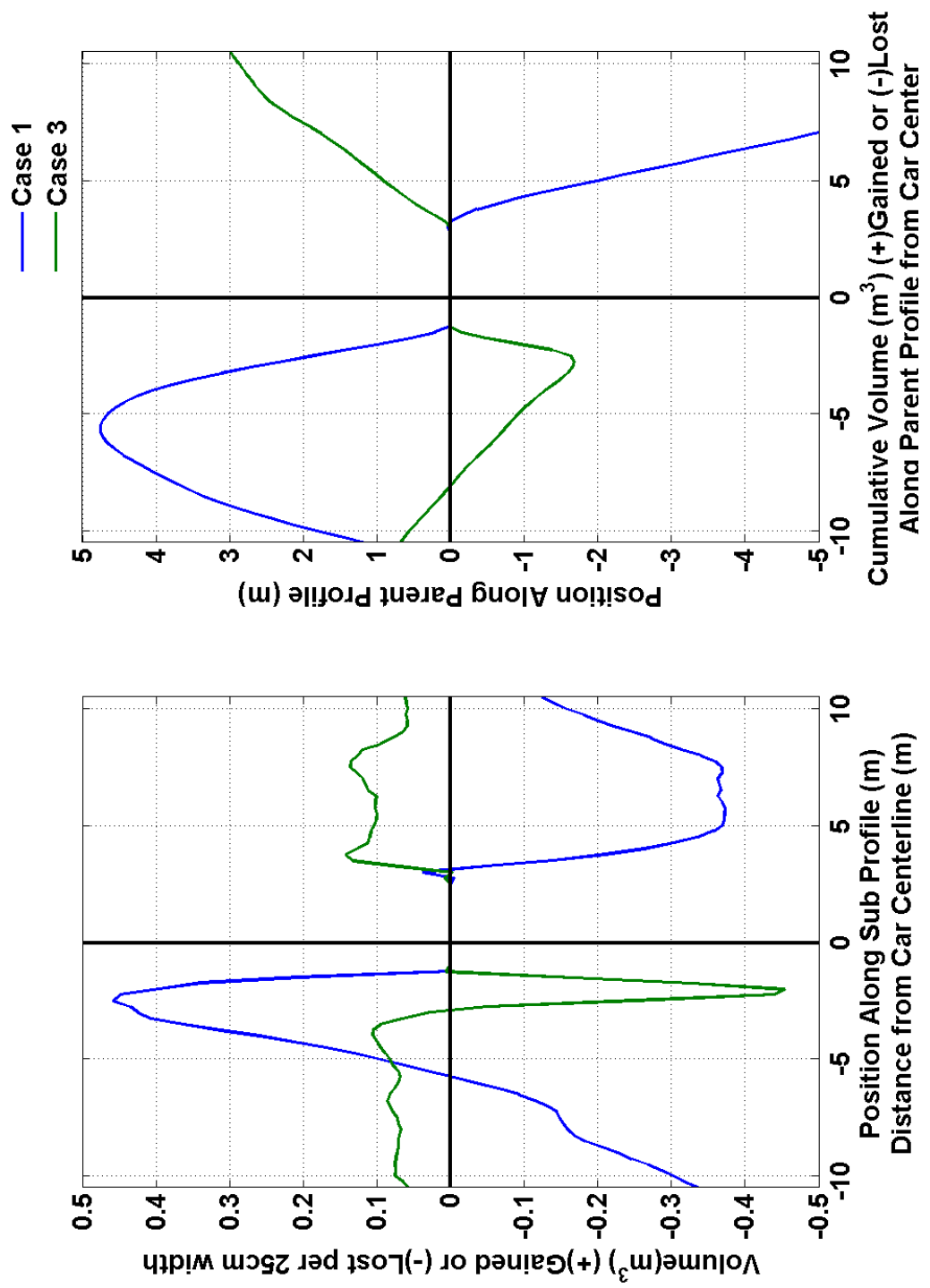
Car #15



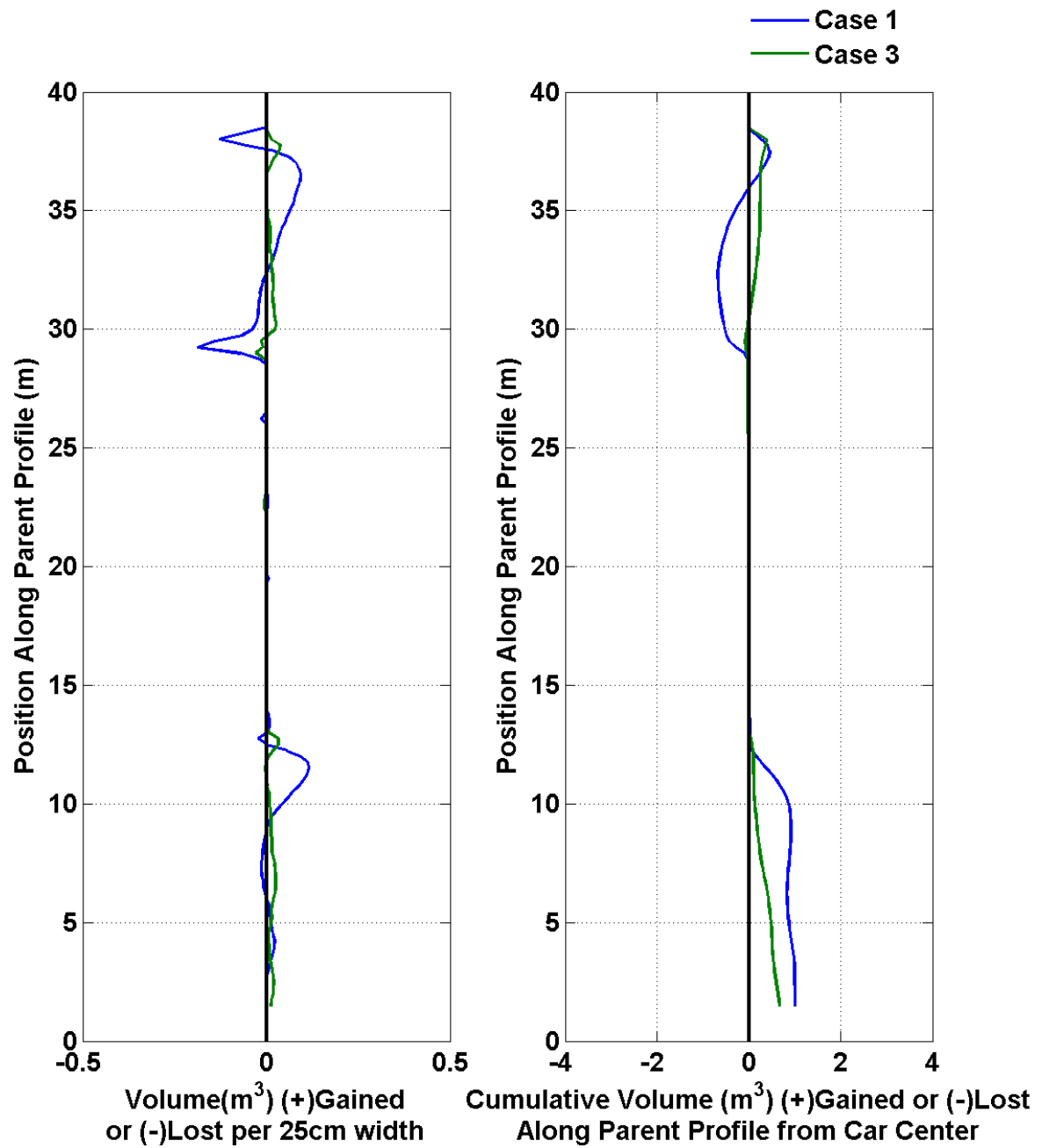
Car #16



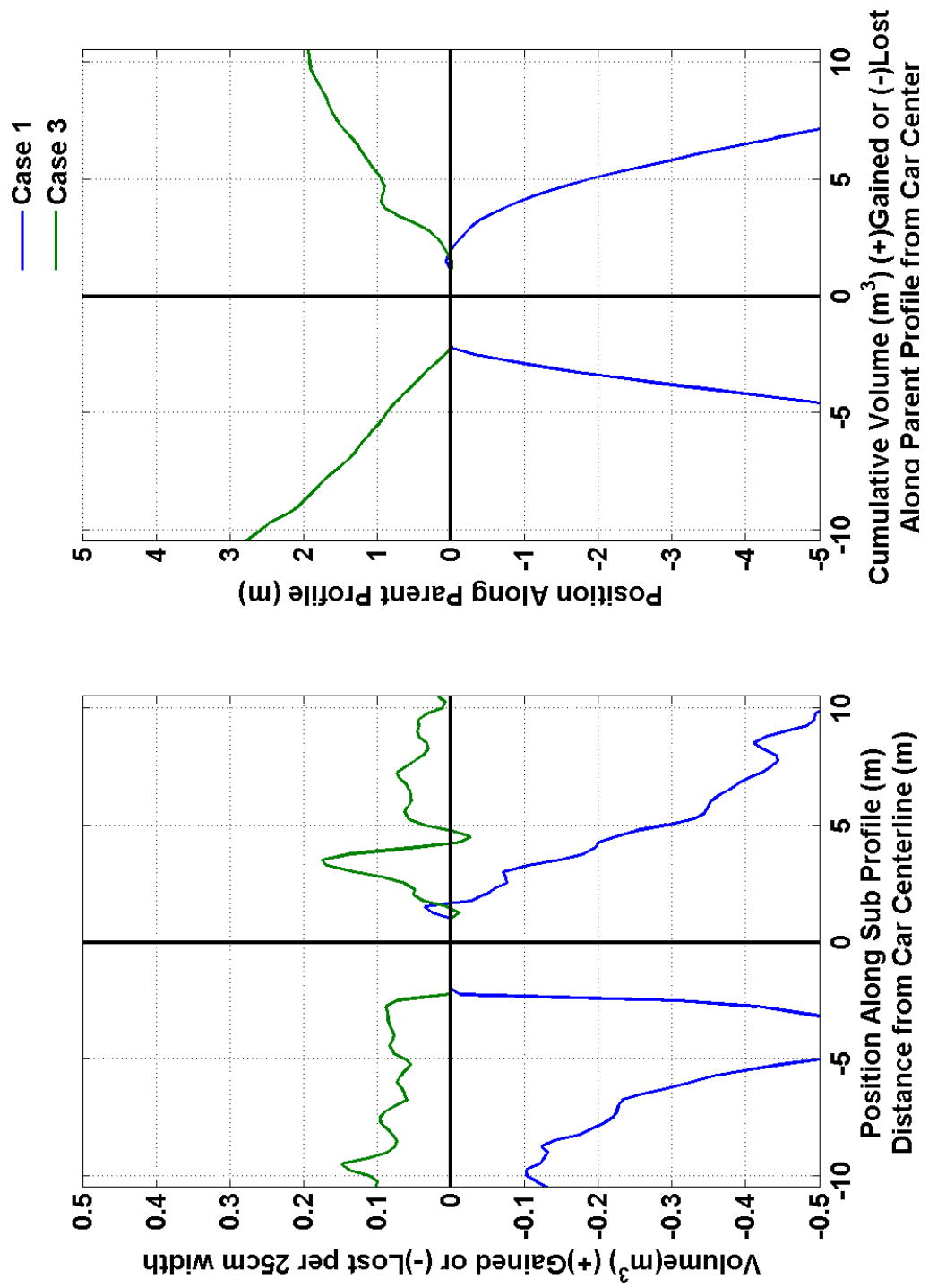
Car #16



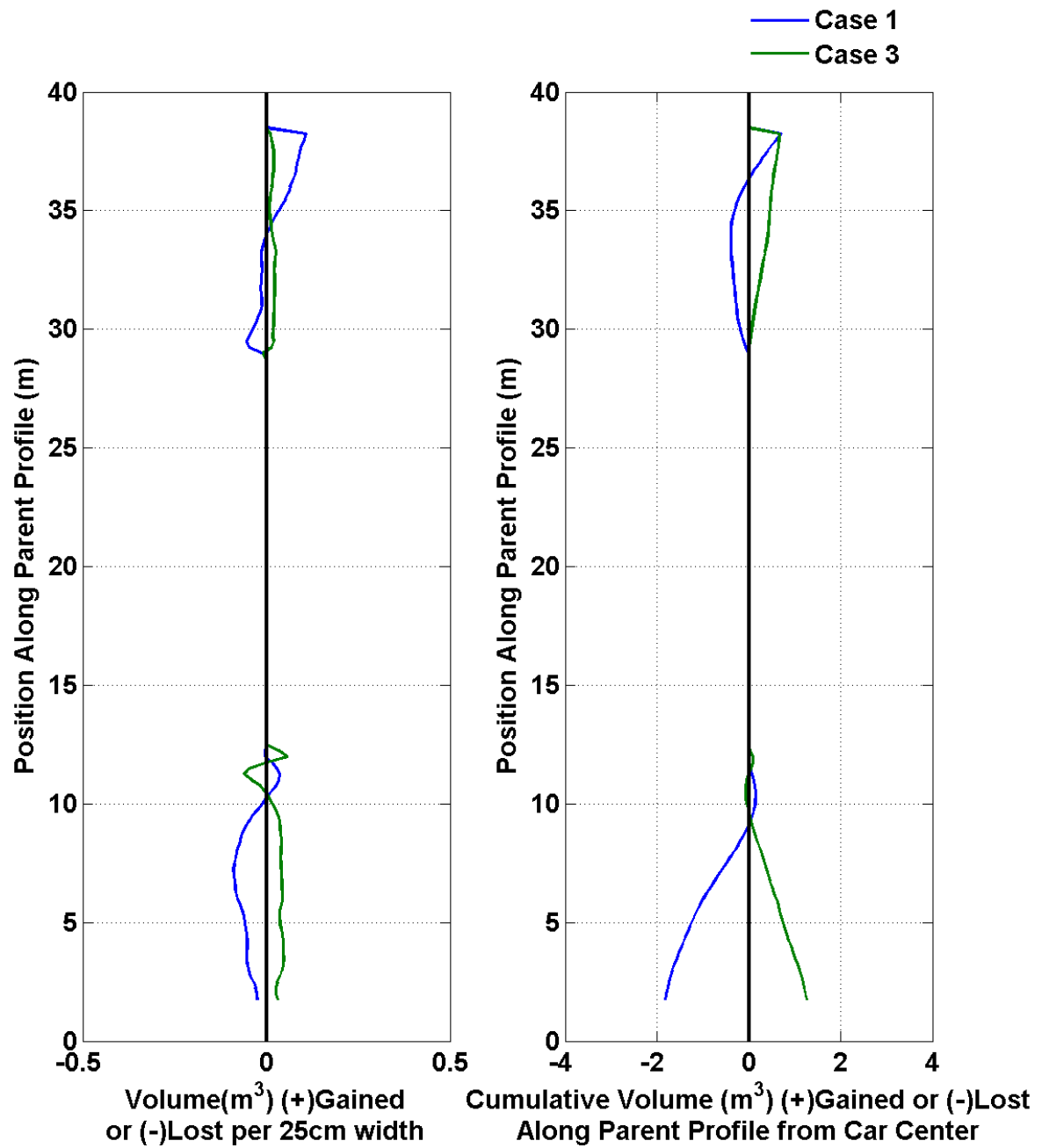
Car #17



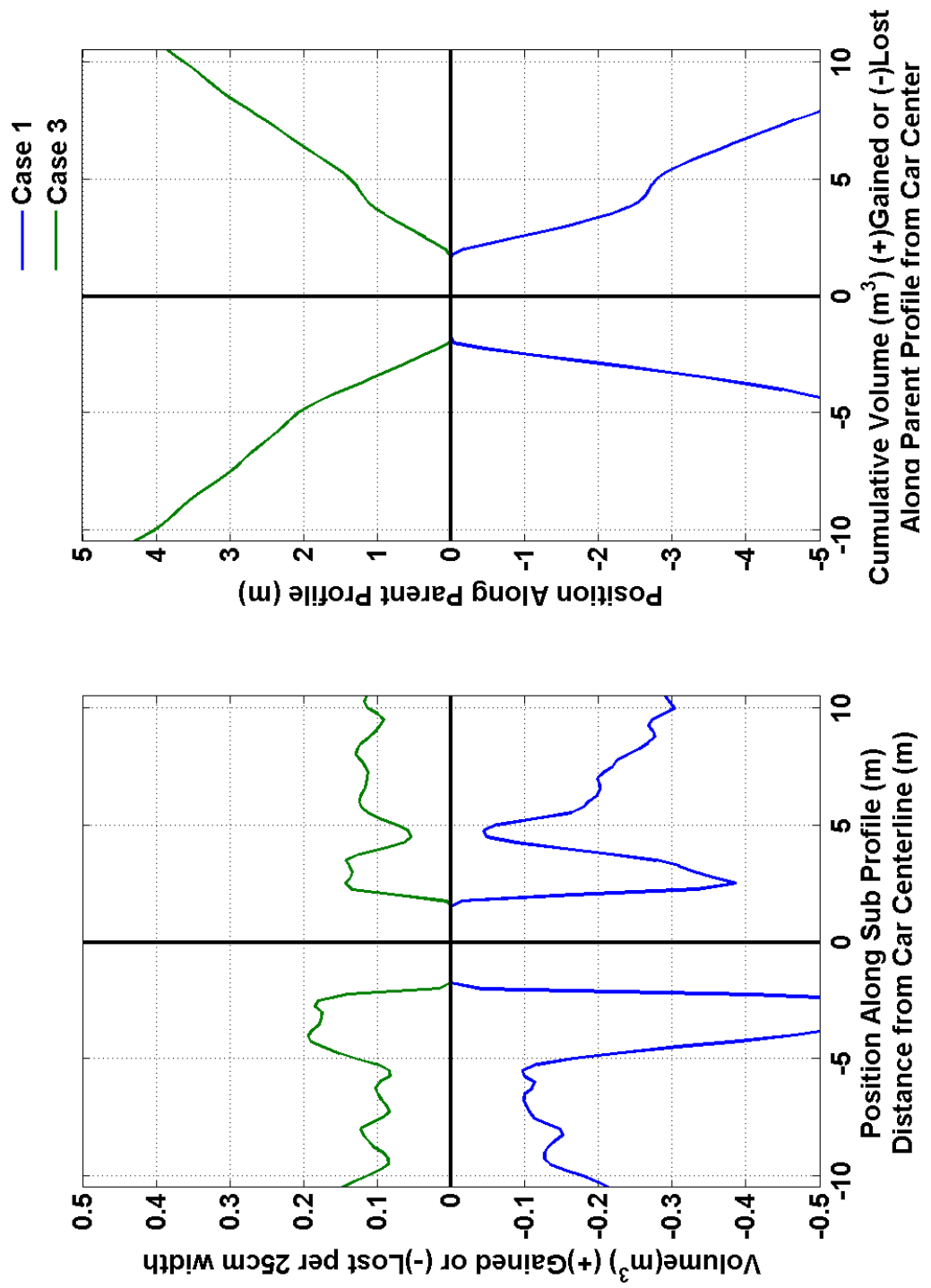
Car #17



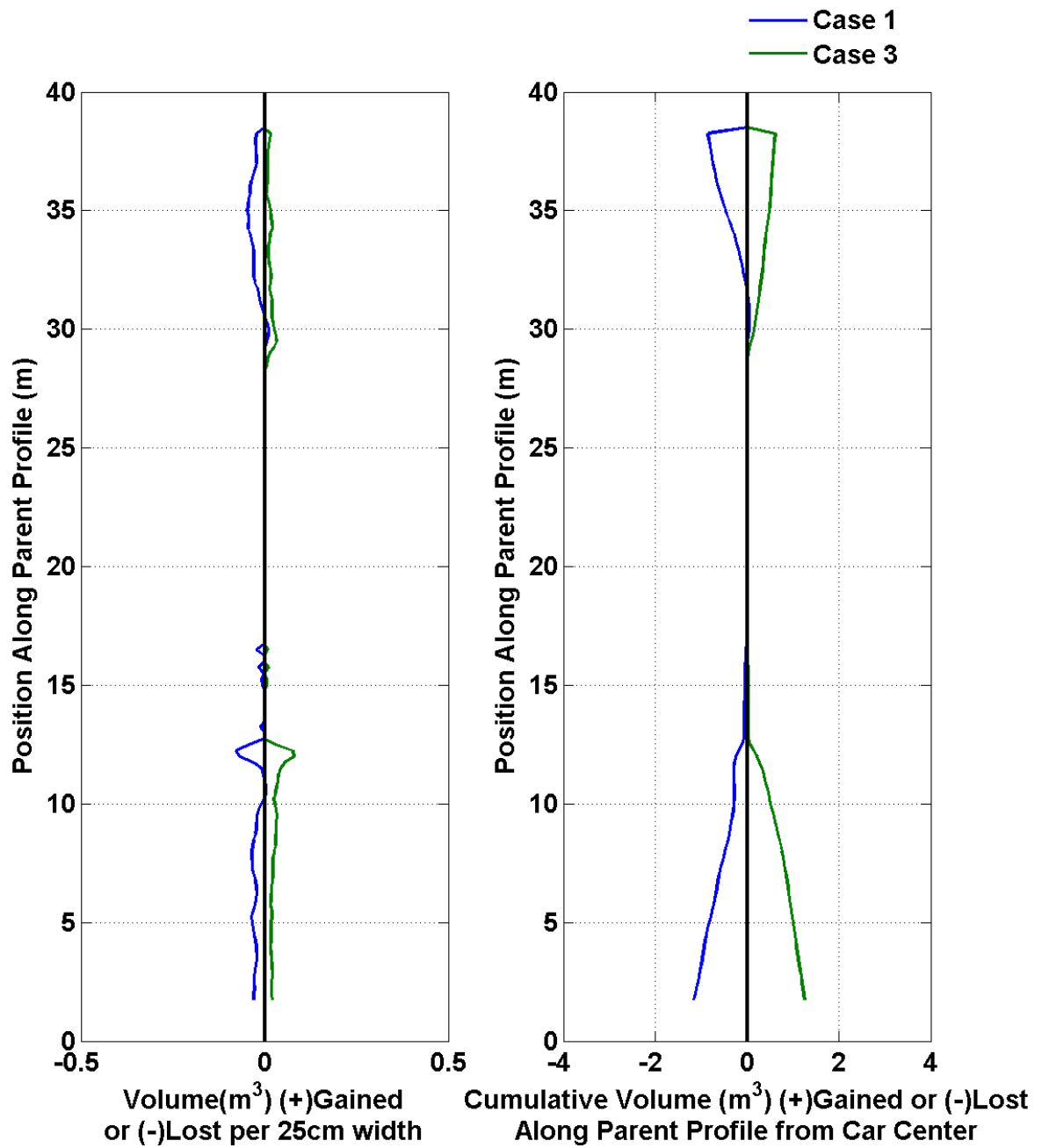
Car #18



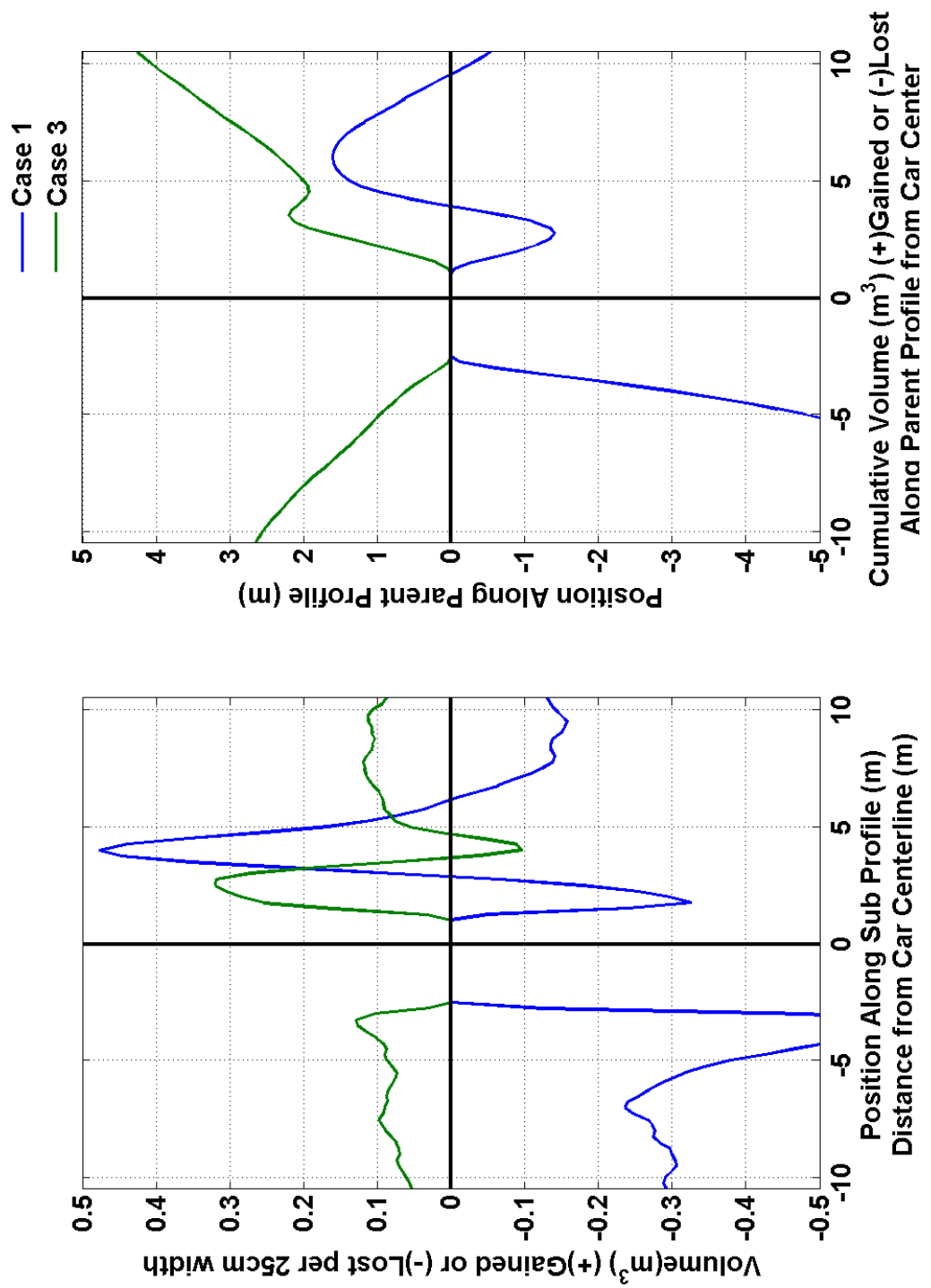
Car #18



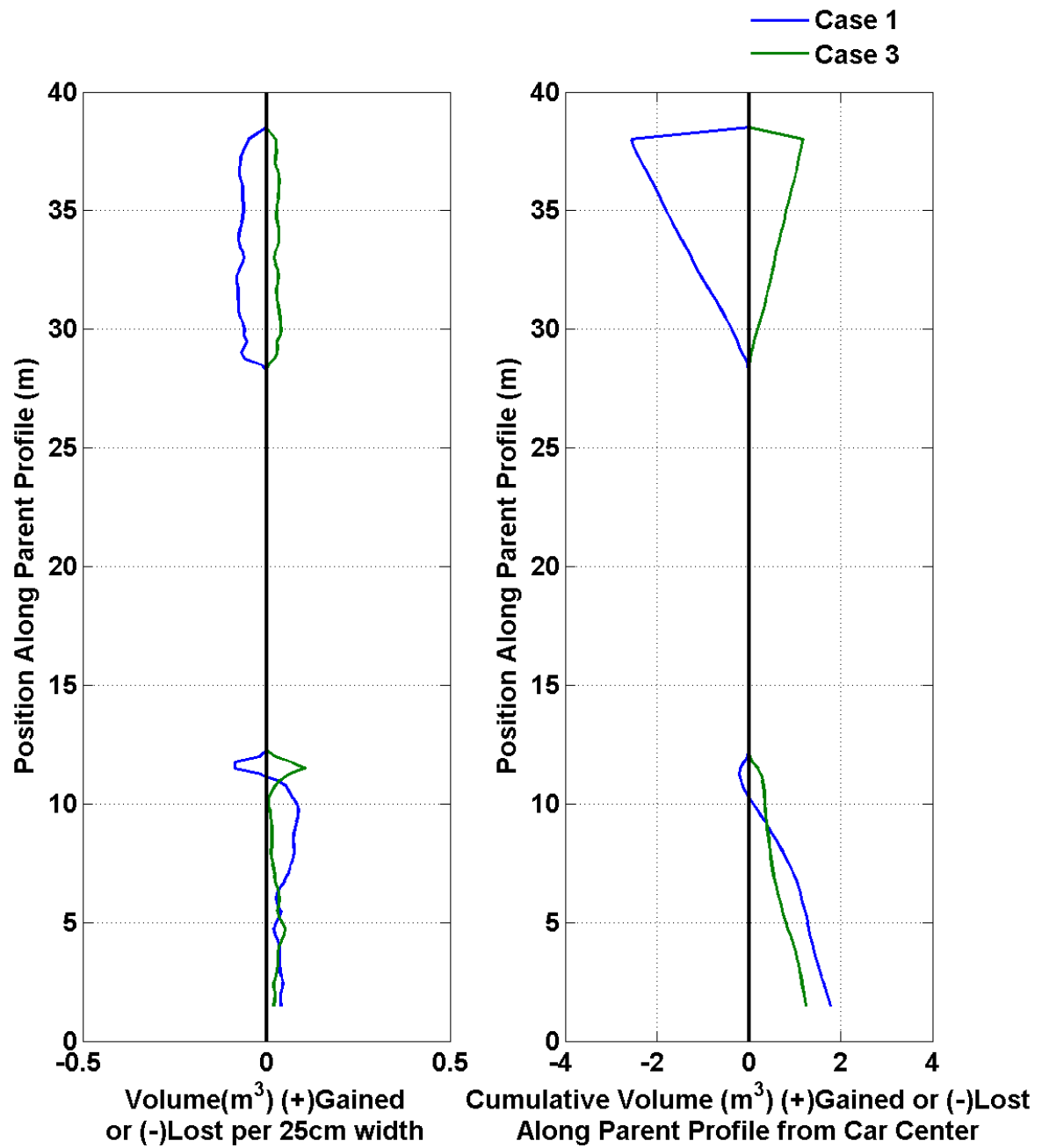
Car #19



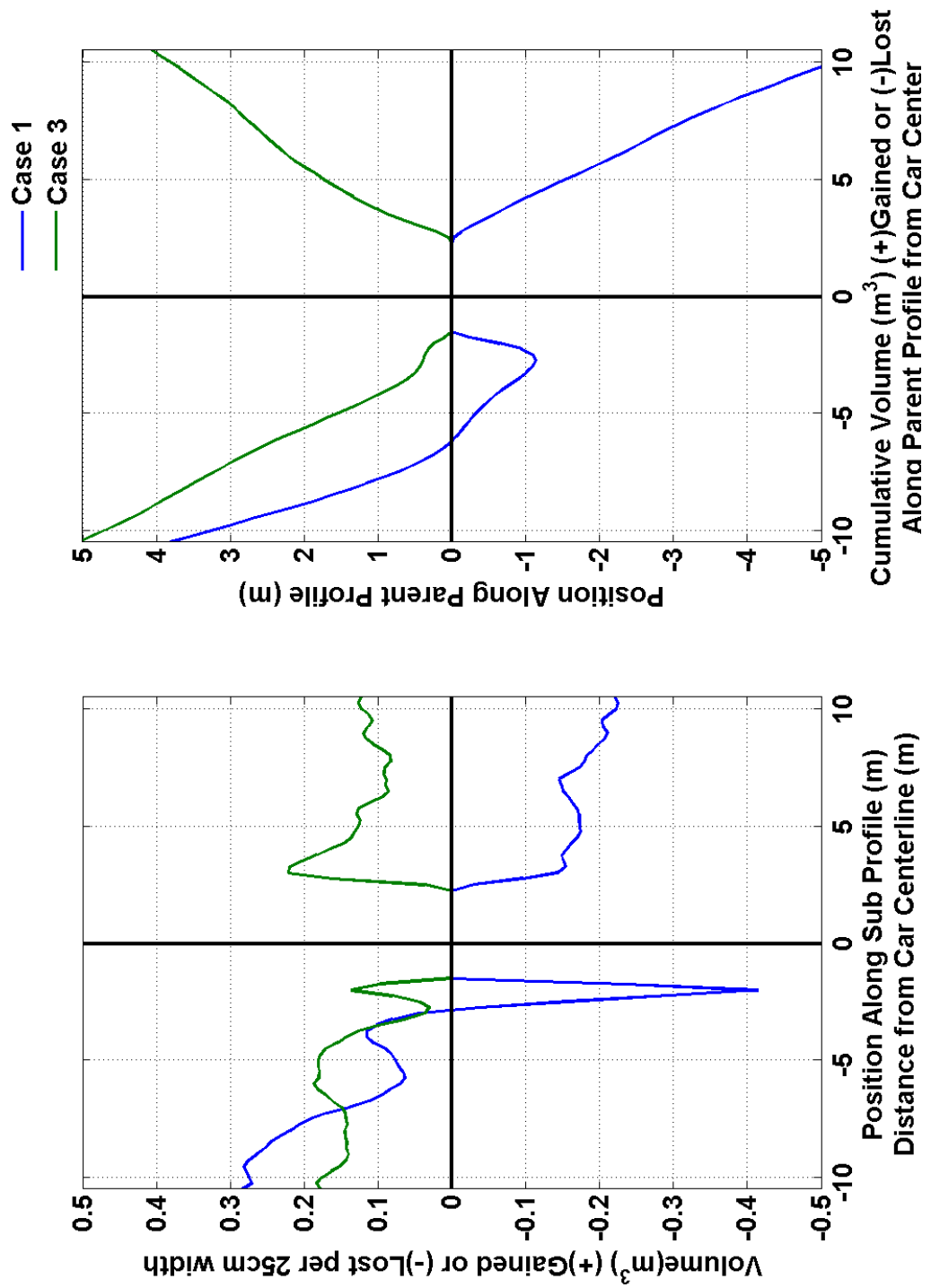
Car #19



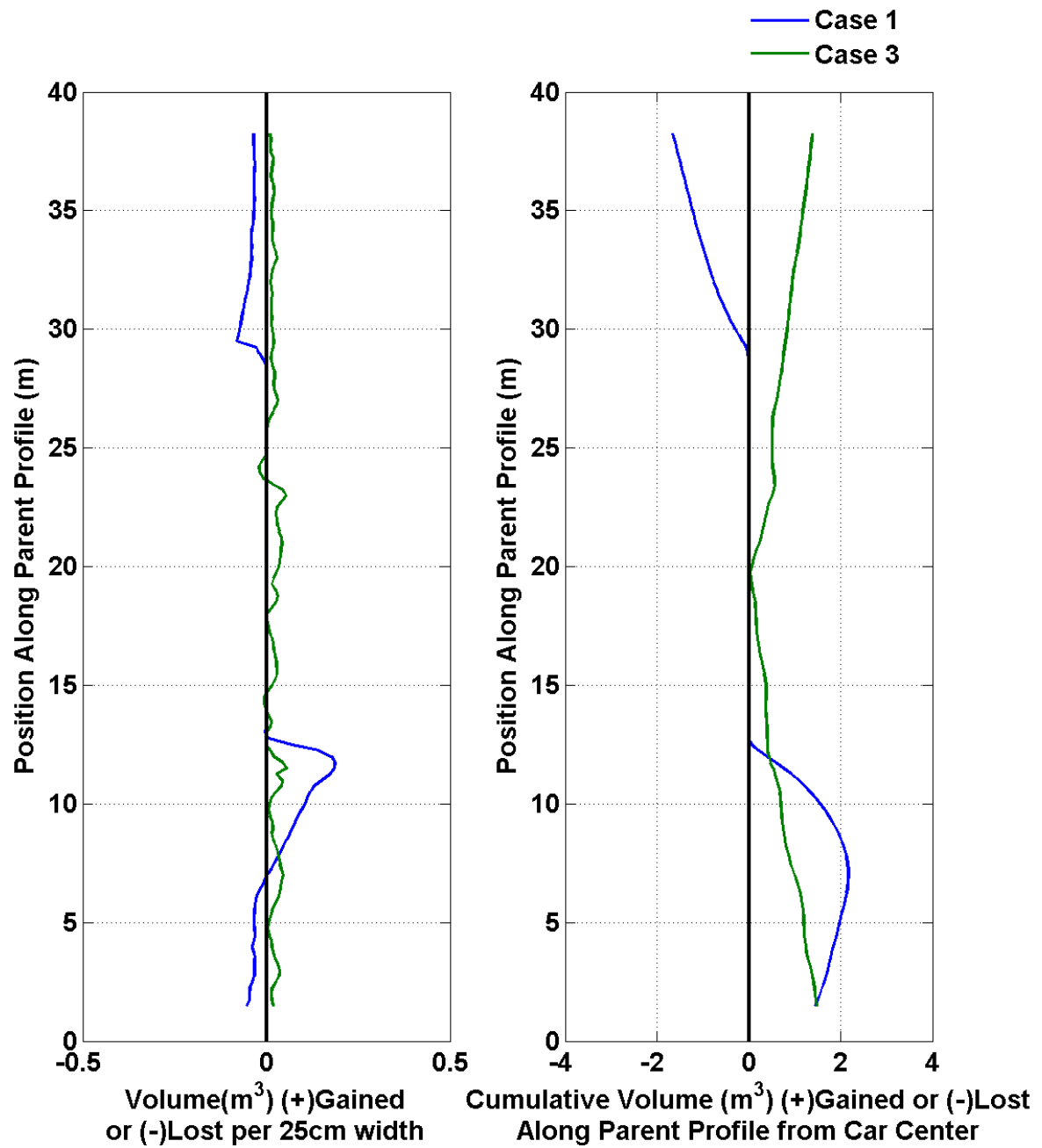
Car #20



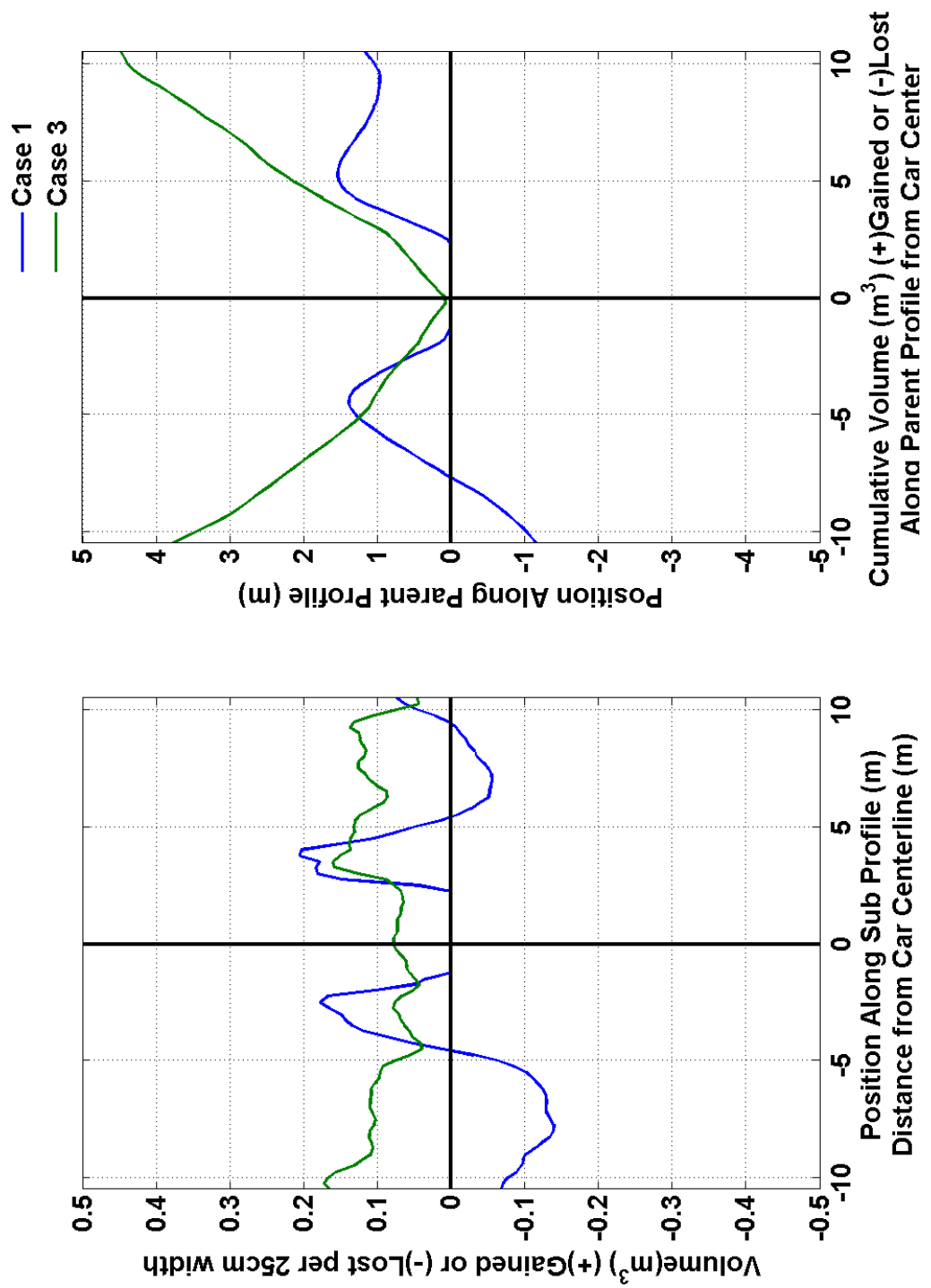
Car #20



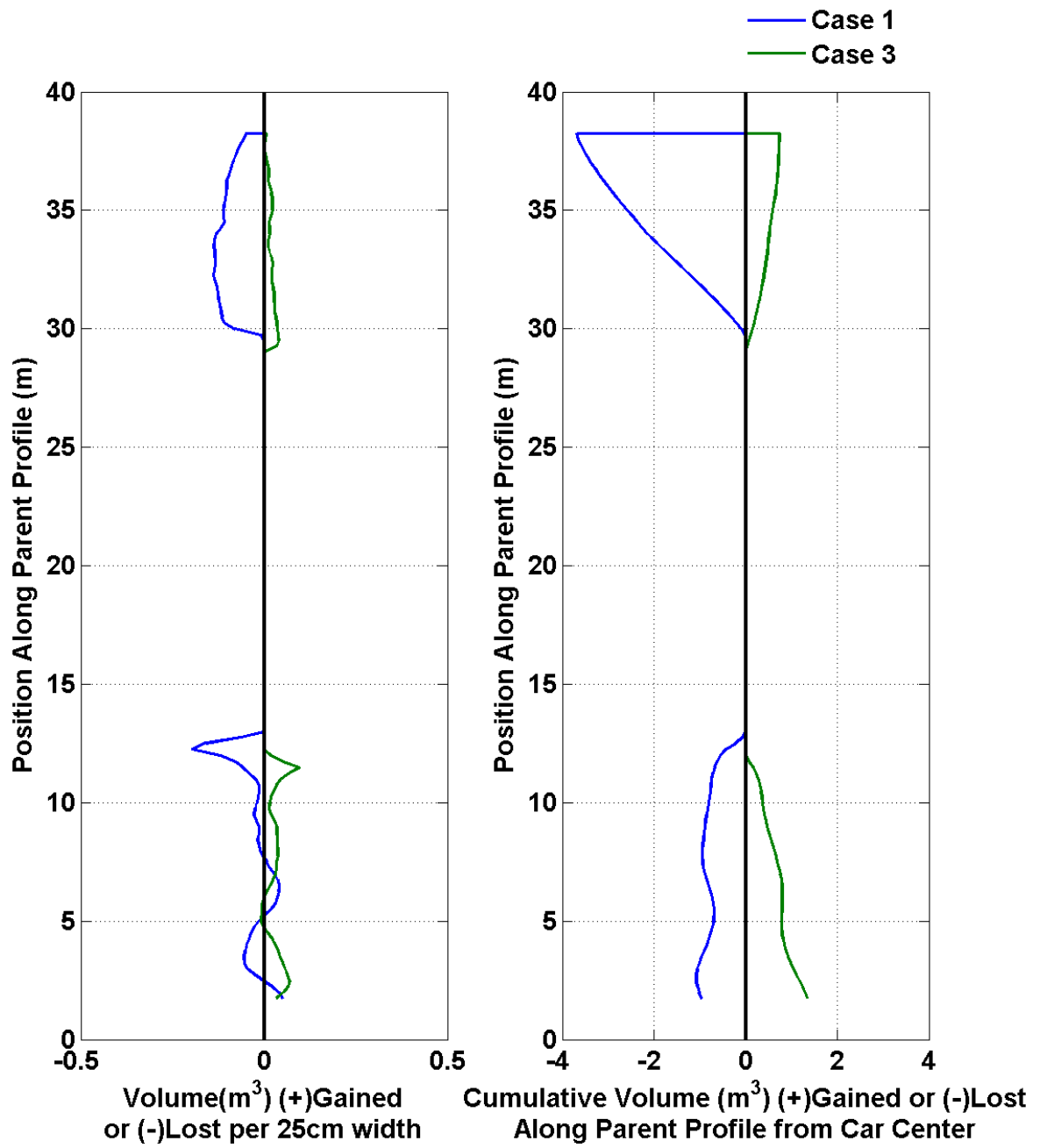
Car #21



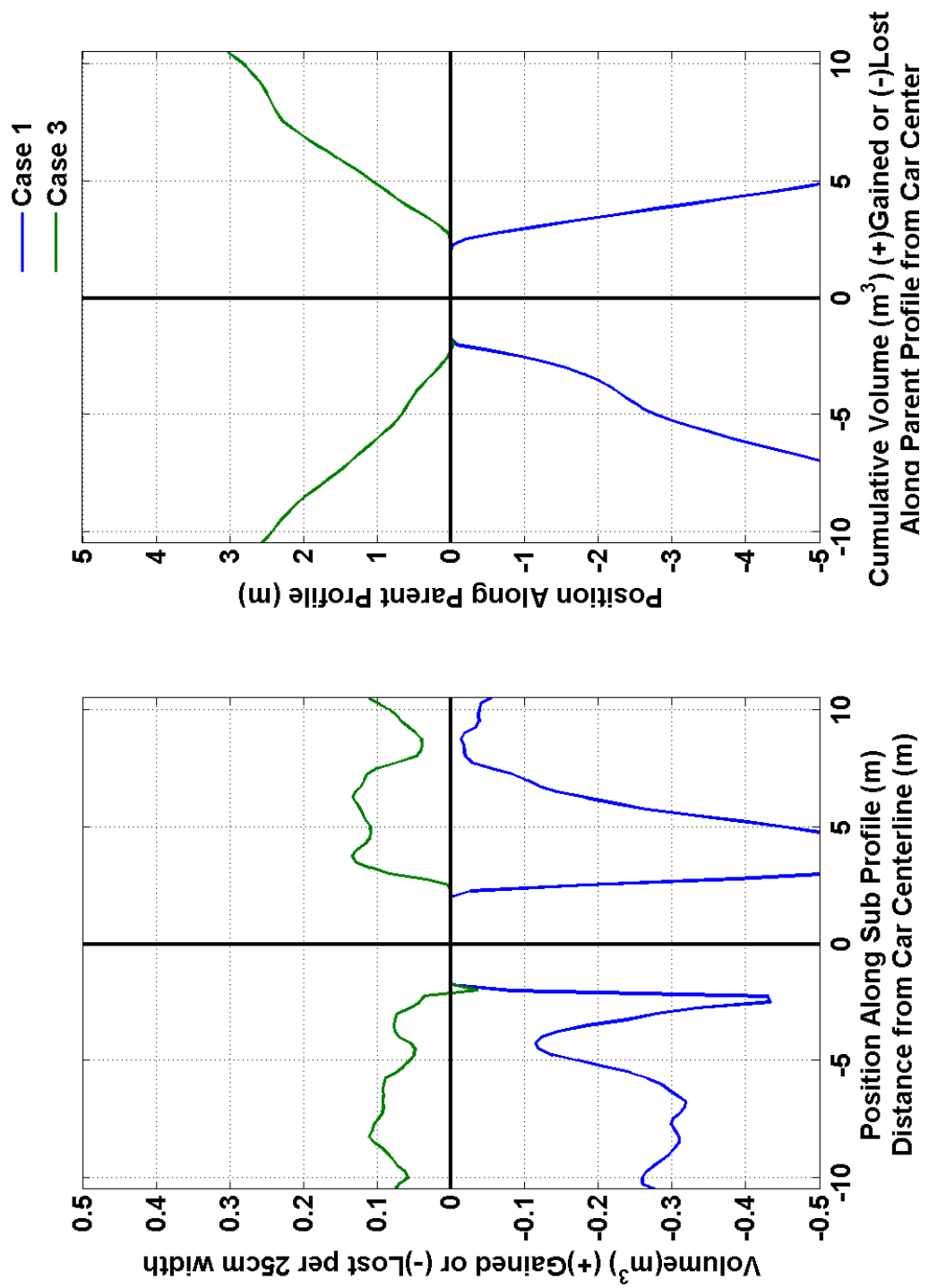
Car #21



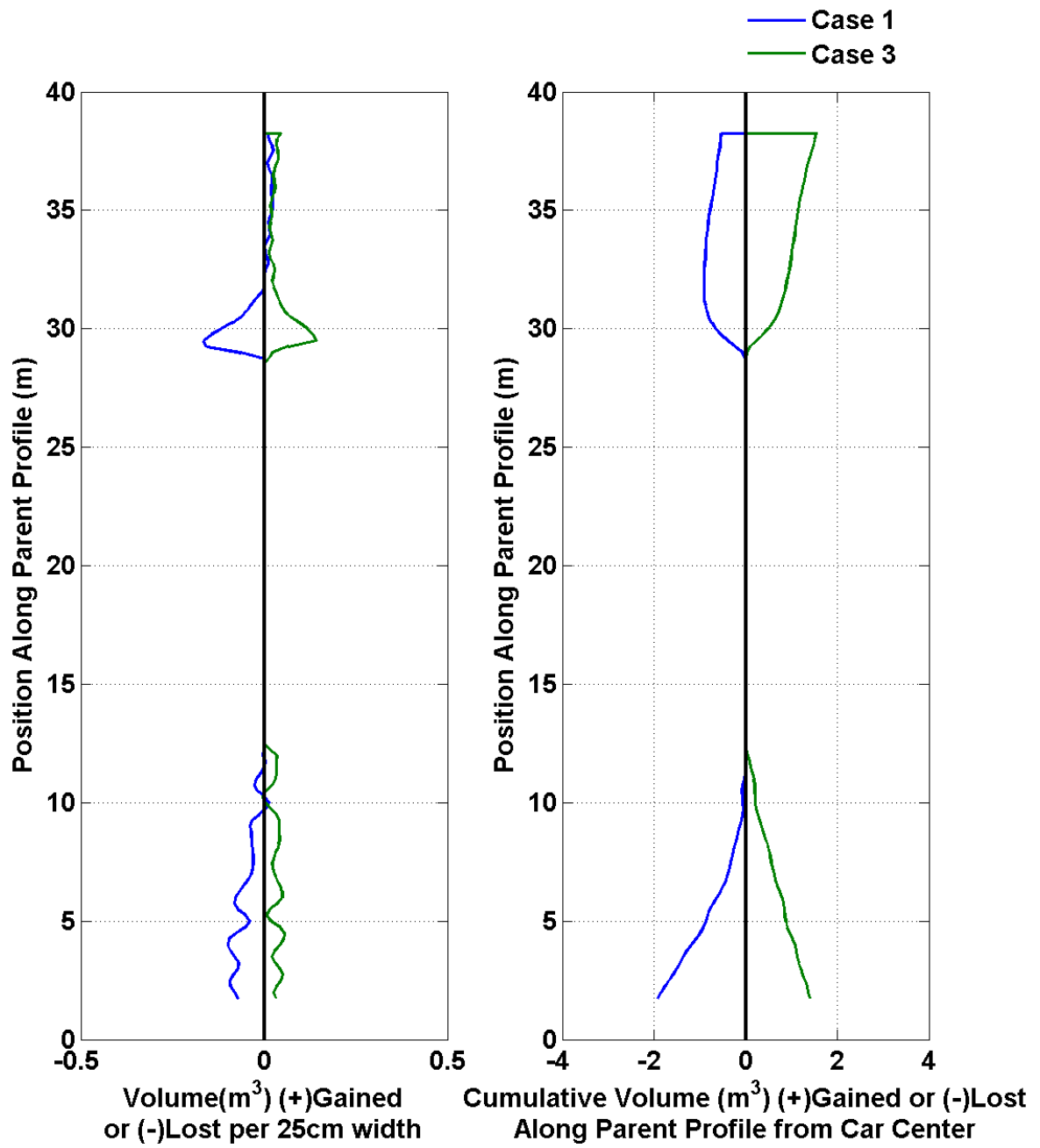
Car #22



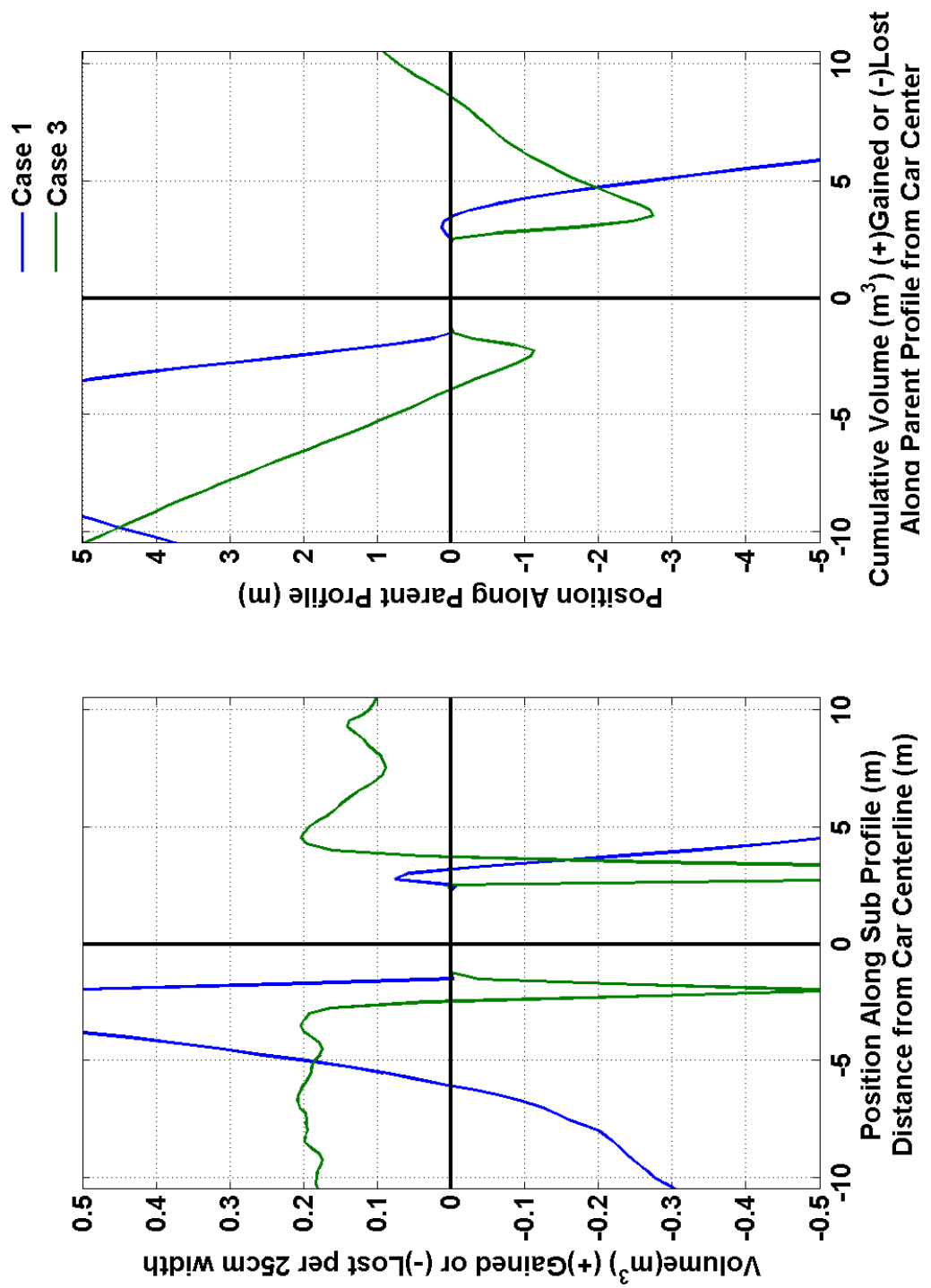
Car #22



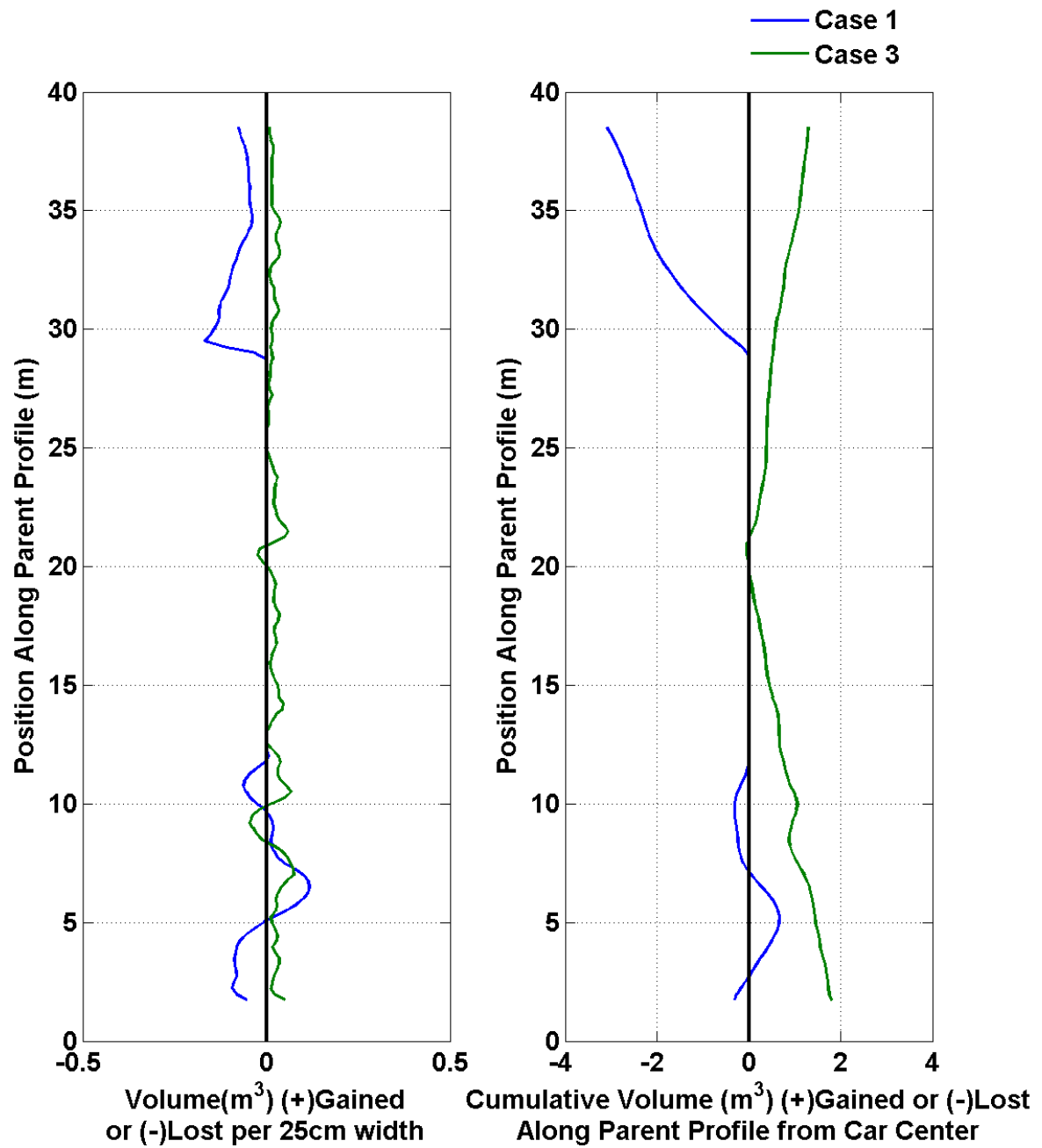
Car #23



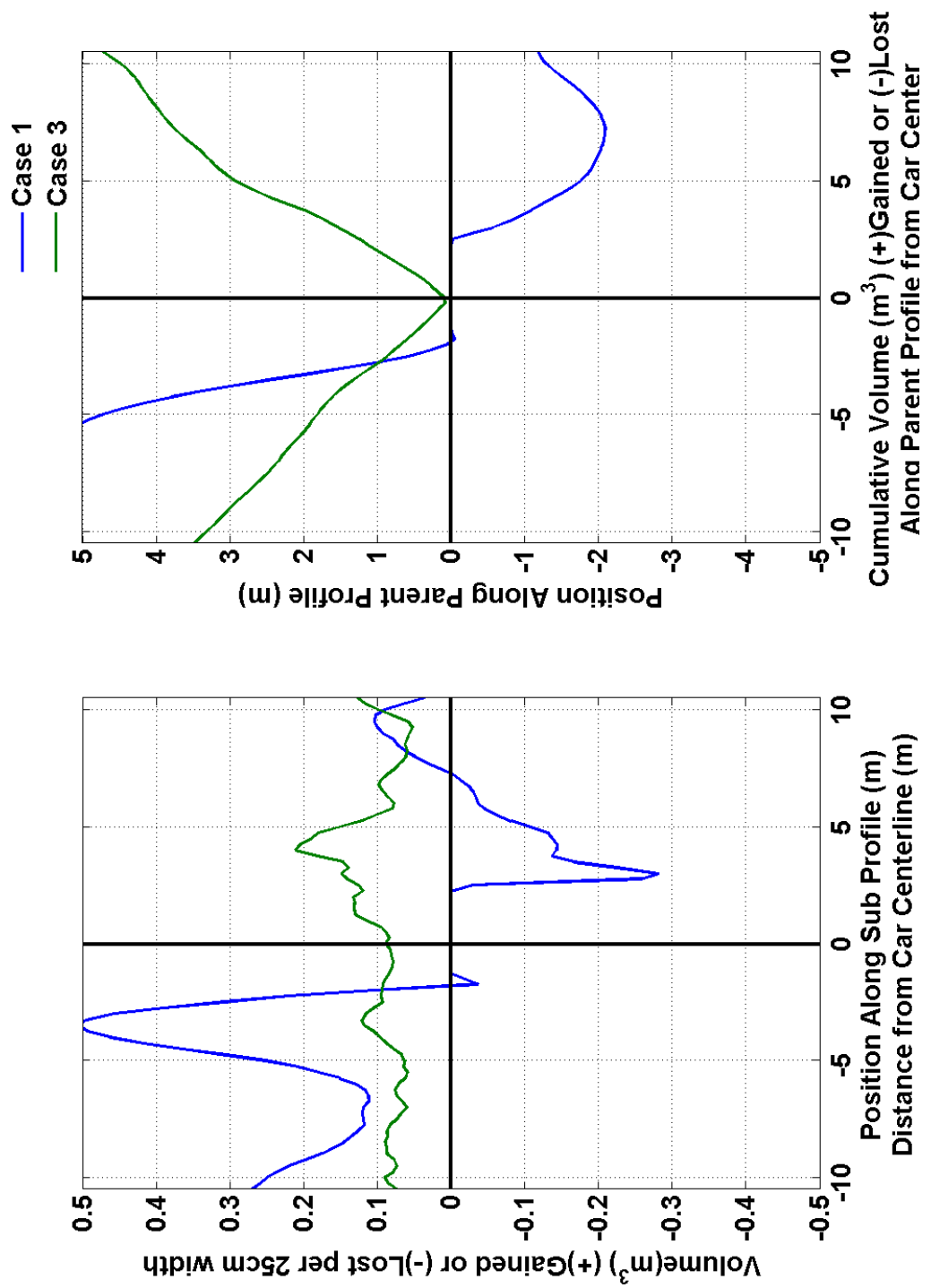
Car #23



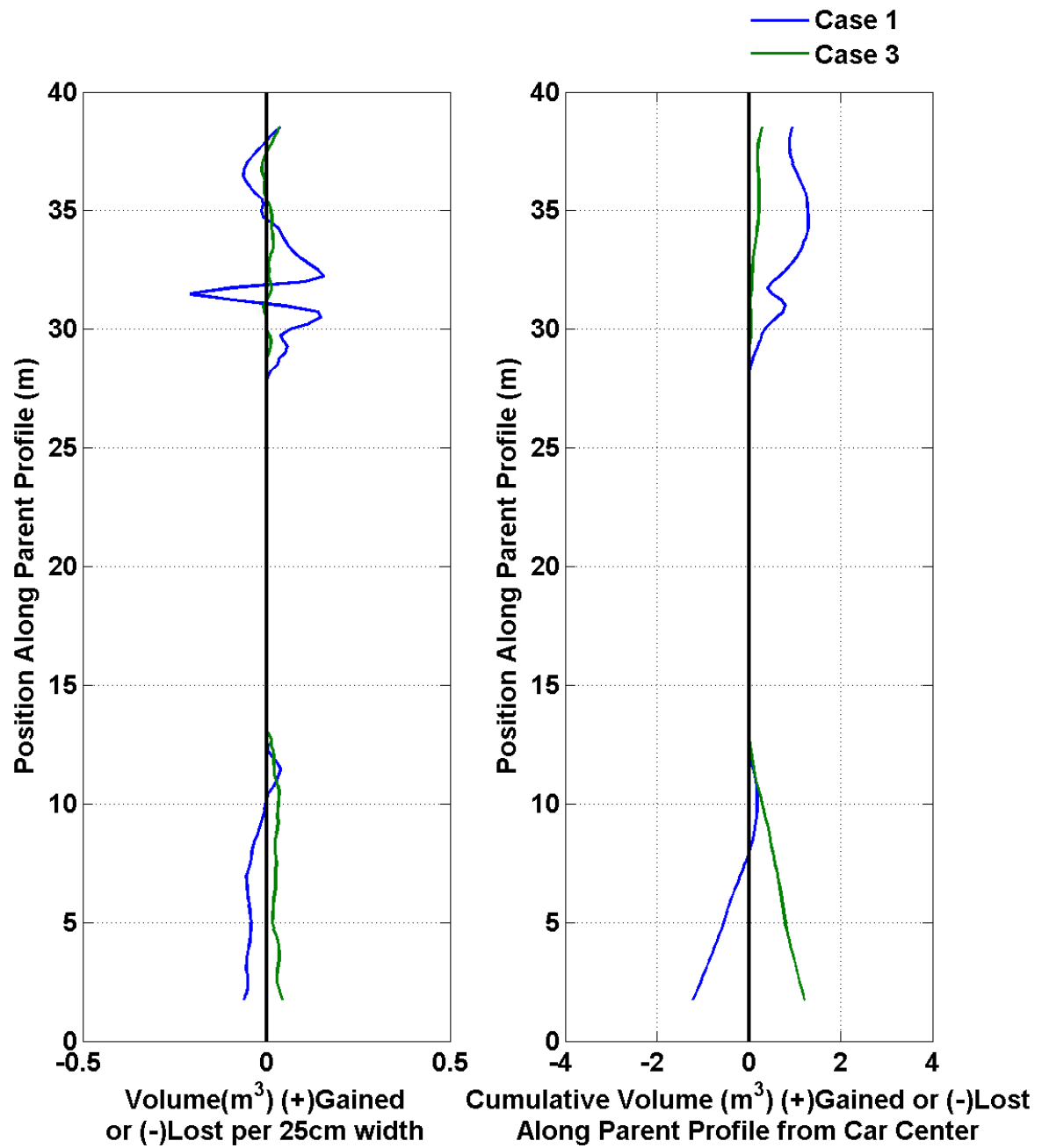
Car #24



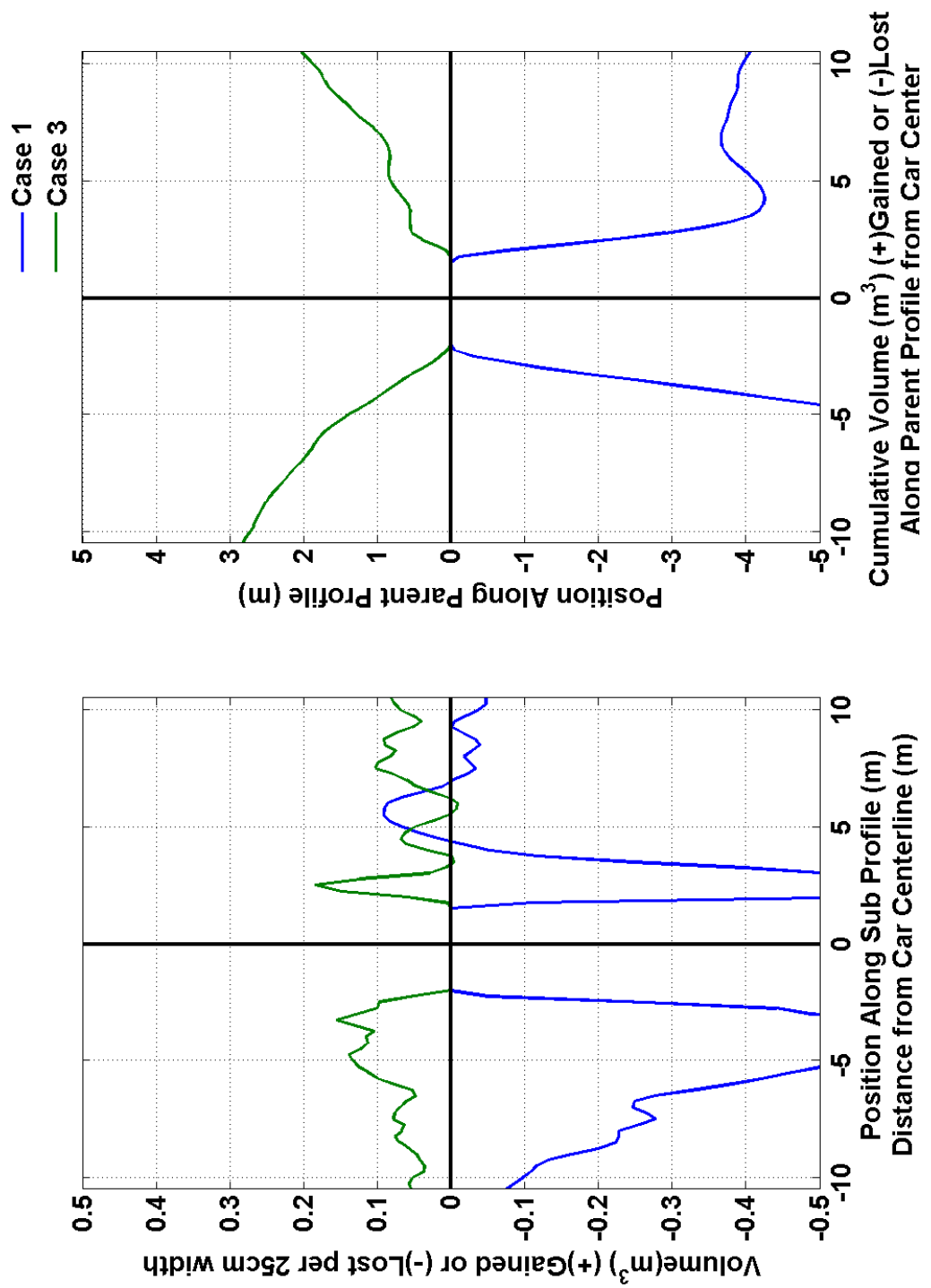
Car #24



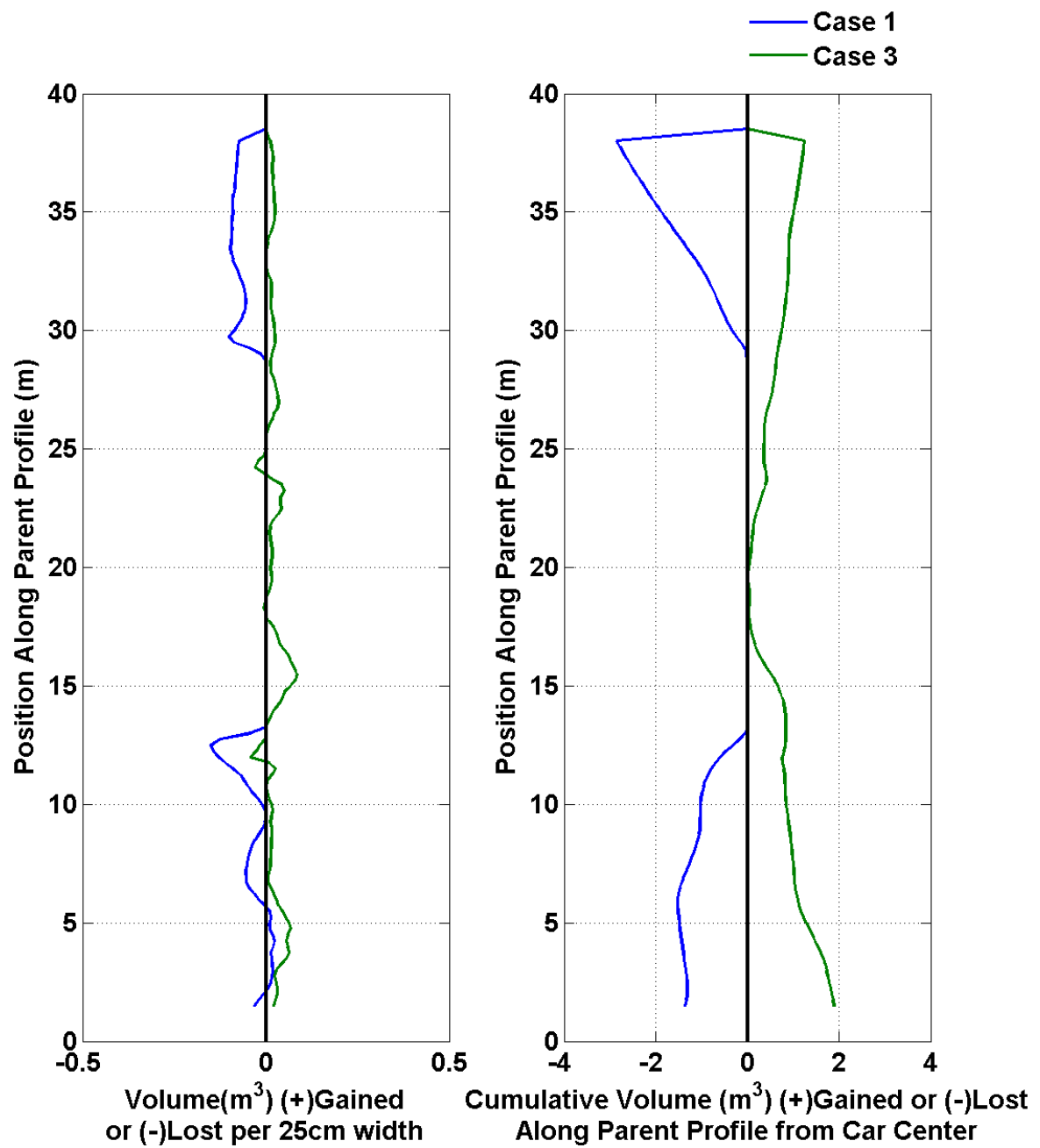
Car #25



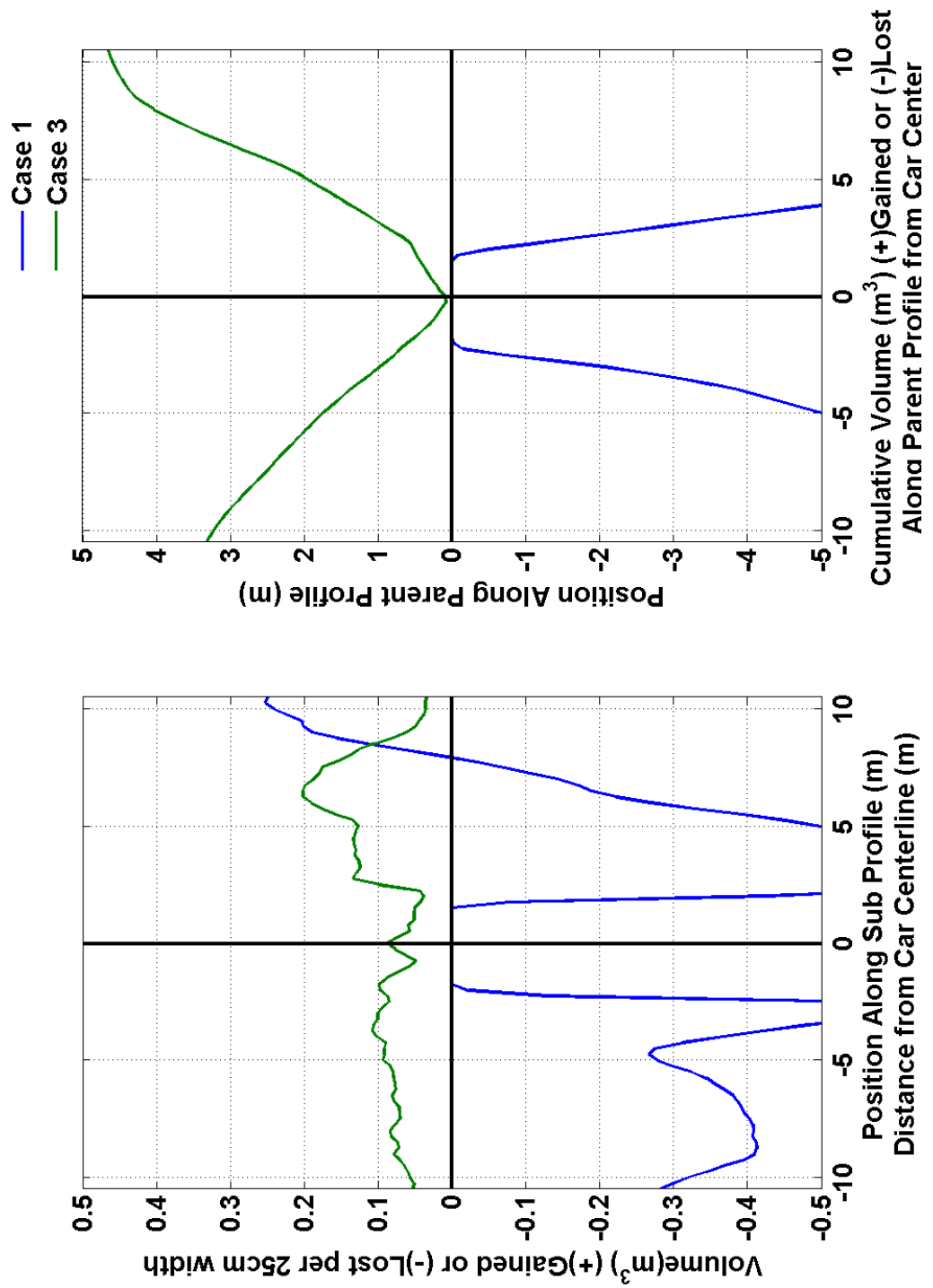
Car #25



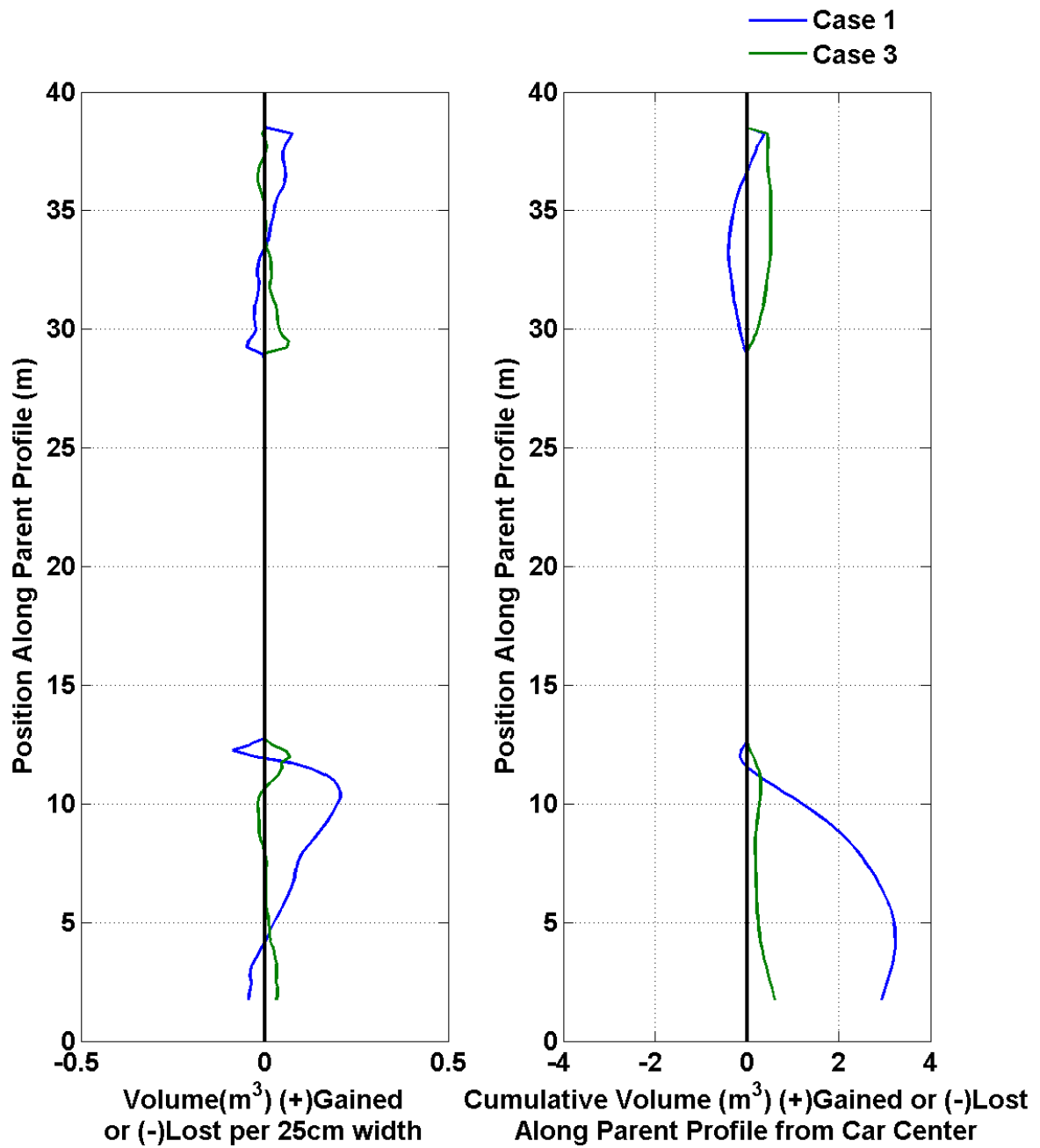
Car #26



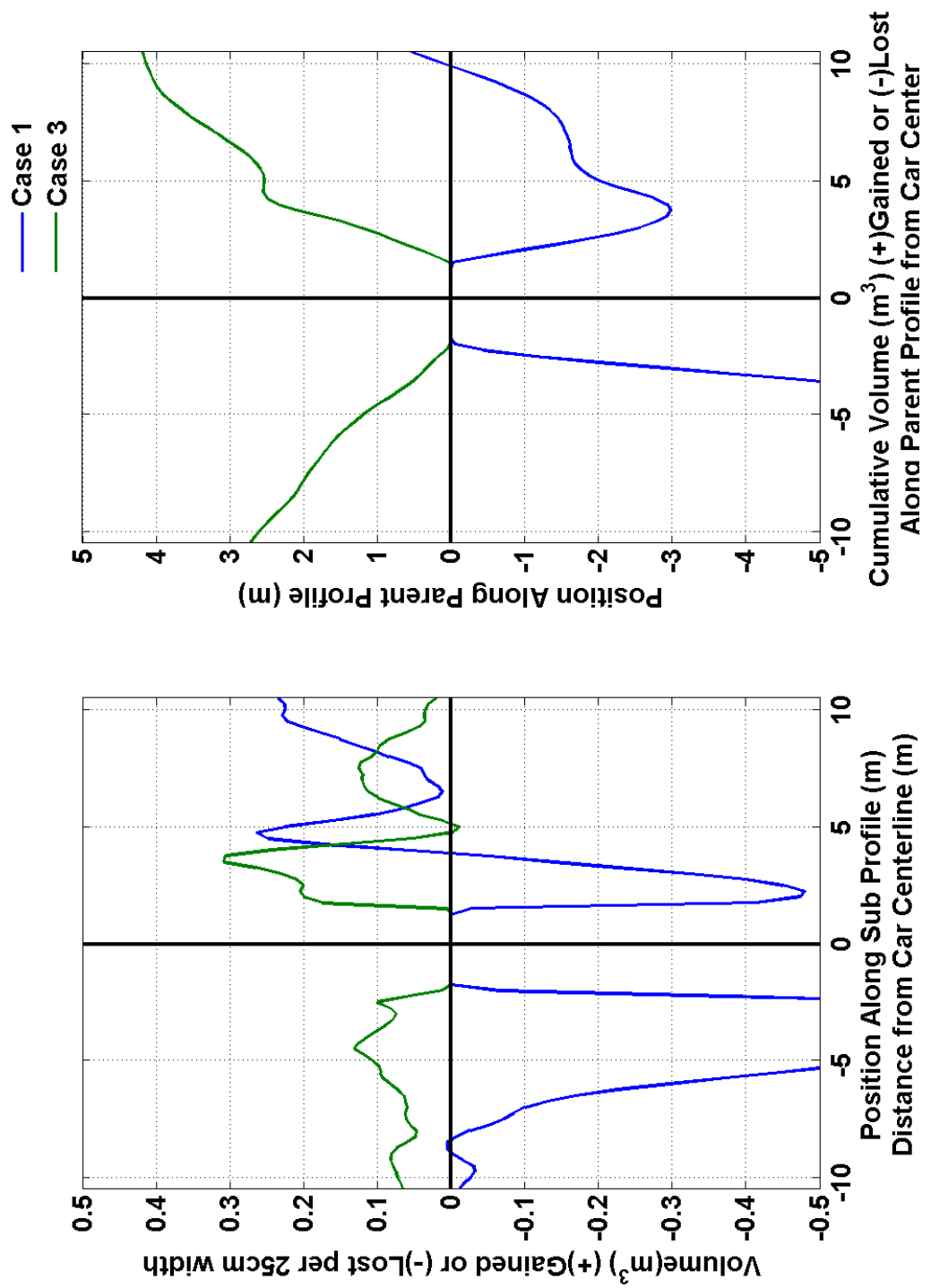
Car #26



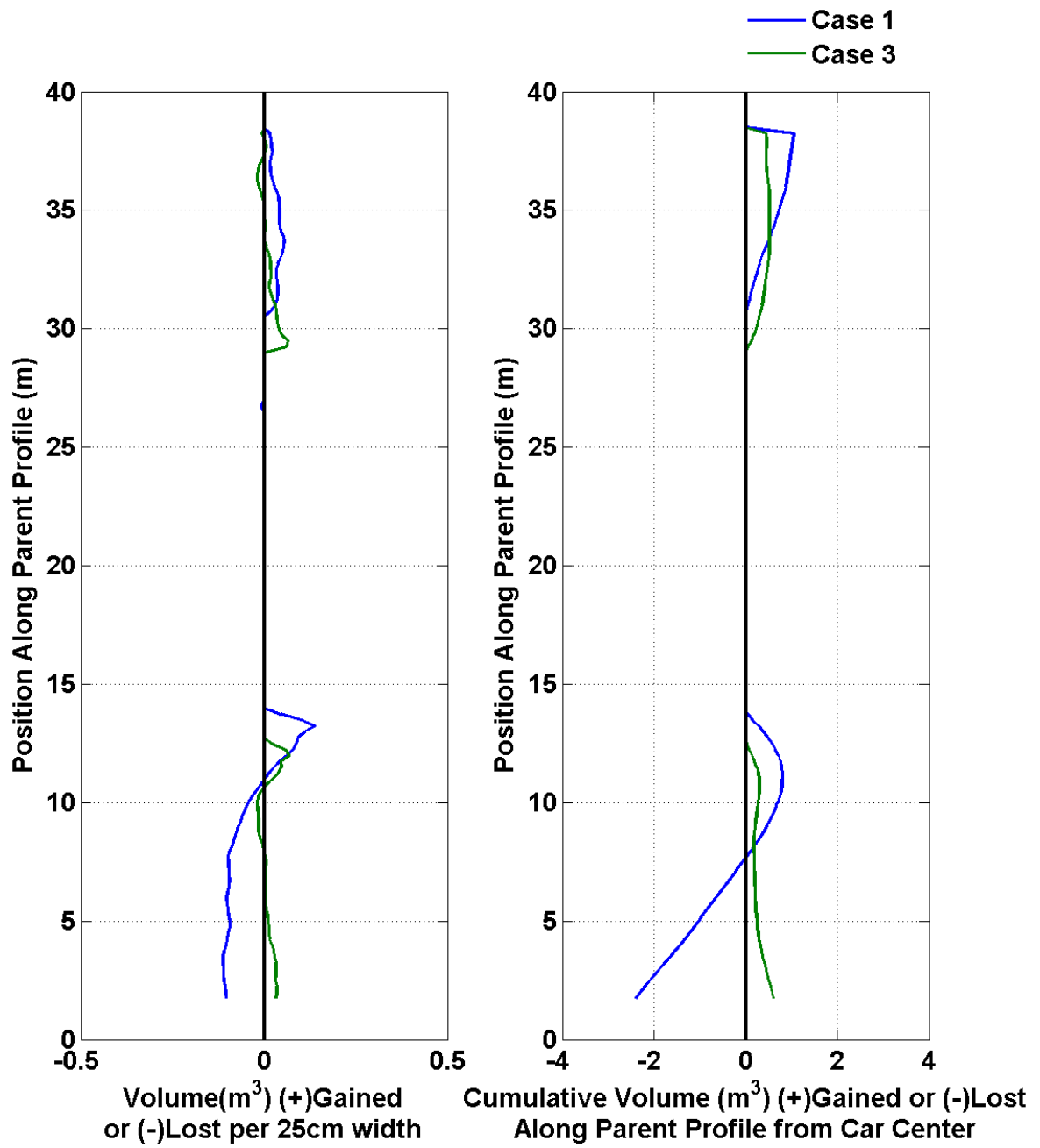
Car #27



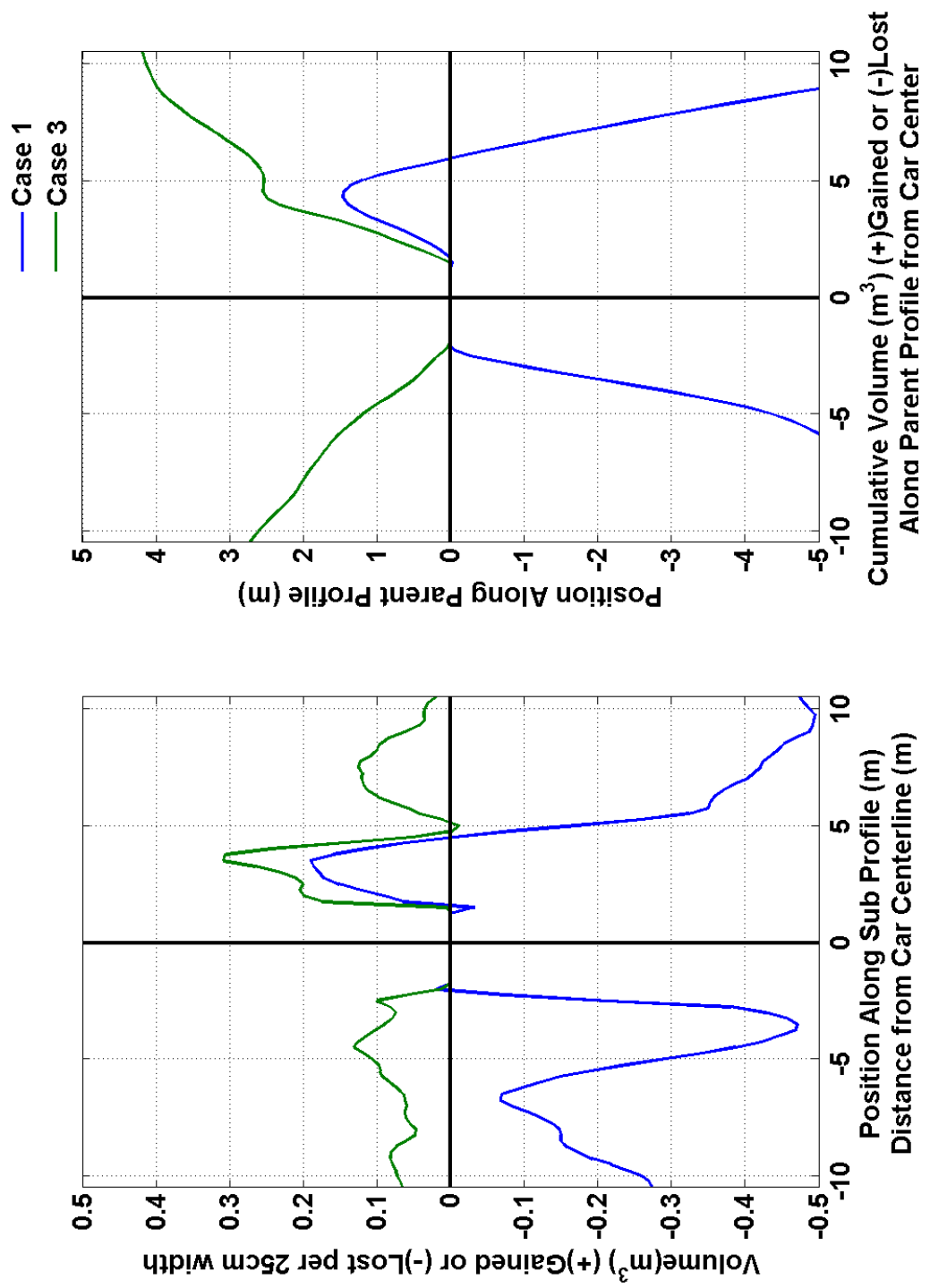
Car #27



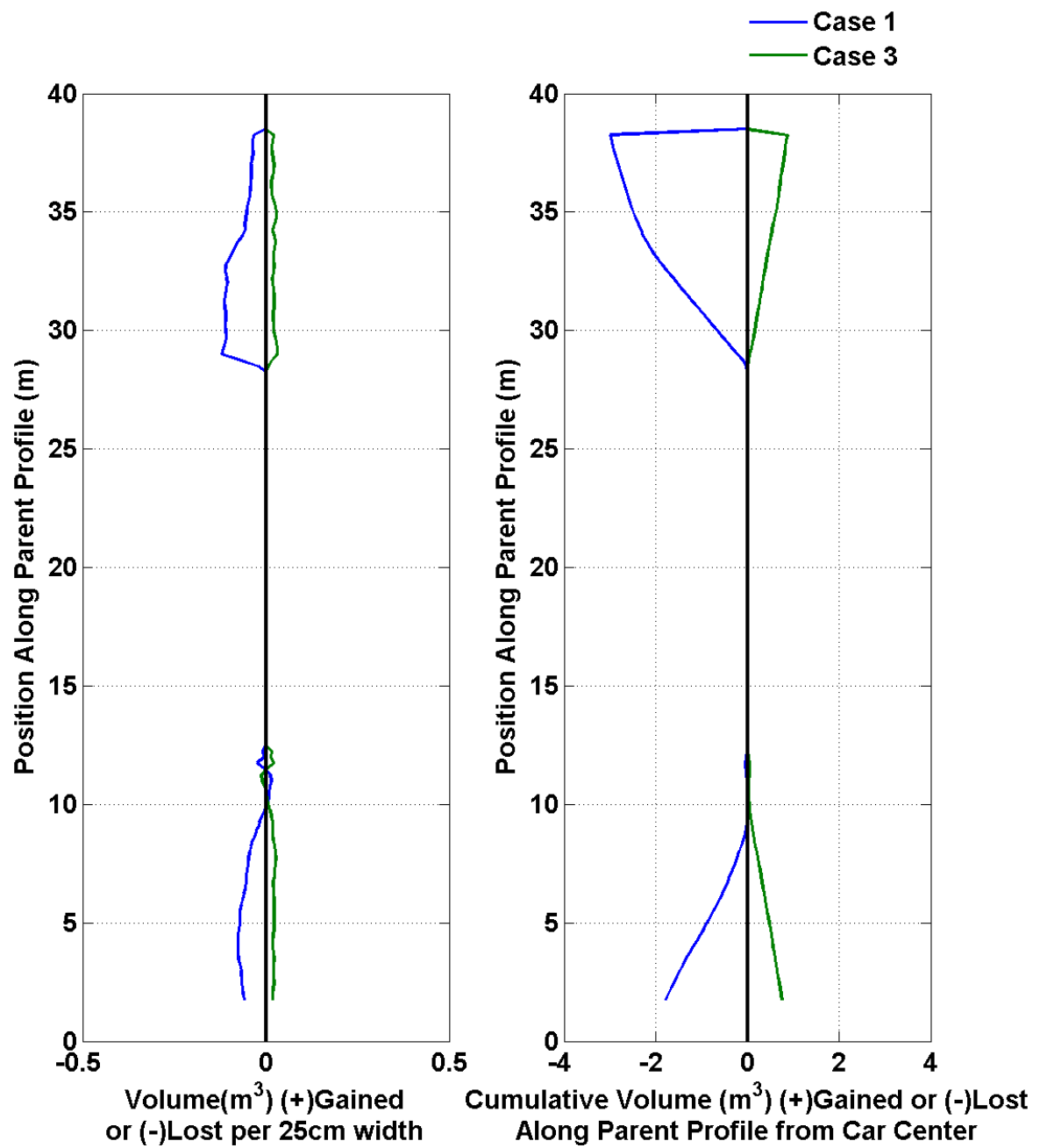
Car #28



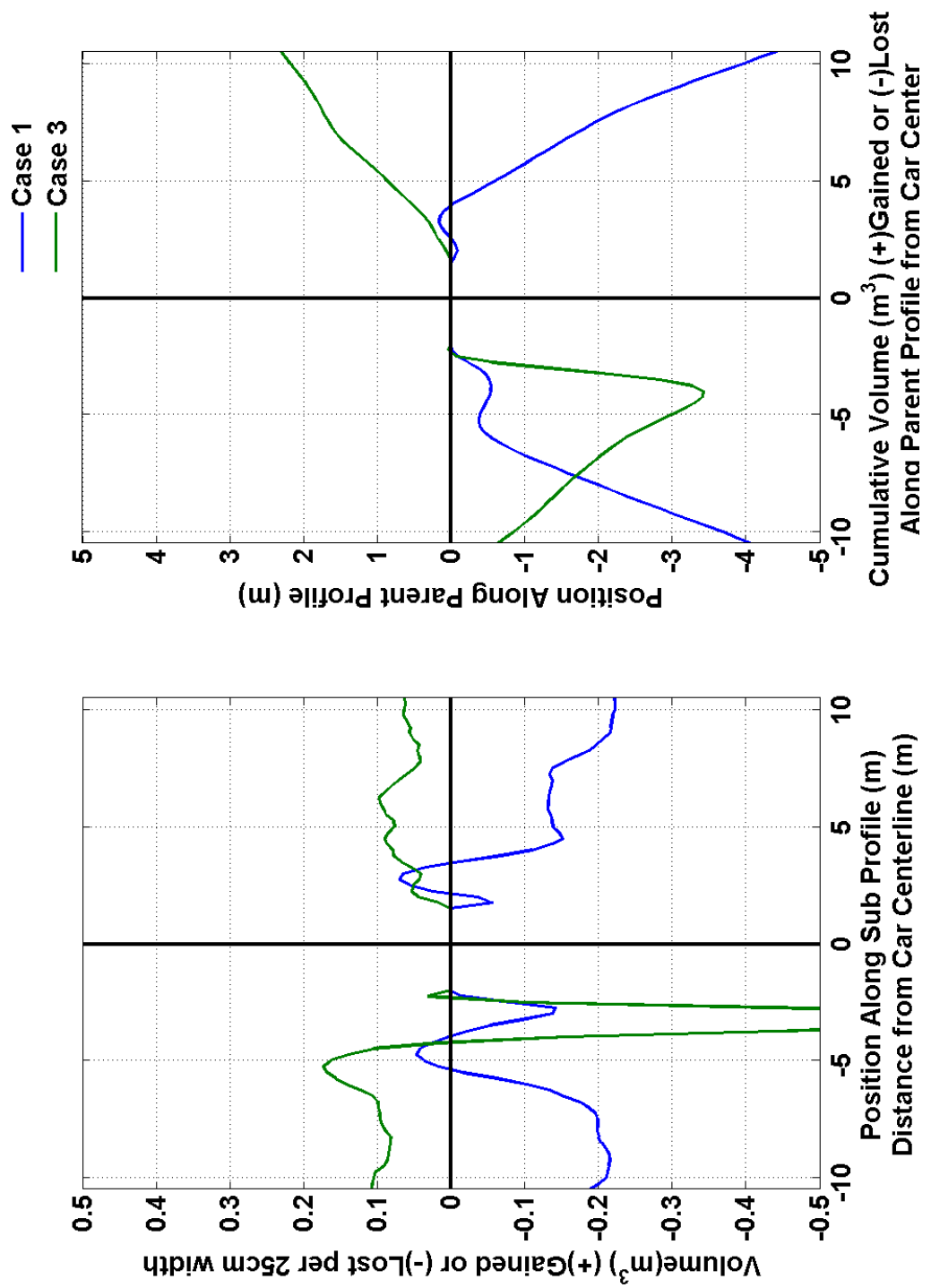
Car #28



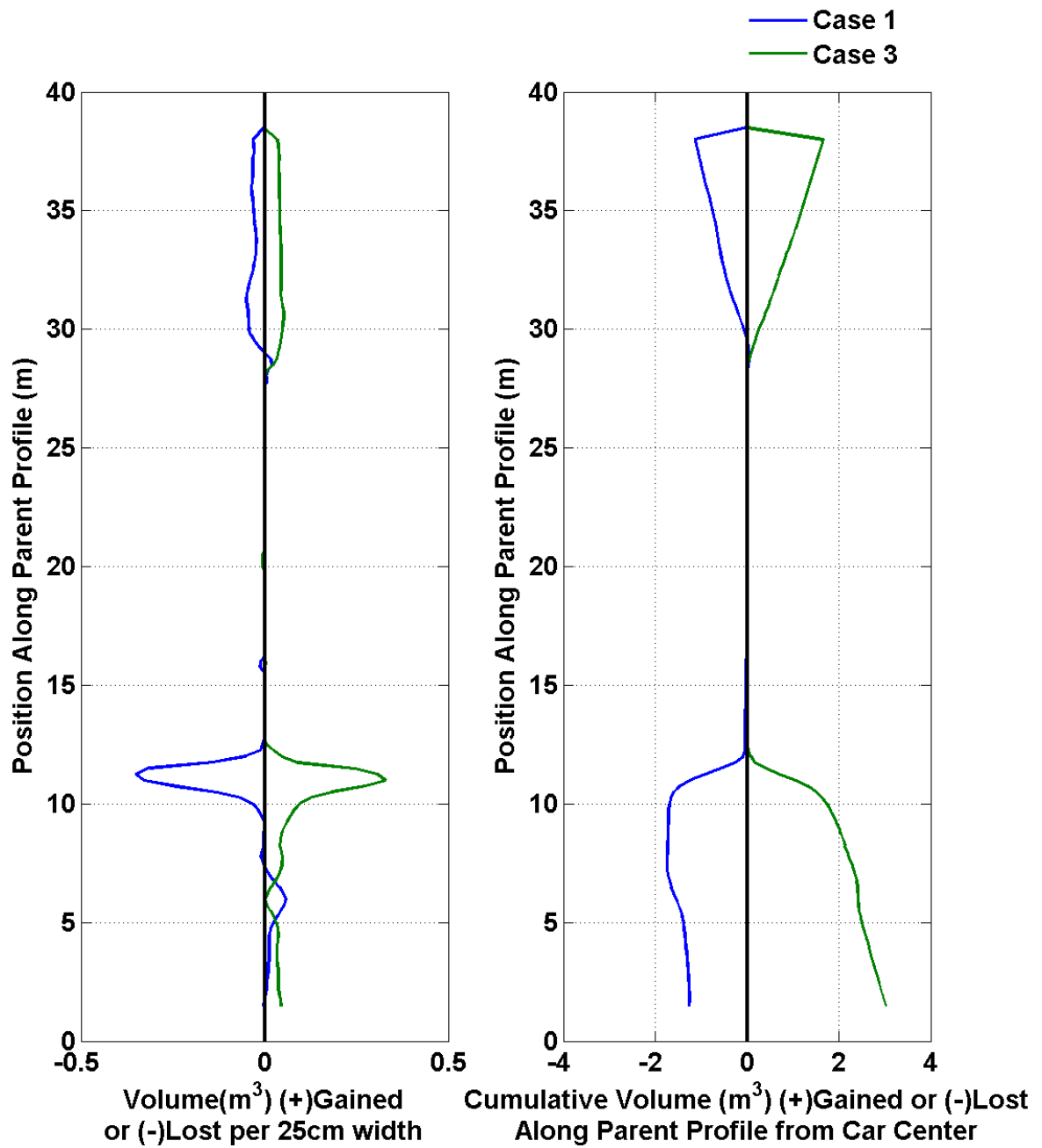
Car #29



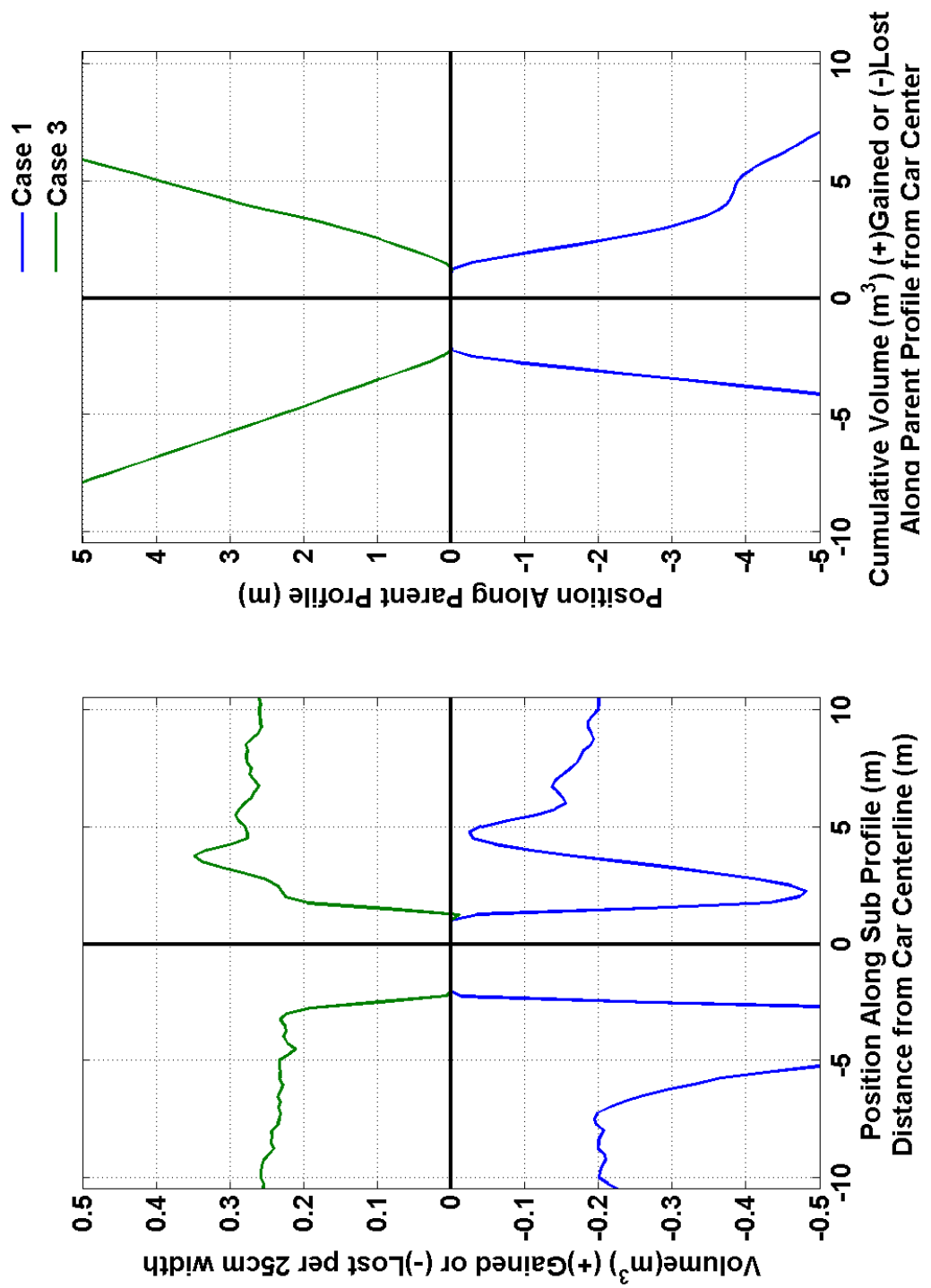
Car #29



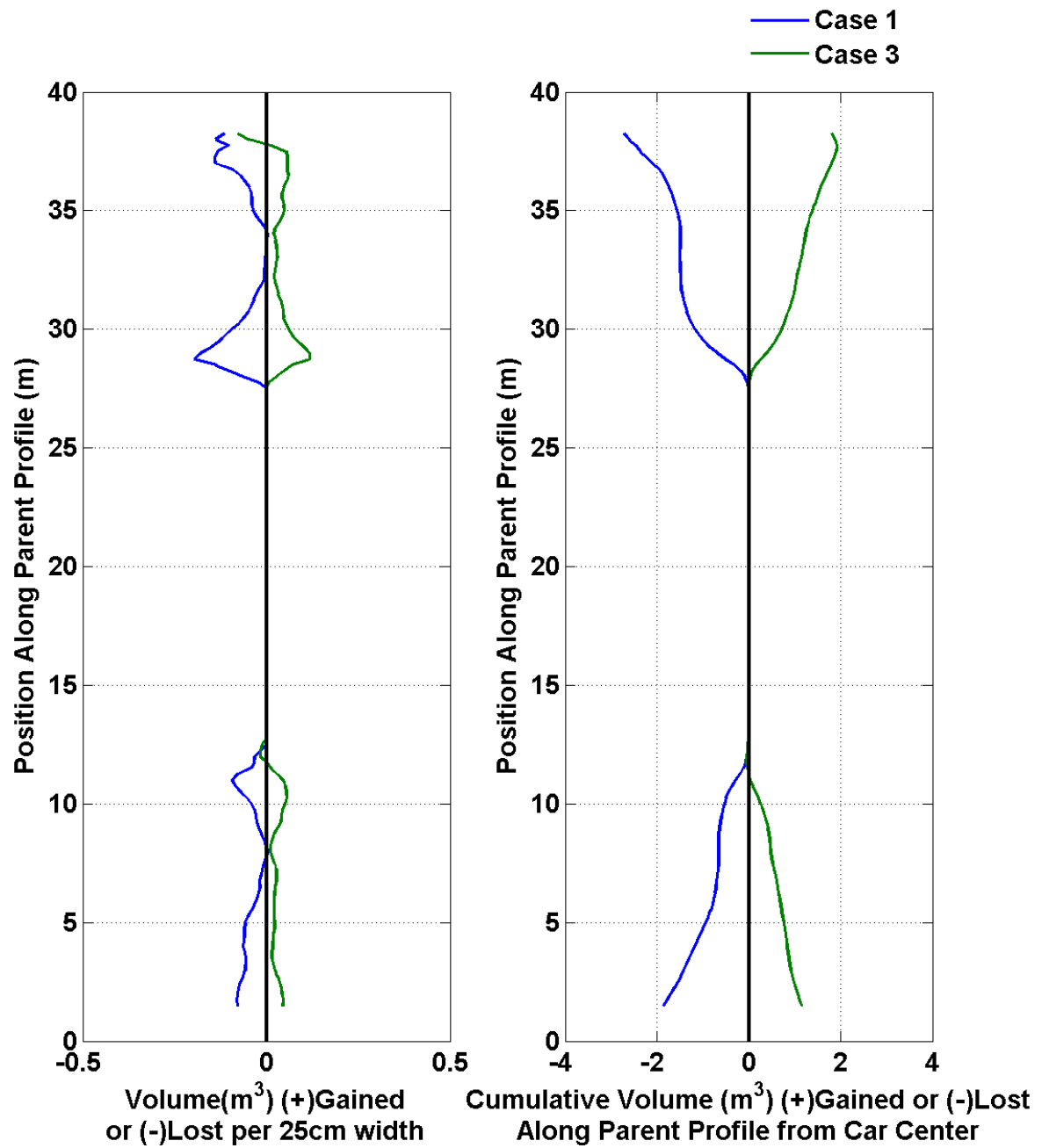
Car #30



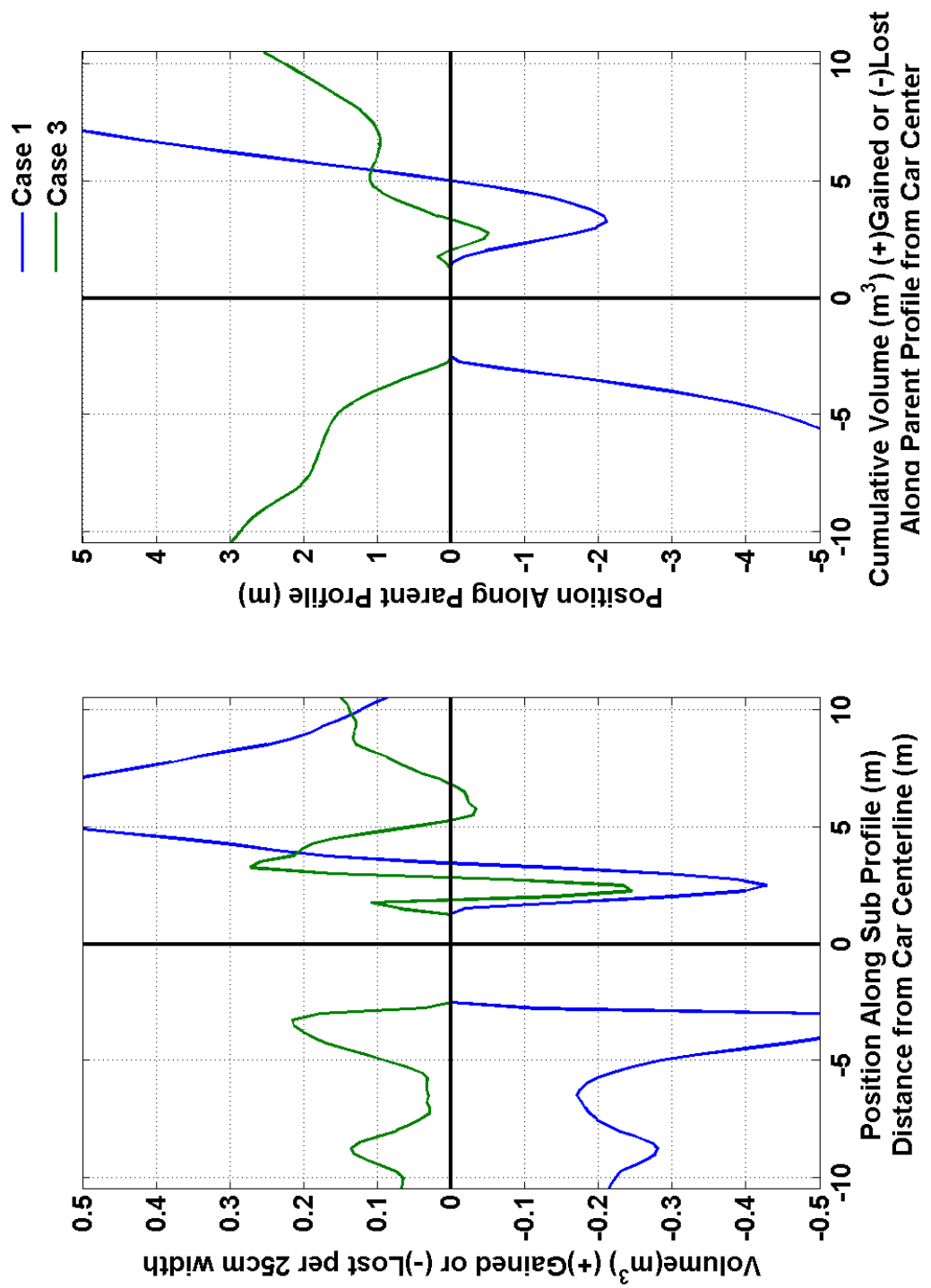
Car #30



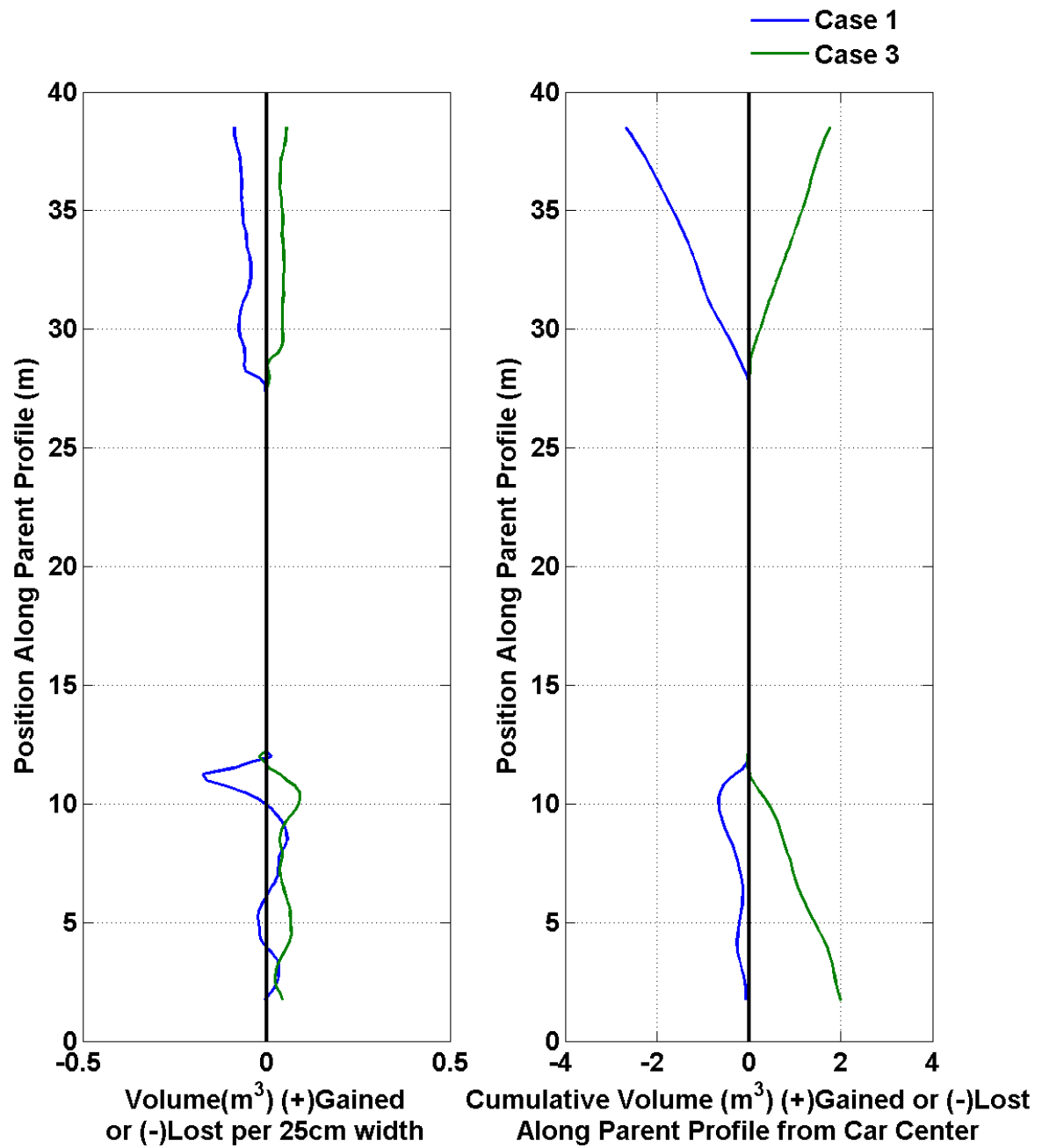
Car #31



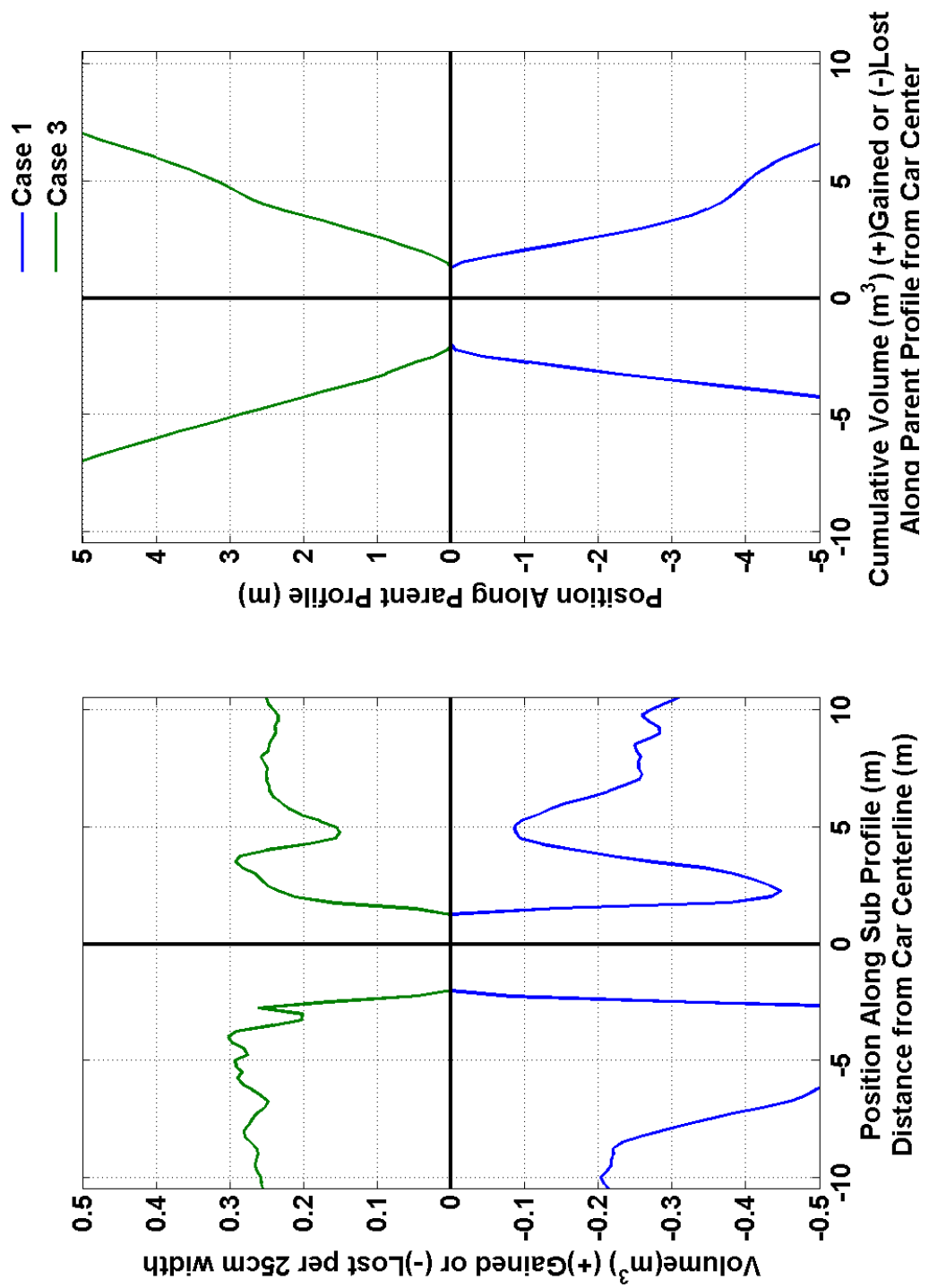
Car #31



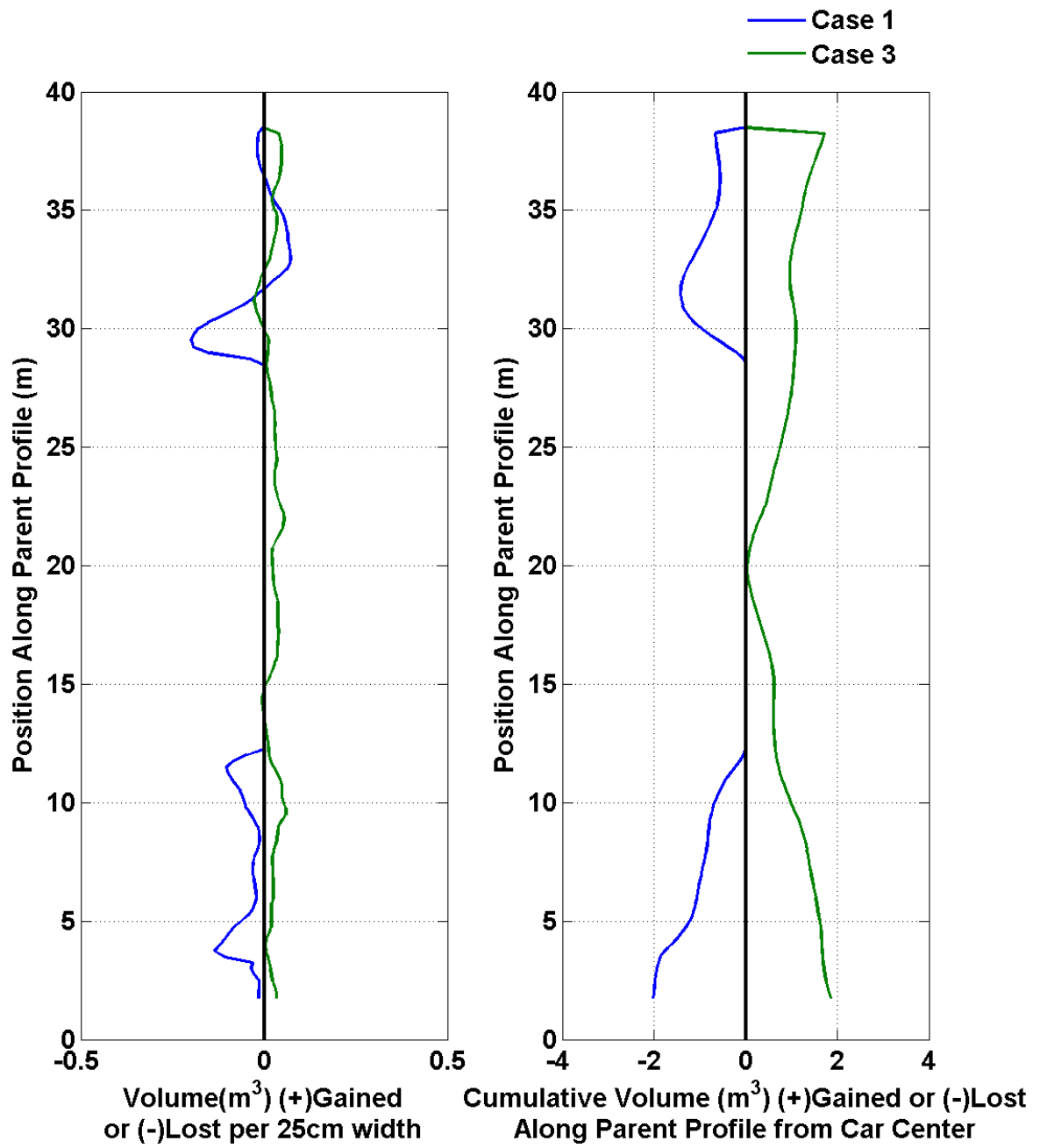
Car #32



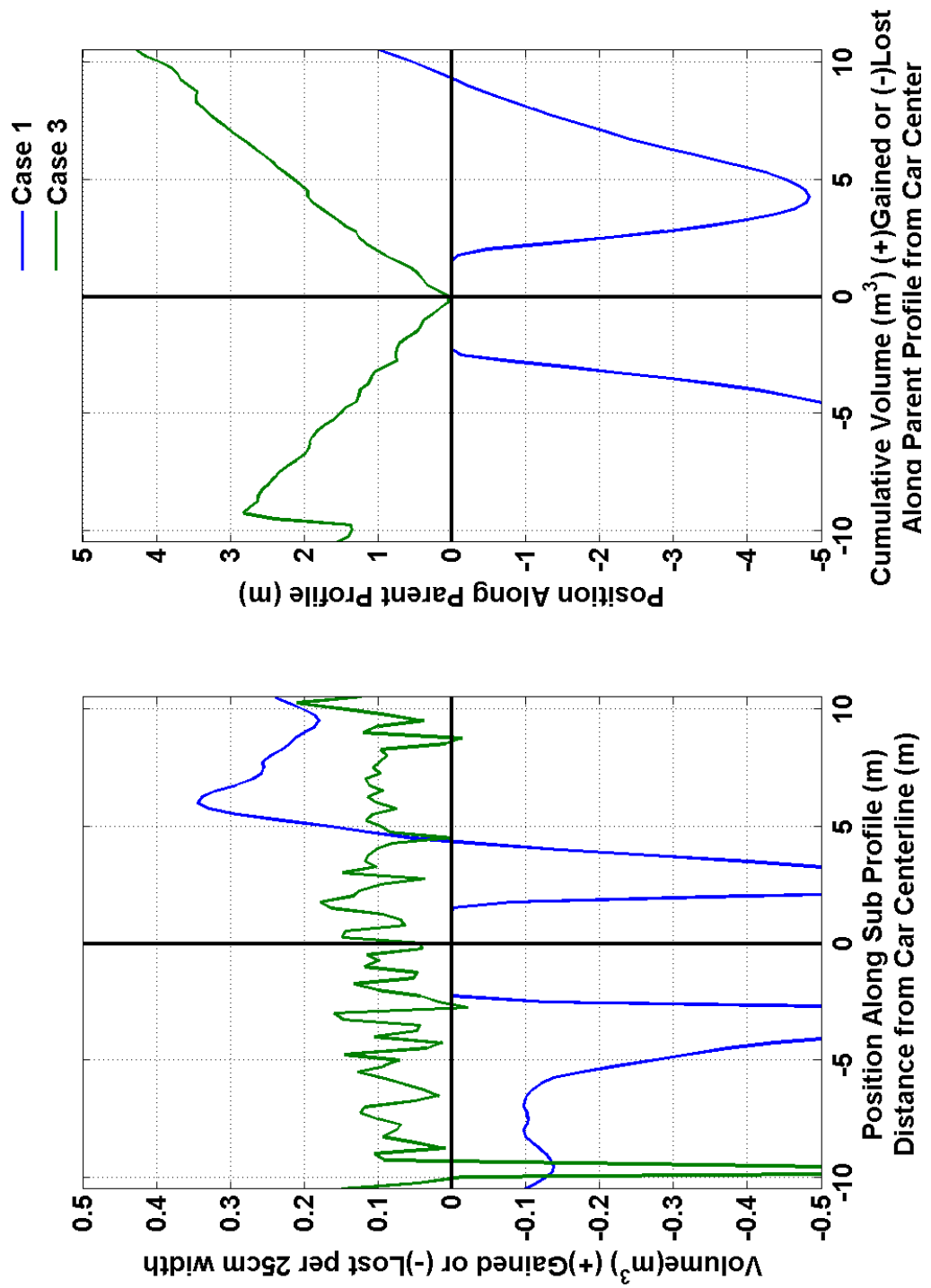
Car #32



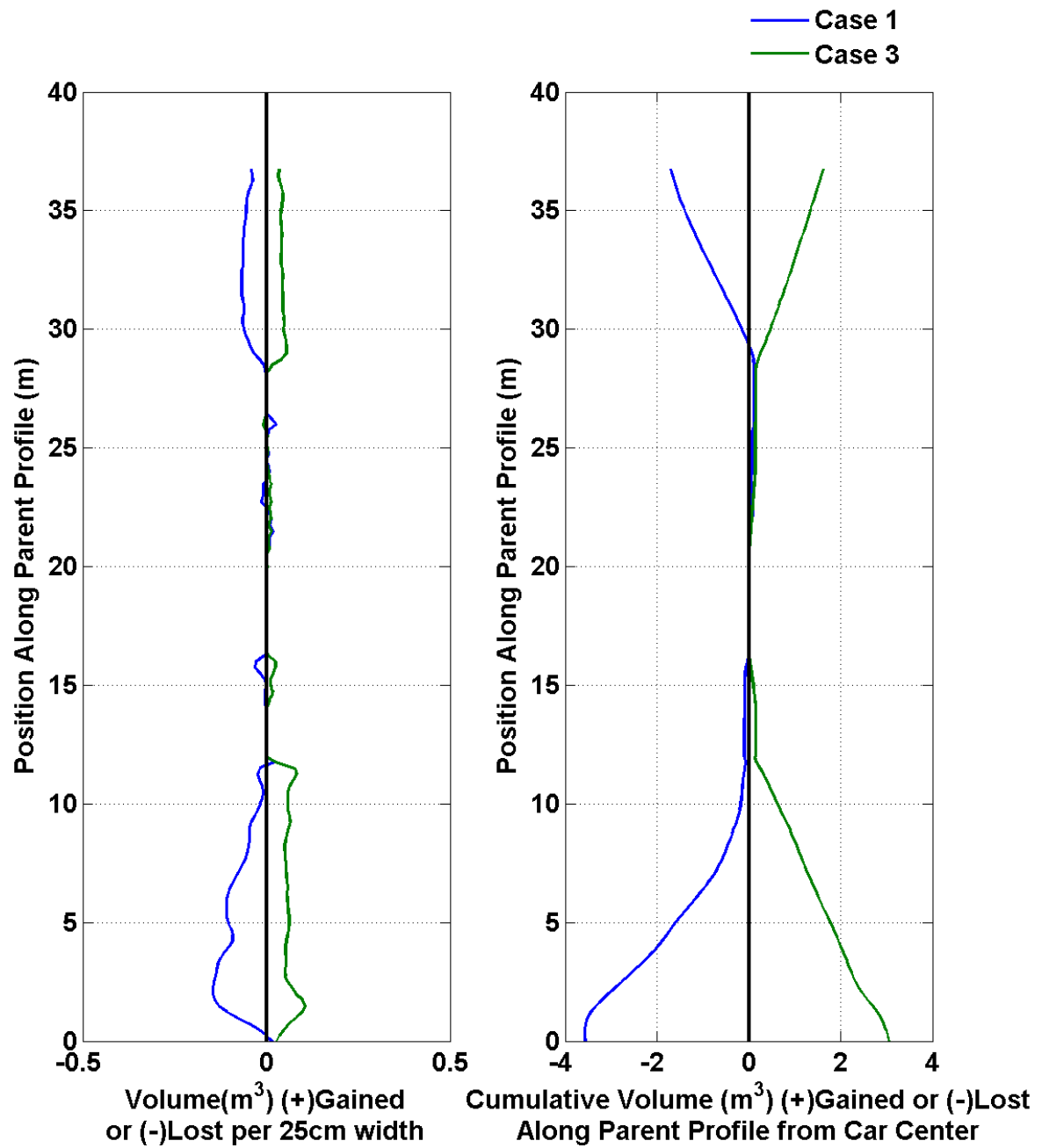
Car #33



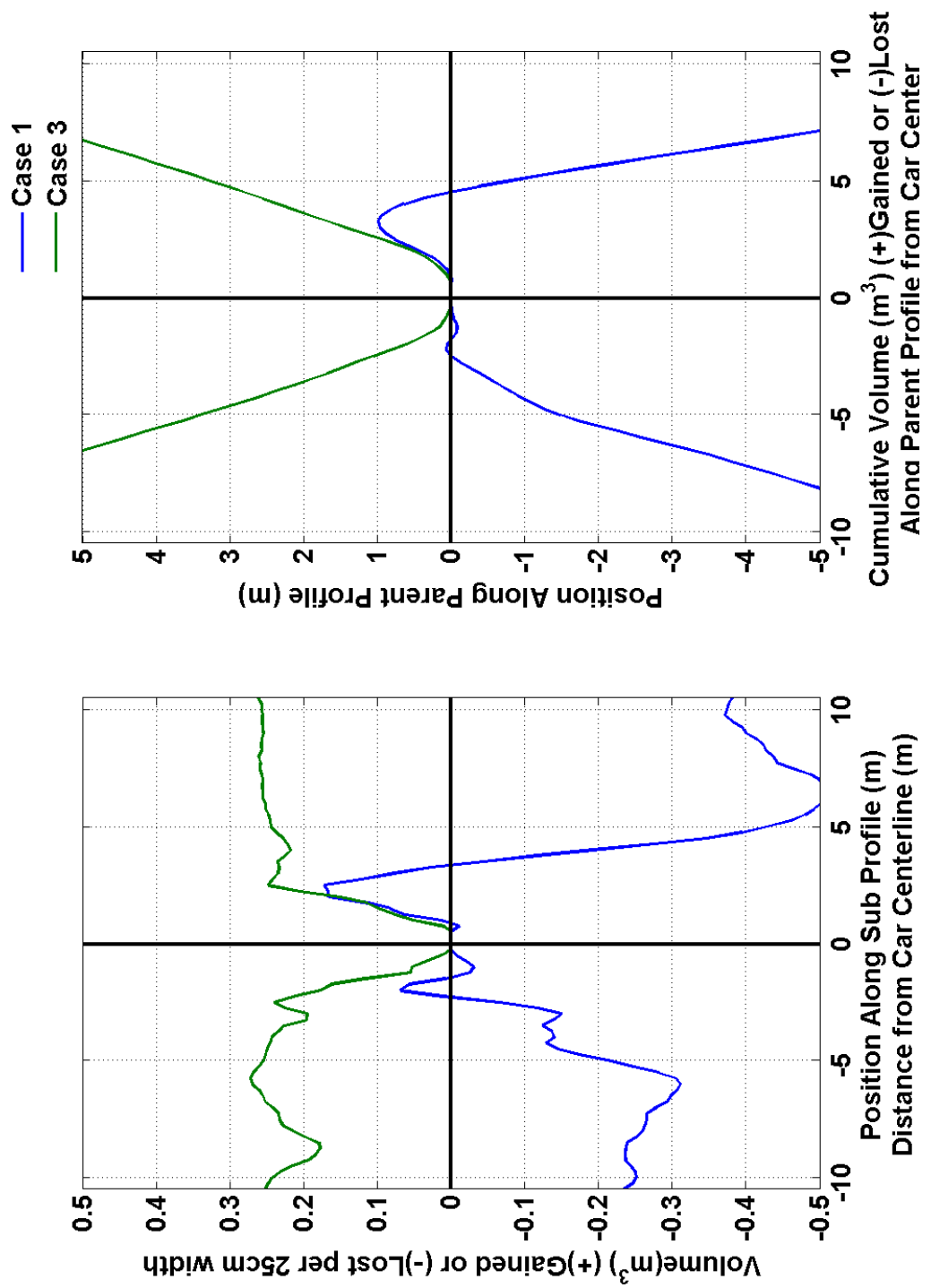
Car #33



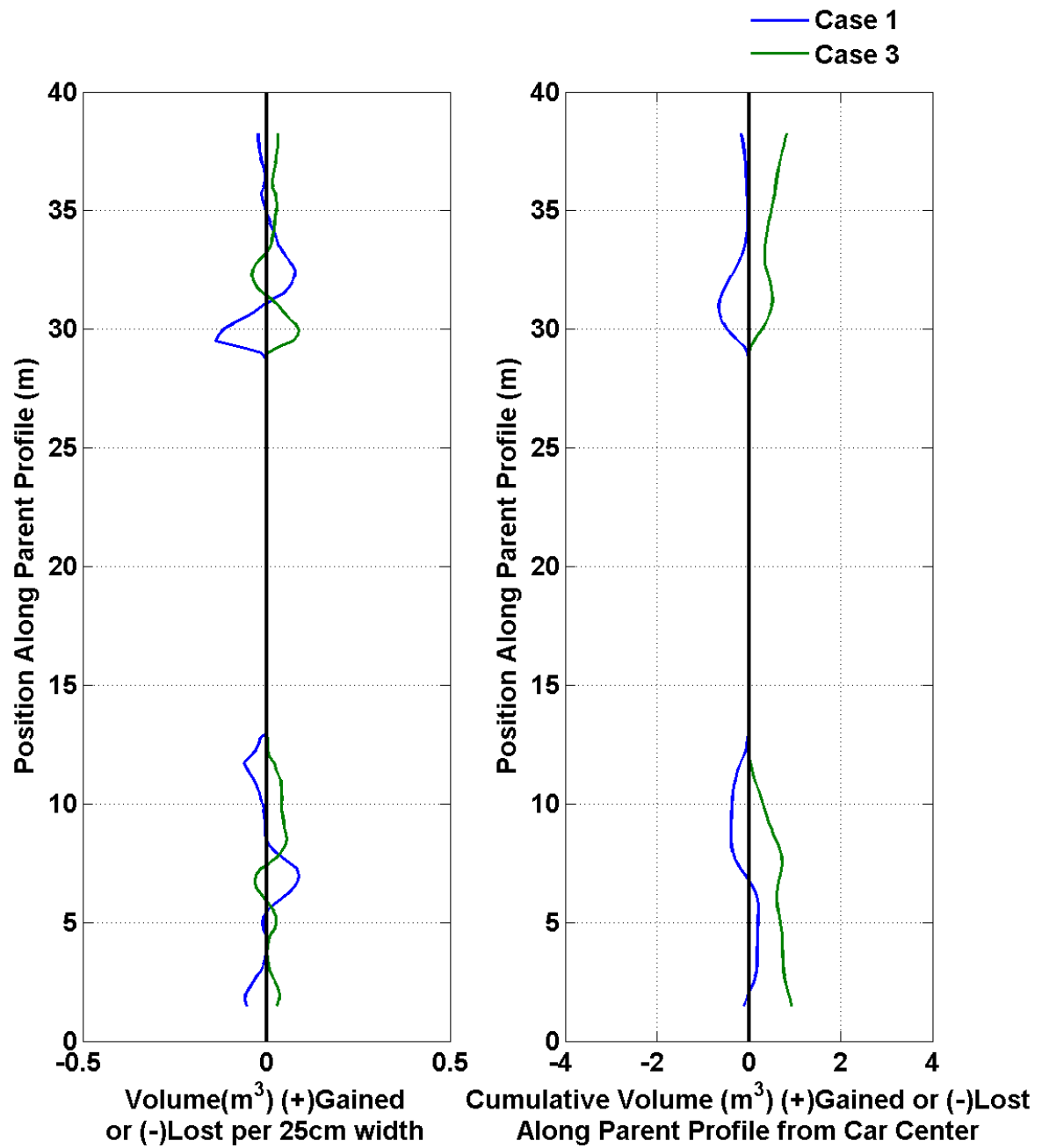
Car #34



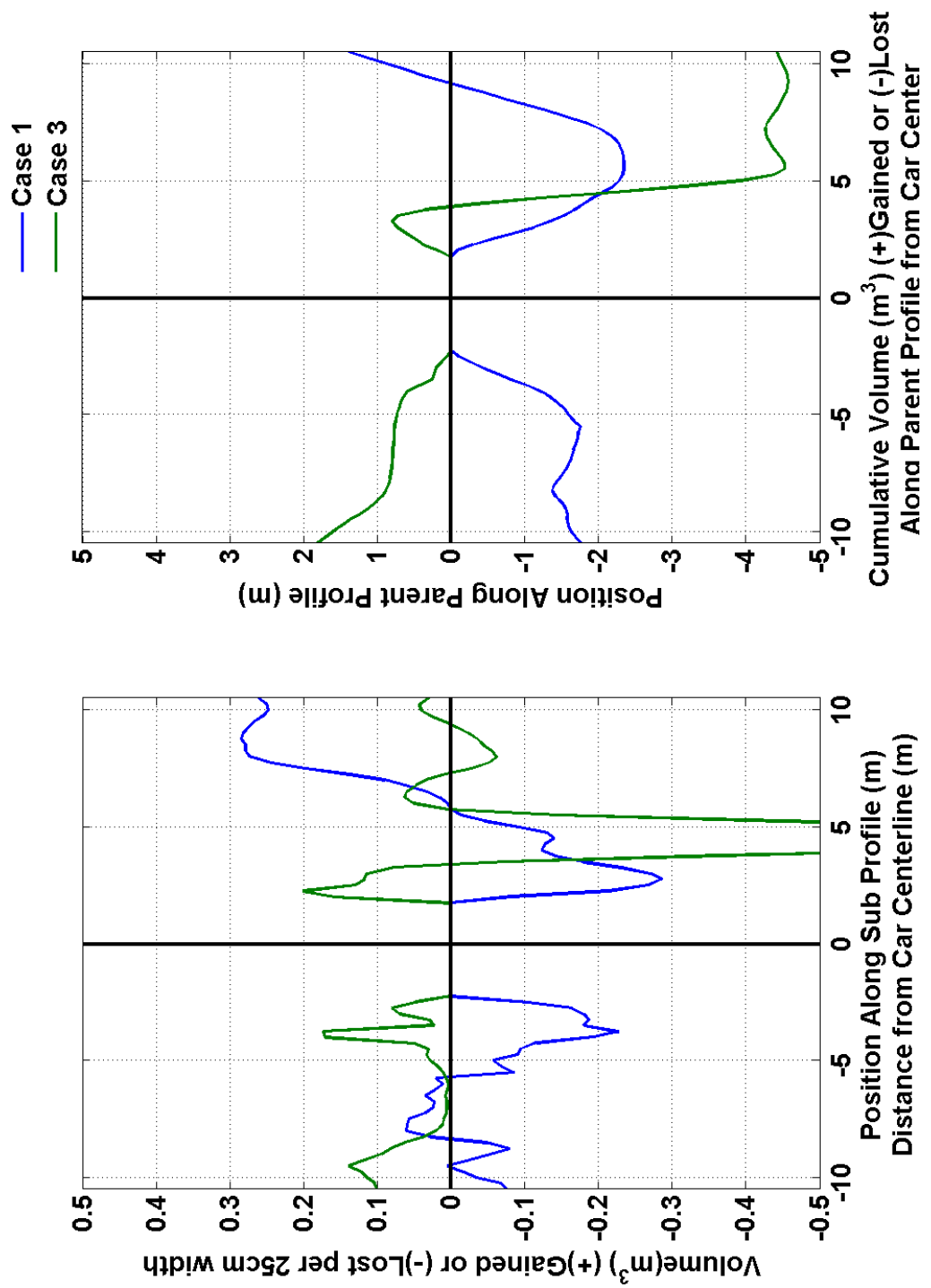
Car #34



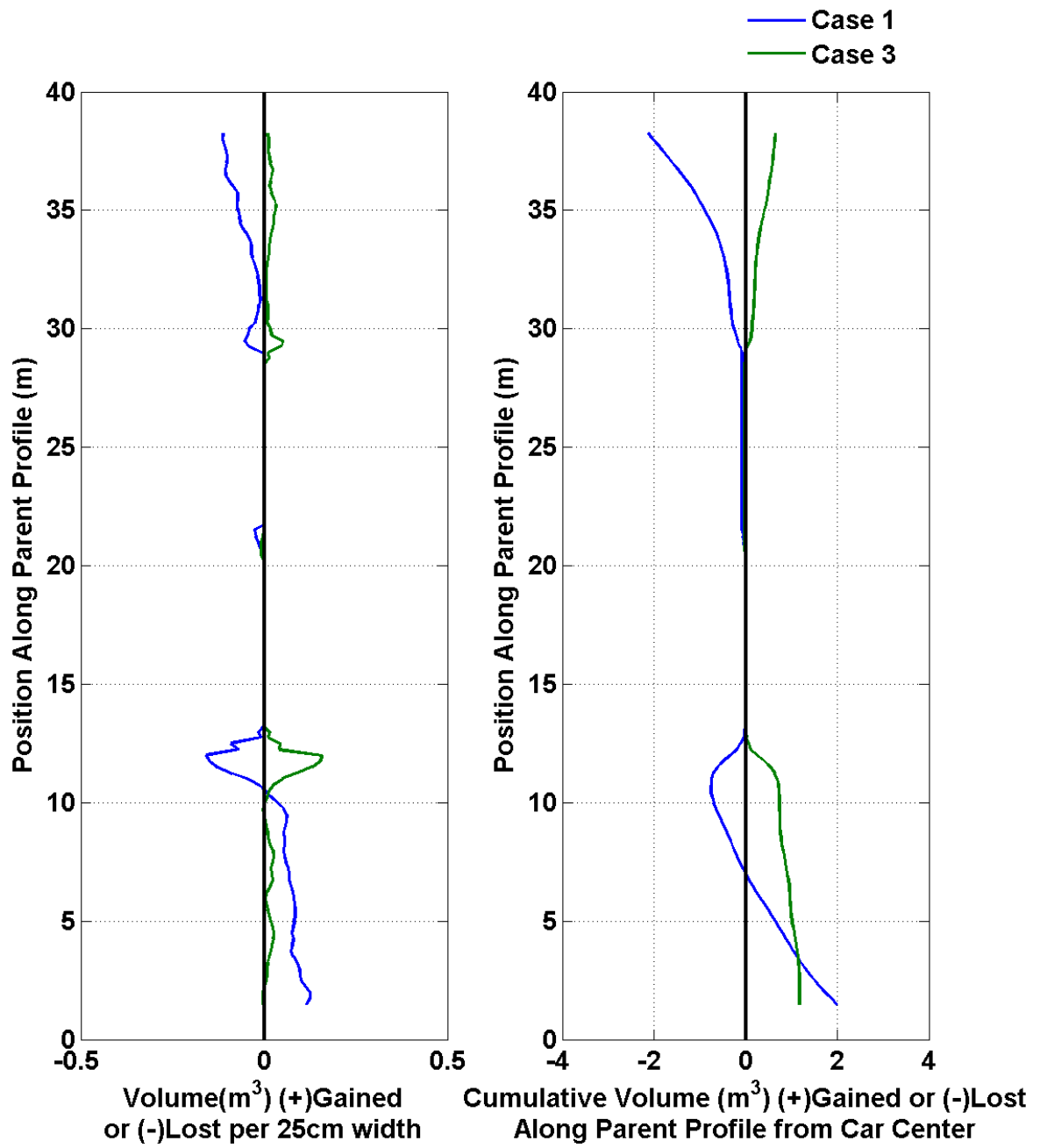
Car #35



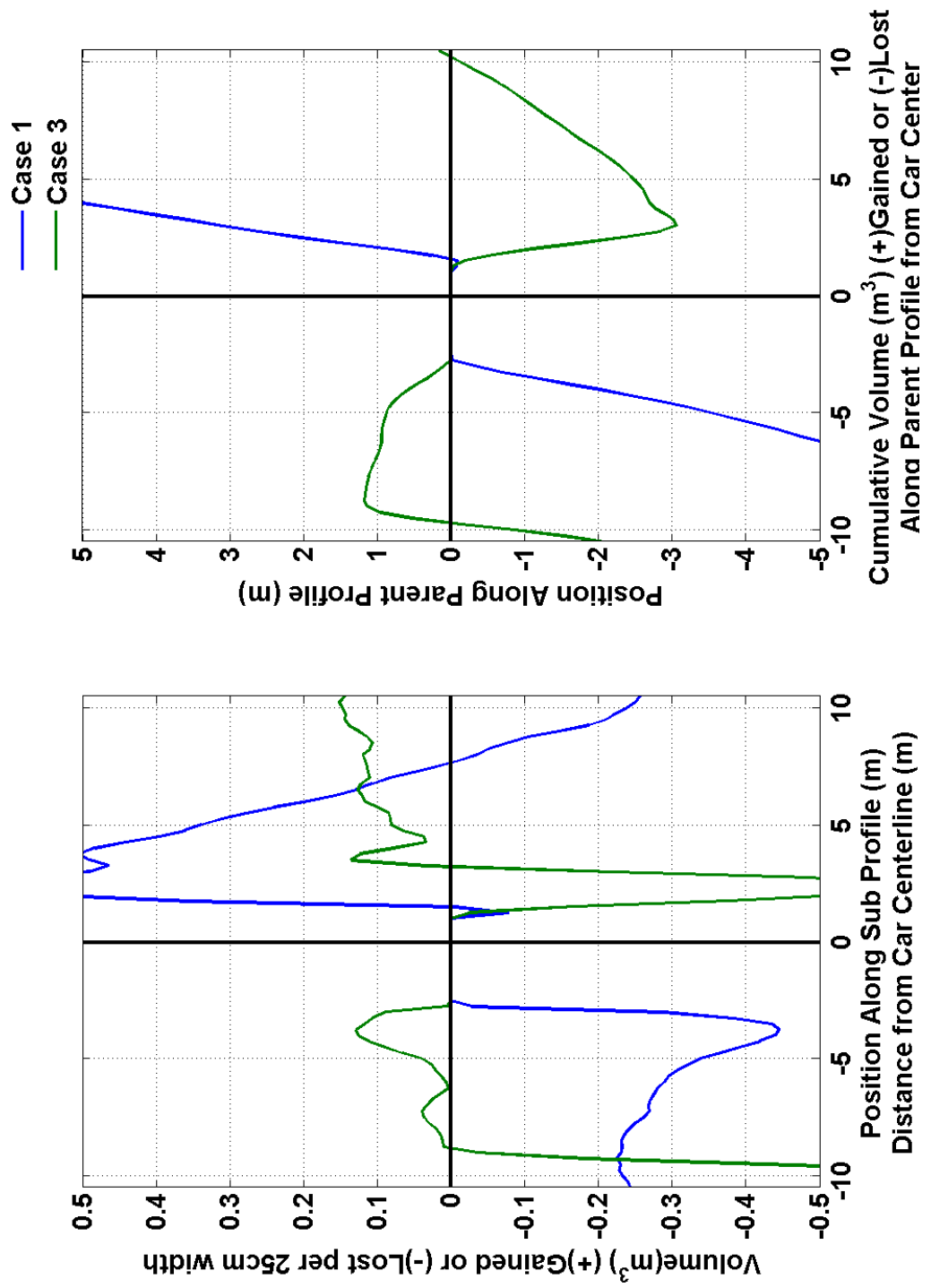
Car #35



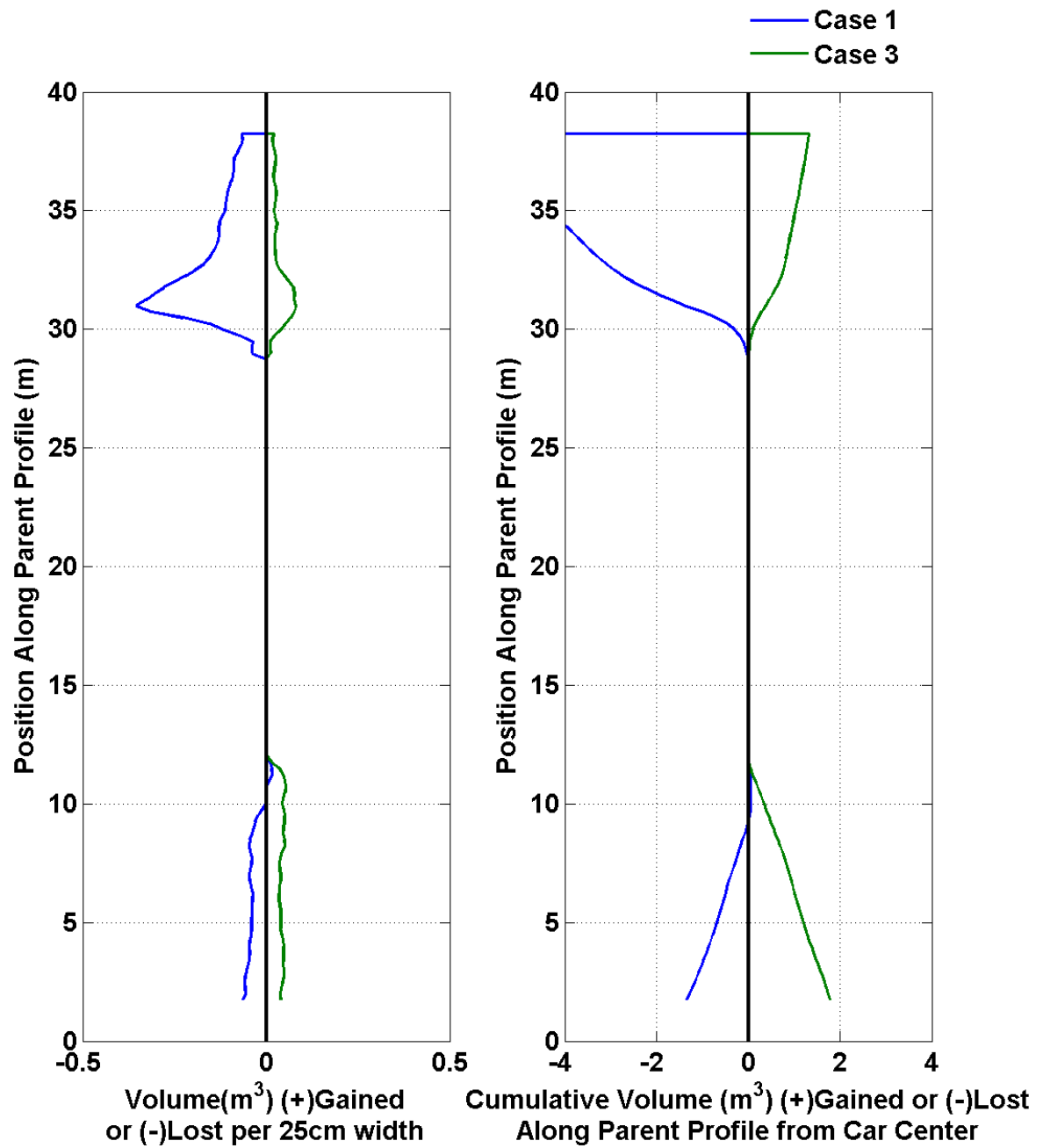
Car #36



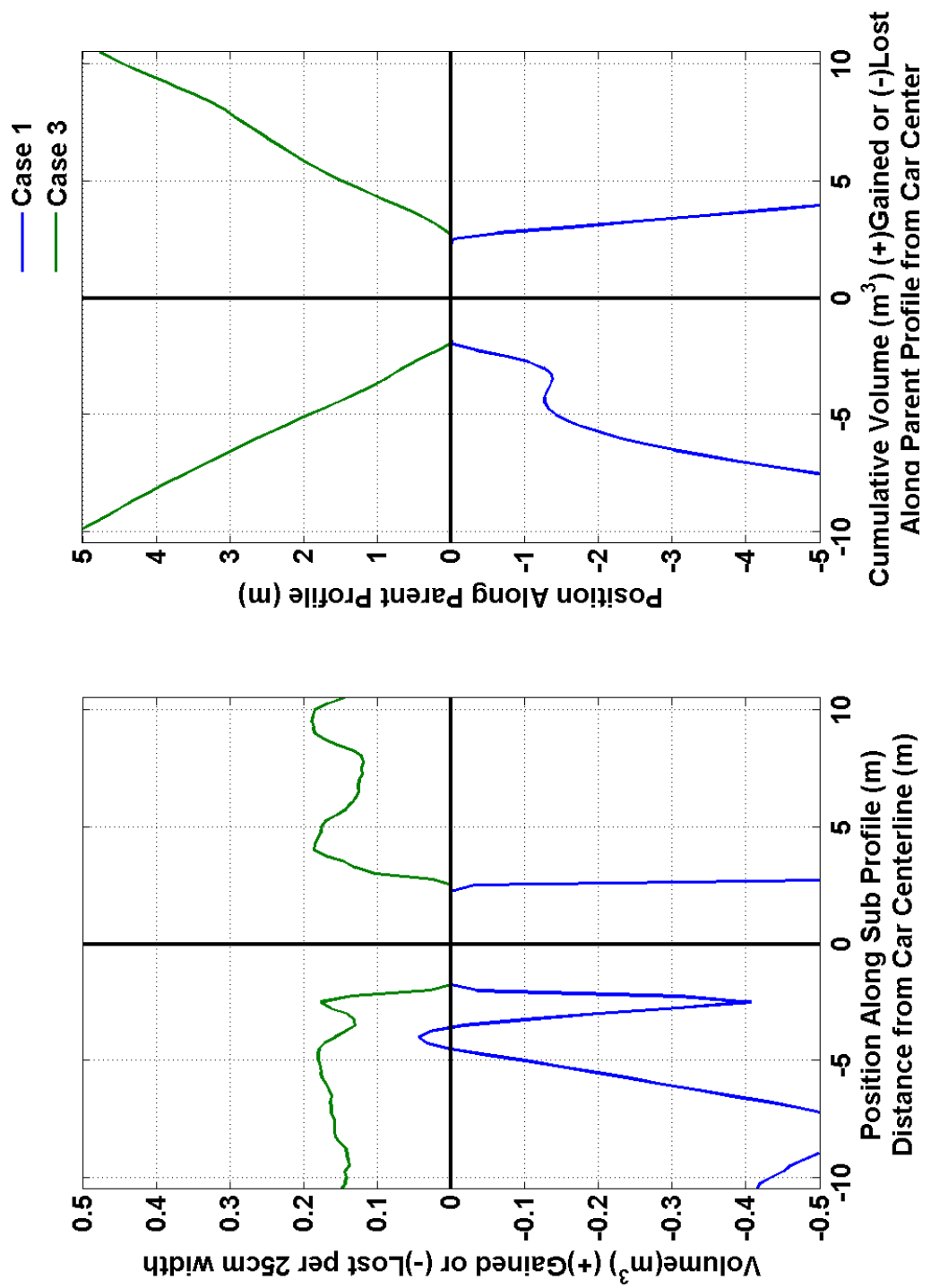
Car #36



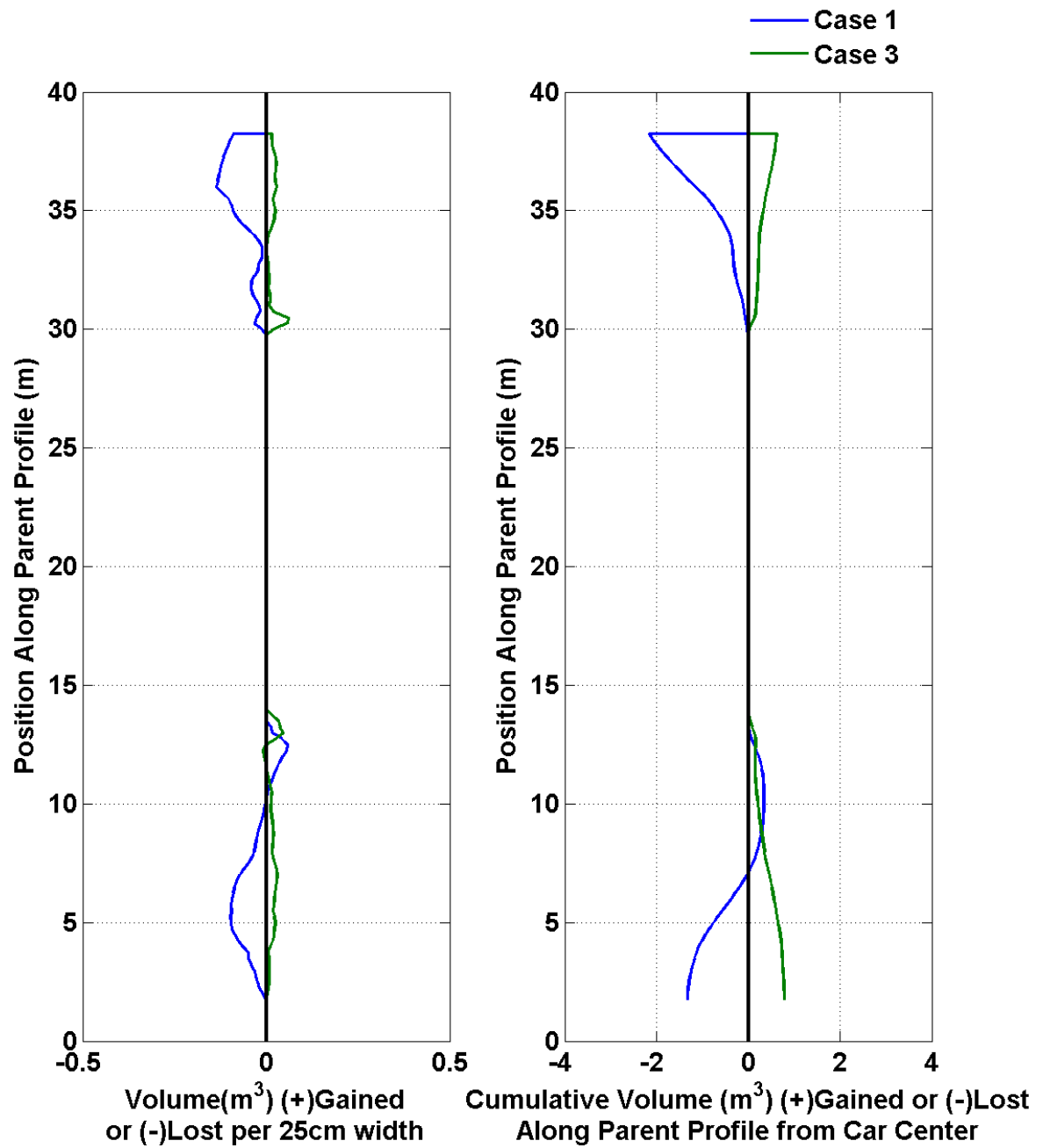
Car #37



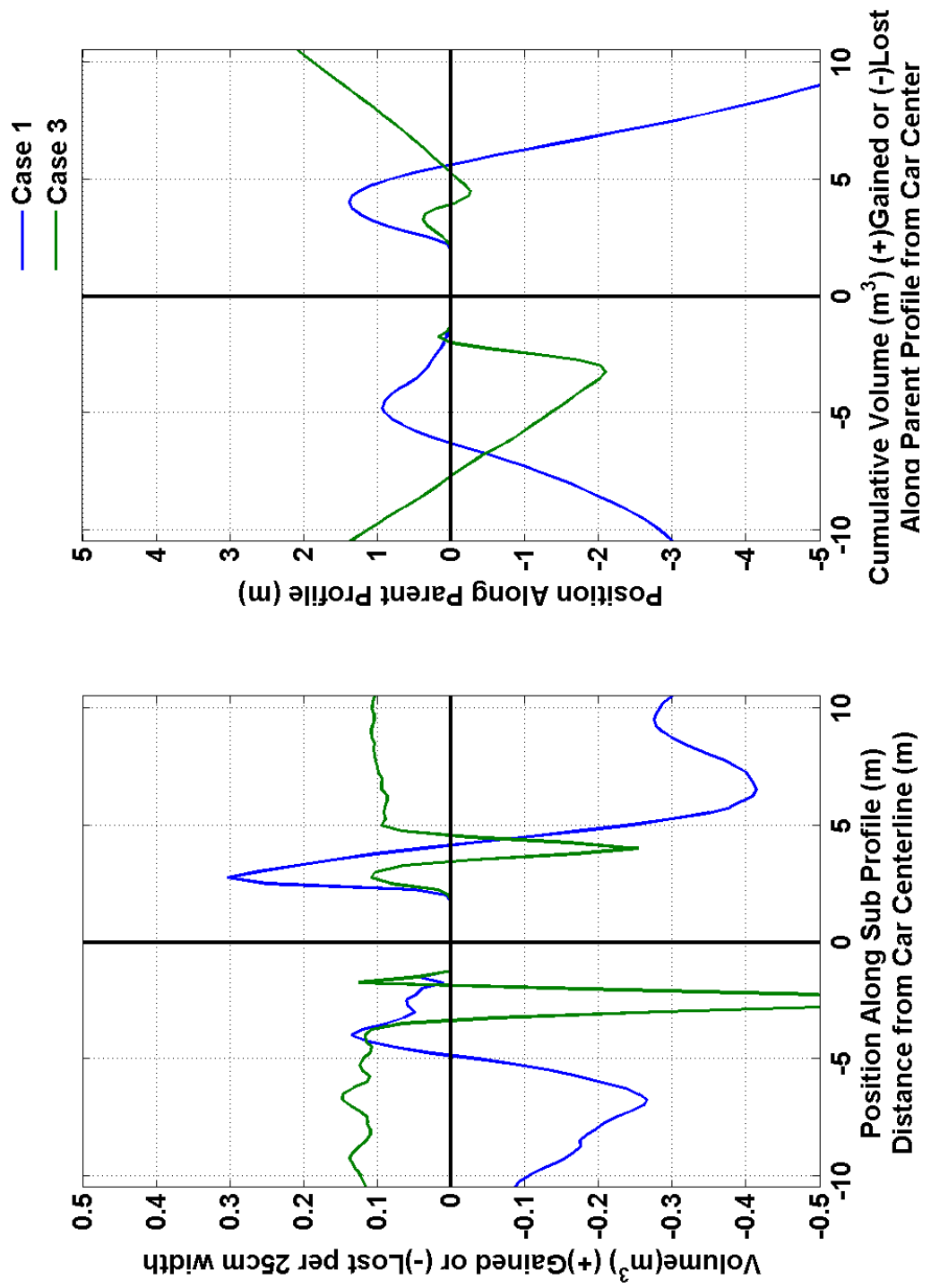
Car #37



Car #38

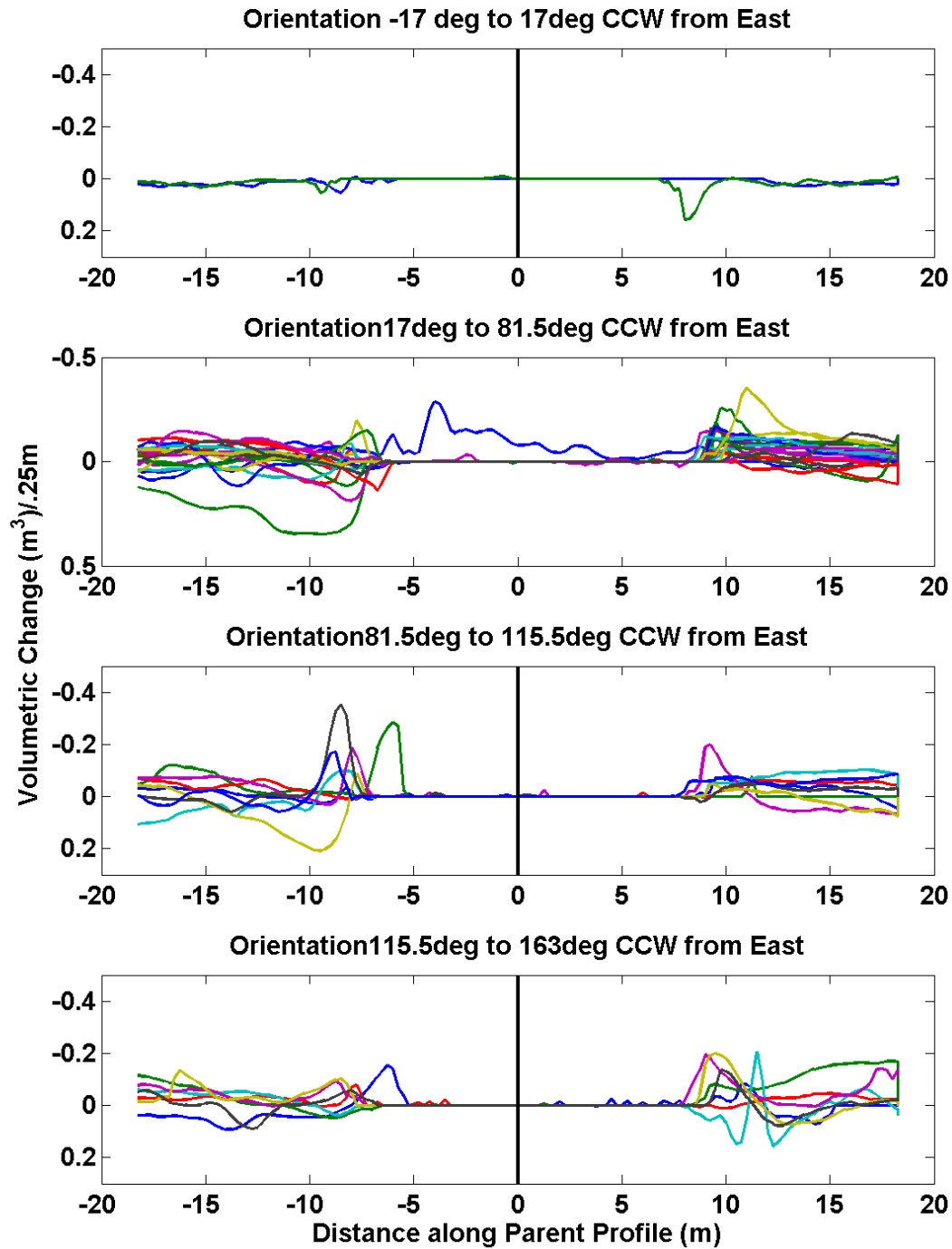


Car #38

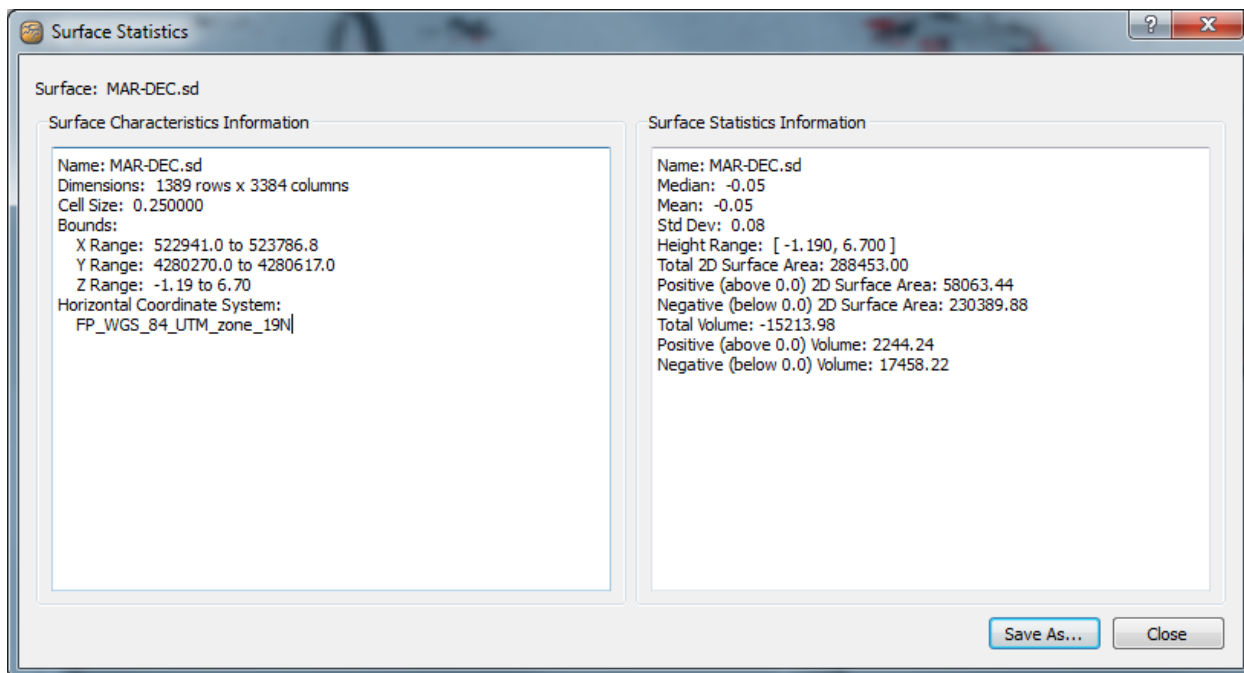
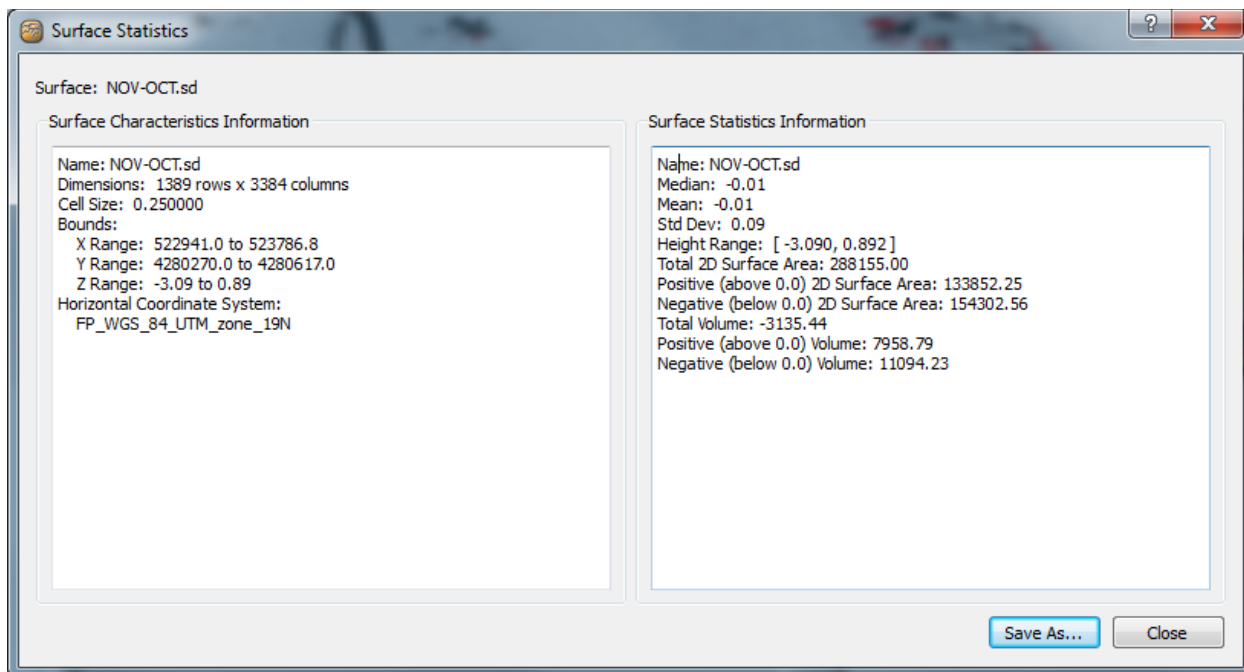


APPENDIX II- Orientation Plots

CASE III Major Axis by Orientation



APPENDIX III- Difference Surface Statistics



APPENDIX IV- MATLAB Script: Numeric Profiler

```

%%%%%%%%Header$$$$$
close all
clear all
clc

res = .25;
w = 2.67; %m from R26 car wikipedia
l = 15.56; %m from R26 car wikipedia

%VOL_NOV_DEC= ['Trial ' 'Orientation ' 'Depth(m) ' 'Height of Car (m) '];
ii=0
for i=100:5:285
    ii=ii+1;
    trial(ii)=i;
%load OCT Datum Surface for orientation data
file_number=num2str(i);
file_name=strcat(file_number, '.txt');
working_file=importdata(file_name);
test = working_file;
%delete and entries with 0 for depth
g=test(:,6)~=0;
test = test(g,:);
test1 = test;

%%%%%%%%ENTER PARAMETERS OF ANALYSIS%%%%%%%%
%extent of bottom sample

start1 = -2.5*w; %<-- Enter here left side start
finish1 = -2.0*w; %<--Enter here left side finish
start2 = 2.0*w; %<-- Enter here right side start
finish2 = 2.5*w; %<--Enter here right side finish
parentstart = 0; %<--Enter here how far from head to start
parentfinish = 4*w+l; %<--Enter here how far along parent to figure bottom
%top of car measurements
startofcar = max(test(:,2))/2-5; %<--Enter here where to start the top of car average
endofcar = max(test(:,2))/2+5; %<-- End top of car average
widthaveraged = .25*w; %<--This is -.25w to +.25w width

%output is saved in "testtenmatrix.mat" and should be pasted directly into
%excel sheet

%Only look at data within the search parameters above
%only look at data within the desired length of parent
a = (test(:,2)>=parentstart&test(:,2)<=parentfinish);

```

```

test = test(a,:);
%%only look at data on the negative side between limits
b=test(:,3)>=start1&test(:,3)<=finish1;
testleft= test(b,:);
c=test(:,3)>=start2&test(:,3)<=finish2;
testright= test(c,:);
%%combine both left and righth sides (already truncated by 0 depth values
%%and parent serach limits)
testtotal = [testleft;testright];

%length requirements for car bottom profile

% test1 = test(b,:);
% test2 = test(c,:);
% test3 = test(f,:);
% testtotal = [test1;test2;test3];

averagebottomdepth(ii)= mean(testtotal(:,6));
orientationboolean = test(:,3)==0;
om = test(orientationboolean,:);
orientation(ii)= (180/pi)*atan2((om(1,5)-om(length(om),5)),(om(1,4)-om(length(om),4)));

%top of car average
d=test1(:,2)>=startofcar&test1(:,2)<=endofcar;
topofcar = test1(d,:);
e=topofcar(:,3)>=-widthaveraged&topofcar(:,3)<=widthaveraged;
topofcar = topofcar(e,:);
averagetopofcar(ii)= mean(topofcar(:,6));
%height of car
heightofcar(ii) = -(averagebottomdepth(ii)-averagetopofcar(ii));
%data production

if 0==1
metadata = [w l start1 finish1 start2 finish2 parentstart parentfinish ...
startofcar endofcar widthaveraged];
testtenmatrix=[trial orientation averagebottomdepth averagetopofcar heightofcar
metadata];
file_array(i,:)=testtenmatrix(1,:);

plot (XXX,YYY,'LineWidth',2,'Color',[0 0 0]);
%# vertical line
hx = graph2d.constantline(0, 'LineWidth',2,'Color',[0 0 0]);
changedependvar(hx,'x');
hold off
hold off
%saveas(gcf, sprintf('figure%d.fig', i));
%saveas(gcf, sprintf('fig_hist_orient_height.png', i));

```

```

%saveas(gcf, sprintf('improvedfigure%d.pdf', i));
end

end

figure(1)
orient tall
subplot(311)
plot(1:38,orientation, '*')
ylabel ('Orientations (CCW from East) (deg)')
xlabel ('Car #')
subplot(312)
plot(1:38,heightofcar, '*')
ylabel ('Car Height (m)')
xlabel ('Car #')
subplot(313)
plot(1:38,-averagebottomdepth, '*')
ylabel ('Depth (m)')
xlabel ('Car #')
%suptitle ('Defining Paramters of Cars Located withing the Analysis Area')
%saveas(gcf, 'fig_orient_height.fig');
%print(gcf, '-dpng', 'fig_orient_height.png');
%saveas(gcf, 'fig_orient_height.pdf');

figure(2)
orient landscape
subplot(131)
hist(orientation, 18)
ylabel ('# of Cars')
xlabel ('Orientation (CCW from East) (deg)')
subplot(132)
hist(heightofcar, 18)
ylabel ('# of Cars')
xlabel ('Car Height Above Seafloor (m)')
subplot (133)
hist (-averagebottomdepth, 10)
xlabel ('Average Bottom Depth (m)')
ylabel ('# of Cars')
%suptitle ('Distribution of Defining Parameters')
%saveas(gcf, 'fig_hist_orient_height.fig');
%print(gcf, '-dpng', 'fig_hist_orient_height.png');
%saveas(gcf, 'fig_hist_orient_height.pdf');

figure(3)
orient landscape
subplot(311)
plot(orientation,heightofcar, '.')
ylabel ('Height of Car (m)')

```



```

xlabel ('Orientation (CCW from East) (deg)')
subplot(312)
plot(averagebottomdepth,heightofcar,':')
ylabel ('Height of Car (m)')
xlabel ('Depth of Car (m)')
subplot (313)
plot (orientation, averagebottomdepth,':')
xlabel ('Orientation (CCW from East) (deg)')
ylabel ('Depth of Car (m)')
saveas (gcf, 'carstats.png')
%save('car_orient_height.mat','trial','orientation','heightofcar','averagebottomdepth');

```

APPENDIX V- MATLAB Scripts:10X Script

10X Profiler Script

```

%%%%%%%%Header$$$$$
close all
clear all
clc
%%% DEFINE WHICH CAR PROFILE TO BE EXAMINED%%%%%%%%
%%---->remember to change the "X file name in "test=X" to respective number
load testsection
trial= testsection
%test=X10;
A = sortrows(trial,3);
%%%%%%%%ENTER PARAMETERS OF ANALYSIS%%%%%%%%
%extent of bottom sample
w = 2.67; %m from R26 car wikipedia
l = 15.56; %m from R26 car wikipedia
start1 = -2.7*w; %<-- Enter here left side start
finish1 = -2.5*w; %<--Enter here left side finish
start2 = 2.5*w; %<-- Enter here right side start
finish2 = 2.7*w; %<--Enter here right side finish
parentstart = 0; %<--Enter here how far from head to start
parentfinish = 16.75; %<--Enter here how far along parent to figure bottom
%top of car measurements
startofcar = 12; %<--Enter here where to start the top of car average
endofcar = 20; %<-- End top of car average
widthaveraged = .25*w; %<--This is -.25w to +.25w width

%output is saved in "testtenmatrix.mat" and should be pasted directly into
%excel sheet

%%%%%%%% CODE TO ANALYZE DATA%%%%%%%%

%delete and entries with 0 for depth
g=test(:,6)~=0;
test = test(g,:);
test1 = test;

%Only look at data within the search parameters above
%%only look at data within the desired length of parent
a = (test(:,2)>=parentstart&test(:,2)<=parentfinish);
test = test(a,:);
%%only look at data on the negative side between limits
b=test(:,3)>=start1&test(:,3)<=finish1;
testleft= test(b,:);
c=test(:,3)>=start2&test(:,3)<=finish2;
testright= test(c,:);
%%combine both left and righth sides (already truncated by 0 depth values

```

```

%%and parent serach limits)
testtotal = [testleft;testright];

%length requirements for car bottom profile

% test1 = test(b,:);
% test2 = test(c,:);
% test3 = test(f,:);
% testtotal = [test1;test2;test3];

averagebottomdepth = mean(testtotal(:,6));
orientationboolean = test(:,3)==0;
om = test(orientationboolean,:);
orientation = (180/pi)*atan2((om(1,5)-om(length(om),5)).(om(1,4)-om(length(om),4)));

%top of car average
d=test1(:,2)>=startofcar&test1(:,2)<=endofcar;
topofcar = test1(d,:);
e=topofcar(:,3)>=-widthaveraged&topofcar(:,3)<=widthaveraged;
topofcar = topofcar(e,:);
averagetopofcar = mean(topofcar(:,6));
%height of car
heightofcar = (averagebottomdepth-averagetopofcar);
%data production
metadata = [w l start1 finish1 start2 finish2 parentstart parentfinish ...
    startofcar endofcar widthaveraged];
testtenmatrix=[trial orientation averagebottomdepth averagetopofcar heightofcar
metadata]

dlmwrite (num2str(trial),testtenmatrix)

```

APPENDIX VI- MATLAB Script: Wave Data

```
close all
clear all
clc
figure
load Redbird_ADCP.mat
subplot (3,1,1)
plot(OctNov.datewave, OctNov.Hs, 'LineWidth', 2); datetick('x', 'dd-mmm-yyyy',
'keepslimits')
ylim([0 8])
grid on
grid minor
xlabel('Date','FontSize',18, 'FontWeight', 'Bold', 'FontName', 'Times New Roman')
ylabel('Meters','FontSize',18, 'FontWeight', 'Bold', 'FontName', 'Times New Roman')
set(gca, 'FontSize', 16, 'FontName', 'Times New Roman', 'FontWeight', 'normal');
title('Redbird ADCP Wave Height-OctNov', 'FontName', 'Times New
Roman','FontSize',18,'fontweight','bold');
subplot (3,1,2)
plot(OctNov.datewave, OctNov.Dp, 'LineWidth', 2); datetick('x', 'dd-mmm-yyyy',
'keepslimits')
ylim([0 360])
grid on
grid minor
xlabel('Date','FontSize',18, 'FontWeight', 'Bold', 'FontName', 'Times New Roman')
ylabel('Degrees','FontSize',18, 'FontWeight', 'Bold', 'FontName', 'Times New Roman')
set(gca, 'FontSize', 16, 'FontName', 'Times New Roman', 'FontWeight', 'normal');
title('Redbird ADCP Dominant Wave Direction', 'FontName', 'Times New
Roman','FontSize',18,'fontweight','bold');
subplot (3,1,3)
plot(OctNov.datewave, OctNov.Tp, 'LineWidth', 2); datetick('x', 'dd-mmm-yyyy',
'keepslimits')
ylim([0 20])
grid on
grid minor
xlabel('Date','FontSize',18, 'FontWeight', 'Bold', 'FontName', 'Times New Roman')
ylabel('Period (Sec)','FontSize',18, 'FontWeight', 'Bold', 'FontName', 'Times New Roman')
set(gca, 'FontSize', 16, 'FontName', 'Times New Roman', 'FontWeight', 'normal');
title('Redbird ADCP Dominant Wave Period', 'FontName', 'Times New
Roman','FontSize',18,'fontweight','bold');

figure
subplot (3,1,1)
plot(MarJune.datewave, MarJune.Hs, 'LineWidth', 2); datetick('x', 'dd-mmm-yyyy',
'keepslimits')
ylim([0 8])
grid on
```

```

grid minor
xlabel('Date', 'FontSize', 18, 'FontWeight', 'Bold', 'FontName', 'Times New Roman')
ylabel('Meters', 'FontSize', 18, 'FontWeight', 'Bold', 'FontName', 'Times New Roman')
set(gca, 'FontSize', 16, 'FontName', 'Times New Roman', 'FontWeight', 'normal');
title('Redbird ADCP Wave Height-MarJune', 'FontName', 'Times New
Roman', 'FontSize', 18, 'fontWeight', 'bold');
subplot (3,1,2)
plot(MarJune.datewave, MarJune.Dp, 'LineWidth', 2); datetick('x', 'dd-mmm-yyyy',
'keplimits')
ylim([0 360])
grid on
grid minor
xlabel('Date', 'FontSize', 18, 'FontWeight', 'Bold', 'FontName', 'Times New Roman')
ylabel('Degrees', 'FontSize', 18, 'FontWeight', 'Bold', 'FontName', 'Times New Roman')
set(gca, 'FontSize', 16, 'FontName', 'Times New Roman', 'FontWeight', 'normal');
title('Redbird ADCP Dominant Wave Direction', 'FontName', 'Times New
Roman', 'FontSize', 18, 'fontWeight', 'bold');
subplot (3,1,3)
plot(MarJune.datewave, MarJune.Tp, 'LineWidth', 2); datetick('x', 'dd-mmm-yyyy',
'keplimits')
ylim([0 20])
grid on
grid minor
xlabel('Date', 'FontSize', 18, 'FontWeight', 'Bold', 'FontName', 'Times New Roman')
ylabel('Period (Sec)', 'FontSize', 18, 'FontWeight', 'Bold', 'FontName', 'Times New Roman')
set(gca, 'FontSize', 16, 'FontName', 'Times New Roman', 'FontWeight', 'normal');
title('Redbird ADCP Dominant Wave Period', 'FontName', 'Times New
Roman', 'FontSize', 18, 'fontWeight', 'bold');

figure
subplot (3,1,1)
plot(JulySept.datewave, JulySept.Hs, 'LineWidth', 2); datetick('x', 'dd-mmm-yyyy',
'keplimits')
ylim([0 8])
grid on
grid minor
xlabel('Date', 'FontSize', 18, 'FontWeight', 'Bold', 'FontName', 'Times New Roman')
ylabel('Meters', 'FontSize', 18, 'FontWeight', 'Bold', 'FontName', 'Times New Roman')
set(gca, 'FontSize', 16, 'FontName', 'Times New Roman', 'FontWeight', 'normal');
title('Redbird ADCP Wave Height-JulySept', 'FontName', 'Times New
Roman', 'FontSize', 18, 'fontWeight', 'bold');
subplot (3,1,2)
plot(JulySept.datewave, JulySept.Dp, 'LineWidth', 2); datetick('x', 'dd-mmm-yyyy',
'keplimits')
ylim([0 360])
grid on
grid minor
xlabel('Date', 'FontSize', 18, 'FontWeight', 'Bold', 'FontName', 'Times New Roman')

```

```

ylabel('Degrees',FontSize,18,'FontWeight','Bold','FontName','Times New Roman')
set(gca,'FontSize',16,'FontName','Times New Roman','FontWeight','normal');
title('Redbird ADCP Dominant Wave Direction','FontName','Times New
Roman',FontSize,18,'fontweight','bold');
subplot (3,1,3)
plot(JulySept.datewave, JulySept.Tp, 'LineWidth', 2); datetick('x', 'dd-mmm-yyyy',
'keplimits')
ylim([0 20])
grid on
grid minor
xlabel('Date',FontSize,18,'FontWeight','Bold','FontName','Times New Roman')
ylabel('Period (Sec)',FontSize,18,'FontWeight','Bold','FontName','Times New Roman')
set(gca,'FontSize',16,'FontName','Times New Roman','FontWeight','normal');
title('Redbird ADCP Dominant Wave Period','FontName','Times New
Roman',FontSize,18,'fontweight','bold');

```

```

figure
subplot (3,1,1)
plot(AugSept.datewave, AugSept.Hs, 'LineWidth', 2); datetick('x', 'dd-mmm-yyyy',
'keplimits')
ylim([0 8])
grid on
grid minor
xlabel('Date',FontSize,18,'FontWeight','Bold','FontName','Times New Roman')
ylabel('Meters',FontSize,18,'FontWeight','Bold','FontName','Times New Roman')
set(gca,'FontSize',16,'FontName','Times New Roman','FontWeight','normal');
title('Redbird ADCP Wave Height-AugSept','FontName','Times New
Roman',FontSize,18,'fontweight','bold');
subplot (3,1,2)
plot(AugSept.datewave, AugSept.Dp, 'LineWidth', 2); datetick('x', 'dd-mmm-yyyy',
'keplimits')
ylim([0 360])
grid on
grid minor
xlabel('Date',FontSize,18,'FontWeight','Bold','FontName','Times New Roman')
ylabel('Degrees',FontSize,18,'FontWeight','Bold','FontName','Times New Roman')
set(gca,'FontSize',16,'FontName','Times New Roman','FontWeight','normal');
title('Redbird ADCP Dominant Wave Direction','FontName','Times New
Roman',FontSize,18,'fontweight','bold');
subplot (3,1,3)
plot(AugSept.datewave, AugSept.Tp, 'LineWidth', 2); datetick('x', 'dd-mmm-yyyy',
'keplimits')
ylim([0 20])
grid on
grid minor
xlabel('Date',FontSize,18,'FontWeight','Bold','FontName','Times New Roman')
ylabel('Period (Sec)',FontSize,18,'FontWeight','Bold','FontName','Times New Roman')

```

```
set(gca, 'FontSize', 16, 'FontName', 'Times New Roman', 'FontWeight', 'normal');  
title('Redbird ADCP Dominant Wave Period', 'FontName', 'Times New  
Roman', 'FontSize', 18, 'fontWeight', 'bold');
```

APPENDIX VII- MATLAB Script: COMPWAVES

```

close all
clear all
clc
load 4409_2013.txt
load 4409_2012.txt
load WW3_CompRec_4Bo.mat
Wavedata = [X4409_2012;X4409_2013];
for i=1:length(Wavedata);
    Wavedata(i,:)= [Wavedata(i,1:5) Wavedata(i,6:18)];
    Wavedatas(i,:) = [datenum([Wavedata(i,1:5) 0]) Wavedata(i,6:18)];
end
A= Wavedatas(:,3)~=99;
Wavedatas=Wavedatas(A,:);
B= Wavedatas(:,2)~=999;
Wavedatas=Wavedatas(B,:);

MONTH =
Wavedatas(:,1)>=datenum(2012,10,6)&Wavedatas(:,1)<=datenum(2013,07,01);
MONTHcomp =
CompRecdate(:,1)>=datenum(2012,10,6)&CompRecdate(:,1)<=datenum(2013,07,01);
Wavedatas = Wavedatas(MONTH,:);
Waveheight = Wavedatas(:,5)~=99;
Wavedatas = Wavedatas(Waveheight,:);
CompRecdate=CompRecdate(MONTHcomp,:);
CompRecHs = CompRecHs(MONTHcomp,:);
CompRecTp = CompRecTp(MONTHcomp,:);

subplot (3,1,1)
plot(CompRecdate,CompRecHs,'LineWidth', 2); datetick('x', 'dd-mmm-yyyy')
ylim([0 8])
grid on
grid minor
xlabel('Date','FontSize',18, 'FontWeight', 'Bold', 'FontName', 'Times New Roman')
ylabel('Hs (meters)','FontSize',18, 'FontWeight', 'Bold', 'FontName', 'Times New Roman')
set(gca, 'FontSize', 16, 'FontName', 'Times New Roman', 'FontWeight', 'normal');
title('Redbird ADCP Significant Wave Height', 'FontName', 'Times New Roman','FontSize',18,'fontweight','bold');
subplot(3,1,2)
plot(Wavedatas(:,1),Wavedatas(:,2), 'LineWidth', 2); datetick('x', 'dd-mmm-yyyy')
ylim([0 360])
xlim([min(CompRecdate) max(CompRecdate)]);
grid on
grid minor
xlabel('Date','FontSize',18, 'FontWeight', 'Bold', 'FontName', 'Times New Roman')

```



```

ylabel('Direction (deg)',FontSize,18, 'FontWeight', 'Bold', 'FontName', 'Times New Roman')
set(gca, 'FontSize', 16, 'FontName', 'Times New Roman', 'FontWeight', 'normal');
title('Redbird ADCP Dominant Wave Direction', 'FontName', 'Times New Roman',FontSize,18,'fontweight','bold');

subplot(3,1,3)
plot(CompRecdate,CompRecTp, 'LineWidth', 2); datetick('x', 'dd-mmm-yyyy')
ylim([2.5 17])
grid on
grid minor
xlabel('Date',FontSize,18, 'FontWeight', 'Bold', 'FontName', 'Times New Roman')
ylabel('Period (Sec)',FontSize,18, 'FontWeight', 'Bold', 'FontName', 'Times New Roman')
set(gca, 'FontSize', 16, 'FontName', 'Times New Roman', 'FontWeight', 'normal');
title('Redbird ADCP Dominant Wave Period', 'FontName', 'Times New Roman',FontSize,18,'fontweight','bold');

```

APPENDIX VIII- MATLAB Script: Final Wave Plots

```

close all
clear all
clc
load WW3_CompRec_4Bo1
load wavedatas
startdate = datenum(2012,12,5);
enddate = datenum(2013,4,1);

datefilter = CompRecdate>startdate & CompRecdate<enddate;
datefilterfordir = Wavedatas(:,1)>startdate & Wavedatas(:,1)<enddate;
CompRecdate = CompRecdate(datefilter,:);
CompRecHs = CompRecHs(datefilter,:);
CompRecTp = CompRecTp(datefilter,:);
Wavedatas = Wavedatas(datefilterfordir,:);

MAXHS = max(CompRecHs)
MAXTP = max(CompRecTp)
figure
orient landscape
subplot(3,1,1)
plot(CompRecdate,CompRecHs,',' , 'LineWidth', 2); datetick('x', 'dd-mmm-yy')
dumtick=735143+ [ 0 31 60 92 103 131 162 192];
%set(gca,'xtick',dumtick)
ylim([0 10])
xlim([startdate enddate])
grid on
grid minor
%xlabel('Date','FontSize',18, 'FontWeight', 'Bold', 'FontName', 'Times New Roman')
ylabel('Hs (meters)','FontSize',18, 'FontWeight', 'Bold', 'FontName', 'Times New Roman')
set(gca, 'FontSize', 16, 'FontName', 'Times New Roman', 'FontWeight', 'normal');
title('Redbird ADCP Significant Wave Height', 'FontName', 'Times New
Roman','FontSize',18,'fontweight','bold');

subplot(3,1,2)
plot(Wavedatas(:,1),Wavedatas(:,2), ',' , 'LineWidth', 2); datetick('x', 'dd-mmm-yy')
%set(gca,'xtick',dumtick)
ylim([0 360])
xlim([startdate enddate])
% xlim([min(CompRecdate) max(CompRecdate)]);
grid on
grid minor
%xlabel('Date','FontSize',18, 'FontWeight', 'Bold', 'FontName', 'Times New Roman')
ylabel('Direction (deg)','FontSize',18, 'FontWeight', 'Bold', 'FontName', 'Times New
Roman')
set(gca, 'FontSize', 16, 'FontName', 'Times New Roman', 'FontWeight', 'normal');

```

```

title('Redbird ADCP Dominant Wave Direction', 'FontName', 'Times New
Roman','FontSize',18,'fontweight','bold');

subplot(3,1,3)
plot(CompRecdate,CompRecTp,'.','LineWidth', 2); datetick('x', 'dd-mmm-yy')
%set(gca,'xtick',dumtick)
ylim([2.5 17])
xlim([startdate enddate])
grid on
grid minor
%xlabel('Date','FontSize',18, 'FontWeight', 'Bold', 'FontName', 'Times New Roman')
ylabel('Period (Sec)','FontSize',18, 'FontWeight', 'Bold', 'FontName', 'Times New Roman')
set(gca, 'FontSize', 16, 'FontName', 'Times New Roman', 'FontWeight', 'normal');
title('Redbird ADCP Dominant Wave Period', 'FontName', 'Times New
Roman','FontSize',18,'fontweight','bold');
saveas(gcf, 'DEC_MAR_wavedate.png')

```

APPENDIX IX- MATLAB Script: Find Minor Scour

```

%%%%%%%%Header$$$$$
close all
clear all
clc
load('car_orient_height.mat')
res = .25;
w = 2.67; %m from R26 car wikipedia
l = 15.56; %m from R26 car wikipedia
%trim data set
Desiredheight = .8*l;%m
Desiredwidth = 8*w;%m

%VOL_NOV_DEC= ['Trial ' 'Orientation ' 'Depth(m) ' 'Height of Car (m) '];
ii=0
for i=100:5:285
    ii=ii+1;
    %load OCT Datum Surface for orientation data
    file_number=num2str(i);
    file_name=strcat(file_number, '.txt');
    working_file=importdata(file_name);
    %d% test = working_file;
    trial(ii)=i;
    %load NOV-OCT Difference Surface
    file_numberdiffOCT_NOV=num2str(i+1);
    file_namediffOCT_NOV=strcat(file_numberdiffOCT_NOV, '.txt');
    working_filediffOCT_NOV=importdata(file_namediffOCT_NOV);
    A = sortrows(working_filediffOCT_NOV,3);
    %load DEC-NOV Difference Surface
    file_numberdiffNOV_DEC=num2str(i+2);
    file_namediffNOV_DEC=strcat(file_numberdiffNOV_DEC, '.txt');
    working_filediffNOV_DEC=importdata(file_namediffNOV_DEC);
    B = sortrows(working_filediffNOV_DEC,3);
    %load MAR_DEC Difference Surface
    file_numberdiffMAR_DEC=num2str(i+2);
    file_namediffMAR_DEC=strcat(file_numberdiffMAR_DEC, '.txt');
    working_filediffMAR_DEC=importdata(file_namediffMAR_DEC);
    C = sortrows(working_filediffMAR_DEC,3);
    %load JUL_MAR Difference Surface
    file_numberdiffJUL_MAR=num2str(i+4);
    file_namediffJUL_MAR=strcat(file_numberdiffJUL_MAR, '.txt');
    working_filediffJUL_MAR=importdata(file_namediffJUL_MAR);
    E = sortrows(working_filediffJUL_MAR,3);

```

```

%trim matrix by .5*difference between data set height and desired height
%from both sides
test2=A;
y1=((max(test2(:,2))-Desiredheight)/2);
y2=(max(test2(:,2))-(max(test2(:,2))-Desiredheight)/2);
x1=-Desiredwidth/2;
x2=Desiredwidth/2;
trim = test2(:,2)>=y1 & test2(:,2)<=y2&test2(:,3)>=x1 & test2(:,3)<=x2 ;

test2 = test2(trim,:);
A = A(trim,:);
B = B(trim,:);
C = C(trim,:);
E = E(trim,:);

numx=floor((x2-x1)/res);
numy=length(A)/numx;
for jj=1:numx

    dumj=(1:numy)+(jj-1)*numy;

    %jj dumj(1) max(dumj)]
    VOLA(ii,jj)=sum(A(dumj,6))*res^2;
    VOLC(ii,jj)=sum(C(dumj,6))*res^2;
    xpos(jj)=A(dumj(1),3);

end
totsuma(ii,ceil(numx/2):numx)=cumsum(VOLA(ii,ceil(numx/2):numx));
totsuma(ii,floor(numx/2):-1:1)=cumsum(VOLA(ii,floor(numx/2):-1:1)) ;
totsumc(ii,ceil(numx/2):numx)=cumsum(VOLC(ii,ceil(numx/2):numx));
totsumc(ii,floor(numx/2):-1:1)=cumsum(VOLC(ii,floor(numx/2):-1:1)) ;

figure(ii);
clf
hold on
orient landscape
subplot (1,2,1);
plot (xpos,VOLA(ii,:),xpos,VOLC(ii,:));
axis ([-10.5 10.5 -.5 .5])

text(-9.9,.60,[' Orientation=' num2str(orientation(ii)) ' deg'])
text (-9.9,.57, [' Car Depth=' num2str(averagebottomdepth(ii)) 'm'])
text (-9.9,.54,[' Height of Car=' num2str(abs(heightofcar(ii))) 'm'])
ylabel ('Volume(m^3) (+)Gained or (-)Lost per 25cm width');
xlabel ({'Position Along Sub Profile (m)';'Distance from Car Centerline (m)'});
hold on
XXX= xpos;

```

```

YYY= zeros(1,length(xpos));
hx = graph2d.constantline(0, 'LineWidth',2,'Color',[0 0 0]);
changedependvar(hx,'x');
plot (XXX,YYY,'LineWidth',2,'Color',[0 0 0]);
grid on
subplot(1,2,2)
plot(xpos,totsuma(ii,:),xpos,totsumc(ii,:));
hold on
XXX= xpos;
YYY= zeros(1,length(xpos));
hx = graph2d.constantline(0, 'LineWidth',2,'Color',[0 0 0]);
changedependvar(hx,'x');
plot (XXX,YYY,'LineWidth',2,'Color',[0 0 0]);
grid on
axis ([-10.5 10.5 -5 5])
%title (['Car #' num2str(ii)])
legend1 = legend ('Case 1', 'Case 2')
set(legend1,...
    'Position',[0.732843137254902 0.908497202238208 0.145588235294118
0.100719424460432]);
legend ('boxoff')
xlabel ({'Cumulative Volume (m^3) (+)Gained or (-)Lost'; 'Along Parent Profile from Car
Center'});
ylabel ('Position Along Parent Profile (m)');
suptitle (['Car #' num2str(ii)])
saveas(gcf, sprintf('figure%dminor.png', ii));
hold off
end

save('MINORSCOUR.mat','VOLA','VOLC','totsuma','totsumc','xpos');
if 0==1
volc =
[VOLC(1:3,:);VOLC(5:6,:);VOLC(8,:);VOLC(11:14,:);VOLC(16:20,:);VOLC(22:23,:);VOLC(25,:
);VOLC(27:32,:);VOLC(35:38,:)];
TOTSUMc =
[totsumc(1:3,:);totsumc(5:6,:);totsumc(8,:);totsumc(11:14,:);totsumc(16:20,:);totsumc(22:2
3,:);totsumc(25,:);totsumc(27:32,:);totsumc(35:38,:)];
figure;
clf
hold on
orient landscape
subplot (1,2,1);
plot (xpos,volc);
hold on
hold on
% XXX= ;
% YYY=zeros(length(VOLA));
% YYY(1,:)= floor(length(VOLA)/2);

```

```

hx = graph2d.constantline(0, 'LineWidth',2,'Color',[0 0 0]);
changedependvar(hx,'x');
%plot (XXX,YYY,'LineWidth',2,'Color',[0 0 0]);
grid on
axis ([-11 11 -1.25 1.25])

% text(-.49,43,[' Orientation=' num2str(orientation(ii)) ' deg'])
% text (-.49,42,[' Car Depth=' num2str(averagebottomdepth(ii)) 'm'])
% text (-.49,41,[' Height of Car=' num2str(abs(heightofcar(ii))) 'm'])
ylabel ({'Volume(m^3) (+)Gained'; 'or (-)Lost per 25cm width'});
xlabel ('Position Along Sub Profile (m)');
subplot(1,2,2)
plot(xpos, TOTSUMc);
hx = graph2d.constantline(0, 'LineWidth',2,'Color',[0 0 0]);
changedependvar(hx,'x');
%plot (XXX,YYY,'LineWidth',2,'Color',[0 0 0]);
grid on
axis ([-11 11 -15 15])
%title (['Car #' num2str(ii)])
%legend1 = legend ('Case 1', 'Case 2');
%set(legend1,...
% 'Position',[0.732843137254902 0.908497202238208 0.145588235294118
0.100719424460432]);
legend ('boxoff')
xlabel ({'Cumulative Volume (m^3) (+)Gained or (-)Lost'; 'Along Parent Profile from Car
Center'});
ylabel ('Position Along Parent Profile (m)');
suptitle (['All Cars Case 2'])
saveas(gcf, 'figminor_allcars_CASE2.png')
end
% figure % create new figure
% subplot(2,2,1) % first subplot
% plot(x,y1)
%figure creation
% figure;
% hold on
% subplot (2,1,1);
% plot (xpos,VOLA,xpos,VOLC);
%
% subplot(2,1,2)
% plot(xpos,totsuma,xpos,totsumc);
%

% if 0==1
% NOV_DEC_VOL=VOLA';
% legend('OCT-NOV','NOV-DEC','DEC-MAR','MAR-JUL')
% hold on

```

```

% %plot (DC, VOLC);
% XXX= DA;
% YYY= zeros(1,length(DA));
% hold on
% plot (XXX,YYY,'LineWidth',2,'Color',[0 0 0]);
% grid on
% %grid minor
% title (['Car #' num2str(trial) ' Orientation=' num2str(testtenmatrix(1,2))...
%   ' deg Car Depth=' num2str(testtenmatrix(1,3)) 'm'...
%   ' Height of Car=' num2str(abs(testtenmatrix(1,5))) 'm']);
% xlabel ('Car Widths From Car Centerline (-)Left (+)Right');
% ylabel ('Volume(m^3/0.25m width) of Sediment (+)Gained or (-)Lost Along Test
Section');
% axis([-3.25 3.25 -1 1])
% %# vertical line
% hx = graph2d.constantline(0, 'LineWidth',2,'Color',[0 0 0]);
% changedependvar(hx,'x');
% hold off
%
% subplot(2,1,2);
% hold on
% plot (DA,TOTSUMA,DB,TOTSUMB,DC,TOTSUMC,DE,TOTSUME);
% NOV_DEC_SUM=TOTSUMA;
% legend('OCT-NOV','NOV-DEC','DEC-MAR','MAR-JUL')
% %plot (DC, TOTSUMC);
% grid on
% %refline(0,0)
% %grid minor
% title ('Cumulative Volume Gained(+) or Lost(-) as a F(Distance from Centerline)');
% xlabel ('Car Widths From Car Centerline (-)Left (+)Right');
% ylabel ('Cumulative Volume Change (m^3)');
% axis([-3.25 3.25 -5 5]);
% %set(gca,'linewidth',3)
% hold on
% plot (XXX,YYY,'LineWidth',2,'Color',[0 0 0]);
% %# vertical line
% hx = graph2d.constantline(0, 'LineWidth',2,'Color',[0 0 0]);
% changedependvar(hx,'x');
% hold off
% hold off
% saveas(gcf, sprintf('figure%d.fig', ii));
% saveas(gcf, sprintf('figure%d.png', ii));
% saveas(gcf, sprintf('improvedfigure%d.pdf', ii));
%
% %%% end
% cardata=file_array(:,1)~=0;
% CARDATA=file_array(cardata,:);

```



```
%  
save('minor_scour','file_array','VOL_OCT_NOV','VOL_NOV_DEC','VOL_DEC_MAR','VOL_M  
AR_JUL','TOT_OCT_NOV','TOT_NOV_DEC','TOT_DEC_MAR','TOT_MAR_JUL','DA','DB','DC','DE  
');  
% end
```

APPENDIX X- MATLAB Script: Find Major Scour

```

%%%%%%%%Header$$$$$
close all
clear all
clc

load('car_orient_height.mat')
res = .25;
w = 2.67; %m from R26 car wikipedia
l = 15.56; %m from R26 car wikipedia
%trim data set
Desiredheight = 8*w+l;%m
Desiredwidth = w;%m

%VOL_NOV_DEC= ['Trial ' 'Orientation ' 'Depth(m) ' 'Height of Car (m) '];
ii=0
for i=100:5:285
    ii=ii+1;
    %load OCT Datum Surface for orientation data
    file_number=num2str(i);
    file_name=strcat(file_number, '.txt');
    working_file=importdata(file_name);
    %d% test = working_file;
    trial(ii)=i;
    %load NOV-OCT Difference Surface
    file_numberdiffOCT_NOV=num2str(i+1);
    file_namediffOCT_NOV=strcat(file_numberdiffOCT_NOV, '.txt');
    working_filediffOCT_NOV=importdata(file_namediffOCT_NOV);
    A = sortrows(working_filediffOCT_NOV,2);
    %load DEC-NOV Difference Surface
    file_numberdiffNOV_DEC=num2str(i+2);
    file_namediffNOV_DEC=strcat(file_numberdiffNOV_DEC, '.txt');
    working_filediffNOV_DEC=importdata(file_namediffNOV_DEC);
    B = sortrows(working_filediffNOV_DEC,2);
    %load MAR_DEC Difference Surface
    file_numberdiffMAR_DEC=num2str(i+2);
    file_namediffMAR_DEC=strcat(file_numberdiffMAR_DEC, '.txt');
    working_filediffMAR_DEC=importdata(file_namediffMAR_DEC);
    C = sortrows(working_filediffMAR_DEC,2);
    %load JUL_MAR Difference Surface
    file_numberdiffJUL_MAR=num2str(i+4);
    file_namediffJUL_MAR=strcat(file_numberdiffJUL_MAR, '.txt');
    working_filediffJUL_MAR=importdata(file_namediffJUL_MAR);
    E = sortrows(working_filediffJUL_MAR,2);

    %trim matrix by .5*difference between data set height and desired height

```

```

%from both sides
test2=A;
y1=((max(test2(:,2))-Desiredheight)/2);
y2=((max(test2(:,2))-(max(test2(:,2))-Desiredheight)/2);
x1=-Desiredwidth/2;
x2=Desiredwidth/2;
trim = test2(:,2)>=y1 & test2(:,2)<=y2 & test2(:,3)>=x1 & test2(:,3)<=x2 ;

```

```

A = A(trim,:);
B = B(trim,:);
C = C(trim,:);
E = E(trim,:);
numx=11; %length(A)/numy;
numy= length(A)/numx; %ceil((y2-y1)/res);

```

```

for jj=1:numy

```

```

    dumjy=(1:numx)+(jj-1)*numx;

```

```

    %[[jj dumj(1) max(dumj)]
    VOLA(ii,jj)=sum(A(dumjy,6))*res^2;
    VOLC(ii,jj)=sum(C(dumjy,6))*res^2;
    xpos(jj)=A(dumjy(1),3);
    ypos(jj)=A(dumjy(1),2);

```

```

end

```

```

    totsuma(ii,ceil(numy/2):numy)=cumsum(VOLA(ii,ceil(numy/2):numy));
    totsuma(ii,floor(numy/2):-1:1)=cumsum(VOLA(ii,floor(numy/2):-1:1)) ;
    totsumc(ii,ceil(numy/2):numy)=cumsum(VOLC(ii,ceil(numy/2):numy));
    totsumc(ii,floor(numy/2):-1:1)=cumsum(VOLC(ii,floor(numy/2):-1:1)) ;
figure(ii);
clf
hold on
orient tall
subplot (1,2,1);
plot (VOLA(ii,:),ypos,VOLC(ii,:),ypos);
hold on
hold on
% XXX= ;
% YYY=zeros(length(VOLA));
% YYY(1,:)= floor(length(VOLA)/2);
hx = graph2d.constantline(0, 'LineWidth',2,'Color',[0 0 0]);
changedependvar(hx,'x');
%plot (XXX,YYY,'LineWidth',2,'Color',[0 0 0]);

```

```

grid on
axis ([-0.5 0.5 0 40])

text(-.49,43,[' Orientation=' num2str(orientation(ii)) ' deg'])
text (-.49,42,[' Car Depth=' num2str(averagebottomdepth(ii)) 'm'])
text (-.49,41,[' Height of Car=' num2str(abs(heightofcar(ii))) 'm'])
xlabel ({'Volume(m^3) (+)Gained'; 'or (-)Lost per 25cm width'});
ylabel ('Position Along Parent Profile (m)');
subplot(1,2,2)
plot(totsuma(ii,:),ypos,totsumc(ii,:),ypos);
hx = graph2d.constantline(0, 'LineWidth',2,'Color',[0 0 0]);
changedependvar(hx,'x');
%plot (XXX,YYY,'LineWidth',2,'Color',[0 0 0]);
grid on
axis ([-4 4 0 40])
%title (['Car #' num2str(ii)])
legend1 = legend ('Case 1', 'Case 2');
set(legend1,...
    'Position',[0.732843137254902 0.908497202238208 0.145588235294118
    0.100719424460432]);
legend ('boxoff')
xlabel ({'Cumulative Volume (m^3) (+)Gained or (-)Lost'; 'Along Parent Profile from Car
Center'});
ylabel ('Position Along Parent Profile (m)');
suptitle (['Car #' num2str(ii)])

% saveas(gcf, sprintf('figure%d.fig', ii));
saveas(gcf, sprintf('figure%dmajor.png', ii));
% saveas(gcf, sprintf('improvedfigure%d.pdf', ii));
%print('-dpng', sprintf('figure%d.png', ii), '-r1000')
end
% figure % create new figure
% subplot(2,2,1) % first subplot
% plot(x,y1)
%figure creation
save('MAJORSCOUR.mat','VOLA','VOLC','totsuma','totsumc','ypos');
if 0==1
%%CASE I Alpha
%
% NOCHANGE(1,:)=totsuma(1,:);
% NOCHANGE(2,:)=totsuma(11,:);
% NOCHANGE(3,:)=totsuma(19,:);
% NOCHANGE(4,:)=totsuma(35,:);
% NOCHANGE(5,:)=totsuma(36,:);
% NOCHANGE(6,:)=totsuma(25,:);
% plot(NOCHANGE,ypos);
hx = graph2d.constantline(0, 'LineWidth',2,'Color',[0 0 0]);

```

```

changedependvar(hx,'x');
%plot (XXX,YYY,'LineWidth',2,'Color',[0 0 0]);
grid on
axis ([-4 4 0 40])
%title (['Car #' num2str(ii)])
%legend1 = legend ('Case 1', 'Case 2');
%set(legend1,...
    % 'Position',[0.732843137254902 0.908497202238208 0.145588235294118
0.100719424460432]);
legend ('boxoff')
xlabel ({'Cumulative Volume (m^3) (+)Gained or (-)Lost'; 'Along Parent Profile from Car
Center'});
ylabel ('Position Along Parent Profile (m)');
%supitle (['All Cars Case 1'])
saveas(gcf, 'figmajor_CASE1_NOCHANGE.png')
end
if 0==1
Volc=[VOLC(1:8,:);VOLC(10:20,:);VOLC(22:23,:);VOLC(25:26,:);VOLC(27:32,:);VOLC(34:38
,:)];
TOTSUMC=[totsumc(1:8,:);totsumc(10:20,:);totsumc(22:23,:);totsumc(25:26,:);totsumc(27:
32,:);totsumc(34:38,:)];
figure;
clf
hold on
orient tall
subplot (1,2,1);
plot (Volc,ypos);
hold on
hold on
% XXX= ;
% YYY=zeros(length(VOLA));
% YYY(1,:)= floor(length(VOLA)/2);
hx = graph2d.constantline(0, 'LineWidth',2,'Color',[0 0 0]);
changedependvar(hx,'x');
%plot (XXX,YYY,'LineWidth',2,'Color',[0 0 0]);
grid on
axis ([-0.5 0.5 0 40])

% text(-.49,43,[' Orientation=' num2str(orientation(ii)) ' deg'])
% text (-.49,42,[' Car Depth=' num2str(averagebottomdepth(ii)) 'm'])
% text (-.49,41,[' Height of Car=' num2str(abs(heightofcar(ii))) 'm'])
xlabel ({'Volume(m^3) (+)Gained'; 'or (-)Lost per 25cm width'});
ylabel ('Position Along Parent Profile (m)');
subplot(1,2,2)
plot(TOTSUMC,ypos);
hx = graph2d.constantline(0, 'LineWidth',2,'Color',[0 0 0]);
changedependvar(hx,'x');
%plot (XXX,YYY,'LineWidth',2,'Color',[0 0 0]);

```

```

grid on
axis ([-4 4 0 40])
%title (['Car #' num2str(ii)])
%legend1 = legend ('Case 1', 'Case 2');
%set(legend1,...
% 'Position',[0.732843137254902 0.908497202238208 0.145588235294118
0.100719424460432]);
legend ('boxoff')
xlabel ({'Cumulative Volume (m^3) (+)Gained or (-)Lost'; 'Along Parent Profile from Car
Center'});
ylabel ('Position Along Parent Profile (m)');
suptitle (['All Cars Case 2'])
saveas(gcf, 'figmajor_allcars_MARCHDEC.png')
end
if 0==1
figure;
hold on
subplot (1,2,1);
plot (VOLA,ypos);

subplot(1,2,2)
plot(totsuma,ypos);

end

% if 0==1
% NOV_DEC_VOL=VOLA';
% legend('OCT-NOV','NOV-DEC','DEC-MAR','MAR-JUL')
% hold on
% plot (DC, VOLC);
% XXX= DA;
% YYY= zeros(1,length(DA));
% hold on
% plot (XXX,YYY,'LineWidth',2,'Color',[0 0 0]);
% grid on
% grid minor
% title (['Car #' num2str(trial) ' Orientation=' num2str(testtenmatrix(1,2))...
% ' deg Car Depth=' num2str(testtenmatrix(1,3)) 'm'...
% ' Height of Car=' num2str(abs(testtenmatrix(1,5))) 'm']);
% xlabel ('Car Widths From Car Centerline (-)Left (+)Right');
% ylabel ('Volume(m^3/0.25m width) of Sediment (+)Gained or (-)Lost Along Test
Section');
% axis([-3.25 3.25 -1 1])
% # vertical line
% hx = graph2d.constantline(0, 'LineWidth',2,'Color',[0 0 0]);
% changedependvar(hx,'x');
% hold off
%
```

```

% subplot(2,1,2);
% hold on
% plot (DA,TOTSUMA,DB,TOTSUMB,DC,TOTSUMC,DE,TOTSUME);
% NOV_DEC_SUM=TOTSUMA;
% legend('OCT-NOV','NOV-DEC','DEC-MAR','MAR-JUL')
% plot (DC, TOTSUMC);
% grid on
% reline(0,0)
% grid minor
% title ('Cumulative Volume Gained(+) or Lost(-) as a F(Distance from Centerline)');
% xlabel ('Car Widths From Car Centerline (-)Left (+)Right');
% ylabel ('Cumulative Volume Change (m^3)');
% axis([-3.25 3.25 -5 5]);
% set(gca,'linewidth',3)
% hold on
% plot (XXX,YYY,'LineWidth',2,'Color',[0 0 0]);
% # vertical line
% hx = graph2d.constantline(0, 'LineWidth',2,'Color',[0 0 0]);
% changedependvar(hx,'x');
% hold off
% hold off
% saveas(gcf, sprintf('figure%d.fig', ii));
% saveas(gcf, sprintf('figure%d.png', ii));
% saveas(gcf, sprintf('improvedfigure%d.pdf', ii));
%
% % end
% cardata=file_array(:,1)~=0;
% CARDATA=file_array(cardata,:);
%
save('major_scour','file_array','VOL_OCT_NOV','VOL_NOV_DEC','VOL_DEC_MAR','VOL_M
AR_JUL','TOT_OCT_NOV','TOT_NOV_DEC','TOT_DEC_MAR','TOT_MAR_JUL','DA','DB','DC','DE
');
% end

```

APPENDIX XI– MATLAB Script: Scour Orientation Minor

```

close all
clear all
clc
load car_orient_height.mat
load MINORSCOUR.mat
depth = averagebottomdepth'
height = heightofcar'
ort = orientation'
trial = trial'
YYY=zeros(1,length(xpos));
%%%%%%%%%%%%%%%%%%%%%%%%%%%%%%%%%%%%%%%%%%%%%%%%%%%%%%%%%%%%%%%%%%%%%%%%%Enter degrees to look at%%%%%%%%%%%%%%%%%%%%%%%%%%%%%%%%%%%%%%%%%%%%%%%%%%%%%%%%%%%%%%%%%%%%%%%%%
a= 0
b= 17
c= (b-(b-a)/2)+90-(b-a)
d = c+2*(b-a)
if 1==1
    e=180-b
    f=180
end

Orientation = ort>a & ort<b;
Orientation90= ort>c & ort<d;
Orientation180= ort>e & ort<f;
FirstPlot= [(trial(Orientation,:)-100)/5+1;(trial(Orientation180,:)-100)/5+1]
SecondPlot = (trial(Orientation90,:)-100)/5+1'

% for ii=1:38
%   hdvolc(ii,:)=-(depth(ii)*VOLC(ii,:))/(height(ii));
%   hdtotsumc(ii,:)=-(depth(ii)*totsumc(ii,:))/(height(ii));
% end
%%%%%%%%%%%%%%%%%%%%%%%%%%%%%%%%%%%%%%%%%%%%%%%%%%%%%%%%%%%%%%%%%%%%%%%%%-->Pick a storm and uncomment section, pick plot DA VS TOT or
%%%%%%%%%%%%%%%%%%%%%%%%%%%%%%%%%%%%%%%%%%%%%%%%%%%%%%%%%%%%%%%%%%%%%%%%%Noralized2
%%%%%%%%%%%%%%%%%%%%%%%%%%%%%%%%%%%%%%%%%%%%%%%%%%%%%%%%%%%%%%%%%%%%%%%%%OCT_NOV%%%%%%%%%%%%%%%%%%%%%%%%%%%%%%%%%%%%%%%%%%%%%%%%%%%%%%%%%%%%%%%%%%%%%%%%%
figure
orient landscape
subplot (211)
plot (xpos,VOLA(Orientation,:),xpos,flipplr(VOLA(Orientation180,:)))
title (['Orientation -17 deg to ' num2str(b) ' deg']);
xlabel ('Distance From Car Centerline (-)Left (+)Right (m)');
ylabel ('Volumetric Change(m^3)/.25m');
legend ('Car 16', 'Car 36','Location','northeastoutside');
%axis([-3.25 3.25 -10 10]);

```



```

%set(gca,'linewidth',3)
hold on
plot (xpos,YYY,'LineWidth',2,'Color',[0 0 0]);
%# vertical line
hx = graph2d.constantline(0, 'LineWidth',2,'Color',[0 0 0]);
changedependvar(hx,'x');
%axis ([-10.5 10.5 -1 .5])
subplot (212)
plot (xpos,VOLA(Orientation90,:))
legend ('Car 8','Car 10','Car 12','Car 13','Car 15','Car 27',...
'Car 30','Car 32','Location','southeastoutside');
hold on
plot (xpos,YYY,'LineWidth',2,'Color',[0 0 0]);
title (['Orientation' num2str(c) ' deg to ' num2str(d) ' deg']);
xlabel ('Distance From Car Centerline (-)Left (+)Right (m)');
ylabel ('Volumetric Change(m^3)/.25m');
axis([-10.5 10.5 -.75 .5]);
%set(gca,'linewidth',3)
hold on
%plot (XXX,YYY,'LineWidth',2,'Color',[0 0 0]);
%# vertical line
hx = graph2d.constantline(0, 'LineWidth',2,'Color',[0 0 0]);
changedependvar(hx,'x');
%axis ([-10.5 10.5 -10 10])
%saveas(gcf, 'figminor_orient_CASE2_VOLC.png')

figure
orient landscape
subplot (211)
plot (xpos,totsuma(Orientation,:),xpos,flipr(totsuma(Orientation180,:)))
title (['Orientation -17 deg to ' num2str(b) ' deg']);
xlabel ('Distance From Car Centerline (-)Left (+)Right (m)');
ylabel ('Cumulative Volume (m^3)');
legend ('Car 16', 'Car 36','Location','northeastoutside');
%axis([-3.25 3.25 -10 10]);
%set(gca,'linewidth',3)
hold on
plot (xpos,YYY,'LineWidth',2,'Color',[0 0 0]);
%# vertical line
hx = graph2d.constantline(0, 'LineWidth',2,'Color',[0 0 0]);
changedependvar(hx,'x');
axis ([-10.5 10.5 -5 5])
subplot (212)
plot (xpos,totsuma(Orientation90,:))
legend('Car 8','Car 10','Car 12','Car 13','Car 15','Car 27',...
'Car 30','Car 32','Location','southeastoutside');
hold on
plot (xpos,YYY,'LineWidth',2,'Color',[0 0 0]);

```

```

title (['Orientation' num2str(c) ' deg to ' num2str(d) ' deg']);
xlabel ('Distance From Car Centerline (-)Left (+)Right (m)');
ylabel ('Cumulative Volume (m^3)');
%axis([-3.25 3.25 -10 10]);
%set(gca,'linewidth',3)
hold on
%plot (XXX,YYY,'LineWidth',2,'Color',[0 0 0]);
%# vertical line
hx = graph2d.constantline(0, 'LineWidth',2,'Color',[0 0 0]);
changedependvar(hx,'x');
%axis ([-10.5 10.5 -1 10])
%saveas(gcf, 'figminor_orient_CASE2_totsumc.png')
% file_array_Oct_Nov = (Orientation,:);
% Tot_Oct_Nov = TOT_OCT_NOV(Orientation,:);
% Tot_Oct_Nov=Tot_Oct_Nov(:,1:numel(DA));
% plot(DA,Tot_Oct_Nov)

% hold
%Normalize by depth and the height of the car.
% for i=1:numel(Tot_Oct_Nov(:,1))
% NormalHieght(:,i) =
(Tot_Oct_Nov(i,:)/abs(file_array_Oct_Nov(i,5)))/abs(file_array_Oct_Nov(i,3));
% end
% plot(DA,NormalHieght)
%%%%%%%%%%%%%%%%%%%%%%%%%%%%%%%%%%%%%%%%%%%%%%%%%%%%%%%%%%%%%%%%%%%%%%%%%NOV_DEC%%%%%%%%%%%%%%%%%%%%%%%%%%%%%%%%%%%%%%%%%%%%%%%%%%%%%%%%%%%%%%%%%%%%%%%%%
%%%%%%%%%%%%%%%%%%%%%%%%%%%%%%%%%%%%%%%%%%%%%%%%%%%%%%%%%%%%%%%%%%%%%%%%%5
% file_array_Nov_Dec = file_array(Orientation,:);
% Tot_Nov_Dec = TOT_NOV_DEC(Orientation,:);
% Tot_Nov_Dec=Tot_Nov_Dec(:,1:numel(DA));
% %plot(DB,Tot_Nov_Dec)
% hold
% for i=1:numel(Tot_Nov_Dec(:,1))
% NormalHieght(:,i) =
(Tot_Nov_Dec(i,:)/abs(file_array_Nov_Dec(i,5)))/abs(file_array_Nov_Dec(i,3));
% end
% plot(DB,NormalHieght)
%%%%%%%%%%%%%%%%%%%%%%%%%%%%%%%%%%%%%%%%%%%%%%%%%%%%%%%%%%%%%%%%%%%%%%%%%DEC_MAR%%%%%%%%%%%%%%%%%%%%%%%%%%%%%%%%%%%%%%%%%%%%%%%%%%%%%%%%%%%%%%%%%%%%%%%%%
%%%%%%%%%%%%%%%%%%%%%%%%%%%%%%%%%%%%%%%%%%%%%%%%%%%%%%%%%%%%%%%%%%%%%%%%%5
% file_array_Dec_Mar = file_array(Orientation,:);
% Tot_Dec_Mar = TOT_DEC_MAR(Orientation,:);
% Tot_Dec_Mar=Tot_Dec_Mar(:,1:numel(DA));
% plot(DA,Tot_Dec_Mar)
% hold
% for i=1:numel(Tot_Dec_Mar(:,1))
% NormalHieght(:,i) =
(Tot_Dec_Mar(i,:)/abs(file_array_Dec_Mar(i,5)))/abs(file_array_Dec_Mar(i,3));
% end
% plot(DC,NormalHieght)

```

```

%%%%%%%%%%%%%%%%%%%%%%%%%%%%%%%%%%%%%%%%%%%%%%%%%%%%%%%%%%%%%%%%%%%%%%%%%
%%%%%%%%%%%%%%%%%%%%%%%%%%%%%%%%%%%%%%%%%%%%%%%%%%%%%%%%%%%%%%%%%%%%%%%%%
% Tot_Mar_Jul = TOT_MAR_JUL(Orientation,:);
% Tot_Mar_Jul=Tot_Mar_Jul(:,1:numel(DA));
% plot(DA,Tot_Mar_Jul)
% hold
% for i=1:numel(Tot_Mar_Jul(:,1))
% NormalHieght(:,i) =
(Tot_Mar_Jul(i,:)/abs(file_array_Mar_Jul(i,5)))/abs(file_array_Mar_Jul(i,3));
% end
% plot(DC,NormalHieght)

```

APPENDIX XII- MATLAB Script Find Scour Orientation Major

```

close all
clear all
clc
load car_orient_height.mat
load MAJORSCOUR.mat
depth = averagebottomdepth'
height = heightofcar'
ort = orientation'
trial = trial'

%%%%%%%%%%%%%%%%%%%%%%%%%%%%%%%%%%%%%%%%%%%%%%%%%%%%%%%%%%%%%%%%%%%%%%%%Enter degrees to look at%%%%%%%%%%%%%%%%%%%%%%%%%%%%%%%%%%%%%%%%%%%%%%%%%%%%%%%%%%%%%%%%%%%%%%%%
a= 0
b= 25
c= (b-(b-a)/2)+90-(b-a)
d = c+2*(b-a)
if 1==1
    e=180-b
    f=180
end

Orientation = ort>a & ort<b;
Orientation90= ort>c & ort<d;
Orientation180= ort>e & ort<f;
FirstPlot= [(trial(Orientation,:)-100)/5+1;(trial(Orientation180,:)-100)/5+1]
SecondPlot = (trial(Orientation90,:)-100)/5+1'
%%%%%%%%%%%%%%%%%%%%%%%%%%%%%%%%%%%%%%%%%%%%%%%%%%%%%%%%%%%%%%%%%%%%%%%%-->Pick a storm and uncomment section, pick plot DA VS TOT or
%%%%%%%%%%%%%%%%%%%%%%%%%%%%%%%%%%%%%%%%%%%%%%%%%%%%%%%%%%%%%%%%%%%%%%%%Normalized2
%%%%%%%%%%%%%%%%%%%%%%%%%%%%%%%%%%%%%%%%%%%%%%%%%%%%%%%%%%%%%%%%%%%%%%%%OCT_NOV%%%%%%%%%%%%%%%%%%%%%%%%%%%%%%%%%%%%%%%%%%%%%%%%%%%%%%%%%%%%%%%%%%%%%%%%
%%%%%%%%%%%%%%%%%%%%%%%%%%%%%%%%%%%%%%%%%%%%%%%%%%%%%%%%%%%%%%%%%%%%%%%%
figure
subplot (121)
plot (VOLC(Orientation,:),ypos-20,flipplr(VOLC(Orientation180,:),ypos-20)
title (['Orientation -25 deg to ' num2str(b) 'deg CCW from East']);
ylabel ('Distance along Parent Profile (m)');
xlabel ('Volumetric Change (m^3)/.25m');
set(gca,'ydir','reverse')
%axis([-3.25 3.25 -10 10]);
%set(gca,'linewidth',3)
hold on
%plot (XXX,YYY,'LineWidth',2,'Color',[0 0 0]);
%# vertical line
hx = graph2d.constantline(0, 'LineWidth',2,'Color',[0 0 0]);
changedependvar(hx,'x');
axis ([-.3 .3 -20 20])
subplot (122)
plot (VOLC(Orientation90,:),ypos-20)

```

```

title (['Orientation' num2str(c) 'deg to ' num2str(d) 'deg CCW from East']);
ylabel ('Distance along Parent Profile (m)');
xlabel ('Volumetric Change (m^3)/.25m');
set(gca,'ydir','reverse')
%axis([-3.25 3.25 -10 10]);
%set(gca,'linewidth',3)
hold on
%plot (XXX,YYY,'LineWidth',2,'Color',[0 0 0]);
%# vertical line
hx = graph2d.constantline(0, 'LineWidth',2,'Color',[0 0 0]);
changedependvar(hx,'x');
axis ([-.3 .3 -20 20])
%axis ([-8 8 0 40])
saveas(gcf, 'figmajor_orient_CASE1_VOLC.png')

```

```

figure
subplot (121)
plot (totsumc(Orientation,:),ypos-20,flipr(totsumc(Orientation180,:)),ypos-20)
title (['Orientation -25 deg to ' num2str(b) 'deg CCW from East']);
ylabel ('Distance along Parent Profile (m)');
xlabel ('Cumulative Volume (m^3)');
set(gca,'ydir','reverse')
%axis([-3.25 3.25 -10 10]);
%set(gca,'linewidth',3)
hold on
%plot (XXX,YYY,'LineWidth',2,'Color',[0 0 0]);
%# vertical line
hx = graph2d.constantline(0, 'LineWidth',2,'Color',[0 0 0]);
changedependvar(hx,'x');
axis ([-5 5 -20 20])
subplot (122)
plot (totsumc(Orientation90,:),ypos-20)
title (['Orientation' num2str(c) 'deg to ' num2str(d) 'deg CCW from East']);
ylabel ('Distance along Parent Profile (m)');
xlabel ('Cumulative Volume (m^3)');
set(gca,'ydir','reverse')
%axis([-3.25 3.25 -10 10]);
%set(gca,'linewidth',3)
hold on
%plot (XXX,YYY,'LineWidth',2,'Color',[0 0 0]);
%# vertical line
hx = graph2d.constantline(0, 'LineWidth',2,'Color',[0 0 0]);
changedependvar(hx,'x');
axis ([-8 8 -20 20])
saveas(gcf, 'figmajor_orient_CASE1_totsumc.png')

```

```

% file_array_Oct_Nov = (Orientation,:);
% Tot_Oct_Nov = TOT_OCT_NOV(Orientation,:);
% Tot_Oct_Nov=Tot_Oct_Nov(:,1:numel(DA));
% plot(DA,Tot_Oct_Nov)

% hold
% Normalize by depth and the height of the car.
% for i=1:numel(Tot_Oct_Nov(:,1))
% NormalHieght(:,i) =
(Tot_Oct_Nov(i,:)/abs(file_array_Oct_Nov(i,5)))/abs(file_array_Oct_Nov(i,3));
% end
% plot(DA,NormalHieght)
%%%%%%%%%%%%%%%%%%%%%%%%%%%%%%%%%%%%%%%%%%%%%%%%%%%%%%%%%%%%%%%%%%%%%%%%%NOV_DEC%%%%%%%%%%%%%%%%%%%%%%%%%%%%%%%%%%%%%%%%%%%%%%%%%%%%%%%%%%%%%%%%%%%%%%%%%
%%%%%%%%%%%%%%%%%%%%%%%%%%%%%%%%%%%%%%%%%%%%%%%%%%%%%%%%%%%%%%%%%%%%%%%%%5
% file_array_Nov_Dec = file_array(Orientation,:);
% Tot_Nov_Dec = TOT_NOV_DEC(Orientation,:);
% Tot_Nov_Dec=Tot_Nov_Dec(:,1:numel(DA));
% %plot(DB,Tot_Nov_Dec)
% hold
% for i=1:numel(Tot_Nov_Dec(:,1))
% NormalHieght(:,i) =
(Tot_Nov_Dec(i,:)/abs(file_array_Nov_Dec(i,5)))/abs(file_array_Nov_Dec(i,3));
% end
% plot(DB,NormalHieght)
%%%%%%%%%%%%%%%%%%%%%%%%%%%%%%%%%%%%%%%%%%%%%%%%%%%%%%%%%%%%%%%%%%%%%%%%%DEC_MAR%%%%%%%%%%%%%%%%%%%%%%%%%%%%%%%%%%%%%%%%%%%%%%%%%%%%%%%%%%%%%%%%%%%%%%%%%
%%%%%%%%%%%%%%%%%%%%%%%%%%%%%%%%%%%%%%%%%%%%%%%%%%%%%%%%%%%%%%%%%%%%%%%%%5
% file_array_Dec_Mar = file_array(Orientation,:);
% Tot_Dec_Mar = TOT_DEC_MAR(Orientation,:);
% Tot_Dec_Mar=Tot_Dec_Mar(:,1:numel(DA));
% plot(DA,Tot_Dec_Mar)
% hold
% for i=1:numel(Tot_Dec_Mar(:,1))
% NormalHieght(:,i) =
(Tot_Dec_Mar(i,:)/abs(file_array_Dec_Mar(i,5)))/abs(file_array_Dec_Mar(i,3));
% end
% plot(DC,NormalHieght)
%%%%%%%%%%%%%%%%%%%%%%%%%%%%%%%%%%%%%%%%%%%%%%%%%%%%%%%%%%%%%%%%%%%%%%%%%MAR_JUL%%%%%%%%%%%%%%%%%%%%%%%%%%%%%%%%%%%%%%%%%%%%%%%%%%%%%%%%%%%%%%%%%%%%%%%%%
%%%%%%%%%%%%%%%%%%%%%%%%%%%%%%%%%%%%%%%%%%%%%%%%%%%%%%%%%%%%%%%%%%%%%%%%%5
% Tot_Mar_Jul = TOT_MAR_JUL(Orientation,:);
% Tot_Mar_Jul=Tot_Mar_Jul(:,1:numel(DA));
% plot(DA,Tot_Mar_Jul)
% hold
% for i=1:numel(Tot_Mar_Jul(:,1))
% NormalHieght(:,i) =
(Tot_Mar_Jul(i,:)/abs(file_array_Mar_Jul(i,5)))/abs(file_array_Mar_Jul(i,3));
% end
% plot(DC,NormalHieght)

```